

**Investigating the therapeutic potential of
ATR, CHK1 and WEE1 inhibitors in cervical cancer**



**A thesis submitted for the degree of
Doctor of Medicine**

**Stuart Rundle
Northern Institute for Cancer Research
June 2020**

**Supervisors:
Professor Nicola J Curtin
Dr Yvette Drew
Mr Ali Kucukmetin**

Abstract

Introduction: Cervical cancer is the 4th most common cause of cancer-related death in women. It is caused by infection with high-risk HPV (HR-HPV). Current therapy with cisplatin and radiotherapy acts by damaging DNA. The DNA damage response (DDR), critical for survival following endogenous and therapeutic DNA damage, comprises signalling to cell cycle checkpoints and DNA repair. HR-HPV inactivates p53 and pRB and thereby the G1/S checkpoint, making cervical cancer an ideal target for inhibition of intra-S and G2/M cell cycle checkpoints. This thesis directly compares the efficacy of inhibitors of the S and G2/M checkpoints: ATR, CHK1 and WEE1 as single agents and as sensitisers to cisplatin and ionising radiation in cervical cancer cell lines

Methods: A panel of 6 cervical cancer cell lines with different histopathology and HPV status were used. DDR protein expression and inhibition of ATR, CHK1 and WEE1 by VE-821, PF-477736 and MK-1775, respectively were measured by Western blot. Checkpoint proteins were measured in a TMA of human cervical cancer by IHC. Cytotoxicity of inhibitors and combinations with cisplatin or IR was determined by clonogenic assay. Cell cycle analysis with propidium iodide was used to investigate cell cycle changes.

Results: The expression of DDR and checkpoint proteins varied in both cell lines and the TMA. There was a modest spectrum of sensitivity to cisplatin, IR and the inhibitors but the rank order was different for each agent, which was not related to the levels of DDR proteins in general but low ATM was associated with VE-821 sensitivity. The inhibitors were used at fixed concentrations for chemo- and radio-sensitisation studies: 1 μ M VE821, 50 nM PF-477736 and 100 nM MK-1775 reflecting their relative target inhibition potency and intrinsic cytotoxicity. Greater sensitisation was observed with cisplatin than IR, with VE-821 having the greatest and MK-1775 the least effect. Cisplatin caused S-phase accumulation that was reduced by the kinase inhibitors in 4/6 cell lines but increased in the other 2. The effects were more marked for VE-821 and PF-477736 vs MK-1775 and were not related to cisplatin sensitisation.

Conclusions: Cytotoxicity and sensitisation effects were not explained by protein expressions or enzyme inhibition. The effect of the inhibitors on cisplatin-induced S-phase arrest varied across the cell line panel and did not correlate with sensitisation data. Analysis was hampered by the size of the panel and their similarity. Further work with a larger, more

diverse panel of cell lines is required before the mechanisms and potential biomarkers of response to ATR, CHK1 and WEE1 inhibition in cervical cancer can be identified.

Acknowledgements

Firstly, I would like to thank Nicola Curtin for her enthusiastic support and guidance throughout the time I have spent at the NICR undertaking these studies. Her patient understanding and counselling through times where juggling the demands of my academic and clinical workload have nearly overwhelmed me have done so much to lead to the completion of this thesis. I would also like to thank Ali Kucukmetin for helping me keep perspective in my clinical training throughout, and Yvette Drew for her support and advice.

Thanks also go to all of the staff at the Northern Gynaecological Oncology Centre, Gateshead who I have worked with over the last three and a half years. They have always understood my need to be 'at the university' without question and have allowed me generous liberties at times to help me get to this point. In particular I have to acknowledge the contribution of Rachel O'Donnell who has often pointed me in the right direction and helped me problem-solve so many issues.

Amongst many people at the NICR who have helped me along the way Liz Matheson, Lucy Gentles and Callum Kirk have been especially helpful with technical assistance and encouragement through the trickier times.

Thanks to the generous patients who have donated samples for mine and others research and to the trustees and members of the Northern Cancer Care and Research Society (NCCRS), whose generous funding allowed me the resources to perform the investigations described herein.

Finally, thanks as always to Steve and Judy, my parents. They are always there, even though for the most part, I'm sure they have no idea what I'm talking about.

Dedication

To Jonny, whose patience knows no limits. We have never known life without this.

List of Abbreviations

ANOVA	Analysis of variance
ATCC	American Type Culture Collection
ATM	Ataxia Telangiectasia Mutated
ATR	Ataxia Telangiectasia Mutated and Rad3 related
ATRi	ATR inhibitor
ATRIP	ATR-interacting protein
BCA	Bicinchoninic acid
BioCoSHH	Control of substances hazardous to health (biological)
CDK1	Cyclin dependent kinase 1
CDK2	Cyclin dependent kinase 2
CDK4	Cyclin dependent kinase 4
CHK1	Checkpoint kinase 1
CHK2	Checkpoint kinase 2
CHK1i	CHK1 inhibitor
CIN	Cervical intra-epithelial neoplasia
COSHH	Control of substances hazardous to health
dC	deoxy-Cytosine
DDR	DNA damage response
DIW	De-ionised water
DMEM	Dulbecco's modified Eagle's medium
DMSO	Dimethyl-sulfoxide
DNA	Deoxyribonucleic acid
DNA-PK	DNA protein kinase
DNA-PKcs	DNA-PK catalytic subunit
DSB	Double strand break
dU	deoxy-Uracil
EDTA	Ethylenediaminetetraacetic acid
ECL	Enhanced Chemiluminescence
EMEM	Eagle's minimum essential medium
E6AP	E6-associated protein

FBS	Foetal Bovine Serum
FIGO	International Federation of Gynecology and Obstetrics
HDI	Human Development Index
HECT	Homologous to E6AP C-Terminus
HNSCC	Head and neck squamous cell cancer
HPV	Human papilloma virus
HR-HPV	High-risk Human papilloma virus
HRP	Horseradish peroxidase
HRR	Homologous recombination repair
IBSCC	International Biological Study on Cervical Cancer
IC ₅₀	Concentration at 50% enzyme inhibition
IR	Ionising radiation
Ku	Ku70-Ku80 heterodimer
LC ₅₀	Concentration required for 50% colony survival
LD ₅₀	Dose required for 50% colony survival
mAb	Monoclonal antibody
MGMT	DNA-methyltransferase
NaCl	Sodium chloride
NER	Nucleotide excision repair
NHEJ	Non-homologous end joining
pAb	Polyclonal antibody
PARP	Poly-ADP ribose polymerase
PBS	Phosphate buffered saline
pCDK1 ^{Y15}	CDK1 phosphorylated at tyrosine residue 15
pCHK1 ^{S296}	CHK1 phosphorylated at serine residue 296
pCHK1 ^{S345}	CHK1 phosphorylated at serine residue 345
PCR	Polymerase chain reaction
PF ₅₀	Ratio of LC ₅₀ (cisplatin) or LD ₅₀ (IR) in absence/presence of inhibitor
PF _{0.3-cis}	Ratio of survival at 0.3 μ M cisplatin in absence/presence of inhibitor
PF _{2-IR}	Ratio of survival at 2 Gy IR absence/presence of inhibitor
PI	Propidium iodide
pRB	Retinoblastoma protein

p53	Tumour protein 53 (gene product)
RB1	Retinoblastoma 1 (gene)
RIPA	Radioimmunoprecipitation (buffer)
RNA	Ribonucleic acid
RNase	Ribonuclease
ROS	Reactive oxygen species
RPA	Replication protein A
RPMI	Roswell Park Memorial Institute (media)
SAM	S-adenosyl-methionine
SCC	Squamous cell cancer
SD	Standard deviation
SEM	Standard error of the mean
shRNA	Short hairpin RNA
siRNA	Small interfering RNA
SRB	Sulforhodamine B
SSB	Single strand break
TBS	Tris-buffered saline
TBST	Tris-buffered saline with 0.5% Tween-20
TOPOI	Topoisomerase-I
TOPOII	Topoisomerase-II
TOPBP1	Topoisomerase-2 binding-protein-1
TP53	Tumour protein 53 (gene)
WEE1i	WEE1 inhibitor
4NQO	4-Nitroquinoline 1-oxide
8-OHdG	8-hydroxy-2'-deoxyguanine

List of Figures

Figure 1.1 Phylogenic tree of human papillomavirus (HPV).....	4
Figure 1.2 HPV infection progressing to cervical cancer through pre-invasive disease	6
Figure 1.3 Schematic representation of the cell cycle and DNA damage checkpoints.	7
Figure 1.4 A stalled replication fork resulting from a DNA lesion	8
Figure 1.5 p53 and pRB at the G1/S cell cycle checkpoint.	11
Figure 1.6 ATR recruitment and activation at stalled replication forks and sites of DNA damage and repair.	17
Figure 1.7 The regulation of CDK activity by ATR, CHK1 and WEE1.	18
Figure 1.8 Simplified schematic diagram of the role of ATR, CHK1 and WEE1 in homologous recombination repair (HRR).	22
Figure 2.1 Diagram showing the layout of an individual 96-well plate used for SRB growth assays.	44
Figure 2.2 Example of 6-well plate layout for cisplatin potentiation colony formation assay.	47
Figure 2.3 Example of 6-well plate layout for IR potentiation colony formation assay.	48
Figure 2.4 The layout of a 96 well plate used for BCA protein assays.....	53
Figure 2.5 Example of a standard curve generated by linear regression analysis of absorbance at 256 nm for a series of standard serum albumin solutions.	53
Figure 2.6 An example of a cell cycle profile of unperturbed HeLa cells.	56
Figure 3.1 Photograph showing HeLa cell colonies.	63
Figure 3.2 Representative examples of growth curves for ME180 and HT-3 cells at five different seeding densities.....	65
Figure 3.3 Baseline protein expression in unperturbed cells.	68
Figure 3.4 Expression of cell cycle checkpoint and NHEJ proteins.....	69
Figure 3.5 Scatter plots showing correlations between baseline protein expressions of pairs of proteins in human cervical cancer cell lines.	71

Figure 3.6 Scatter plots of cell cycle checkpoint and DDR protein expression vs cell line doubling times.	72
Figure 4.1 Representative Western blots showing protein bands corresponding to ATR and the principal phosphorylation targets of ATR CHK1 and WEE1 in HeLa cells.....	81
Figure 4.2 Concentration dependent inhibition of ATR by VE-821.	83
Figure 4.3 Activation of ATR by cisplatin and inhibition by VE-821.	84
Figure 4.4 Concentration dependent inhibition of CHK1 by PF-477736.	85
Figure 4.5 Activation of CHK1 by cisplatin and inhibition by PF-477736.	86
Figure 4.6 Concentration dependent inhibition of WEE1 by MK-1775.....	87
Figure 4.7 Activation of WEE1 by cisplatin and inhibition by MK-1775.	88
Figure 4.8 Single agent cytotoxicity of VE-821 in the cervical cancer cell line panel.	89
Figure 4.9 Single agent cytotoxicity of PF-477736 in the cervical cancer cell line panel.	90
Figure 4.10 Single agent cytotoxicity of MK-1775 in the cervical cancer cell line panel.....	91
Figure 4.11 Scatter plots of target enzyme % inhibition vs cytotoxicity (LC ₅₀).	93
Figure 4.12 <i>Scatter plots of target enzyme % inhibition vs cytotoxicity (% colony survival at fixed inhibitor concentrations).</i>	94
Figure 4.13 Scatter plots of ATM and DNA-PKcs expression vs single agent cytotoxicity.....	96
Figure 5.1 Cisplatin cytotoxicity in the cervical cell line panel.	104
Figure 5.2 Correlations between cisplatin cytotoxicity and relative activation of target enzymes by cisplatin in cervical cancer cell lines.	105
Figure 5.3 Ionising radiation cytotoxicity in the cervical cell line panel.....	106
Figure 5.4 Correlations IR cytotoxicity and baseline expression of target enzymes cervical cancer cell lines.	107
Figure 5.5 Colony survival of cervical cancer cell lines exposed to cisplatin ± VE-821.	108
Figure 5.6 Colony survival of cervical cancer cell lines exposed to cisplatin ± PF-477736...	110
Figure 5.7 Colony survival of cervical cancer cell lines exposed to cisplatin ± MK-1775. ...	112

Figure 5.8 Correlations between cell line sensitisation to cisplatin by MK-1775 and baseline expression of WEE1 in cervical cancer cell lines.	114
Figure 5.9 Colony survival of cervical cancer cell lines exposed to IR \pm VE-821.....	116
Figure 5.10 Correlations between sensitisation to IR by VE-821 and sensitivity to IR alone.	117
Figure 5.11 Colony survival of cervical cancer cell lines exposed to IR \pm PF-477736.	119
Figure 5.12 Colony survival of cervical cancer cell lines exposed to IR \pm MK-1775.	121
Figure 5.13 Correlations between MK-1775 sensitisation of cell lines to cisplatin cytotoxicity and baseline expression of target enzymes in cervical cancer cell lines.....	122
Figure 5.14 Heatmaps showing the relative sensitisation of cervical cancer cell lines to cisplatin and IR by VE-821, PF-477736 and MK-1775.	125
Figure 6.1 Representative example of cell cycle profile histograms showing cell cycle distributions of SiHa cells with and without treatment using cisplatin +/- VE-821, PF-477736 and MK-1775.....	129
Figure 6.2 Cell cycle profiles of cervical cancer cell lines treated with VE-821 and cisplatin as single agents and in combination.	132
Figure 6.3 Cell cycle profiles of cervical cancer cell lines treated with PF-477736 and cisplatin as single agents and in combination.	133
Figure 6.4 Cell cycle profiles of cervical cancer cell lines treated with MK-1775 and cisplatin as single agents and in combination.	134
Figure 6.5 Changes in S-phase and G2/M-phase populations in cells treated with cisplatin-inhibitor combinations compared to cells treated with cisplatin alone.	135
Figure 6.6 Correlations between target enzyme inhibition and effect of 1 μ M VE-821, 50 nM PF-477736 and 100 nM MK-1775 on cell cycle profile changes induced by 3 μ M cisplatin.	137
Figure 6.7 Correlations between ATR and CHK1 expression and effect of 1 μ M VE-821 on cell cycle profile changes induced by 3 μ M cisplatin.....	138
Figure 6.8 Correlations between ATR and CHK1 expression and effect of 50 nM PF-477736 on cell cycle profile changes induced by 3 μ M cisplatin.	139
Figure 7.1 Tissue microarray layout containing duplicate cores from 11 patient samples and 2 positive control cores.....	145

Figure 7.2 Micrographs of human testes positive control tissue demonstrating CHK1 staining.....	148
Figure 7.3 Micrographs of human testes positive control tissue demonstrating ATR staining but inadequate WEE1 staining	148
Figure 7.4 Micrographs of representative TMA cores stained for ATR (top) and CHK1 (bottom).....	149
Figure 7.5 Correlations between ATR and CHK1 expression in clinical tumour samples	151
Figure 7.6 Correlation between ATR and CHK1 mRNA expression in TCGA data.....	152
Figure 7.7 Kaplan-Meier plots showing survival of kinase high vs low expression from the TCGA study of cervical cancer dataset	154
Figure 8.1 Schematic representation of proposed balance of DNA damage checkpoint and repair reactions influencing cell cycle progression in response to DNA damage.	164

List of Tables

Table 1.1 Cervical cancer treatment options and 5-year survival by stage at presentation.	2
Table 1.2 Key cell cycle factors associated with the G1/S cell cycle checkpoint.....	10
Table 1.3 Principal described DNA repair pathways, activating lesions and causative agents or insults.....	15
Table 1.4 Key cell cycle factors at the intra-S and G2/M DNA damage cell cycle checkpoints	20
Table 1.5 DNA damaging agents, lesions and repair pathways.	21
Table 1.6 Potent and specific small molecule inhibitors of ATR, CHK1 and WEE1.....	26
Table 1.7 Studies describing replication stress inducing transformations that promote S-phase entry that evidence potential synthetic lethality with ATR, CHK1 or WEE1 inhibition.	29
Table 2.1 Human cervical cancer cell lines used and their specific growth media for continuous culture.	42
Table 2.2 Primary and secondary antibodies used for Western blot experiments to determine the baseline expression of key DDr and cell cycle checkpoint proteins, their manufacturer, and experimental dilutions.	50
Table 3.1 Cervical cell lines used in experiments, their HPV status, histological sub-type and TP53/RB1 status.	62

Table 3.2 Doubling times and cloning efficiency for six cervical cancer cell lines.....	66
Table 4.1 LC ₅₀ values for each VE-821, PF-477736 and MK-1775 in all six cervical cancer cell lines.	92
Table 4.2 Concentration specific target enzyme inhibition and inhibition of colony survival for the cervical cancer cell lines using 1 μ M VE-821, 50 nM PF-477736 and 100 nM MK-1775.	95
Table 5.1 Sensitisation of cervical cancer cell lines to cisplatin by VE-821.	109
Table 5.2 Sensitisation of cervical cancer cell lines to cisplatin by PF-477736.	111
Table 5.3 Sensitisation of cervical cancer cell lines to cisplatin by MK-1774.	113
Table 5.4 Sensitisation of cervical cancer cell lines to IR by VE-821.	117
Table 5.5 Sensitisation of cervical cancer cell lines to IR by PF-477736.....	118
Table 5.6 Sensitisation of cervical cancer cell lines to IR by MK-1775	120
Table 6.1 Percent-single cell populations per cell cycle phase for six cervical cancer cell lines exposed to cisplatin +/- inhibitors drugs.....	131
Table 7.1 Antibodies and dilutions used for IHC staining of clinical TMA slides.	146
Table 7.2 Modified H-score results for individual cores from a cervical cancer TMA stained for ATR and CHK1.....	150
Table 7.3 Clinical, diagnostic, treatment and follow-up data for cervical cancer patients who donated tumour samples to these investigations.....	153
Table 7.4 Survival of cervical cancer patients from the TCGA study of cervical cancer dataset by checkpoint kinase expression.....	155

Contents

1	Introduction.....	1
1.1	Cervical cancer – Morbidity, mortality and current treatment	1
1.2	Cervical cancer and high-risk HPV.....	3
1.2.1	Cervical cancer is strongly associated with high-risk HPV.....	3
1.2.2	HPV-driven cervical cancer pathogenesis	5
1.3	Cell cycle control and the DNA damage checkpoints.....	7
1.3.1	p53 and pRB at the G1/S checkpoint	9
1.3.2	High-risk HPV interaction with p53 and pRB.....	11
1.4	The DNA damage response and the ATR-CHK1-WEE1 axis	12
1.4.1	DNA repair pathways	13
1.4.2	ATR-CHK1-WEE1 activation.....	15
1.4.3	ATR, CHK1 and WEE1 at the Intra-S and G2/M checkpoints.....	17
1.4.4	ATR, CHK1 and WEE1 in DNA repair.....	20
1.5	ATR, CHK1 and WEE1 inhibitors.....	23
1.5.1	Target validation by genetic downregulation	23
1.5.2	Development of ATR, CHK1 and WEE1 inhibitors	24
1.6	Single agent activity and determinants of sensitivity for inhibition of the ATR-CHK1-WEE1 axis.....	28
1.6.1	Oncogene driven replication stress as a sensitiser to ATR, CHK1 or WEE1 inhibition	28
1.6.2	DDR abnormalities as determinants of sensitivity to ATR, CHK1 or WEE1 inhibition.	30
1.7	Pre-clinical data: chemo-sensitisation and radio-sensitisation	32
1.7.1	Combinations with platinum chemotherapy agents.....	32
1.7.2	Combinations with ionising radiation	35
1.8	ATR, CHK1 and WEE1 inhibitors in clinical practice	37
1.9	Aims and Objectives:.....	38
2	Materials and Methods.....	40
2.1	General laboratory practice.....	40
2.2	Chemicals and Reagents	40
2.3	Cell Culture	40
2.4	SRB assay	43
2.4.1	Determination of cell line growth rate by SRB assay	43
2.4.2	Data analysis	44
2.5	Colony formation assay.....	45
2.5.1	Cell preparation and fixation	45
2.5.2	Single agent cytotoxicity assay.....	46
2.5.3	Cisplatin potentiation cytotoxicity assay	46
2.5.4	Radio-potentiation cytotoxicity assay.....	48
2.5.5	Data Analysis.....	49
2.6	Western blot	49

2.6.1	Preparation of cell lysates	51
2.6.2	BCA assay	52
2.6.3	Gel electrophoresis	54
2.6.4	Antibody staining and chemi-luminescence	54
2.6.5	Data Analysis	55
2.7	Cell cycle analysis	55
2.7.1	Preparation of samples for cell cycle analysis	56
2.7.2	Fluorescence cytometry and data analysis	57
2.8	Tissue microarray and Immunohistochemistry	57
2.9	Data analysis and statistics	58
3	<i>Characterisation of cervical cancer cell lines.....</i>	59
3.1	Introduction	59
3.1.1	Cervical cancer cell lines as a useful pre-clinical tool	59
3.1.2	Choosing cervical cancer cell lines to represent clinical conditions	60
3.2	Aims and Objectives	60
3.3	Materials and methods	61
3.3.1	Cervical cancer cell lines	61
3.3.2	Determination of cell doubling times by SRB assay	61
3.3.3	Determination of cloning efficiency by colony formation assay	62
3.3.4	Determination of baseline protein expression by Western blot	63
3.4	Results	64
3.4.1	Cell line doubling times and cloning efficiency	64
3.4.2	Baseline expression of checkpoint and DDR proteins	66
3.4.3	Correlations between protein expressions	70
3.4.4	Correlations between cell growth and protein expressions	72
3.5	Discussion	72
3.6	Conclusions	76
4	<i>Target enzyme activity and single agent cytotoxicity</i>	77
4.1	Introduction	77
4.2	Aims and objectives	78
4.3	Materials and methods	79
4.3.1	Investigations of enzyme activation and inhibition by western blot	79
4.3.2	Single agent cytotoxicity of inhibitors of ATR, CHK1 and WEE1	80
4.4	Results	81
4.4.1	Activation of the ATR-CHK1-WEE1 pathway by cisplatin	81
4.4.2	Target enzyme inhibition: ATR and VE-821	81
4.4.3	Target enzyme inhibition: CHK1 and PF-477736	84
4.4.4	Target enzyme inhibition: WEE1 and MK-1775	86
4.5	Single agent cytotoxicity	89
4.5.1	ATR inhibitor single agent cytotoxicity: VE-821	89
4.5.2	CHK1 single agent cytotoxicity: PF-477736	90
4.5.3	WEE1 inhibitor single agent cytotoxicity: ML-1775	91
4.6	Correlations between cell line characteristics, target inhibition and single agent cytotoxicity.	93
4.6.1	Correlations between enzyme inhibition and single agent cytotoxicity	93
4.6.2	Correlations with baseline protein expressions	95

4.7	Discussion	97
4.8	Conclusions	99
5	<i>Sensitisation of cervical cancer cell lines to cisplatin and ionising radiation using inhibitors of ATR, CHK1 and WEE1</i>	101
5.1	Introduction	101
5.2	Aims and Objectives	102
5.3	Materials and methods	102
5.3.1	Colony formation assays with cisplatin and ionising radiation	102
5.4	Results	103
5.4.1	Cell line sensitivity to cisplatin and ionising radiation alone	103
5.4.2	Sensitisation of cell lines to cisplatin by ATR, CHK1 and WEE1 inhibitors	107
5.4.3	Sensitisation of cell lines to IR by inhibitors of ATR, CHK1 and WEE1	114
5.5	Discussion	122
5.6	Conclusions	126
6	<i>Evaluation of cell cycle profile changes following cisplatin and inhibitor exposure.</i>	127
6.1	Introduction	127
6.2	Aims and objectives	128
6.3	Materials and Methods	128
6.4	Results	130
6.4.1	Cell cycle responses to single agents	130
6.4.2	Effect of ATR, CHK1 and WEE1 inhibitors on cisplatin-induced cell cycle profile changes.	130
6.4.3	Correlations between cell cycle changes, cell line characteristics and cytotoxicity profiles.....	135
6.5	Discussion	140
6.6	Conclusions	141
7	<i>Exploration of checkpoint protein expression in clinical tumour samples.....</i>	143
7.1	Introduction	143
7.2	Aims and Objectives.....	144
7.3	Materials and methods	144
7.3.1	TMA construction and slide preparation	144
7.3.2	Immunohistochemistry	145
7.3.4	Slide scanning and data analysis	146
7.4	Results	147
7.4.1	Optimisation of antibody dilutions	147
7.4.2	IHC scoring	149
7.4.3	ATR, CHK1 and WEE1 expression in a wider context.	151
7.4.4	Clinical correlation	152
7.5	Discussion and conclusions.....	155
8	<i>Final discussion, conclusions and future directions</i>	157
8.1	Final conclusions	163
8.2	Future directions.....	164
	<i>References.....</i>	167

<i>Appendix.....</i>	<i>188</i>
Poster presentations at scientific conferences	188

1 Introduction

1.1 Cervical cancer – Morbidity, mortality and current treatment

Cervical cancer accounted for over 310,000 cancer deaths worldwide in 2018 despite important advances in the detection of pre-invasive disease through effective screening programmes (Landy et al., 2016, Rebolj et al., 2019) and the availability of vaccines targeted at high-risk human papillomavirus (HPV) (Simms et al., 2019). Cervical cancer remains stubbornly amongst the top four worldwide causes of female cancer death, accounting for 7.5 % of cancer related mortality in women. In low Human Development Index (HDI) settings cervical cancer is the second most common cause of female cancer death and in Western and sub-Saharan Africa it is the most commonly diagnosed cancer in women (Bray et al., 2018). The overwhelming majority of cervical cancers are carcinomas arising from the squamous cells of the ectocervical transition zone or adenocarcinomas (and a variant known as adenosquamous cancers) arising from the glandular endocervix. Both histopathological sub-types have the same aetiology: mucosal infection with human papillomavirus (HPV) and are treated similarly, although adenocarcinomas have a marginally poorer response to non-surgical treatments and a slightly poorer prognosis (Katanyoo et al., 2012, Chen et al., 2014).

In all settings, the likelihood of surviving cervical cancer depends on the stage of the disease. The five-year survival rates from cervical cancer range from 95% in stage 1 disease to just 5% for those with stage 4 disease (CRUK, 2019). Cervical cancer is staged according to the 2018 FIGO (International Federation of Gynaecology and Obstetrics) staging system (Bhatla et al., 2018), which uses a combination of clinical and radiological findings (Table 1.1). Initial treatment is defined by stage at presentation. Early disease, confined to the cervix is usually treated surgically with either a local or radical excision of the tumour, cervix and uterine corpus along with common sites of metastases such as the parametrium and pelvic lymph nodes. Locally advanced disease in which there is evidence of spread to the parametrium or pelvic nodes is usually treated with concurrent radical radiotherapy and cisplatin chemotherapy (Cibula et al., 2018).

Stage	Description	Current 1 st line treatment	5 year Survival
I A	Microscopic invasive disease confined to the cervix with a depth of invasion < 5 mm	Local surgical excision ± pelvic lymph node assessment	95%
I B	Invasive disease confined to the cervix with depth of invasion ≥ 5 mm	Radical surgical excision with pelvic ± para-aortic lymphadenectomy	
II A	Tumour extends to involve upper two-thirds of vagina without parametrial involvement	Radical surgical excision with lymphadenectomy or primary combination platinum based chemo-radiotherapy	50%
II B	Tumour extends to involve the parametrium but not up to the pelvic sidewall	Primary combination platinum based chemo-radiotherapy	
III A	Tumour extends to the lower third of the vagina without but pelvic sidewall involvement	Primary combination platinum based chemo-radiotherapy	40%
III B	Tumour extends to the pelvic sidewall or causes hydronephrosis/non functioning kidney	Primary combination platinum based chemo-radiotherapy	
III C	(1) Pelvic- or (2) para-aortic lymph node metastases	Primary combination platinum based chemo-radiotherapy	
IV A	Spread to adjacent pelvic organs	Primary combination platinum based chemo-radiotherapy	5%
IV B	Spread to extra-pelvic organs	Palliative chemotherapy	

Table 1.1 Cervical cancer treatment options and 5-year survival by stage at presentation.

Staging does not include sub-categorisation that do not affect treatment choices or have significant impacts on survival outcomes, which are based on previous FIGO (2009) staging classifications. Local excision refers to cervical conisation or simple excision of the cervix ± uterine corpus (depending on the tumour size and fertility preservation wishes of the patient). Radical excision refers to excision of the cervix ± uterine corpus with excision of the parametria and upper vagina. Table derived from Bhatla et.al., 2018

For patients who have disease outside of the pelvis at presentation or for those who have recurrent disease in anatomical areas previously treated with radiotherapy, therapeutic options are often limited to palliative chemotherapy, often with platinum-based regimes if the disease is not amenable to salvage surgery (Scatchard et al., 2012). Despite the recent introduction of newer agents such as the anti-vascular endothelial growth factor drug Bevacizumab (Bizzarri et al., 2016, Rosen et al., 2017) into chemotherapy regimens, the prognosis for advanced or recurrent disease remains poor. This underlies the urgent need to find new and effective strategies to treat cervical cancer, including strategies aimed at enhancing the effectiveness of standard of care treatments at all stages of disease.

1.2 Cervical cancer and high-risk HPV

1.2.1 Cervical cancer is strongly associated with high-risk HPV

Cervical cancer is almost ubiquitously a disease resulting from infection of the cervical transition zone by 'high-risk' HPV subtypes (HR-HPV). The HPV family of deoxyribonucleic acid (DNA)-viruses is large and diverse (Figure 1.1) (de Villiers, 2013). The majority of HPV viruses, especially from the *beta*- and *gamma*- types persist in host species as commensals, without causing disease. Others such as the 'low-risk' *alpha*-type HPV-3 can cause benign papillomatous diseases in humans, such as anogenital warts. A relatively small number of *alpha*-HPV viruses are regarded as HR-HPV and are capable of causing malignant disease, most notably in the cervix.

Alpha- HPV types have a greater diversity in their *E6* and *E7* genes than other HPV types. The transcriptional products of these genes: virus proteins E6 and E7 play important roles in host immune evasion and virus genome amplification within the host cell replication machinery (Doorbar et al., 2015). An important feature of HR-HPV E6 and E7 is their respective interactions with host cell tumour protein 53 (p53) and retinoblastoma protein (pRB), and the resulting interference with cell-cycle DNA damage checkpoint control (see section 1.3.1).

Confirmation of the association between HR-HPV and cervical cancer was provided by the International Biological Study on Cervical Cancer (IBSCC), which reported 93% positivity for HR-HPV in 981 cervical cancer patients from 22 countries (Bosch et al., 1995). The relative distribution of HR-HPV sub-types in this study confirmed a predominance of HPV-16 and related sub-types (16, 31, 33, 35, 52 and 58) in squamous cancers (68%), while HPV-18 and related sub-types (18, 39, 45, 59 and 68) predominated in adenocarcinomas and adenosquamous cancers (71% in each), findings that were subsequently corroborated in later studies (Zehbe and Wilander, 1997). Following this, re-analysis of many of the IBSCC HPV-negative specimens using polymerase chain reaction (PCR) targeting HR-HPV *E6* and *E7* genes, which are integral to carcinogenesis established that the worldwide prevalence of HPV in cervical cancer is as high as 99.7% (Walboomers et al., 1999).

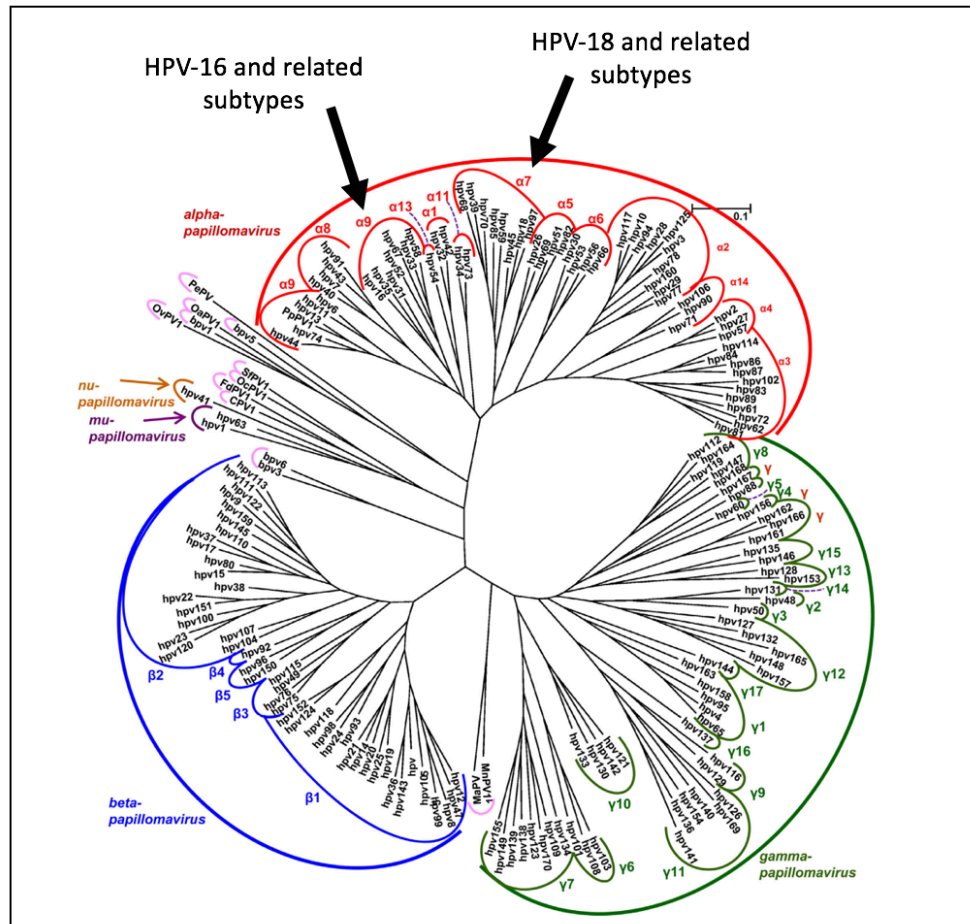


Figure 1.1 Phylogenetic tree of human papillomavirus (HPV).

Most human-disease causing HPV are found amongst the alpha-types. The location of the high-risk HPV subtypes related to HPV-16: most common in squamous cervical cancers, and HPV-18: most common in adenocarcinomas are noted. Diagram adapted from de Villiers, 2013.

The possibility of a truly HPV negative cervical cancer cannot be completely ruled out. However, such an entity appears to be rare and the prevalence of HPV negative cervical cancers is universally accepted to be extremely low. The existence of human cervical cancer cell lines in which there are no detectable HPV DNA sequences, refutes the conclusion that these cancers are non-existent. Characterisation of these cell lines however, suggests that pathogenic mutations of one or both of the tumour suppressor genes: *Tumour Protein 53 (TP53)* and; *Retinoblastoma 1(RB1)* are present. This is in contrast to the situation in HPV positive cell lines, where the cell lines expressed normal gene products at comparatively low levels, indicative of post transcription suppression by The HPV proteins E6 and E7

(Walboomers and Meijer, 1997). This evidence suggests that disruption of the functions of the tumour suppressor proteins p53 and pRB play a vital role in promoting human cervical cancer carcinogenesis in the presence or absence of HR-HPV.

1.2.2 HPV-driven cervical cancer pathogenesis

It is persistent infection of the cervical epithelium with HR-HPV sub-types that increases an individual's risk of developing pre-invasive lesions or cervical cancer (Munoz et al., 2003). The development of pre-invasive cervical lesions known as cervical intra-epithelial neoplasia (CIN) is the pathognomonic prodrome in the development of cervical cancer and these lesions usually appear years before the development of a frankly malignant lesion.

A detailed description of the pathophysiology of CIN progression is beyond the scope of this thesis and is summarised in Figure 1.2 however, it should be noted that the molecular processes in CIN lesions are identical to invasive cancer and the ability to detect CIN in cervical samples underlies the effectiveness of cervical cancer screening programmes. Low grade lesions (CIN-I) may, however regress spontaneously under the influence of host immunity (Tainio et al., 2018), whilst high grade CIN (CIN-II or CIN-III) have a higher risk of progression to cervical cancer (Vink et al., 2013).

The prevalence of HR-HPV infection is as high as 20% in the UK female population (Ramanakumar et al., 2016). It is important to recognise that up to 50% of lower genital tract HR-HPV infections will clear spontaneously within 1 year of detection. The true prevalence of high grade cervical pre-invasive lesions amongst the population is difficult to estimate given the variable uptake of screening and the often-transient nature of the disease, which may not progress to cancer. A Canadian study, conducted in settings similar to the UK, with HPV vaccination and cervical screening programmes estimate an incidence rate for CIN-II or CIN-III of between 1 and 2 per 1000 person years (Racey et al., 2020).

The impact of HPV vaccination on cervical cancer rates is not yet fully understood. The incidence of cervical cancer across all regions of the UK from 2015 to 2017 was approximately 10 per 100,000 women per year. Whilst the incidence rates are projected to

fall under the continued influence of HPV vaccination, rates are expected to remain at above 8 per 100,000 women per year until at least 2040 (Castanon et al., 2018).

In the progression from viral infection, through CIN to cervical cancer, rather than a normal virus-host relationship in which HPV uses the host DNA replication machinery to propagate its life cycle, under certain circumstances viral DNA is integrated into the host genetic material. Viral integration represents a pre-cancer event for the host as integration is associated with dysregulation of the key *E6* and *E7* oncogenes resulting in the promotion of cell proliferation, checkpoint dysfunction and genetic instability through interaction with the gene products of the tumour suppressor genes, TP53 and RB1 (Jeon et al., 1995). The resulting clonal expansion of cells with integrated HR-HPV results in the characteristic pre-invasive cervical lesions and in some cases, invasive cancer (McBride and Warburton, 2017).

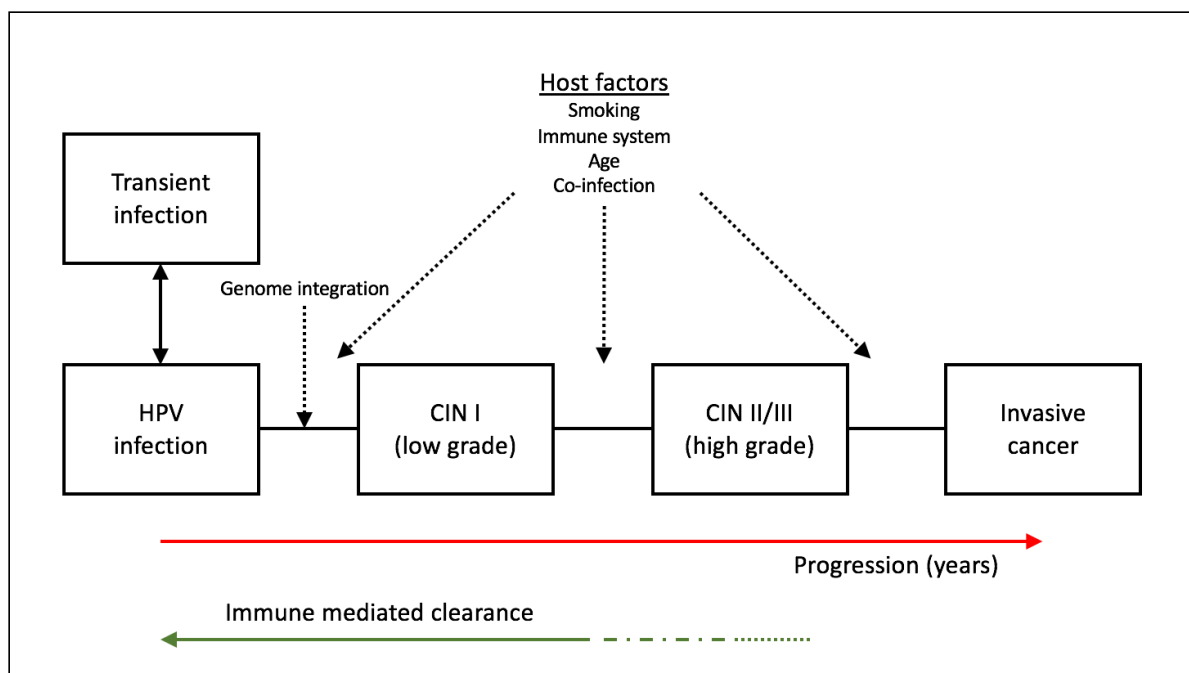


Figure 1.2 HPV infection progressing to cervical cancer through pre-invasive disease

Host factors including age, immunity and smoking status play a role in immune mediated virus clearance. Persistence of infection over years leads to the development of invasive disease in a small number of women. The risk of progression from CIN II/CIN III to invasive cancer is approximately 2% over 10 years. 50% of CIN II lesions may regress spontaneously over 2 years.

1.3 Cell cycle control and the DNA damage checkpoints

Non-dividing cells are frequently referred to as being in resting- or G₀- phase. Dividing cells are described as being in one of four observable cell cycle phases at any one time: G₁, S, G₂ or M (Figure 1.3). G₁ and G₂ phases represent periods of growth and biosynthesis in preparation for DNA replication or synthesis (S-phase) or cell division (M-phase or Mitosis). G₁ cells may enter S-Phase and continue the cell cycle, undergo terminal differentiation (enter G₀) or arrest in G₁ in the face of DNA damage at the G₁/S DNA damage checkpoint. G₁ arrest prevents DNA replication in the presence of problematic DNA lesions and allows time for DNA repair. G₂ cells may also arrest in response to DNA damage at the G₂/M DNA damage checkpoint. This prevents potentially harmful DNA lesions that have occurred during synthesis from being incorporated into the genome of daughter cells following cell division (M-phase or mitosis) (Curtin, 2012, Sancar et al., 2004). A further check on the fidelity of the cell's DNA occurs at the intra-S checkpoint.

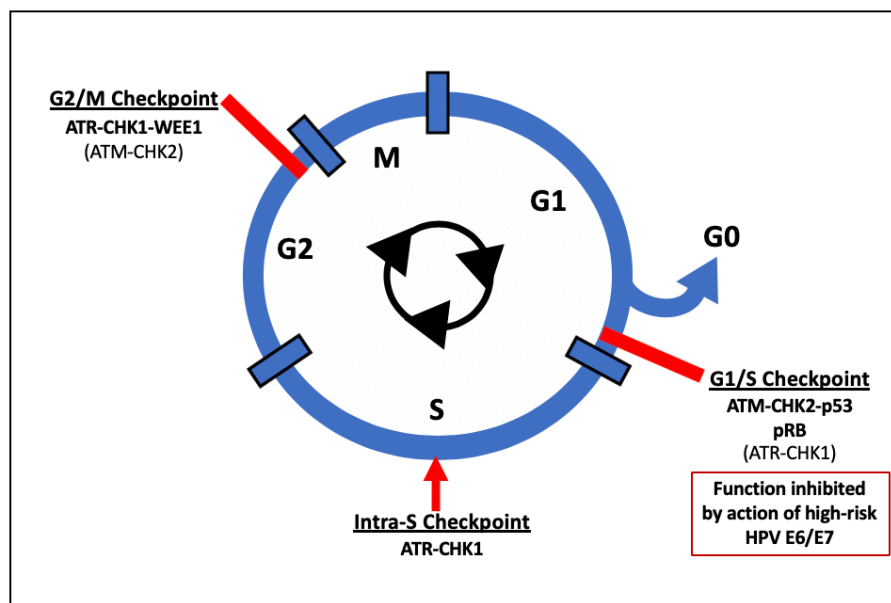


Figure 1.3 Schematic representation of the cell cycle and DNA damage checkpoints.

The principal signalling pathways to each cell cycle checkpoint are shown. DNA damage is signalled to the intra-S and G₂/M transition checkpoints mainly via ATR signalling through Chk1. The G₁/S checkpoint is mainly signalled to via the ATM-Chk2 pathway leading to activation of p53. Closely related to the G₁/S checkpoint is the pRB controlled G₁ restriction point. There is some degree of crossover between ATM and ATR signalling to G₁/S and G₂/M checkpoints. Function of G₁/S checkpoint is inhibited by interactions of p53 and pRB with high-risk HPV proteins E6 and E7 (section 1.3.2)

During S-phase the DNA replication machinery: a complex interplay of helicases, primases and polymerases, operating at the replication fork encounters each base in the genome and is therefore a sensitive probe for DNA lesions (Lodish H, 2000). Lesions that block the progression of replication polymerases result in a stalled replication fork characterised by uncoupling of the helicase (unwinding) and polymerase (replication) functions of the replication machinery. Replication fork stalling and the resulting generation of single stranded DNA is a powerful indicator of replication stress and inducer of signalling to intra-S and G2/M cell cycle checkpoints (Iyer and Rhind, 2017). This signalling occurs principally through Ataxia Telangiectasia and Rad3-related (ATR) mediated signalling pathways (Figure 1.4 and Chapter 1.3) (Cimprich and Cortez, 2008, MacDougall et al., 2007, Maréchal and Zou, 2013).

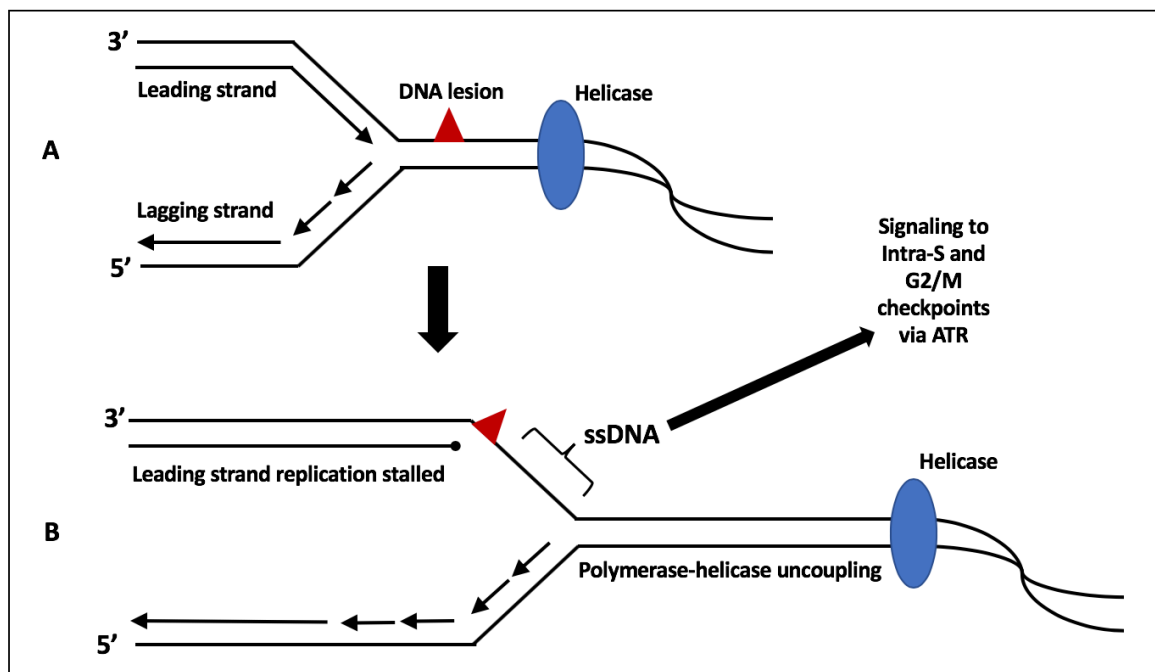


Figure 1.4 A stalled replication fork resulting from a DNA lesion

The DNA replication machinery is preceded by helicase unwinding of the dsDNA. In this case replication of the leading strand is halted by the lesion on the leading strand template, resulting in the presence of ssDNA. The stalled replication fork is characterised by the presence of this ssDNA and the uncoupling of the helicase and polymerase functions of the replication machinery. The stalled replication fork signals to DNA damage checkpoints through ATR.

1.3.1 p53 and pRB at the G1/S checkpoint

In addition to its established roles in the detection and repair of DNA double strand breaks (Maréchal and Zou, 2013), ataxia telangiectasia mutated (ATM) and its immediate downstream kinase, checkpoint kinase 2 (CHK2) play important roles in signalling DNA damage to the G1/S checkpoint (Figure 1.3) (Sancar et al., 2004). ATM and CHK2, and to a lesser extent ATR and checkpoint kinase 1 (CHK1), directly phosphorylate p53. Accumulation of phosphorylated p53 and its action as a transcription factor for p21(CIP1) results in increased p21(CIP1) mediated inhibition of the cyclin dependent kinase-2 (CDK2)/cyclinE complex. CDK2/cyclinE complex function is crucial the progression of the cell into S-phase (Figure 1.5) (Bertoli et al., 2013, Kastan and Bartek, 2004).

Further control of the G1/S transition is exerted by pRB through regulation of the E2F transcription factors. During early G1 phase, pRB binding of E2F proteins inhibits transcription of S-phase proteins. Phosphorylation of pRB under the influence of activated cyclin dependent kinase-4 (CDK4)/cyclinD complex, arising from cyclinD accumulation in response to mitogenic stimuli, results in the dissociation of pRB from E2F allowing E2F to initiate transcription of S-phase proteins (Molinari, 2000). Accumulation of p21(CIP1) also leads to inhibition of CDK4/cyclinD phosphorylation of pRB resulting in reduced E2F activity in the presence of DNA damage or replication stress (Dick and Rubin, 2013) A summary of the characteristics of the key G1/S cell cycle checkpoint proteins and their function at the G1/S transition is given in Table 1.2.

Protein Factors	Description	Function at the G1/S transition
ATM	<ul style="list-style-type: none"> PIKK serine/threonine kinases DNA damage sensor protein Principle activating DNA lesion is DSB 	<ul style="list-style-type: none"> Phosphorylates and activates CHK2 and p53 in response to DNA damage
CDK2	<ul style="list-style-type: none"> Cyclin dependent serine/threonine kinase Catalytic sub-unit of CDK2/cyclin complexes Activated by complexation with cyclins Activity regulated by p21(CIP1) mediated inhibition 	<ul style="list-style-type: none"> CDK2/Cyclin E complexation activates histone gene transcription Supports DNA replication through assembly of pre-replication complex and allows progression into S-phase
CHK2	<ul style="list-style-type: none"> Serine/threonine kinase DNA damage effector protein Principle activator is phosphorylation by ATM Key substrates include p53 and cdc25 phosphatases 	<ul style="list-style-type: none"> Phosphorylates and stabilizes p53 p53 accumulation results in increased transcription of p21(CIP1) p21(CIP1) inhibits CDK2/cyclin E complex function
E2F	<ul style="list-style-type: none"> Transcription factor family with key role at G1/S transition Binding to pRB prevents interaction with transcriptional machinery 	<ul style="list-style-type: none"> E2F activator factors mediate S-phase protein transcription and promote of S-phase entry
pRB	<ul style="list-style-type: none"> Pocket protein (allows functional binding of other proteins) Allows reversible suppression of DNA replication through binding of transcription factors 	<ul style="list-style-type: none"> pRB binding to E2F transcription factors inhibit E2F function: Transcription of S-phase proteins and promotion of entry to S-phase.
p21(CIP1)	<ul style="list-style-type: none"> ATP competitive inhibitor of CDK/cyclin protein complex Primary mediator of p53 induced cell cycle arrest 	<ul style="list-style-type: none"> P21(CIP1) binding to CDK2/cyclin E complex inactivates its kinase activity Inactive CDK2/cyclin E prevents progression to S-phase
p53	<ul style="list-style-type: none"> Transcription factor with key role in regulation of cell cycle progression Interaction (phosphorylation) with ATM and CHK2 in response to DNA damage results in accumulation of p53 	<ul style="list-style-type: none"> Phosphorylated form acts as transcription factor for p21(CIP1) Transcription of p21(CIP1) leads to inhibition of CDK2/cyclin E complex function

Table 1.2 Key cell cycle factors associated with the G1/S cell cycle checkpoint.

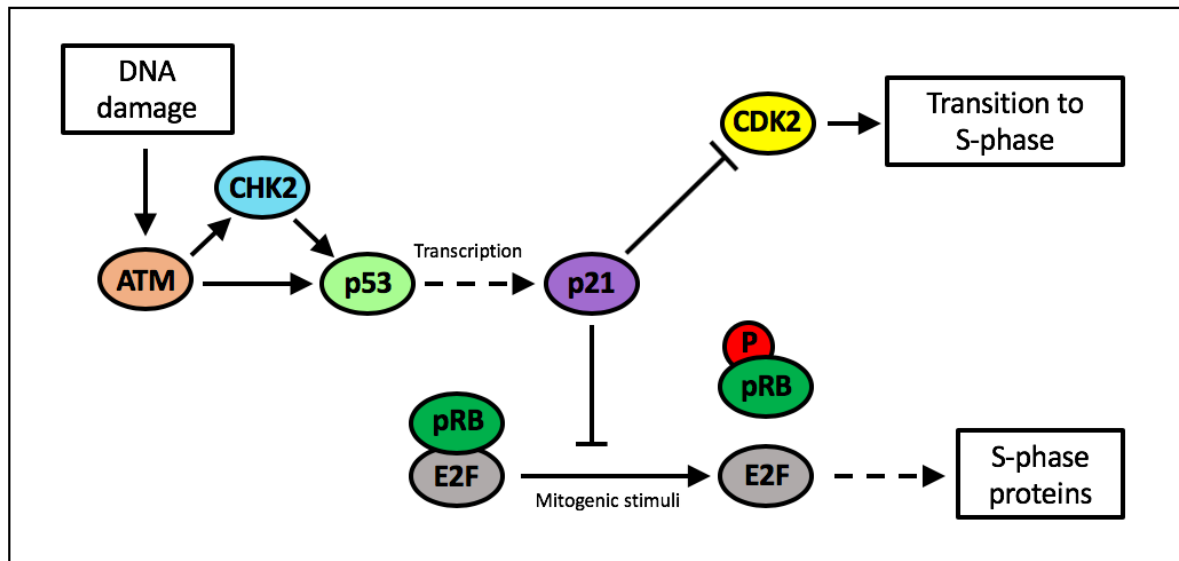


Figure 1.5 p53 and pRB at the G1/S cell cycle checkpoint.

Activation of p53 resulting from phosphorylation by both ATM and CHK2 (and to a lesser extent, ATR and CHK1, not shown) results in increased transcription of p21(CIP1) and inhibition of CDK2 mediated promotion of transition to S-phase. This pathway interacts with the pRB controlled transcription of S-Phase proteins, needed for DNA synthesis by the E2F transcription factors via inhibition of pRB phosphorylation and dissociation from E2F by p21(CIP1).

1.3.2 High-risk HPV interaction with p53 and pRB

The most important feature associated with HR-HPV subtypes is the ability of viral proteins E6 and E7 to interact with and disrupt the activity of the tumour suppressor gene products: p53 and pRB. The vast majority of cervical cancers express wild-type p53 and pRB and it is thought that functional depletion of these proteins by E6 and E7 and the resulting loss of G1 checkpoint control is key to carcinogenesis in HPV associated cervical cancer (Munger et al., 1992). The loss of G1/S checkpoint function as a key inducer of cervical squamous carcinoma and adenocarcinoma is supported by the observation of mutated p53 and pRb in HPV negative cervical cancer cell lines (section 1.2.1).

Viral protein E6 interacts with a cellular protein known as E6 associated protein (E6AP). Following binding, E6AP catalyses degradation of p53 by multi-ubiquitination. E6AP is a prominent member of the HECT (homologous to E6AP C Terminus) E3 ubiquitin ligase family (Huibregtse et al., 1995): enzymes which mediate recognition of proteins targeted for degradation by the ubiquitin proteasome pathway (Livneh et al., 2016). The exact nature of the interaction between E6, E6AP and p53 is not clear, however recent evidence suggests that E6 binding of E6AP induces a conformational change in the protein-substrate complex allowing p53 access to the catalytic site of E6AP, facilitating ubiquitin transfer (Sailer et al., 2018). Though low-risk HPV E6 may bind E6AP, the degradation of p53 by activated E6AP appears to be an exclusive property of E6 from HR-HPV subtypes (Tommasino et al., 2003, Thomas et al., 1999).

Stable complex formation between HPV viral protein E7 and pRB is thought to interfere with CDK4/cyclinD phosphorylation of pRB when bound to E2F transcription factors (Songcock et al., 2017), resulting in reduced free E2F and therefore inhibition of transcription of key S-phase proteins in late G1 phase. Though this property of E7 appears to be consistent across multiple sub-types of human papilloma viruses, the affinity of E7 from low-risk HPV subtypes for human pRB has been shown to be considerably lower than that for E7 from HPV-16 and HPV-18, the most commonly identified HR-HPV sub-types detected in cervical cancer (Munger et al., 1989).

Deficiency in G1/S checkpoint control by mutation or loss of either p53 or pRB are thought to be one of the most common defects in cancer cells (Massague, 2004). These defects, however open therapeutic opportunities through manipulation of the S-phase and G2/M checkpoints on which the cell has become reliant to prevent mitotic catastrophe (Curtin, 2012). Targeting the checkpoint kinases ATR, CHK1 and WEE1 on whose function these checkpoints rely provides such a therapeutic opportunity.

1.4 The DNA damage response and the ATR-CHK1-WEE1 axis

DNA damage occurs continuously, with an estimated $10^4 - 10^5$ lesions per cell per day caused by products of normal cell functions (Hoeijmakers, 2001). Endogenous lesions such as abasic sites and base transitions, caused by depurination or cytosine deamination,

respectively as well as methylations and oxidative lesions account for the majority of these (Ciccia and Elledge, 2010). Environmental DNA damage may also result in a heavy burden for the cell through, for example, UV radiation induced pyrimidine dimers and 6-4 photoproducts (Hoeijmakers, 2001).

As well as the elimination of cells with irrevocably damaged DNA by apoptosis, and interruption of the cell's progression through the cell cycle via activation of DNA damage checkpoints (Chapter 1.2), the cell's response to DNA damage includes the removal of lesions through lesion-specific DNA repair pathways (Table 1.2) (Sancar et al., 2004). These three interconnected processes are collectively referred to as the DNA damage response (DDR). The DNA damage response is characterised by the presence and activity of detector, signalling and effector proteins in coordinated pathways that lead to the induction of DNA repair and checkpoint engagement. ATR recruitment to sites of DNA damage and the subsequent signalling of this damage to the cells DDR machinery is one such pathway. The ATR-CHK1-WEE1 pathway not only signals to checkpoint activation, as described in Chapter 1.3, but also to a number of DNA repair pathways. The following section briefly describes DNA repair pathways. This is followed by an overview of ATR-CHK1-WEE1 activation, their roles at the intra-S and G2/M cell cycle checkpoint and finally, ATR-CHK1 signalling in DNA repair

1.4.1 DNA repair pathways

A summary of the principal described DNA repair pathways, the lesions that they repair and examples of endogenous, environmental and therapeutic inducers of those lesions are given in Table 1.3. Replication errors, resulting from mis-incorporation of bases into the DNA strand, base deletions or insertions are dealt with by mismatch repair (Jiricny, 2006). The simplest lesions, resulting from S-adenosyl-methionine (SAM) methylation or alkylation of guanine are directly repaired by DNA methyltransferase (MGMT) demethylation (Curtin, 2012). Base modifications, reactive oxygen species (ROS)-induced oxidation (e.g. 8-OHdG), methylation and deamination (dC to dU) are repaired by base excision repair (BER), which includes base removal, SSB generation and the downstream

pathway of SSB repair. SSBR can also act on frank SSB (e.g .ROS or IR-induced) or topoisomerase I-linked lesions (Curtin, 2012, Wallace, 2014).

DNA double strand breaks (DSB) are less numerous though more toxic to the cell than SSBs. DSBs also occur as a result of ROS induced damage, directly or through a failure to repair SSBs. Therapeutic induction of DSBs commonly occurs through the use of topoisomerase II (TOPOII) poisons, or antimetabolites that cause collapsed replication forks and ionising radiation (Curtin, 2012). The cell is reliant on two pathways for the restoration of DNA integrity in the face of DSBs. Non-homologous end joining (NHEJ) accounts for the repair of the majority of lesions in all phases of the cell cycle but predominates in G0 and G1 phase (Shrivastav et al., 2008). NHEJ is rapid and not without error (Mahaney et al., 2009). In G2 and M-phase, where a template strand of DNA is available, DSBs may be repaired by homologous recombination repair (HRR). HRR is a highly complex process that results in high fidelity re-synthesis of the damaged segment of DNA (Shrivastav et al., 2008).

Platinum exposure results in the formation of bulky DNA adducts, which along with intra-strand crosslinks, UV induced 6-4 photoproducts (6-4PPs) and damage resulting from aromatic hydrocarbon exposure are repaired by the nucleotide excision repair (NER) pathway (Marteijn et al., 2014). Along with these helix distorting adducts, exposure to platinum agents also results in inter-strand crosslinks. NER shares components with and contributes to inter-strand crosslink (ICL) repair (Deans and West, 2011). The role and contribution of the ATR-CHK1 pathway in DNA repair will be further discussed in Chapter 1.4.4.

Repair pathway	Lesions repaired	Endogenous insults	Environmental insults	Therapeutic insults
Direct repair	O ⁶ -methylguanine	S-adenosyl-methionine (SAM)	Nitrosamines Bile acids	Temozolomide (TMZ) Alkylating agents
BER/SSBR	Single strand break 8-oxoguanine Uracil	SAM Reactive oxygen species (ROS) Trapped topoisomerase I (TOPOI) Base deamination	Ionising radiation (IR)	TMZ IR TOPOI poisons Antimetabolites
NER	6-4 photoproducts (6-4PP) Cyclopurines Bulky adducts	ROS	Ultraviolet radiation (UV) Tobacco smoke	Cisplatin Carboplatin
NHEJ	Double strand breaks (DSB)	IR Trapped topoisomerase II (TOPOII)	ROS	IR TOPOI poisons
HRR	DSB Stalled replication forks	Unrepaired SSB	IR	TMZ TOPOI poisons Anti-metabolites
ICL repair	ICL	Malonic dialdehyde	Acrolein Crotonaldehyde	Cisplatin Carboplatin Mitomycin C
MMR	Base mismatch	Replication errors SAM	-	TMZ Nucleoside analogues

Table 1.3 Principal described DNA repair pathways, activating lesions and causative agents or insults

Table is derived from Curtin 2012 and gives examples of endogenous and environmental agents which may give rise to lesions repaired by the specific DNA repair pathways listed. Therapeutic insults refer to commonly used DNA damaging cancer therapies.

1.4.2 ATR-CHK1-WEE1 activation

ATR is a phosphatidyl inositol 3' kinase-related kinases (PIKK) family member that is closely related in structure to ATM, another DNA damage sensing kinase that has considerable crossover in signalling function with ATR (Figure 1.3) (Maréchal and Zou, 2013). ATR is activated by the presence of single stranded DNA (ssDNA) that arises at stalled replication forks (Figure 1.4) or DNA damage repair pathway intermediates such as nucleotide excision repair (NER) intermediates and resected double strand breaks (DSB) (Figure 1.6) (MacDougall et al., 2007, Cimprich and Cortez, 2008). The scale of ATR activation may be proportional to the amount of ssDNA present, signalled through increasing complexation of replication protein-A (RPA) with the exposed ssDNA lengths (Choi et al., 2010).

ATR interacting protein (ATRIP) localises ATR to the ssDNA-RPA complex (Cortez et al., 2001, Ball et al., 2007). RPA-ssDNA complexation also results in the RAD-17 mediated recruitment of the heterotrimeric ring complex: 9-1-1 comprised of RAD9-RAD1-HUS1. The 9-1-1 complex recruits DNA-topoisomerase-2-binding protein-1 (TOPBP1) to the site of DNA damage. The

recruitment of TOPBP1 appears to be a crucial step in ATR activation and subsequent phosphorylation events (Burrows and Elledge, 2008, Shiotani and Zou, 2009). Following activation by TOPBP1, ATR phosphorylates its main effector kinase, checkpoint protein 1 (CHK1).

ATR activates CHK1 by phosphorylation at two serine residues (S317 and S345) in a claspin dependent reaction (Walworth and Bernards, 1996, Walworth et al., 2000, Liu et al., 2000). Claspin transiently localises CHK1 to the site of DNA damage following recruitment by phosphorylated-RAD17 (Liu et al., 2006, Kumagai and Dunphy, 2000). RAD17 is phosphorylated by ATR following ATR localisation at the DNA damage site (Wang et al., 2006). Following activation, CHK1 dissociates from the nuclear chromatin, signalling the DNA damage to ATR-CHK1 dependent checkpoint reactions and DDR pathways (Smits and Gillespie, 2015).

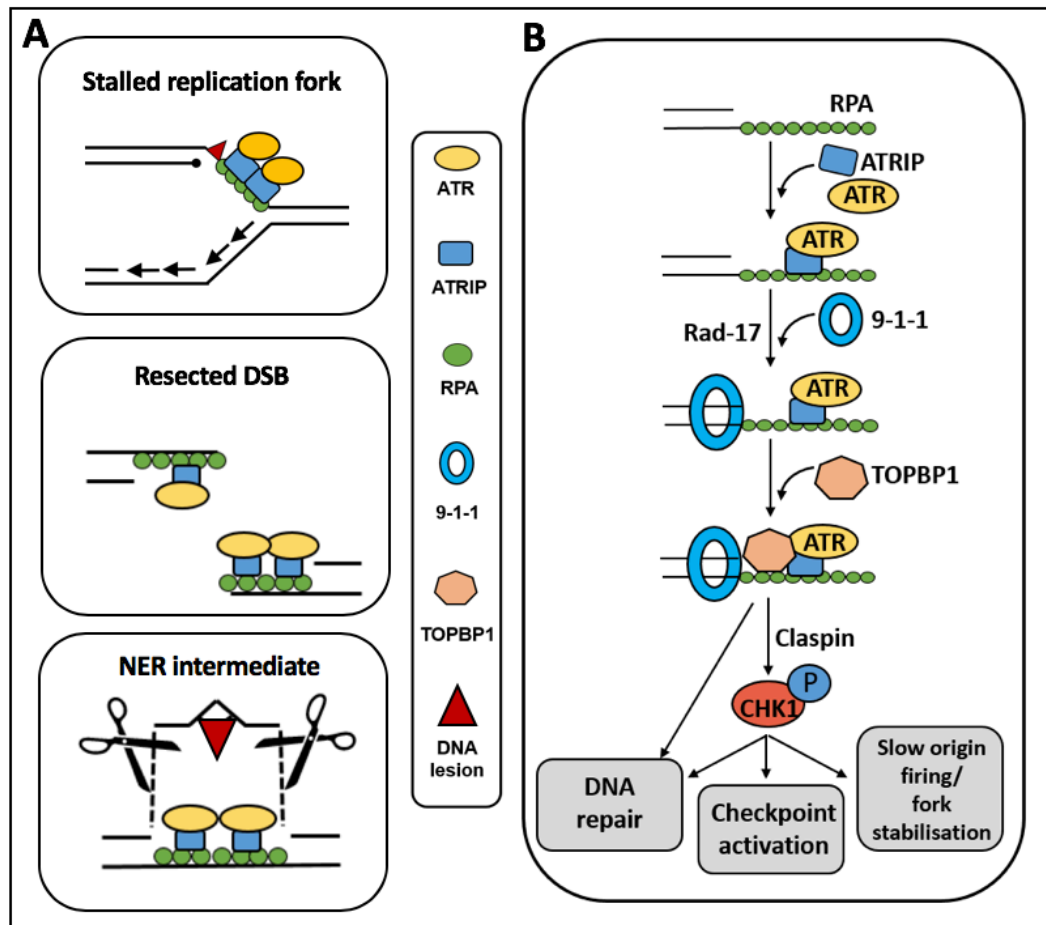


Figure 1.6 ATR recruitment and activation at stalled replication forks and sites of DNA damage and repair.

A: Lesions that activate ATR are stalled replication forks, resected DSBs and NER intermediates. All lesions have the presence of ssDNA in common, which complexes with RPA and recruits ATR to the lesion via ATRIP. **B:** The ssDNA-RPA complex also recruits 9-1-1 and TOPBP1 to the damage site. TOPBP1 mediated ATR activation results in CHK1 phosphorylation and activation of the downstream, DDR effects of ATR activation. Figure derived from Rundle et al, 2017.

1.4.3 ATR, CHK1 and WEE1 at the Intra-S and G2/M checkpoints.

Following activation of ATR and CHK1 at sites of DNA damage, during DNA repair or through replication stress characterised by stalled replication forks, phosphorylation of CHK1 substrates may result in arrest in S-phase or at the G2/M transition. Important CHK1 phosphorylation targets are WEE1 and the cell division cycle (cdc) proteins: cdc25A and cdc25C. WEE1 activation results in direct inhibitory phosphorylation of cyclin dependent kinase 1 (CDK1) and CDK2 at threonine14/tyrosine15. CHK1 phosphorylation of cdc25 phosphatases targets these proteins for degradation, resulting in a reduction in the removal

of the inhibitory phosphorylations from CDK1/2. The combined effect is one of a reduction in CDK activity (Figure 1.7) (Sorensen and Syljuasen, 2012).

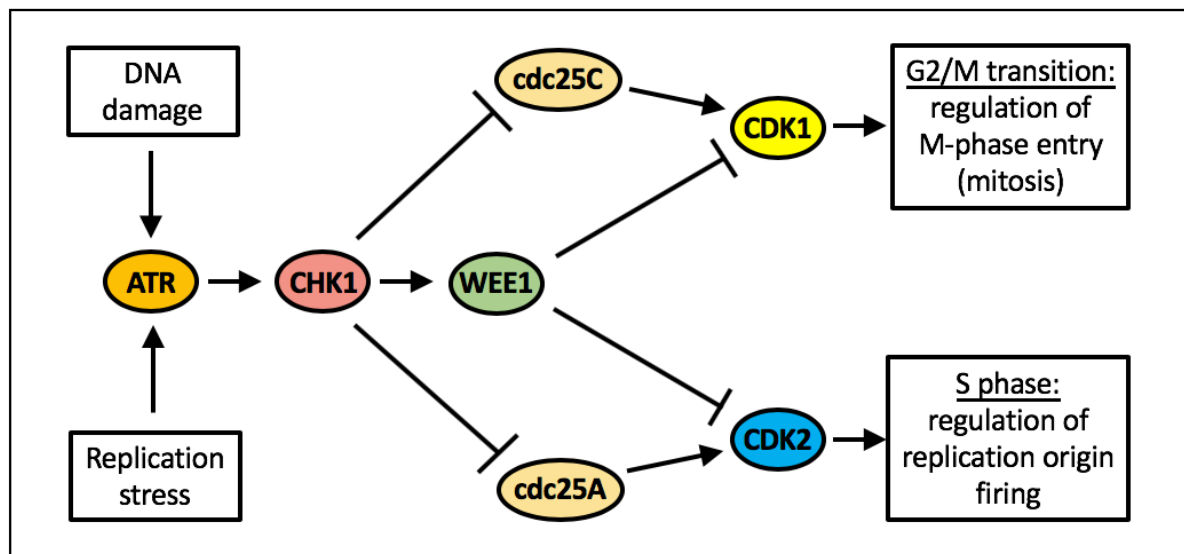


Figure 1.7 The regulation of CDK activity by ATR, CHK1 and WEE1.

CDK phosphorylation at tyrosine 15 results in negative regulation of cell cycle progression at the G2/M transition and negative regulation of replication origin firing in S-phase. DNA damage or replication stress signalled through ATR activation results in CHK1 phosphorylation of WEE1 and the cdc25 phosphatases. Activated WEE1 phosphorylates CDK1/2, inhibiting M-phase entry and replication origin firing. CHK1 phosphorylation of cdc25A/C targets these proteins for degradation, reducing CDK dephosphorylation.

In S-phase, CDK2 activity initiates replication origin firing. Inhibition of CDK2 by phosphorylation (maintained through the combined effects of CHK1 mediated inhibition of the phosphatase cdc25A and WEE1 kinase activation) therefore reduces the accumulation of stalled replication forks and the depletion of nucleotides in the face of DNA lesions that prevent replication fork progression (Beck et al., 2012, Parsels et al., 2018). This effectively prevents the cell from progressing through S-phase, resulting in S-phase arrest. Active CDK2 is a key protein in the pathway for the loading of cdc45L and co-factors onto the nuclear chromatin and the subsequent binding of helicase and DNA polymerase- α (pol- α) that is required for replication initiation (Zheng et al., 2017). In addition to contributing to the inhibition of new replication origin firing, ATR and CHK1 appear to have important roles in the stabilisation of stalled replication forks, preventing replication fork collapse and thus

further reducing DNA-damage induced replication stress (Paulsen and Cimprich, 2007, Friedel et al., 2009).

At the G2/M checkpoint, CHK1 phosphorylation of WEE1 and cdc25C results in inhibition of CDK1 through the maintenance of the inhibitory phosphorylation at tyrosine residue 15: CDK1(Y15) (Mueller and Haas-Kogan, 2015). Arrest at the G2/M transition prevents entry of the cell to mitosis. This action then, prevents either the permanent loss or disruption of genetic information through passage to daughter cells, or in the case of major DNA damage, immediate mitotic catastrophe (Sorensen and Syljuasen, 2012, Chen et al., 2003, Dai and Grant, 2010) A summary of the characteristics of the key G2/M and intra-S cell cycle checkpoint proteins and their function through S-phase and at the G2/M transition is given in Table 1.4.

Protein Factors	Description	Function in S-phase and at the G2/M transition
ATR	<ul style="list-style-type: none"> PIKK serine/threonine kinases DNA damage sensor protein Principle activator is single stranded DNA associated with lesions characterised by replication stress 	<ul style="list-style-type: none"> Phosphorylates and activates CHK1 in response to DNA damage
CDK1	<ul style="list-style-type: none"> Cyclin dependent serine/threonine kinase Catalytic sub-unit of CDK1/cyclin A complexes Activated by complexation with cyclins Target of cdc25C phosphatase and WEE1 	<ul style="list-style-type: none"> Active CDK1/cyclin A regulates entry to mitosis by regulating mitotic events at the centrosome
CDK2	<ul style="list-style-type: none"> Cyclin dependent serine/threonine kinase Catalytic sub-unit of CDK2/cyclin A complexes Activated by complexation with cyclins Target of cdc25A phosphatase and WEE1 	<ul style="list-style-type: none"> In S-phase CDK2 disassociates from cyclin E and associates with cyclin A CDK2/cyclin A regulates DNA replication through regulation of DNA replication origin firing
cdc25A/C	<ul style="list-style-type: none"> Protein tyrosine phosphatases Activated by CHK1 phosphorylation in response to DNA damage and replication stress 	<ul style="list-style-type: none"> cdc25C removes inhibitory phosphorylations in the CDK1 active site allowing activity of CDK1/Cyclin A and entry to mitosis (M-phase) cdc25A removes inhibitory phosphorylations in the CDK2 active site allowing activity of CDK2/cyclin A and progression through S-phase
CHK1	<ul style="list-style-type: none"> Serine/threonine kinase DNA damage effector protein Principle activator is phosphorylation by ATM Key substrates include WEE1 kinase and cdc25 phosphatases 	<ul style="list-style-type: none"> Phosphorylation of WEE1 Phosphorylation of cdc25 proteins targets these for degradation Combined effect is to down-regulate CDK/cyclin mediated cell cycle progression
WEE1	<ul style="list-style-type: none"> Serine/threonine kinase DNA damage effector protein Principal activator is phosphorylation by CHK1 Key substrates include CDK/cyclin complexes 	<ul style="list-style-type: none"> Phosphorylation of target sites in CDK1/2 active sites prevents CDK/cyclin mediated M-phase entry and DNA replication origin regulation

Table 1.4 Key cell cycle factors at the intra-S and G2/M DNA damage cell cycle checkpoints

1.4.4 ATR, CHK1 and WEE1 in DNA repair

The removal of DNA lesions and restoration of DNA integrity is performed by discreet DNA repair pathways that are largely dependent on the nature of the DNA lesion and therefore, the causative insult or DNA damaging agent as described in section 1.4.1 (Table 1.3). Current therapies for cervical cancer: platinum chemotherapy and ionising radiation cause different DNA lesions that are repaired by different pathways.

In addition to its role in DNA damage checkpoint reactions, ATR and its associated downstream kinase: CHK1 play important roles in a number of DNA repair pathways. These include a role for ATR in the regulation of recruitment of key proteins to the Fanconi anaemia pathways for inter-strand crosslink repair (Shigechi et al., 2012, Andreassen et al., 2004) and also to nucleoside excision repair (NER) (Wu et al., 2007).

DNA damaging agent	DNA lesion	DNA repair pathway
Methylation	O ⁶ -methylguanine	Direct repair by DNA methyltransferase (MGMT)
Alkylation Deamination Oxygen radicals	Apyrimidinic sites 8-oxoguanine Single strand breaks (SSB)	Base excision repair (BER) Single strand break repair (SSBR)
Ultraviolet radiation (UV)	6-4 photoproducts (6-4PP) Cyclobutane-pyrimidine dimer (CPD)	Nucleotide excision repair (NER)
Polycyclic hydrocarbons	Bulky base adducts	
Platinum agents	Intra-strand crosslinks	
	Inter-strand crosslinks	Inter-strand crosslink (ICL) repair
Ionising radiation (IR)	Double strand breaks (DSB) + SSB	BER/SSBR Non-homologous end joining (NHEJ) Homologous recombination repair (HRR)
Replication errors	Base mismatch	Mismatch repair

Table 1.5 DNA damaging agents, lesions and repair pathways.

DNA damaging agents cause distinct DNA lesions that are repaired through specific repair pathways. Table derived from Hoeijmakers 2001.

ATR, CHK1 and WEE1 are also involved in the regulatory mechanisms of homologous recombination repair (HRR), an important repair pathway for lesions associated with both cisplatin and ionising radiation (IR) treatment. ATR phosphorylates and activates the key HRR regulatory protein BRCA1 (Tibbetts et al., 2000), whilst CHK1 is involved in the recruitment and activation of BRCA2 and RAD51 recombinase (Sorensen et al., 2005) (Figure 1.8). Cells treated with ATR or CHK1 inhibitors show reductions in HRR function by RAD51 foci assays in response to hydroxyurea or gemcitabine induced replication stress (Parsels et al., 2009, Morgan et al., 2010, Peasland et al., 2011). A coupling of the HRR and checkpoint signalling roles of ATR has recently been described. ATR inhibits cyclin dependent kinases (CDKs) at the cell cycle checkpoint through phosphorylation of CHK1 and subsequently of

WEE1 (section 1.3.2). Evidence now exists to suggest that CDK inhibition also promotes HRR function (Buisson et al., 2017).

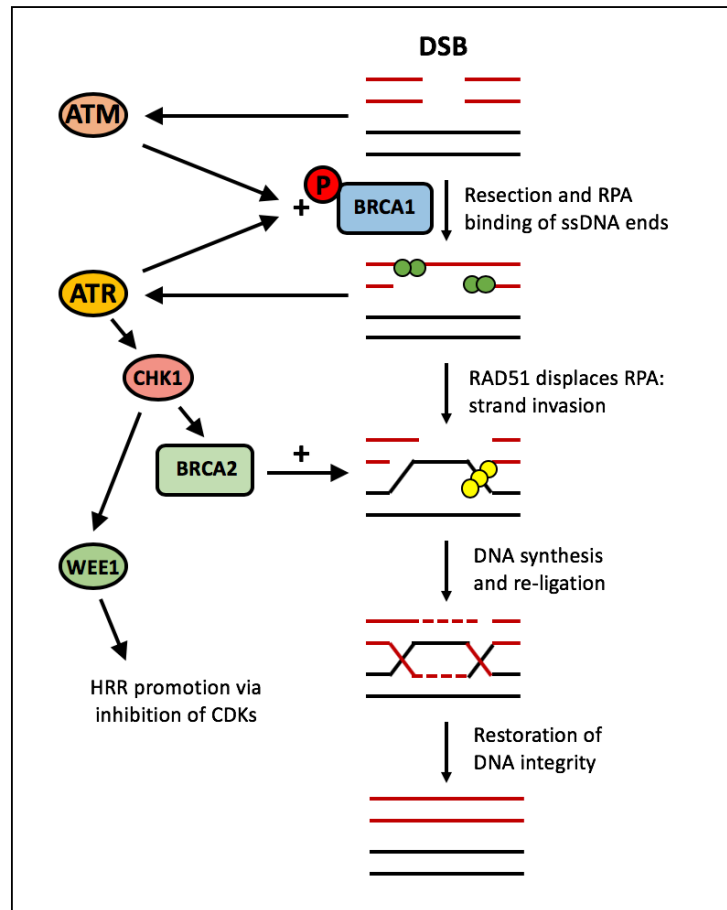


Figure 1.8 Simplified schematic diagram of the role of ATR, CHK1 and WEE1 in homologous recombination repair (HRR).

BRCA1 phosphorylation by ATM and ATR is a key step in the initiation of HRR. ATR further promotes HRR function through activation of CHK1, which has a role in the recruitment and activation of BRCA2. BRCA2 is necessary for RAD51 recruitment. CHK1 activation of WEE1 and subsequent CDK inhibition further promotes HRR function.

1.5 ATR, CHK1 and WEE1 inhibitors

1.5.1 Target validation by genetic downregulation

Homozygous disruption of ATR or CHK1 or WEE1 is incompatible with life at an early embryonic stage, highlighting the importance of the pathway (Brown and Baltimore, 2000, Takai et al., 2000). Seckel syndrome, a human genetic condition caused by reduced expression of ATR secondary to a hypomorphic mutation of the ATR gene is characterised by growth retardation and microcephaly, but not increased carcinogenesis (O'Driscoll et al., 2003). Kinase-dead ATR cells, where an inactive form of the kinase acts as a negative inhibitor to native ATR function have been shown to be sensitive to DNA damaging agents (Cliby et al., 2002, Nghiem et al., 2001) including IR and platinum and failed to arrest at the G2/M checkpoint (Cliby et al., 1998).

CHK1 knockdown by small interfering RNA (siRNA) or short hairpin RNA (shRNA) also sensitises cells to a variety of DNA damaging agents (Carrassa et al., 2004, Flatten et al., 2005, Ganzinelli et al., 2008, Pan et al., 2009, Azorsa et al., 2009). However, unlike ATR knockdown, the results are less convincing for sensitisation of platinum agents: for example, CHK1 downregulation failed to sensitise HCT-116, HeLa or U2OS cells to cisplatin (Wagner and Karnitz, 2009). Genetic downregulation or knockdown of WEE1 has been reported to increase cell susceptibility to DNA damage by exogenous DNA damaging agents and also to result in increased apoptotic cell death in p53 deficient cervical cancer cell lines through G2/M checkpoint abrogation (Pappano et al., 2014, Wang et al., 2004), though studies are fewer in number than those for ATR and CHK1.

It has been suggested that the downregulation of ATR, CHK1 or WEE1 sensitises p53 deficient cells to a greater extent than cells with normal p53 function (Pan et al., 2009, Ganzinelli et al., 2008) and that targeting the ATR-CHK1-WEE1 pathway would lead to greater effects in p53-mutant tumours. However, this has been contradicted in some studies: siRNA downregulation of ATR has been observed to be equally efficacious as a sensitiser of U2OS p53-wild type and HeLa p53-defective cells to the topoisomerase I poisons camptothecin and SN-38 (Flatten et al., 2005). In addition, CHK1 downregulation by

siRNA caused similar sensitisation of paired p53-wild type and p53-defective U2OS cells to irinotecan and cisplatin (Zenvirt et al., 2010). Furthermore, in U2OS cells with G1-checkpoint deficiencies caused by other abnormalities (cyclin D1, cyclin E1, MDM2 or CDK2 overexpression or infection by HPV) ATR knockdown resulted in sensitisation to DNA damage that was reversed by p21 or p27 induced expression (Nghiem et al., 2001). Overall, it is likely that G1/S checkpoint deficiency, rather than p53 status is a key determinant of sensitivity to downregulation of ATR, CHK1 or WEE1 function. A similar pattern of results is seen when the enzymes are inhibited by specific, potent small molecule inhibitors.

1.5.2 Development of ATR, CHK1 and WEE1 inhibitors

The potent and selective kinase inhibitors targeting ATR, CHK1 and WEE1 that have been developed for clinical use (listed in Table 1.6) are reversible, ATP competitive inhibitors. These molecules bind to the target principally through hydrogen bond formation between the inhibitor molecule and residues within the ATP binding pockets of the kinases (Knight and Shokat, 2005). A common feature of the inhibitor molecules is a hydrophobic tail which, following binding interacts with the catalytic sites on the enzyme. This interaction prevents conformational changes that are required for activation and cycling of the target enzyme (Roskoski, 2015).

Early inhibitors of ATR and CHK1, such as UCN-01 were initially developed with other targets in mind and consequently showed poor selectivity and potency against these enzymes (Senderowicz, 2000). More recently, potent and selective inhibitors have been developed, though the development of WEE1 inhibitors has lagged behind that of ATR and CHK1 inhibitors. A number of these compounds, with a focus of those for which significant pre-clinical data is available are detailed in Table 1.3 and their development is described herein.

ATR inhibitor development

Caffeine was amongst the first natural product observed to inhibit ATR, sensitising cells to UV induced DNA damage (Sarkaria et al., 1999). However, other DDR enzymes including ATM and DNA protein kinase catalytic subunit (DNA-PKcs) are also inhibited by caffeine and its

potency against ATR is much less than that seen for more modern inhibitors (ATR IC₅₀ = 1.1 mM). Schisandrin B was another naturally occurring compound that was identified as a potent ATR inhibitor (ATR IC₅₀ = 7.3 µM). It is much more specific for ATR than caffeine making abrogation of UV induced G2/M checkpoint induction much more readily attributable to inhibition of ATR (Nishida et al., 2009).

Amongst the first novel compounds, NU6027 was found to be a more potent inhibitor of ATR than of its intended developmental target, CDK2 (Peasland et al., 2011). The first highly specific and potent ATR inhibitor identified with this target in mind was ETP-46464, which was identified by screening a pool of PI-3K inhibitors (likely to be enriched for ATR inhibitors due to the similarities between the two PIKK enzyme family members), utilising a screening platform specific for ATR inhibition (Toledo et al., 2011). Poor pharmacokinetics, however prevented its development into a clinical candidate.

Further ATR specific screening assays enabled the identification of precursors to the related aminopyrazine compounds VE-821 and VE-822 (Charrier et al., 2011, Fokas et al., 2012). Both compounds show >100-fold selectivity for ATR versus other DDR kinases such as ATM and DNA-PKcs and have extensive pre-clinical data related to them in anti-cancer investigations. Favourable toxicological profiles and pre-clinical *in vivo* performance have led to VE-822 being introduced into clinical trials as VX-970 (Fokas et al., 2012, O'Carrigan B, 2016). Another screen using compounds with structural similarities to known PIKK inhibitors led to the development of a series of morpholone compounds into AZ20 (Foote et al., 2013) and AZD6738 (Vendetti et al., 2015). AZ20 development was limited by its poor aqueous solubility but AZD6738 progressed to clinical trials as an orally bioavailable drug.

ATR inhibitors		
Name	IC ₅₀ /Ki	Specificity
NU6027	ATR IC ₅₀ = 1 nM	ATR, CDK1 (Ki = 2.5 <u>uM</u>), CDK2 (Ki = 1.3 <u>uM</u>)
ETP-46464	ATR IC ₅₀ = 25 nM	ATR
VE-821	ATR IC ₅₀ = 26 nM	>100-fold ATR vs ATM/DNA-PK
VE-822/VX-970	ATR IC ₅₀ = 0.2nM	>100-fold ATR vs ATM/DNA-PK
AZ20	ATR IC ₅₀ = 5 nM	>600-fold ATR vs ATM/DNA-PK/PI-3K
AZD6738	ATR IC ₅₀ = 1nM	ATR
CHK1 inhibitors		
Name	IC ₅₀ /Ki	Specificity
AZD7762	CHK1 IC ₅₀ = 5 nM	Equally potent: CHK1/CHK2
V158411	CHK1 IC ₅₀ = 4.4 nM	Equally potent: CHK1/CHK2
PF-477736	CHK1 Ki = 4.9 nM	100-fold CHK1 vs CHK2
MK-8776/SCH900776	CHK1 IC ₅₀ = 3 nM	500-fold CHK1 vs CHK2
CCT244747	CHK1 IC ₅₀ = 8 nM	>1000-fold CHK1 vs CHK2
CCT245737/SRA-737	CHK1 IC ₅₀ = 1.3 nM	>1500-fold CHK1 vs CHK2
LY2603618	CHK1 IC ₅₀ = 7 nM	>1500-fold CHK1 vs CHK2
WEE1 inhibitors		
Name	IC ₅₀	Specificity
AZD1775/ MK-1775	WEE1 IC ₅₀ = 5.2 nM	WEE1

Table 1.6 Potent and specific small molecule inhibitors of ATR, CHK1 and WEE1.

Inhibitors for which there is considerable pre-clinical data available are given, along with the chemical group to which they belong and data supporting their specificity for the target enzyme. Table is adapted from Rundle et al. 2017.

CHK1 inhibitor development

Structure based drug design led to the development of AZD7762 from a thiophene carboxamide urea compound identified in high throughput screening (Oza et al., 2012). Like the similarly developed compound, V158411 (Massey et al., 2015) these small molecule inhibitors show dual CHK1 and CHK2 inhibitor activity with greater CHK1 selectivity in cell-based assays. Truly selective CHK1 inhibitors were first seen with the development of PF-477736 (Blasina et al., 2008) and the pyrazole compound SCH900776 (now known as MK-8776) (Guzi et al., 2011), which show a 100-fold and 500-fold selectivity for CHK1 over CHK2, respectively (Matthews et al., 2013). Extensive pre-clinical data is available for both drugs though detailed descriptions of their development are limited.

A number of pyrazine compounds have been developed and described as potent and specific inhibitors of CHK1: high throughput and virtual screening for fragment hits, followed by structure-based drug design led to the development of CCT244747 and CCT245737 (Walton et al., 2012, Walton et al., 2016). These compounds show over 1000-fold selectivity for CHK1 over CHK2 and were the first orally bioavailable CHK1 inhibitors. CCT245737 has now entered clinical trials as SRA-737. A further pyrazine derived compound, LY2603618 and its follow-on drug LY2606368 also show >1000-fold selectivity for CHK1 and the latter has also entered clinical trials (King et al., 2014, Hong et al., 2016).

WEE1 inhibitor development

The development of clinically promising WEE1 inhibitors has been hindered by difficulties in establishing target specificity. Early WEE1 inhibitors such as the pyrido-pyrimidine derivative, PD0166285 or the pyrolo-carbazole derivative, PD0407842 were potent ($WEE1\ IC_{50} < 100\text{ nM}$) but non-selective. These compounds showed significant interference with other DDR targets such as MYT1 and CHK1 (Panek et al., 1997, De Witt Hamer et al., 2011). MK-1775 is a pyrazolo-pyrimidine derivative that is the first and so far, only potent selective inhibitor of WEE1 that has shown promise as a clinical candidate (Mizuarai et al., 2009, Hirai et al., 2009). Now known as AZD1775 or its commercial name: Adavertotib, it has been taken

forward into clinical trials and used in combinations including with platinum agents (Pillie et al., 2019).

1.6 Single agent activity and determinants of sensitivity for inhibition of the ATR-CHK1-WEE1 axis

1.6.1 Oncogene driven replication stress as a sensitiser to ATR, CHK1 or WEE1 inhibition

Whilst much attention is focussed on the ability of these potent and specific inhibitors of ATR, CHK1 and WEE1 to potentiate the cytotoxic effects of existing genotoxic chemotherapy treatments (section 1.6), investigations of the potential for existing characteristics of cancer cells to act as determinants of sensitivity are also described. Oncogene transformations, with particular focus on those which promote S-phase entry or result in increased levels of replication stress through loss of control of the G1/S cell cycle checkpoint have been shown to promote sensitivity to inhibition G2/M checkpoint manipulation by ATR-CHK1-WEE1 axis inhibition. A summary of this evidence is presented in Table 1.7.

Whilst the oncogene transformations that are detailed in Table 1.7 are rarely present in cervical cancer cells, the evidence presented supports the hypothesis that inhibitors of ATR, CHK1 and WEE1 are a potentially effective strategy as single agents against cervical cancer cells rendered G1/S checkpoint deficient through p53 or pRB insufficiency either by HPV driven degradation or by mutation.

Study	RS-inducer	Sensitiser	Effect
Murga et al. 2011	Myc overexpression	ATR hypomorphism	In-vivo: reduction in lymphoma rates in ATR deficient mice
		CHK1i (UCN-01)	In-vivo: tumour regression in Eμ-Myc mice (lymphoma model)
Gilad et al. 2010	Ras overexpression	ATR siRNA /shRNA knockdown	In vitro: reduction in cell doublings (MEF cells)
		ATR hypomorphism	In-vivo: Increased tumourigenesis (multiple sites)
Vendetti et al. 2015	K-Ras mutation	ATRi (AZD6738)	In-vitro: reduction in colony formation
Toledo et al. 2011	Cyclin E1 overexpression	ATRi (ETP46464)	In-vitro: increase in H2AX foci in MEF cells
Foot et al. 2013	K-Ras mutation	ATRi (AZ20)	In-vivo: growth inhibition in K-Ras mutated colorectal cancer xenografts
Morgado-Palacin et al 2016	N-Ras mutation	ATRi (AZ20)	In vivo: growth inhibition in N-Ras mutated AML xenografts
Williamson et al. 2016	ARID1A knockdown/mutation	ATRi (VE-821/VE-822)	In-vitro: increased toxicity in ARID1A knockdown cell lines. In-vivo: growth inhibition in ARID1A mutated colorectal cancer xenografts
Chen et al. 2018	Cyclin E1 overexpression	WEE1i(MK-1775)	In-vitro: increased toxicity of TNBC cell lines

Table 1.7 Studies describing replication stress inducing transformations that promote S-phase entry that evidence potential synthetic lethality with ATR, CHK1 or WEE1 inhibition.

The Oncogene is the mutation or transformation which renders the cell susceptible to ATR, CHK1 or WEE1 inhibition. The sensitiser is the mode of ATR, CHK1 or WEE1 inhibition or silencing used. ATRi = small molecule ATR inhibitor, CHK1i = small molecule CHK1 inhibitor and WEE1i = WEE1 small molecule inhibitor.

1.6.2 DDR abnormalities as determinants of sensitivity to ATR, CHK1 or WEE1 inhibition.

Exploiting the concept of synthetic lethality for cancer treatment is well described. In its simplest form, the simultaneous alteration of the function of two genes or proteins that, in isolation are not essential for cell viability, causes cell death. In the case of cancer treatment, if one of these genes represents an oncogene, tumour suppressor gene or oncogenic process/pathway that is dysfunctional in the cancer cell, the other may become a candidate for inhibition or knockdown. The result of endogenous dysfunction of one gene product plus inhibition of the other would result in selective killing of the cancer cell (Curtin, 2012, Lord and Ashworth, 2017).

The most commonly cited example of therapeutic synthetic lethality is the use of poly (ADP-ribose) polymerase (PARP) inhibitors (PARPi) to selectively kill cells that are HRR defective (Bryant et al., 2005, Farmer et al., 2005). The enzyme PARP1 is an essential component of the cell's response to endogenous or therapy induced SSB. PARP1 binding to DNA induces its catalytic function. This function synthesises negatively charged poly (ADP-ribose) chains on target proteins (PARylation), which acts as a recruitment signal for DNA repair effector proteins. Dissociation of PARP1 from the site of DNA damage occurs following auto-PARylation (Eustermann et al., 2015), however PARPi function to disrupt auto-PARylation, trapping PARP1 on the DNA double helix (Pommier et al., 2016). The result is disruption of PARP1 catalytic function, as well as the inability of the cell to process the DNA-PARP1 complex at the replication fork. Resolution of this lesion requires HRR function, involving BRCA1 and BRCA2 tumour suppressor genes. In cells that have defective BRCA1/2, HRR is also dysfunctional, leading to the inability to resolve the replication fork lesion and cell death (Lord and Ashworth, 2017).

ATR and CHK1 are crucial to the functioning of HRR and inhibition of these kinases has been shown to convey synthetic lethality in cells lacking BER function through knockdown of x-ray cross-complementing protein 1 (XRCC1) in a reversal of the situation described for PARP

inhibitors (Peasland et al., 2011, Sultana et al., 2013, Middleton et al., 2015). Defects in BER are relatively common in cancers and exploiting this through ATR pathway inhibition is a therapeutic option. Defects in HRR itself have also been shown to confer sensitivity to ATR, CHK1 and WEE1 inhibition: Chinese hamster ovary cells with inactivated XRCC3 or BRCA2 (both of which are involved in recruitment and function of RAD51 to HRR) resulted in increased sensitivity to the ATR inhibitor, VE-821 and inhibition of RAD51 itself conferred sensitivity to VE-821 and the CHK1 inhibitor AZD7762 (Middleton et al., 2015, Krajewska et al., 2015). In an siRNA screen for determinants to sensitivity to the WEE1 inhibitor MK-1775, HRR genes including RAD51, BRCA1 and BRCA2 increased sensitivity in short survival assays but validation in clonogenic survival assays was hindered by the effects of silencing the HRR genes themselves on cell viability (Aarts et al., 2015).

Other DNA repair related determinants of sensitivity to ATR and CHK1 inhibition include disruptions in non-homologous end joining (NHEJ), Fanconi anaemia (FA) and nucleotide excision repair (NER) pathways. Knockdown of the key nucleotide excision repair (NER) enzyme: excision repair cross-complementing protein 1 (ERCC1) and its co-factors has been shown to render cells sensitive to ATR and CHK1 inhibition, though the validity of this as a therapeutic strategy for NER deficient cancers is unclear as inactivation of other NER enzymes did not increase sensitivity to ATR or CHK1 inhibition (Mohani et al., 2014).

The NHEJ heterotrimer DNA protein kinase (DNA-PK) consists of the catalytic sub-unit DNA-PKcs, Ku70a and Ku80. High levels of DNA-PKcs expression have been correlated with sensitivity to ATR and CHK1 inhibition. In contrast to this, Ku80 depletion was observed to be associated with sensitivity to ATR inhibition with VE-821 (Middleton et al., 2015). Interestingly pRB has been reported to have a role in Ku protein stabilisation within the DNAPK complex in addition to its role in the G1/S cell cycle checkpoint (Cook et al., 2015, Huang et al., 2015). This may be an important factor when considering the sensitivity of cervical cancer cells to ATR inhibition given the effects of HR-HPV protein E7 on pRB function.

Isogenic cell line pairs differing in FA pathway function alone were differentially sensitive to pharmacological CHK1 inhibition with UCN-01 and another early CHK1 inhibitor GO6976,

with FA deficient cells showing the greater sensitivity. Confirmation that this relationship was valid *in vivo* was achieved using pharmacological CHK1 inhibition in FANCD2 knockdown zebra fish embryos (Chen et al., 2009). Knock down of FA pathway genes FANCM and BRIP1 also sensitised a variety of human cancer cell lines to WEE1 inhibition with MK-1775 (Aarts et al., 2015).

Finally, due the complimentary functions and close relationships between ATR and ATM in the DDR, it has been suggested that ATM deficiency may prove to be synthetically lethal with ATR inhibition. ATR inhibition by AZD6738 and VE-821 has shown selective cytotoxicity in ATM deficient cells and this was further confirmed in ATM deficient chronic lymphocytic leukaemia (CLL) xenografts (Kwok et al., 2016, Middleton et al., 2015). The mechanism of ATRi cytotoxicity in ATM deficient cells is proposed to involve a loss of ATM stimulated HRR function, and therefore reduced ability of the cell to resolve lesions arising from collapsed replication forks that result from the replication stress induced by ATR inhibition. Additionally, the combined loss of cell cycle control that results from defective or impaired ATR/CHK2 and ATM/CHK1/p53 pathways is likely to compound the sensitivity of the ATM deficient cell to ATR inhibition (Kwok et al., 2016).

1.7 Pre-clinical data: chemo-sensitisation and radio-sensitisation

Potent and selective inhibitors of ATR, CHK1 and WEE1 have been developed as outlined in the previous sections. These drugs have been extensively investigated with respect to their single agent cytotoxicity and as sensitisers of DNA damaging chemotherapy agents and IR (Rundle et al., 2017, Pilie et al., 2019). The following sections review the literature that describes the effects of these drugs for sensitising cancer cells, *in-vitro* and *in vivo*, with particular reference to potentiation of existing standard of care treatment in cervical cancer: platinum-based chemotherapy and IR.

1.7.1 Combinations with platinum chemotherapy agents

ATR inhibitors

ATR is activated by the single-stranded DNA fragments that arise from NER intermediates and at stalled replication forks, both of which arise as a result of inter- and intra-strand

crosslinks caused by platinum agents. ATR is also a key enzyme in the FANC/HRR DNA repair pathways that resolve inter-strand crosslinks, which also arise following platinum treatment (Eastman, 1990, Siddik, 2003, Demarcq et al., 1994). It is not surprising then, that potentiation of platinum agents by ATR inhibitors is widely reported. Caffeine mediated potentiation of cis-platin cytotoxicity through ATR inhibition and abrogation of the G2/M checkpoint was one of the earliest observations made regarding prototype ATR inhibitors (Roberts and Kotsaki-Kovatsi, 1986, Yazlovitskaya and Persons, 2003) and was a precursor to investigations using the more selective, specifically developed inhibitors.

The potent and selective ATR inhibitor, VE-821 caused a 10-fold potentiation of cisplatin cytotoxicity in p53-mutant or ATM deficient human colon cancer cells and showed synergistic activity in ATM-null fibroblasts in combination with cisplatin (Reaper et al., 2011, Teng et al., 2015). VE-822 (VX-970) showed promise as a potentiator of cisplatin in lung cancer cells with similar results seen in gemcitabine-VX-970 combinations (Hall et al., 2014). In this study, p53 deficient cells again showed the greatest potentiation of cisplatin by VX-970 but a significant potentiation was also seen with AZD6738 in a further panel of non-small cell lung cancer (NSCLC) cell lines with other DDR abnormalities including ATM deficiency and K-ras mutation (Vendetti et al., 2015). ETP-46464 increased the cytotoxic effects of cisplatin in a range of gynecological cancer cell lines including those derived from ovarian, endometrial and cervical cancers. These results were independent of p53 status (Teng et al., 2015).

VE-822 and AZD6738 have shown promise with respect to anti-tumour performance *in vivo* in combination with platinum, underlying their progression to clinical trials. VE-822 significantly enhanced the efficacy of cisplatin in mice xenograft models of lung cancer including complete tumour growth inhibition in three platinum insensitive models (Hall et al., 2014). Additionally, a complete response to combination treatment was observed in a cisplatin sensitive tumour, which was sustained for three weeks following cessation of treatment. AZD6738 combinations with cisplatin also resulted in significant tumour growth delay in NSCLC xenograft models in which neither AZD6738 nor cisplatin monotherapy was effective (Vendetti et al., 2015). No significant increase in toxicity was observed in these studies with ATR inhibitor versus cisplatin alone.

CHK1 inhibitors

There is inconsistency in the reported effects of CHK1 inhibitors as a strategy for potentiating platinum induced cytotoxicity and it is suggested that CHK1 activity is not required for resistance to cisplatin (Wagner and Karnitz, 2009). The CHK1/2 inhibitor AZD7762 reversed cisplatin resistance in a panel of p53 mutant NSCLC cell lines (Bartucci et al., 2012) and the same drug also reversed cisplatin resistance in a panel of clear cell ovarian cancer and p53 mutant head and neck squamous cell cancer (HNSCC) cell lines (Itamochi et al., 2014). AZD7762 also potentiated cisplatin toxicity in neuroblastoma cells lines that were G1 checkpoint deficient due to MDM2 amplification or p14 deletion as well as in p53 mutated cases. In this study, an effect was not seen in G1 checkpoint proficient cell lines (Xu et al., 2011).

In contrast to the above examples, MK-8776 failed to sensitise p53 mutated triple negative breast cancer (TNBC) cells to cisplatin (Montano et al., 2012) and whilst V158411 potentiated the effects of platinum agents in a number of cell line panels in a p53 dependent manner, the effects were substantially less than those reported in the same studies for gemcitabine potentiation (Bryant et al., 2014).

Perhaps due to the mixed results observed for CHK1 inhibitor potentiation of cisplatin, *in vivo* xenograft data is less extensive than for ATR inhibitors. Studies with AZD7762, however showed some encouraging results. Co-treatment of xenograft models of ovarian clear cell cancer showed with cisplatin and AZD7762 resulted in greater inhibitory effects than with cisplatin alone (Itamochi et al., 2014) and the same drug was also shown to significantly enhance tumour growth reduction versus cisplatin alone in a variety of NSCLC models with sustained effects being recorded for up to three weeks following treatment (Bartucci et al., 2012).

WEE1 inhibitors

Fewer reports exist of WEE1 inhibitors in combination with cisplatin or carboplatin. Much of the literature concerned with WEE1 potentiation of genotoxic agents focussed on combinations with anti-metabolites such as gemcitabine or cytarabine, where a p53

dependent sensitisation has been reported across a number of human cancer cell lines including in cervical cancer cell lines (Matheson et al., 2016). MK-1775 has, however been observed to potentiate cisplatin in medulloblastoma cells (Harris et al., 2014) and also increased sensitivity to cisplatin in combination with shRNA p53 knockdown in ovarian cancer cells, with no effect seen in cells with intact p53 (Hirai et al., 2009).

In vivo, MK-1775 potentiated carboplatin in cervical cancer xenografts and showed a reduction in tumour growth when combined with cisplatin in murine models of ovarian cancer (Hirai et al., 2009). As with the data for ATR and CHK1 inhibition, combinations with platinum agents do not appear to significantly alter the toxicity profiles compared to platinum treatment alone in these models and at the doses or concentrations used.

1.7.2 Combinations with ionising radiation

Ionising radiation, usually in combination with cisplatin is the most important treatment modality for locally advanced cervical cancer. IR causes a variety of DNA lesions (Table 1.2) that are potent inducers of the ATR mediated DNA damage response reactions. As such, ATR, CHK1 and WEE1 inhibitors have all been shown to be effective sensitisers of IR effects on tumour cells, *in-vitro* and *in vivo*.

ATR inhibitors

VE-821 has been shown to increase cell killing in combination with IR in a variety of human cancer cell lines, including those derived from cervical cancer, TNBC, HNSCC and colon cancer (Zhang et al., 2016, Pires et al., 2012). Following successful potentiation of IR in pancreatic cancer cells *in-vitro*, VE-822 enhanced tumour growth delay of both single fraction and fractionated IR in pancreatic ductal carcinoma xenografts without increasing toxicity (Fokas et al., 2012). Reports also suggest that VE-821 sensitised cancer cells to IR under hypoxic conditions. Treatment of hypoxic cells (often associated with large, solid organ tumours such as that found in cervical cancer) is often difficult due to their aggressive phenotype and tendency to chemo- and radio-resistance (Bristow and Hill, 2008). However, this finding has not been replicated in tumour models.

CHK1 inhibitors

The dual CHK1/2 inhibitor AZD7762 caused p53 dependent radio sensitisation of glioblastoma, colon, lung, and pancreatic cancer cell lines in clonogenic assays (Mitchell et al., 2010). Conversely, other studies demonstrate sensitisation by AZD7762 of a large number of human cell lines to IR independent of p53 status (Yang et al., 2011, Dillon et al., 2017). In contrast to these results neither AZD7762 or the CHK1 specific inhibitor LY2603618 sensitised a range of radio-resistant cell lines with high levels of DDR protein and oncogene expressions to IR (Zhang et al., 2016). However, both drugs suppressed growth of the radio-resistant cell lines when used as single agents, but not their radio-sensitive parental cells, supporting evidence for CHK1 inhibition as a therapeutic strategy for cells with high levels of endogenous replication stress (see Chapter 1.5.1).

The *in vivo* performance of CHK1 inhibitors as a sensitiser of IR mirrors the results of in-vitro reports. AZD7762 prolonged survival in mouse models of lung cancer metastases (Yang et al., 2011) and more than doubled tumour growth delay following fractionated IR in colorectal cancer xenografts (Mitchell et al., 2010).

WEE1 inhibitors

Whilst there are fewer reports of WEE1 radio-sensitisation, results of MK-1775 combinations with IR appear to be positive. MK-1775 has sensitised high grade glioma (HGG) cells to IR in-vitro and this translated into a significant survival advantage for mice bearing HGG xenografts treated with the combination over those treated with IR alone (Mueller et al., 2014). As with ATR and CHK1 inhibitors, there are reports of p53 dependent sensitisations that are likely to represent the importance of G1/S checkpoint deficiency rather than p53 mutated status specifically: a p53-defective panel of human lung, prostate and breast cancer cell lines showed sensitisation by MK-1775 to IR but no effect was measured in wild-type matched cells (Bridges et al., 2011).

1.8 ATR, CHK1 and WEE1 inhibitors in clinical practice

Four ATR inhibitors are currently undergoing clinical trials and have shown anti-tumour activity as single agents and in combination with other chemotherapy drugs. Amongst these are VE-822 (VX-970) and AZD6738, for which a description of the available pre-clinical data is given in sections 1.5 and 1.6 have been tested in combinations with platinum chemotherapy agents and have available results. VE-822 (as M6620) showed good tolerability as a single agent and achieved a complete response (CR) in patient with metastatic colorectal cancer that showed 100% ATM loss on immunohistochemistry (O'Carrigan B, 2016). AZD6738 monotherapy appeared to be less well tolerated with bone marrow suppression observed with continuous dosing schedules. However, two partial responses (out of 26 enrolled patients) were observed in patients with advanced solid organ tumours (Dillon, 2017).

Combinations with either VX-970/M6620 or AZD6738 have proved to be more problematic with respect to dose limiting toxicities, particularly in relation to bone marrow suppression. Despite frequent dose delays and interruptions due to neutropenia, a phase 1 trial, which combined VX-970 with carboplatin in 15 patients saw a sustained partial response in one patient and stable disease maintained in 8 others over 6-months (O'Carrigan B, 2016). Furthermore, in another cohort, combinations of VX-970 with cisplatin showed anti-tumour activity in patients with previously platinum resistant or refractory disease (Shapiro, 2016). AZD6738 combinations with carboplatin have resulted in 3 three observed partial responses, two of which were in patients with ATM deficient tumours (ovarian clear cell cancer and colorectal cancer) (Yap, 2016).

Trials of CHK1 inhibitors as single agents and in combinations with other chemotherapy drugs have been hampered by severe dose limiting toxicities including bone marrow suppression, cardiotoxicity and severe thrombo-embolic events (Pilie et al., 2019). Three CHK1 inhibitors are currently undergoing clinical trials, including LY2602638 (Prexasertib) and CCT245737 (SRA737). A phase II trial of Prexasertib has demonstrated tumour responses in 5 out of 22 patients with advanced BRCA wild-type high grade serous ovarian cancer (HGSOC) (Lee, 2016). This result is notable due to the high frequency of p53 mutation present in HGSOC.

The only selective WEE1 inhibitor to enter trials is AZD1775 (MK-1775). The progress of this drug through trials has been hampered by the need for unconventional dosing schedules dictated by cumulative toxicity effects. A phase I study has reported a PR in two out of 25 patients, both of whom had BRCA-2 mutant tumours. However, given the pre-clinical data that suggests a strong selectivity for response to WEE1 inhibition in p53 deficient tumours, none of the p53 mutant tumours in this trial responded to AZD1775 therapy (Do et al., 2015). However, a phase II trial reported that addition of AZD1775 to carboplatin and paclitaxel chemotherapy in 122 patients with advanced p53-mutant ovarian cancer resulted in an increase in progression free survival (Oza, 2015). Another Phase II trial reported a greater overall response rate in p53 mutant vs p-53 null-type tumours (Leijen et al., 2016).

1.9 Aims and Objectives:

Cervical cancer is associated with HR-HPV infection, and the E6 and E7 viral proteins are responsible for p53 degradation and inactivation of pRb, thereby abrogating the G1 checkpoint in a similar manner to cells with pathogenic mutations in p53 and pRB. Inhibition of the intra-S and/or G2/M checkpoint with an ATR, CHK1 or WEE1 inhibitor may therefore selectively sensitise cervical cancer cells with dysfunctional G1 control to DNA damaging agents (e.g. IR and cisplatin). Furthermore, data indicates that DNA-PKcs overexpression and ATM deficiency are potential determinants of sensitivity to ATR-CHK1 pathway inhibition and therefore may render cells more sensitive to ATR, CHK1 and WEE1 inhibition alone or in combination with IR and cisplatin. The aim of this work was (i) to directly compare ATR, CHK1 and WEE1 inhibitors for their ability to kill cervical cancer cells and to chemo- and radio-sensitise these cells, (ii) identify determinants of sensitivity and (iii) to explore the underlying mechanisms.

Hypotheses to be tested:

1. The cervical cancer cell lines will display a spectrum of sensitivity to cisplatin and IR as well as ATR, CHK1 and WEE1 inhibitors alone that will be related to the expression of DDR proteins

2. ATR, CHK1 and WEE1 inhibitors will sensitise cervical cancer cells to IR and cisplatin and that sensitisation will be dependent on HR-HPV and p53/pRb status and consequent impairment of G1 cell cycle control

2 Materials and Methods

2.1 General laboratory practice

All experiments were performed to Newcastle University standards for safe working regulations and with adherence to the Control of Substances Hazardous to Health (CoSHH) and Biological CoSHH (BioCoSHH) regulations. Culture of live cell line material was conducted in a class II biosafety cabinet within in a dedicated tissue culture laboratory.

2.2 Chemicals and Reagents

Unless stated otherwise, chemicals and reagents were purchased from Sigma-Aldrich (Poole, Dorset UK). Cisplatin (*cis*-Diammineplatinum(II) dichloride) stock solution was prepared by dissolution in sterile 0.9% w/v sodium chloride (NaCl) solution at 1 mM, filter sterilised through a 0.2 micron filter, aliquoted and stored at -20 °C. All inhibitors were purchased from Selleckchem.com. (Houston, Texas USA). A stock solution of VE-821 (ATR inhibitor) was prepared by dissolution in flame sealed, sterile dry dimethyl-sulfoxide (DMSO) from flame-sealed vials at 20 nM, aliquoted and stored at -80 °C. Stock solutions of PF-477736 (CHK1 inhibitor) and MK-1775 (WEE1 inhibitor) were prepared by dissolution in dry DMSO at 10 mM, aliquoted and stored at -80 °C.

2.3 Cell Culture

Six human cervical cancer cell lines were used: HeLa; SiHa; C33A; CaSki; ME-180; and HT-3. Cell lines were purchased from the American Type Culture Collection (ATCC) cell biology collection and authenticated by short tandem repeat (STR) profiling according to institutional protocols. Cells were stored under liquid nitrogen at -190 °C. For experimental use, cells were thawed and transferred to 25 cm² tissue culture flasks in cell specific growth media containing 2 mM L-glutamine and 10% v/v foetal bovine serum (FBS) (table 2.1). Cells were then incubated at 37 °C, 5% CO₂ and 95% humidity. Growth medium was changed after 24 hours, once the cells were observed to have adhered to the bottom of the culture flask. When the cells reached 60% confluence, they were harvested: cells were washed twice with 10 ml sterile phosphate buffered saline (PBS) and incubated in 10% Trypsin-

ethylenediaminetetraacetic acid (trypsin-EDTA) for 5-10 minutes until they were observed to have detached from the flask. Cells were then resuspended in full culture medium to neutralise the trypsin and seeded into 75 cm² tissue culture flasks for ongoing culture.

Continuous cell culture was maintained by serial passage of cells at 60% – 80% confluence to maintain exponential growth. Cells were used for experiments at post-authentication passage number 30 or less to limit the effects of genetic drift that can occur at high passage numbers. Cells were passaged at least once following thawing and prior to use. For experimental use, cultured cells were harvested as outlined above. Early passage, exponentially growing cells were frozen for future use in 2 ml aliquots of $1 - 2 \times 10^6$ cells/ml and in cell specific freezing medium (cell specific growth medium with 10% FBS and 10% DMSO). Cells in freezing medium were immediately frozen at -80 °C for 24 hours prior to transfer to storage under liquid nitrogen.

To avoid cross contamination, one cell line and corresponding dedicated media and reagents were handled exclusively at any one time within the biosafety cabinet. The cabinet was cleaned thoroughly with 70% ethanol between experiments using different cell lines. All media was prepared in aseptic conditions, sterility checked, stored at 4 °C and warmed to 37 °C prior to use. All continuously cultured cells lines were regularly tested for mycoplasma infection according to NICR protocols.

Cell line	Growth medium
HeLa	EMEM +2 mM L-glutamine, 10% FBS, 100 IU/ml penicillin and 100 ug/ml streptomycin
SiHa	EMEM +2 mM L-glutamine, 10% FBS, 100 IU/ml penicillin and 100 ug/ml streptomycin
C33A	EMEM +2 mM L-glutamine, 10% FBS, 100 IU/ml penicillin and 100 ug/ml streptomycin
CaSki	DMEM +2 mM L-glutamine, 10% FBS, 100 IU/ml penicillin and 100 ug/ml streptomycin
ME-180	RPMI +2 mM L-glutamine, 10% FBS, 100 IU/ml penicillin and 100 ug/ml streptomycin
HT-3	RPMI +2 mM L-glutamine, 10% FBS, 100 IU/ml penicillin and 100 ug/ml streptomycin

Table 2.1 Human cervical cancer cell lines used and their specific growth media for continuous culture. EMEM = Eagle's Minimum Essential Medium, DMEM = Dulbecco's Modified Eagles Medium, RPMI = Roswell Park Memorial Institute (medium), FBS = Fetal Bovine Serum.

2.4 SRB assay

The Sulforhodamine B (SRB) assay relies on the stoichiometric binding of SRB dye to cell proteins under mildly acidic conditions. The dye is then solubilised into a defined volume of basic solvent. This produces a dye concentration that is directly proportional to the cell mass being measured. Measurement of absorbance at wavelength 510 nm then allows for estimation of the quantity of cell material present (Skehan et al., 1990).

2.4.1 Determination of cell line growth rate by SRB assay

Cell preparation and fixation

Exponentially growing cells were harvested as described in section 2.3, above at 60% confluence and seeded into five rows of six separate 96-well plates in 100 µl full growth medium per well. Each row of an individual 96-well plate contained cells seeded at a different seeding density ranging from 6.75×10^3 cells/well to 1.0×10^5 cells/well to allow for selection of the optimal seeding density for each cell line, as shown in figure 2.1. Cells were incubated at 37 °C and allowed to adhere to the bottom of the wells for 24 hours prior to fixation of the first plate: the 'Day 0 plate'. An individual 96-well plate was then fixed at a recorded time on each of the following 5 days.

Cells were fixed by addition of 25 µl fresh methanol-acetic acid 3:1 (v/v) to each cell-containing well and incubated at 4 °C for at least 60 minutes. Following fixation of the cells in an individual 96-well plate, the plate was washed in slow running tap water and allowed to air dry. Plates were stored at 4 °C until all were fixed, prior to staining.

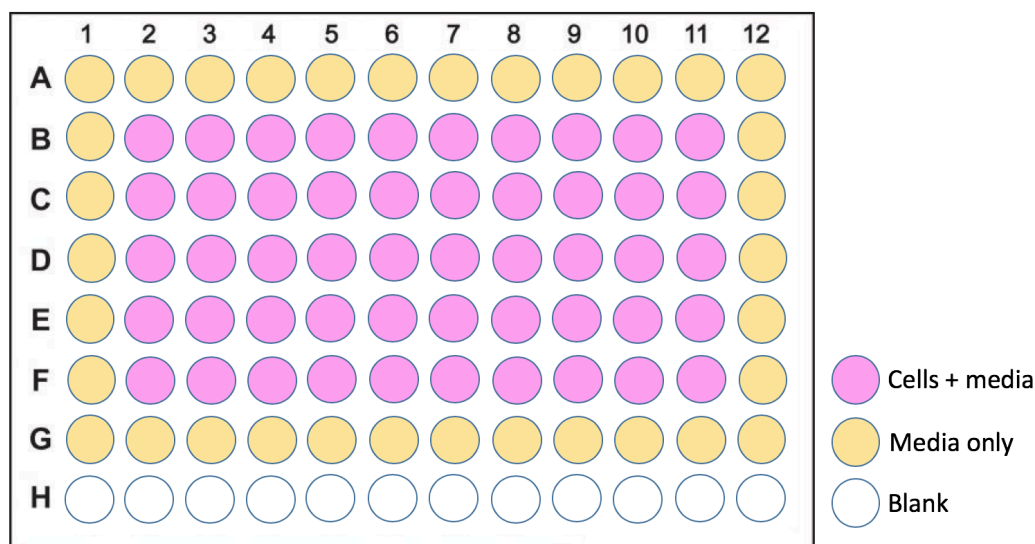


Figure 2.1 Diagram showing the layout of an individual 96-well plate used for SRB growth assays.

Each of five rows (B-F) of a 96-well plate contained cells in full growth media at increasing seeding densities ranging from 6.75×10^3 cells/well to 1.0×10^5 cells/well. Experimental cells are surrounded by wells containing growth media only to reduce 'edge effect' associated with microplate-based assays.

SRB staining and absorbance measurement

When all of the 96-well plates had been fixed, they were allowed to attain room temperature prior to addition of 20 μ l 0.04% w/v SRB to each well. Cells were incubated with the dye at room temperature for 1 hour, washed briskly four times in 1% acetic acid and dried in a drying cabinet at 37 °C. Once dry, 100 μ l of 10 mM Tris-base (pH 10.5) was added to each well and the plates agitated on a plate shaker at room temperature for 10 minutes to solubilise the bound dye. Absorbance at wavelength 510 nM was measured using a FLUOstar® Omega microplate reader.

2.4.2 Data analysis

Absorbance measurements for each individual seeding density (averaged over each row) for each 96-well plate was measured. Data was exported to Graphpad Prism® and curves of \log_{10} Absorbance vs time were constructed. Points on the curve that fall along a straight line represent cells in exponential growth phase, and these were used to calculate the doubling times for each cell line under investigation.

2.5 Colony formation assay

A colony formation (clonogenic survival) assay is a cell survival assay based on the ability of a single cell to grow into a colony of cells. Developed as a method for determining reproductive death of cells after exposure to IR, it can also be used to test the cytotoxic effects of agents in solution (Franken et al., 2006). Cells are seeded out at known densities and the fractional survival of cells following treatment with a cytotoxic insult is calculated based on the number of colonies observed to have survived over the number of cells seeded. When the dose of IR, or concentration of the cytotoxic drug is varied, a survival curve can be constructed

In-vitro results from clonogenic assays have been shown to correlate with *in vivo* clinical drug trial results and tumour response to chemotherapy agents (Salmon et al., 1978). Colony formation assays do, however have some limitations: Whilst the seeding of cell aggregates can be guarded against by disaggregation techniques, this action in itself may disrupt normal cell-cell interactions of importance in the three-dimensional tumour system or micro-environment (Miller et al., 1984); non-dividing and reversibly resting G_0 cells are not assessed in colony formation assays as they are not dividing (Hoffman, 1991). However, while this may be problematic in assessing cells derived from clinical tumours that may be enriched with G_0 phase cells, it is unlikely to represent a significant problem in rapidly proliferating, cell line culture experiments. Overall, colony formation assays represent a convenient and reliable way of assessing the cytotoxic effects of drugs and IR on proliferating cell populations.

2.5.1 Cell preparation and fixation

Exponentially growing cells were harvested as described in section 2.3, above at 60% confluence and seeded into 6-well plates at three different seeding densities per drug concentration to allow for differential plating efficiencies and expected cytotoxicity. Cells were incubated at 37 °C and allowed to adhere for 24 hours. Growth media was aspirated from the wells and replaced with medium containing drug, diluted to the desired concentration. All control wells were exposed to growth media with DMSO at an identical

concentration to that used for dilution of the inhibitor drug and not more than 0.5% v/v. Exposure times were 24 hours unless otherwise stated.

At 24 hours exposure, the drug-containing media was aspirated and replaced with full growth media (table 2.1). The cells were incubated for 8 – 14 days, depending on the doubling time of the cell line, allowing for at least 5 doubling-times. Following the desired incubation period colonies were fixed with methanol-acetic acid 3:1 (v/v) and stained with 0.4% w/v crystal violet solution. Colonies of over 30 cells were counted to determine colony survival at each drug concentration used.

2.5.2 Single agent cytotoxicity assay

Serial dilutions of drugs for cytotoxicity assays were made according to the individual experiment requirements. Stock solutions of cisplatin or inhibitor were removed from storage and allowed to thaw to room temperature prior to serial dilution with either 0.9% w/v NaCl (for cisplatin) or DMSO (inhibitors). Final dilutions to achieve experimental concentrations were made in cell line specific growth medium at a DMSO concentration of not more than 0.5% v/v.

2.5.3 Cisplatin potentiation cytotoxicity assay

For colony formation assays investigating the potentiation of the cytotoxic effects of cisplatin by inhibitors of ATR, CHK1 and WEE1, single concentrations of inhibitor drugs were used to potentiate the effects of a range of cisplatin concentrations. Inhibitor concentrations were chosen at which substantial enzymatic inhibition was observed in Western blot analysis of target inhibition, but little inherent cytotoxicity was observed in single agent cytotoxicity assays.

Serial dilutions of cisplatin stock solution in NaCl were prepared as described in section 2.5.2, above. Final dilutions were prepared in duplicate in growth media containing either: the chosen concentration of inhibitor in DMSO; or an equivalent concentration of DMSO only as control. Identical series of 6-well plates (Figure 2.2) were therefore incubated, fixed and

analysed. The percentage survival of colonies in wells treated with cisplatin + inhibitor relative to the cisplatin only controls represents the potentiation effect of the inhibitor drug.

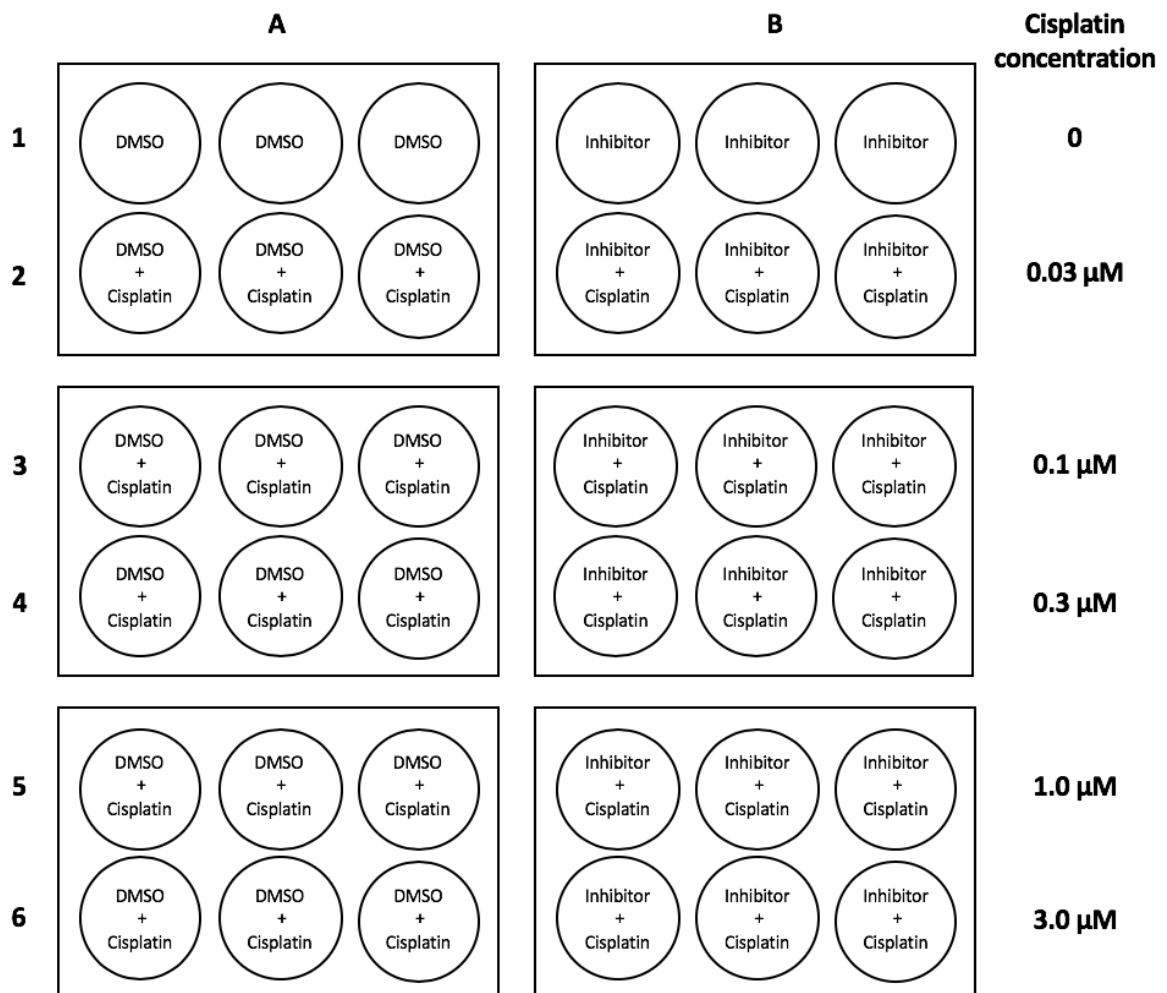


Figure 2.2 Example of 6-well plate layout for cisplatin potentiation colony formation assay.

*Identical series of 6-well plates containing media with either **A**: DMSO + cisplatin concentrations or **B**: inhibitor + cisplatin concentrations were incubated as described in chapter 2.5.3. Colony survival was normalised to DMSO or inhibitor only controls (Row 1). Rows 2 -6 contained increasing concentrations of cisplatin of between 0.03 μM and 3.0 μM*

2.5.4 Radio-potential cytotoxicity assay

The same concentrations of inhibitors were used to investigate any potential of these drugs to potentiate the cytotoxic effect of ionising radiation (IR) in colony formation assays.

Growth media containing either: the chosen concentration of inhibitor in DMSO; or an equivalent concentration of DMSO only as control were added to each well of a series of 6 well plates. Each plate contained 1 row of three wells containing inhibitor, and one row of three wells as control. The 6-well plates containing known seeding densities of cells, and inhibitor or DMSO in growth media were then immediately exposed to increasing doses of ionising radiation and incubated, fixed and analysed as described in section 5.1 (figure 2.2). The percentage survival of colonies in wells treated with IR + inhibitor relative to the IR only controls represents the potentiation effect of the inhibitor drug.

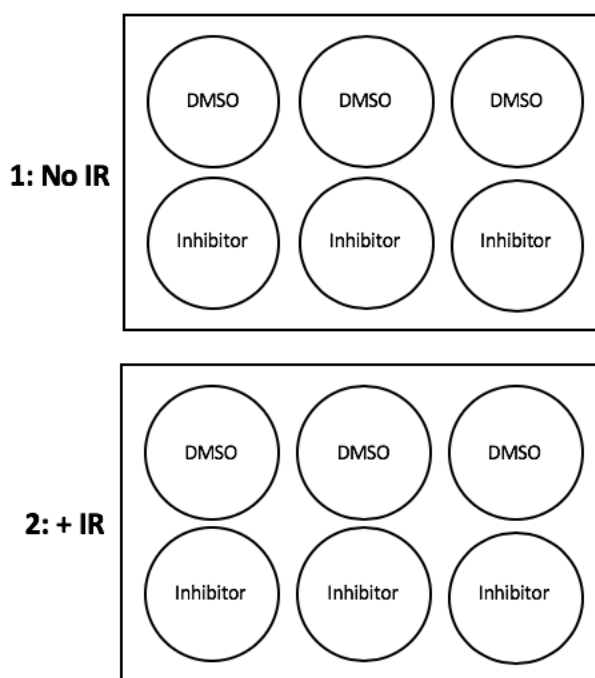


Figure 2.3 Example of 6-well plate layout for IR potentiation colony formation assay.

*Identical series of 6-well plates containing cells + media with either DMSO or inhibitor were exposed to no IR (**plate 1**) increasing doses of IR (**Plate 2 and higher**) and incubated as described in chapter 2.5.3. Colony survival was normalised to DMSO or inhibitor controls (Plate 1). Irradiated plates were exposed to 2 Gy, 4 Gy or 6 Gy of IR.*

2.5.5 Data Analysis

Following fixation and staining, colonies were counted manually, and the percentage survival calculated in Microsoft Excel®. Percentage survival results for each cell for each biological repeat were copied to Graphpad Prism® and the mean and standard deviation of survival for each individual condition calculated. Survival curves were plotted. For cisplatin and IR potentiation experiments, two-way analysis of variance (ANOVA) was conducted to detect significant potentiation effects.

2.6 *Western blot*

Western blot was used to measure the relative expression of cell cycle checkpoint kinases and other DDR proteins. Western blot was also used to assess the activation of ATR, CHK1 and WEE1 by cisplatin in each cell line and the inhibition of these kinases by their respective small molecule inhibitors: VE-821; PF-477736; and MK-1775, by staining for the principle activation target of each enzyme (Table 2.2, Target Protein).

Western blot is a semi-quantitative method for assessing protein expression. Proteins from whole cell lysates are separated by their molecular weight by gel electrophoresis and transferred onto a cellulose blotting membrane. The membrane is incubated with a sequence of primary antibodies (antibodies raised against the protein under investigation) and secondary antibodies that are conjugated to horseradish peroxidase (HRP). Addition of a chemi-luminescence substrate to the HRP conjugated secondary antibody allows for analysis by correlating the intensity of the chemi-luminescence with the amount of protein present.

Cell Cycle Kinase	Target protein (activated)	Mol. Wt. of target protein (kDa)	Antibody used	Supplier, product	Antibody dilution
ATR	pCHK1 ^{S345}	56	Anti-Phospho-CHK1 (S345) Rabbit mAb	Cell Signalling, 2348	1:1000 in 5% BSA
CHK1	pCHK1 ^{S296}	56	Anti-Phospho-CHK1 (S296) Rabbit pAb	Cell Signalling, 2349	1:1000 in 5% BSA
WEE1	pCDK1 ^{Y15}	34	Anti-Phospho-CDK1 (Y15) Rabbit pAb	Cell Signalling, 9111	1:1000 in 5% BSA
	Protein	Mol. Wt. of protein (kDa)	Antibody used	Supplier, product	Antibody dilution
	ATR	250	Anti-ATR (N-19) Goat mAb	Santa-Cruz, 1887	1:500 in 5% milk
	CHK1	56	Anti-CHK1 (G-4) Mouse mAb	Santa-Cruz, 8408	1:500 in 5% milk
	WEE1	96	Anti-WEE1 (B-11) Mouse mAb	Santa-Cruz, 5285	1:500 in 5% milk
	CDK1	34	Anti-CDK1 (POH1) Mouse mAb	Cell signalling, 9116	1:1000 in 5% BSA
	ATM	350	Anti-ATM (D2E2) Rabbit mAb	Cell signalling, 2873	1:1000 in 5% BSA
	DNA-PKcs	450	Anti-DNA-PKcs (H-163) Rabbit pAb	Santa-Cruz, 9051	1:500 in 5% milk
	Ku80		Anti-Ku80 (EPR3468) Rabbit mAb	Abcam, ab3114	1:500 in 5% milk
	Ku70		Anti-Ku70 (N3H10) Mouse mAb	Abcam, ab80592	1:500 in 5% milk
	α -tubulin	50	Anti- α -tubulin Mouse monoclonal	Sigma, T6074	1:80000 in 5% milk
			Polyclonal goat anti-rabbit IgG/HRP	Dako, PO447	1:2000 in 5% milk
			Polyclonal goat anti-mouse IgG/HRP	Dako, PO448	1:2000 in 5% milk
			Polyclonal Donkey anti-goat IgG/HRP	Santa-Cruz, 2020	1:2000 in 5% milk

Table 2.2 Primary and secondary antibodies used for Western blot experiments to determine the baseline expression of key DDR and cell cycle checkpoint proteins, their manufacturer, and experimental dilutions.

HRP = Horseradish Peroxidase, pAB = polyclonal antibody, mAb = monoclonal antibody, 5% BSA = Bovine serum albumin % w/v in TBS-Tween 20, 5% milk = dried skimmed milk 5% w/v in TBS-Tween 20.

2.6.1 Preparation of cell lysates

Preparation of lysates from untreated cells

For the determination of baseline protein expression in each of the cell lines, cell lysates were prepared from cells that were not exposed to genotoxic agents or inhibitors.

Exponentially growing cells were seeded into 10 cm tissue culture dishes and incubated at 37 °C in 10 ml of growth media. At 60% confluence, cells were washed twice in PBS. Cells were incubated for 5 minutes at room temperature with 300 µl radioimmunoprecipitation (RIPA) lysis buffer and 1:100 protease inhibitor cocktail (ThermoFisher-Scientific, Rockford, USA) prior to mechanical agitation and transfer to Eppendorf tubes for centrifugation at 16000 g for 5 minutes. The supernatant was removed and stored at -80 °C until analysis.

Preparation of lysates from drug-treated cells

For the determination of the levels of phosphorylated proteins associated with activation or inhibition of enzymes by the genotoxic agents and inhibitors under investigation, cells were treated with combinations of drugs as described in the individual experimental protocols (see sections 3.3 and 4.3). Exponentially growing cells were seeded into wells of 6-well plates and cultured at 37 °C to 60% confluence. Growth media was replaced with treatment media containing the drug combinations and cells were further cultured until the desired time for lysis. Cells were washed twice in PBS and cultured for 10 minutes on ice with 70 µl per well of Phosphosafe extraction reagent (Novogen/Merk KGaA, Darmstadt, Germany) with 1:100 protease inhibitor cocktail (ThermoFisher-Scientific, Rockford, USA) prior to mechanical agitation, transfer to Eppendorf tubes and centrifugation at 16000 g for 5 minutes. Supernatant was removed and stored at -80 °C. To avoid repeated freeze-thaw cycles, a 10 µl aliquot of all lysate samples was diluted with 40 µl de-ionised water (DIW) and used for BCA assay.

2.6.2 BCA assay

In order to measure the relative amounts of specific proteins in multiple samples by Western blot, each experimental sample analysed should be of identical overall protein concentration. This is achieved by dilution of whole cell lysates for each experimental sample to the equivalent protein concentration of the sample with the lowest value. In order to determine the overall protein concentration of the lysate, bicinchoninic acid assay (BCA assay) was performed using a Pierce protein assay kit (ThermoFisher-Scientific, Rockford, USA).

The BCA assay relies on the ability of peptide bonds within proteins to reduce copper (II) sulphate (Cu^{2+} ions) to Cu^+ . The amount of Cu^{2+} reduced is stoichiometric with the amount of protein present. Following this reduction reaction, bicinchoninic acid molecules complex with the Cu^+ ions forming a purple coloured complex that absorbs light at a wavelength of 562 nm. Therefore, absorption of light at 562 nm correlates with the amount of protein present in the reaction solution (Smith et al., 1985).

The protein concentrations in 1:5 dilutions of whole cell lysates were measured in quadruplicate alongside known dilutions of a standard solution of bovine serum albumin. 10 μl aliquots of dilute lysate and protein standards were pipetted in quadruplicate into individual wells of a 96-well plate as shown in figure 2.3. Using deionised water (DIW) as a blank-control, 190 μl Pierce assay reagent was added to each well and the plate was incubated at 37 °C for 30 minutes. Absorbance at 562 nM was measured using a FLUOstar® Omega microplate reader. Protein concentrations were calculated by fit to a standard curve determined by linear regression analysis of the bovine serum albumin standards (figure 2.4).

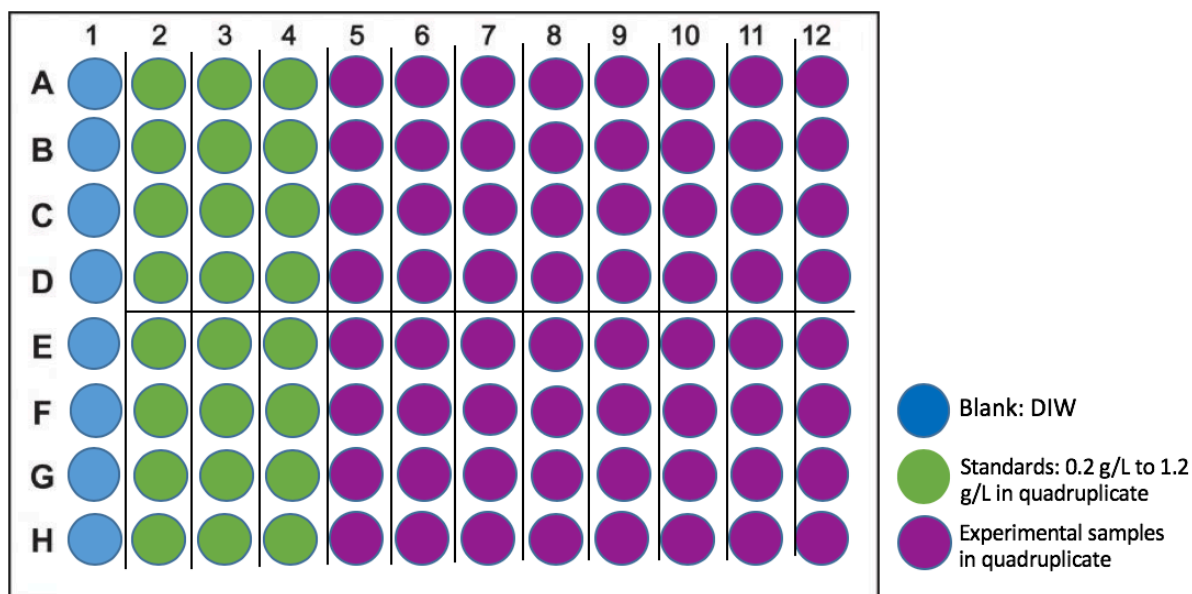


Figure 2.4 The layout of a 96 well plate used for BCA protein assays

DIW was used as a blank control in column A. Protein standard dilutions were added to columns B to D. 1:5 dilutions of whole cell lysates were added to remaining wells in quadruplicate prior to the addition of Pierce reagent and incubation at 37°C for 30 minutes.

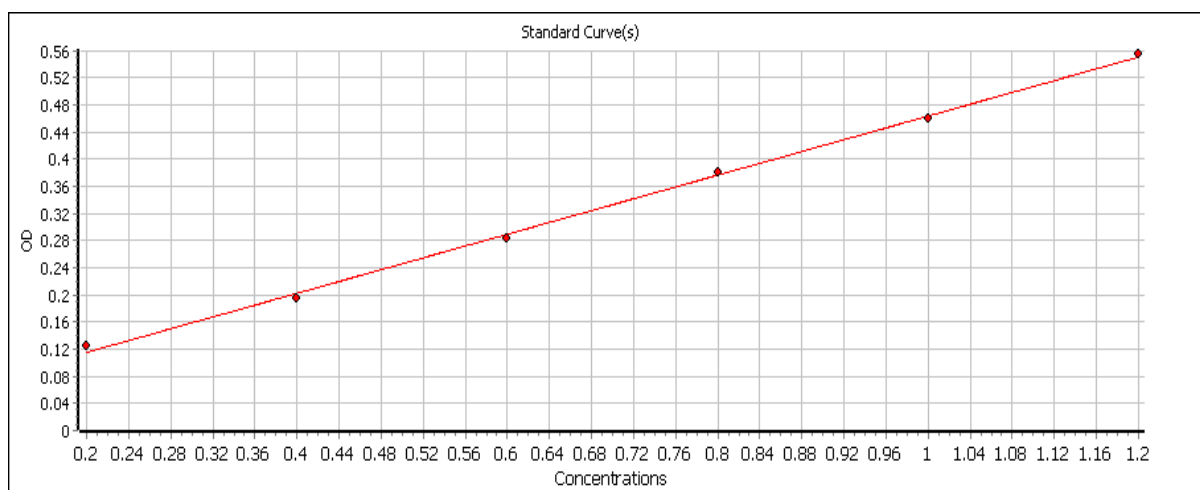


Figure 2.5 Example of a standard curve generated by linear regression analysis of absorbance at 256 nm for a series of standard serum albumin solutions.

Protein concentrations of whole cell lysates were determined by fit of the average of absorbance values, measured in quadruplicate to the standard curve.

2.6.3 Gel electrophoresis

Unless otherwise stated all reagents for electrophoresis were purchased from Bio-Rad laboratories (Hercules, California USA). Cell lysates were thawed on ice and diluted to a maximum protein concentration of 1.0 mg/ml in DIW, 25% XT sample buffer and 0.5% XT reducing agent. Samples were heated to 94 °C for 5 minutes to allow for protein denaturation and epitope exposure. Once cooled, Samples were loaded as 30 µl aliquots into separate wells of an XT precast 3% - 8% tris-acetate electrophoresis gel. High-mark protein ladder (ThermoFisher-Scientific, Rockford, USA) was loaded into wells at either side of the gel to estimate the molecular weight of the protein bands.

Electrophoresis was driven by a potential difference down the gel of 150 V for 65 minutes in 10% tris-glycine running buffer. Following electrophoresis, the proteins were transferred to a nitrocellulose blotting membrane (Amersham Protran premium 0.45 µm NC) across a potential difference of 100 V for 60 minutes in 10 % tris-glycine transfer buffer and 20% methanol. The membrane was then placed in 5% milk in Tris-Buffered Saline + Tween 20 (TBST) and incubated for at least 60 minutes at room temperature on a rocking platform to prevent non-specific antibody binding during antibody staining.

2.6.4 Antibody staining and chemi-luminescence

The membrane was cut at the appropriate molecular weight markers, to enable multiple proteins to be analysed without stripping and re-probing, as desired and incubated with primary antibodies at the dilutions given in table 2.2. All primary antibodies were incubated with the membrane at 4°C, overnight. Membranes were washed with TBST for 20 minutes prior to incubation with the secondary antibodies at room temperature for at 60 minutes. Following incubation with the secondary antibodies, the membrane was exposed to Clarity Western enhanced chemiluminescence (ECL) substrate for 5 minutes and chemi-luminescence was measured and quantified using a G-box® image analyser (Syngene, Cambridge UK) and associated Gene-Tools® image analyser software.

2.6.5 Data Analysis

Once the intensity of chemiluminescence associated with each protein band of interest was measured it was recorded in Microsoft Excel®. The ratio of intensity of the band of interest to its corresponding loading control protein band minus the background fluorescence was calculated. Values were then imported to Graphpad Prism® for further evaluation and display as detailed in chapters 2 and 3.

2.7 Cell cycle analysis

The cell cycle profile of a population of cells within a sample can be used to determine the effects of drugs and other exogenous influences on the progression of proliferating cells through the cell cycle. The cell cycle profile of a sample containing proliferating cells can be determined using a fluorescent dye that binds to the DNA of the cells and then measuring the intensity of the fluorescence from each cell as it passes through a laser. Propidium Iodide (PI) is a dye that binds stoichiometrically to the DNA and RNA of fixed, permeable cells. PI is maximally excited by lasers at wavelength 493 nM and has maximal emission spectra at 636 nM.

Proliferating cells are fixed and permeabilised with Ethanol, treated with ribonuclease (RNase) to degrade RNA content and then exposed to saturating concentrations of PI. The stoichiometric relationship between bound PI and the DNA content of the cell results in a direct correlation between cell DNA content and cell fluorescence, measured by flow cytometry. Cells in G2-/M-phase will have roughly twice the fluorescence of either G0 (resting) or G1-phase cells, due to there being twice the DNA content in these cells, as they have duplicated their DNA in preparation for mitosis. S-phase cells will have fluorescence on a scale between G0/G1 and G2/M cells, as shown in figure 2.5.

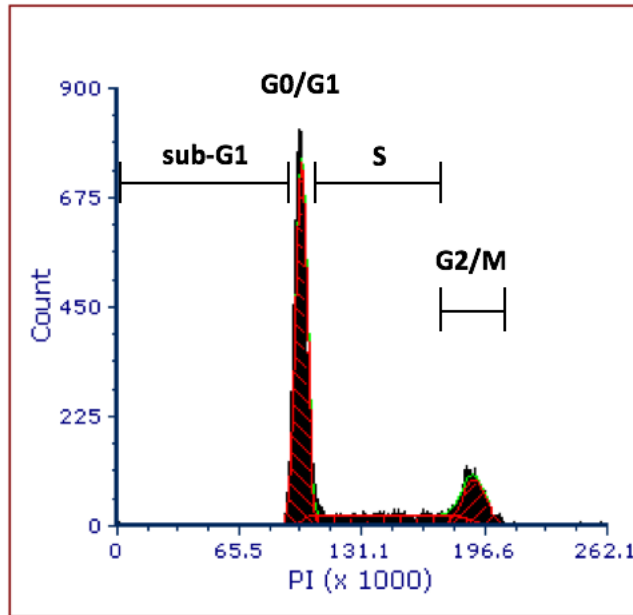


Figure 2.6 An example of a cell cycle profile of unperturbed HeLa cells.

The populations of G₀-/G₁-phase, S-phase and G₂-/M-phase cells are shown along an arbitrary fluorescence scale. G₂- or M-phase cells have twice the fluorescence of the G₁- or G₁-phase cells owing to DNA duplication that occurs in S-Phase. S-phase cells have a DNA content and fluorescence on a scale between the G₀/G₁ and G₂/M populations. Apoptotic cells have fragmented DNA and their fluorescence is less than that of G-phase₁ cells (sub-G₁).

2.7.1 Preparation of samples for cell cycle analysis

Cell harvesting and permeabilisation

Serial dilutions of cisplatin stock solution in NaCl were prepared as described in section 2.5.2, above. Final dilutions were prepared in duplicate in growth media containing either: the chosen concentration of inhibitor in DMSO; or an equivalent concentration of DMSO only as control.

Cells were cultured in 10 cm tissue culture dishes until they were 60% confluent. Growth media was aspirated from the wells and replaced with drug, diluted to the desired concentration in growth media. All control wells were exposed to growth media with DMSO at an identical concentration to that used for dilution of the inhibitor drug and not more than 0.5%. Exposure times were 24 hours.

Following the drug exposure, the drug-containing media was aspirated and reserved to ensure non-adhered cells were not lost to analysis. The cells were washed twice with PBS and incubated with 4 ml trypsin-EDTA until all cells were observed to have detached from the bottom of the culture dish. The cells were then re-suspended in 5 ml PBS and transferred to 20 ml universal tubes with the reserved media and centrifuged at 250G for 3 minutes. The supernatant was discarded, the cells were resuspended in 1 ml ice-cold PBS and transferred to Eppendorf tubes. Following further centrifugation at 250G for 5 minutes, the supernatant was again discarded, and the cells were resuspended in 1 ml 70% ethanol. Cells in ethanol were stored at 4 °C for no longer than 2 weeks.

RNA digestion and PI staining

Cells were removed from cold storage and allowed to reach room temperature before centrifugation at 250 g for 5 minutes. The ethanol supernatant was then discarded, and cells resuspended in 800 µl PBS for 20 minutes. This step was repeated to ensure adequate elimination of ethanol. Bovine RNase A at a final concentration of 1 mg/ml was added to the cell suspension and the cells were incubated at 37 °C for 30 minutes. PI at a final concentration of 400 µg/ml was added to the RNA free cell suspension followed by further 30 minutes at 37 °C.

2.7.2 Fluorescence cytometry and data analysis

Permeabilised and PI stained cells were analysed for DNA content using a BD FACSCanto II flow cytometer. Data was stored and transferred to FCS Express 6® software for analysis. Doublets were excluded, as described in chapter 6 and the sub-G1, G0/G1, S and G2/M populations were determined from the cell cycle histogram.

2.8 Tissue microarray and Immunohistochemistry

A tissue microarray (TMA) was constructed from formalin fixed and paraffin embedded cervical cancer tissue following diagnosis or treatment from patients who consented to biobanking under existing ethical permissions (2012 REC: 12/NE0395. R&D sponsor: NUTH NHS foundation trust No. 6579). The TMA was prepared and IHC undertaken according to the procedures detailed in Chapter 8.3.

2.9 Data analysis and statistics

Statistical analysis of all experimentally generated data was undertaken using Graphpad Prism® statistics software. Pearson correlation analysis was used to explore relationships between data. Where correlation analyses are given, r^2 represents the goodness-of-fit of the data to the linear regression line and the *p-value* represents the probability that the result would have occurred if the correlation co-efficient was zero.

3 Characterisation of cervical cancer cell lines

3.1 Introduction

Due to the strict measurement of tumour dimensions necessary for the accurate staging of cervical cancer and the often-small volume of primary tumour present at diagnosis, harvesting adequate tissue for primary tumour cultures from cervical cancer is rarely possible. Even in advanced or recurrent disease, small biopsies are usually taken to confirm diagnosis, again necessitating fixation and paraffin section of the whole specimen to ensure that adequate material is available for diagnosis and histopathological subtyping prior to non-excisional treatments being undertaken.

3.1.1 Cervical cancer cell lines as a useful pre-clinical tool

Cancer cell lines offer a readily available alternative to primary cultures. Immortalised cell lines have the advantage of providing a theoretically limitless supply of consistent material, supporting reproducible outcomes between researchers and over long-time periods compared to non-immortalised primary cultures. However, care must be taken when interpreting results from experiments with cell lines: while cell lines aim to reproduce the features of their parent primary cells, genotypic and phenotypic characteristics may change over time and serial passage. Additionally, significant heterogeneity may exist in a single culture. Cross culture and contamination with either other cell lines or infective agents such as mycoplasma species may also affect or disrupt cell behaviours or gene expression and must be guarded against and regularly tested for (Kaur and Dufour, 2012). To avoid these problems, one individual cell line of post-authentication passage < 30 was handled exclusively at any one-time, biological safety cabinets were thoroughly cleaned between experiments using different cell lines and regular mycoplasma contamination testing was conducted.

A limited range of cervical cancer cell lines are commercially available, however within their number are some of the most widely used human cancer cell lines used in research today. Most notable are HeLa cells, immortalised from primary cell culture in 1951 this cell line is perhaps the most prolific in modern research (Lucey et al., 2009). HeLa cells have been used

to successfully inform clinical practice in fields as diverse as vaccine development to cancer research (Skloot, 2010). HeLa cells have been reported to be a viable cell line for tumour xenografts in mice (Rastogi et al., 2015, Nin et al., 2014). Similarly, other human cervical cancer cell lines used in the investigations described in this thesis (ME-180, CaSki, SiHa and C33A) have been successfully used to produce murine models of human cervical cancer (Cairns and Hill, 2004, Donat et al., 2014).

3.1.2 Choosing cervical cancer cell lines to represent clinical conditions

Choosing cell lines from a limited commercially available range to be representative of the prevalence and distribution of HPV and histological sub-types prevalent in cervical cancers requires an appreciation of the distribution of these factors in the worldwide population as considered in Chapter 1. Considering the variance in histological and HPV sub-type distribution as well as presence or absence of HPV DNA, and within the limitations of the small number available commercially, a panel of cervical cancer cell lines was chosen to represent: squamous and glandular cancers with common high-risk HPV sub-type (HPV 16 and 18); a rare but observed HPV subtype infection with uncertain oncological significance (HPV 68) (Longuet et al., 1996); and for completeness, two cervical cancer cell lines with no detectable HPV DNA but known pathogenic BP53 and RB1 mutations (Table 3.1).

3.2 *Aims and Objectives*

The aims of the investigations described in this chapter are threefold:

1. to determine the growth rate (doubling time) of the cell lines, as this may be a determinant of sensitivity to cytotoxic drugs and inhibitors of ATR, CHK1 and WEE1;
2. to determine the clonogenic potential (cloning efficiency) of the cervical cancer cell lines for use in future cytotoxicity assays;
3. to establish baseline DDR and G2/M cell cycle checkpoint protein expression as this may reflect HPV/p53/pRB status or be a determinant of sensitivity to inhibition of ATR, CHK1 or WEE1.

3.3 Materials and methods

3.3.1 Cervical cancer cell lines

The cervical cancer cell lines used for experiments described herein were purchased from the American Type Culture Collection (ATCC) Cell Biology Collection and stored in the authenticated cell bank within the Northern Institute for Cancer Research (NICR). The ATCC lists 9 commercially available cell lines derived from human cervical cancer, of which, 6 were chosen for their array of known HPV subtype infection and genotypic characteristics as outlined, above (Table 3.1).

Three of the cell lines are known to be high risk HPV positive: HeLa (HPV 18+), SiHa (HPV 16+) and CaSki (HPV16+ and HPV18+). Two are HPV negative but harbour TP53 +/- RB1 mutations: C33A; and HT-3. One: ME-180, is positive for HPV 68.

3.3.2 Determination of cell doubling times by SRB assay

The doubling times of two cervical cancer cell lines (ME-180 and HT-3) were determined by SRB assay. Cells were seeded in six identical 96 well plates at seeding densities from 6.75×10^3 cells/well to 1.0×10^5 cells/well and incubated for 6 days with fixation of a single 96 well plate at a documented time on each successive day of incubation, as described in section 2.4. The doubling times of the remaining four cell lines used for the experiments described in this thesis (HeLa, SiHa, C33a and CaSki) were determined by SRB assay in work carried out by I. Kotsopoulos (MD thesis, 2018) using the method described here.

Cell Line	Histopathological sub-type and tumour site.	HPV status	Pathogenic mutations
HeLa	Primary cervical adenocarcinoma	HPV 18+	-
SiHa	Primary cervical squamous cell carcinoma	HPV 16+	-
C33A	Primary cervical carcinoma	-	TP53/RB1
CaSki	Cervical carcinoma from metastatic site: small intestine	HPV 16+ HPV 18+	-
ME-180	Cervical squamous cell carcinoma from metastatic site: omentum	HPV 68+	-
HT-3	Cervical carcinoma from metastatic site: lymph node	-	TP53/RB1

Table 3.1 Cervical cell lines used in experiments, their HPV status, histological sub-type and TP53/RB1 status.

3.3.3 Determination of cloning efficiency by colony formation assay

In order to determine the optimal seeding densities for cytotoxic colony formation assays, the cloning efficiency of the six cell lines were determined by undertaking colony formation assays in the absence of cytotoxic agents. Cells were seeded in individual six well plates at known seeding densities and incubated for 7 – 14 days in cell specific full growth media, as described in Chapter 2.5. Incubation time depended on the doubling time of the cell line, allowing for at least 5 doubling-times. Following the desired incubation period colonies were fixed with methanol-acetic acid 3:1 (v/v) and stained with 0.4% crystal violet solution. Colonies of over 30 cells were counted by eye to determine colony survival at each drug concentration used (Figure 3.1). Mean cloning efficiencies in the absence of cytotoxic agents were calculated from three individual experiments. The cloning efficiency for a cell line seeded at a known seeding density in an individual well of a 6-well plate is calculated as follows:

$$\text{Cloning efficiency (\%)} = \left\{ \frac{\text{Number of colonies observed}}{\text{Number of cells seeded}} \right\} \times 100$$

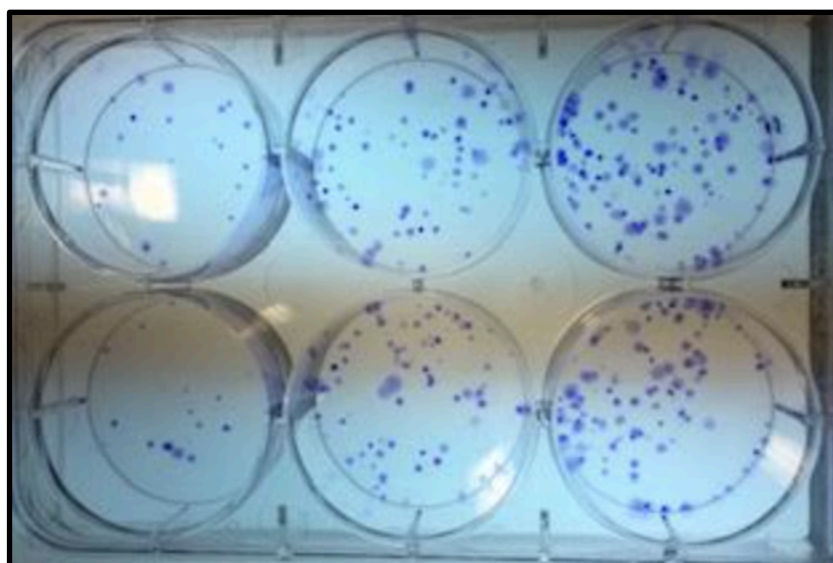


Figure 3.1 Photograph showing HeLa cell colonies.

HeLa cells were seeded at seeding densities of 50, 100 and 200 cells per well in duplicate from left to right. Cells were incubated in full growth media for 10 days (>5 doublings) prior to fixation with methanol-acetic acid 3:1 (v/v). Colonies were stained with 0.4% crystal violet and counted manually.

3.3.4 Determination of baseline protein expression by Western blot

Western blot was used to measure the relative expression of cell cycle checkpoint kinases and DDR proteins. Whole cell lysates were prepared from unperturbed and exponentially growing cells, separated by gel electrophoresis and transferred to a blotting membrane, as described in chapter 2.6. Membranes were incubated with primary and secondary antibodies (table 2.2) prior to exposure to a chemiluminescence agent. The fluorescence of each protein band was measured and normalised to the loading control protein, α -tubulin.

3.4 Results

3.4.1 Cell line doubling times and cloning efficiency

Antiproliferative anticancer agents and cell cycle checkpoint inhibitors are likely to be more cytotoxic to rapidly dividing cells, so it was important to calculate the cell cycle time. Additionally, the cell doubling time is a useful indicator of how long is needed for colony formation in cytotoxicity assays. Calculating the population doubling time is also a useful surrogate for estimating the rate at which the cells grow and the length of the cell cycle for each of the individual cell lines used. Representative growth curves for ME-180 and HT-3 cell lines are shown in Figures 3.2.

When plotted on a log scale, exponentially growing cells will have absorbance values that fall along a straight line. Cells that are confluent, or that are not growing in an exponential growth phase will show a 'plateau'. Data points which indicated pre- or -post exponential growth 'plateau' phase cells, were omitted from the doubling time calculation. Doubling times for each of two replicate experiments for ME-180 cells and HT-3 cells were calculated from the exponential growth phases observed from each of the five technical replicates within that experiment.

Mean doubling times and the standard error of the means for these experiments and those previously undertaken by I. Kotsopoulos are presented in Table 3.2. HeLa, C33A and Caski displayed broadly similar doubling times (around 45 h). SiHa cells grew the slowest (59 hours) and ME-180 cells and HT-3 cells grew the fastest (31 hours).

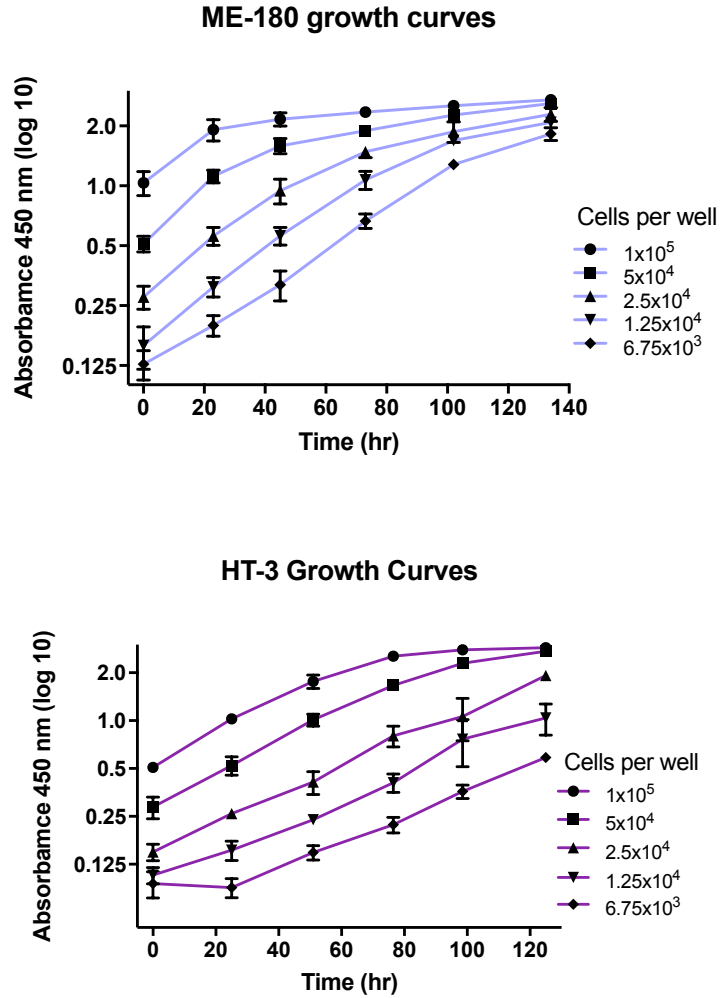


Figure 3.2 Representative examples of growth curves for ME180 and HT-3 cells at five different seeding densities.

Cells were seeded at the densities shown in replicate 96-well plates. After overnight incubation the first plate was fixed (time 0) and the remainder were fixed at daily intervals for 6 days prior to staining all plates with SRB and reading the optical density at 450 nm. Data are mean and SD from a single representative experiment with 6 replicate wells/cell density and time points corresponding to the exact number of hours after time 0 fixation.

Cell Line	Cell doubling time hours \pm SEM (n)	Observed cloning efficiency % \pm SEM (n)
HeLa	44 \pm 3 (3)	47 \pm 2 (3)
SiHa	59 \pm 3 (3)	39 \pm 5 (3)
C33A	46 \pm 5 (3)	73 \pm 13 (3)
CaSki	46 \pm 3 (3)	24 \pm 7 (3)
ME-180	30, 33 (2)	51 \pm 7 (3)
HT-3	37 \pm 2 (3)	22 \pm 1 (3)

Table 3.2 Doubling times and cloning efficiency for six cervical cancer cell lines.

Doubling times were calculated from experiments as shown in Fig 3.2 and 3.1. Data are mean and SEM of the mean doubling time/individual experiment (which was the mean of the 5 technical replicates/experiment). For ME-180 cells, the mean doubling time of two biological replicates are given. Points that fell outside of exponential growth were excluded from analysis. For all other data, the mean and SEM of three biological replicates are given.

The mean cloning efficiencies for each cell line are also shown Table 3.2. CaSki cells and HT-3 cells showed the poorest cloning efficiencies at 22 percent and 23 percent, respectively. C33A cells showed the greatest cloning efficiency at 79 percent. Relative cloning efficiencies showed no relationship to the cell doubling times.

3.4.2 Baseline expression of checkpoint and DDR proteins

In order to confirm that the cells expressed the protein kinases that are key to the functioning of the G2-M cell cycle checkpoint and that are under investigation in this thesis, their expression in unperturbed exponentially growing cells were measured. ATR, CHK1, WEE1 and the principal WEE1 target protein CDK1 levels were measured. Additionally, expression of the important DNA damage signalling kinase: ATM and the key NHEJ proteins: DNA-PKcs; Ku70; and Ku80 were also measured, due to the previously described correlations between expression of these proteins and sensitivity to inhibition of ATR (Chapter 1.6.2). Representative Western blots for the six cervical cancer cell lines used are shown in Figure 3.3.

Potential differences in the expression of cell cycle checkpoint and DDR proteins between the cell lines were investigated. Protein expression was quantified by expressing the

absolute densitometry value associated with the band corresponding to the protein of interest as a ratio to the loading control protein, α -tubulin:

$$\text{Protein expression} = \frac{\text{Protein densitometry value} - \text{background}}{\alpha \text{ tubulin densitometry value} - \text{background}}$$

Variation in α -tubulin expression was noted across the cell line panel. Tubulin and other housekeeping proteins can vary between cells (Li and Shen, 2013). This variation was consistent across individual experimental repeats and was unlikely to represent chance differences in total protein content of individual Western Blot electrophoresis lanes.

There was substantial inter-assay variation, despite normalising expression to the loading control (Figure 3.5). Nevertheless, differences could be detected between the cell lines. Amongst the G2/M checkpoint protein kinases under investigation: there was a 2-fold variation in ATR expression between Caski (lowest) to SiHa (highest); a 3-fold variation in CHK1 expression between SiHa (lowest) to HT3 (highest); and a 5-fold variation in expression of WEE1 between CaSki (lowest) to ME-180 (highest).

HT-3 cells appeared to have very little baseline expression of ATM when compared to the other five cell lines, with a marked difference of over 20-fold in the expression of this protein when compared to any of the other cell lines. In contrast, a difference of less than 3-fold was observed when ATM expression was compared between the other five cell lines.

With regard to the NHEJ proteins measured: DNA-PKcs expression varied considerably across the six cervical cancer cell lines, with a greater than 5-fold variation between HeLa cells (highest) and HT-3 cells (lowest); both Ku70 and Ku80 proteins appeared to be expressed at higher levels in HeLa cells than in any of the other cell lines and this difference was greatest in the case of Ku80, with a 5-fold greater expression than in the cells with the least measured expression (SiHa).

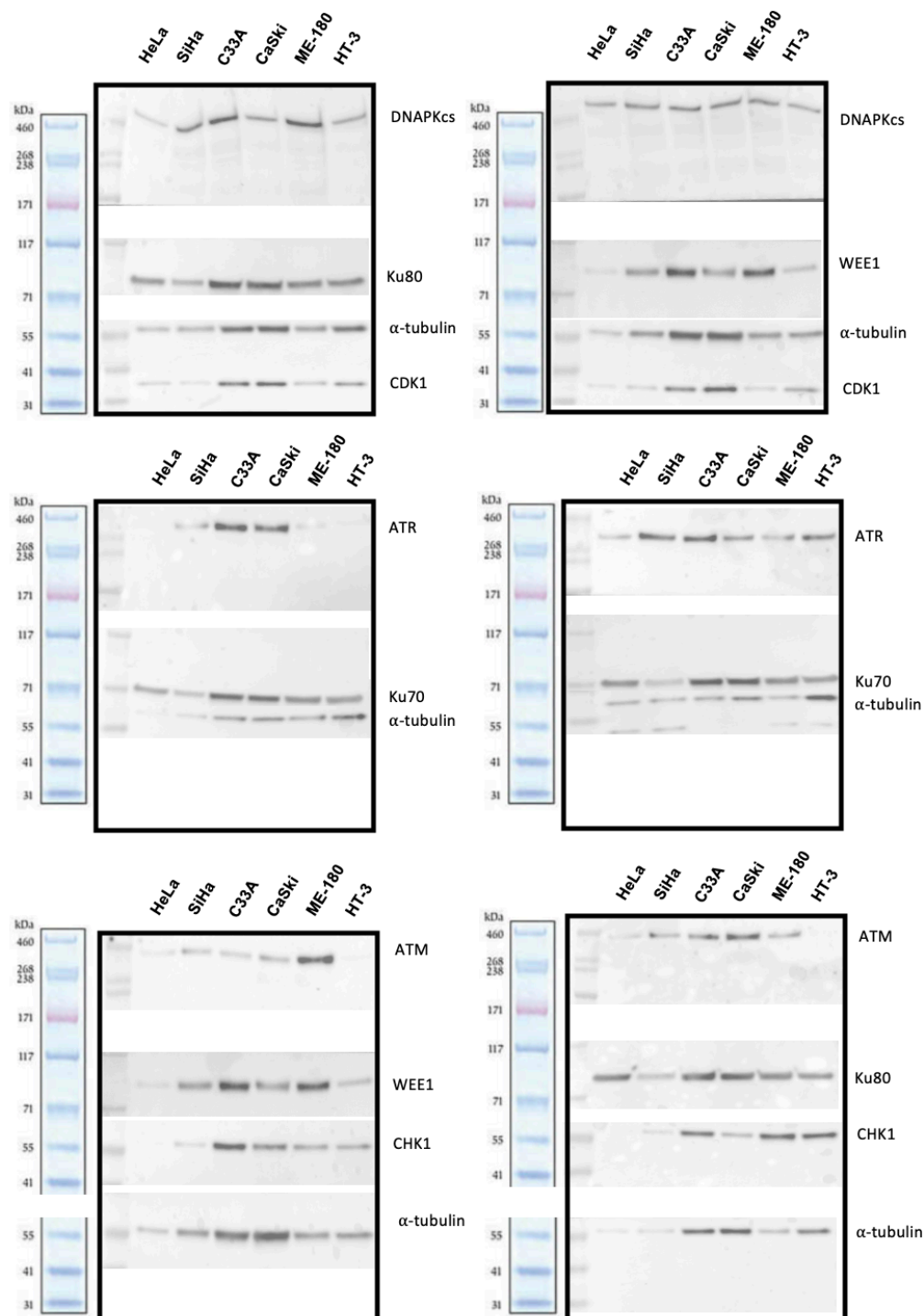


Figure 3.3 Baseline protein expression in unperturbed cells.

Baseline Expression of G2-M cell cycle checkpoint kinases and other key DDR proteins were measured by western blot of cell lysates from exponentially growing cells in the absence of DNA damaging agents. Individual blots showing the expression of cell cycle and DDR proteins representing two individual measurements of expression of each protein are shown. Protein ladder is High-Mark Pre-Stained (Invitrogen, UK).

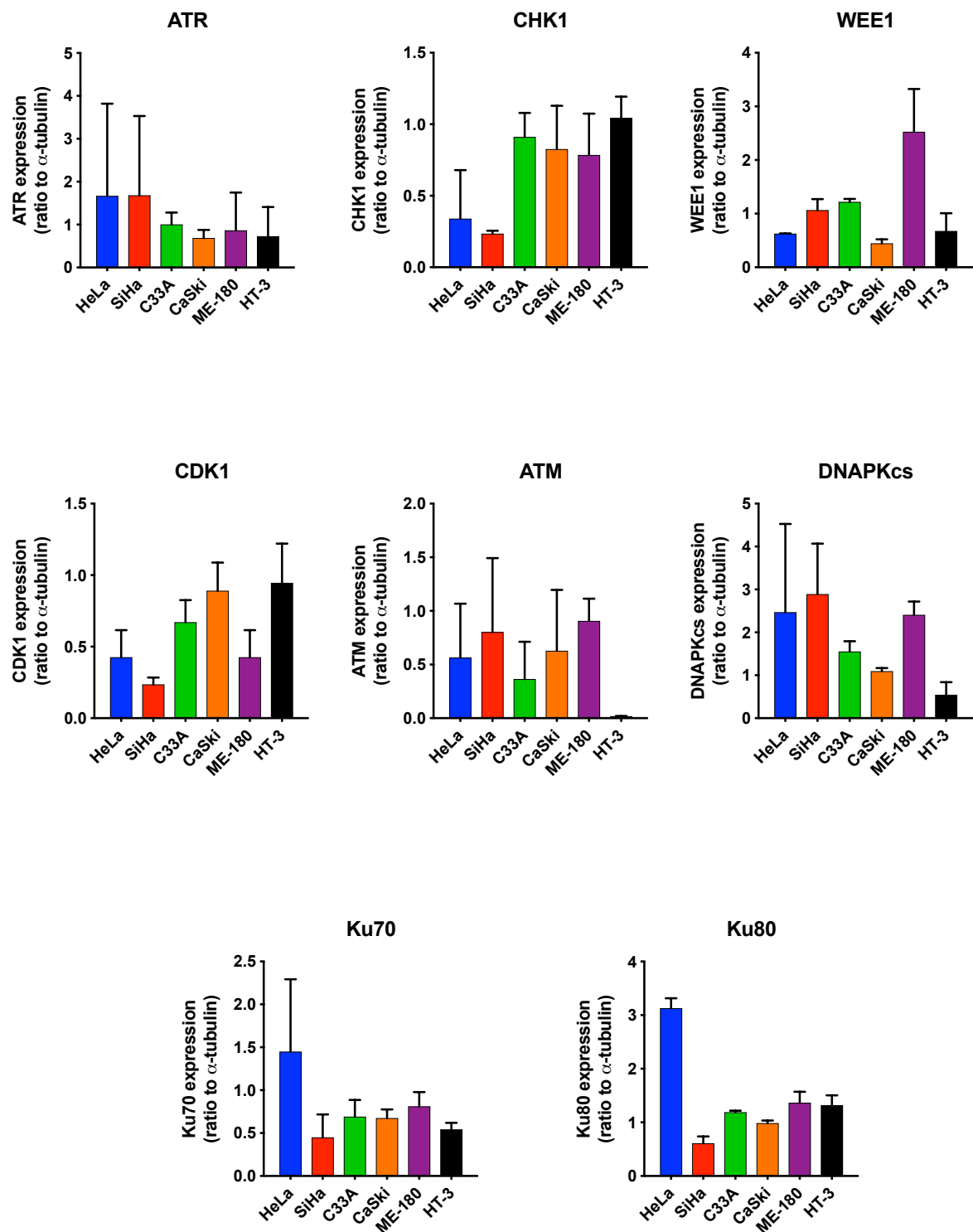


Figure 3.4 Expression of cell cycle checkpoint and NHEJ proteins.

The protein content of exponentially growing cell lysates was measured by densitometry analysis of Western blots. Data are mean and range of expression normalised to the loading control protein, α -tubulin.

3.4.3 Correlations between protein expressions

Relationships between the expression of the key G2/M checkpoint proteins and DDR proteins were investigated by correlation analysis. The baseline expressions of individual proteins were compared between cell lines. No correlations were observed between the levels of expression of ATM and any of the other proteins measured in the cell lines. Similarly, no proteins correlated with the expression of WEE1 in the cell lines. The expression of the Ku proteins, Ku 70 and Ku 80 showed a very strong positive correlation ($r^2 = 0.93$, $p < 0.01$), as expected. The human Ku protein is a heterodimer made up of a single Ku70 and a single Ku80 domain and therefore proportional expression of each protein would be expected in each cell. DNA-PKcs is the catalytic sub-unit of the nuclear DNA dependent protein kinase, DNA-PK. DNA-PK is formed from a stoichiometric interaction between the Ku heterodimer and the DNA-PKcs catalytic sub-unit. Despite this, a correlation between either Ku protein and DNA-PKcs expression was not observed.

Significant negative correlations were observed between: the expression of ATR and both CHK1 and CDK1; and the expression of DNA-PKcs and both CHK1 and CDK1 (figure 3.6). Positive correlations were observed between the expression of CHK1 and CDK1; and between ATR and DNA-PKcs, though this particular relationship did not reach significance (Figure 3.5).

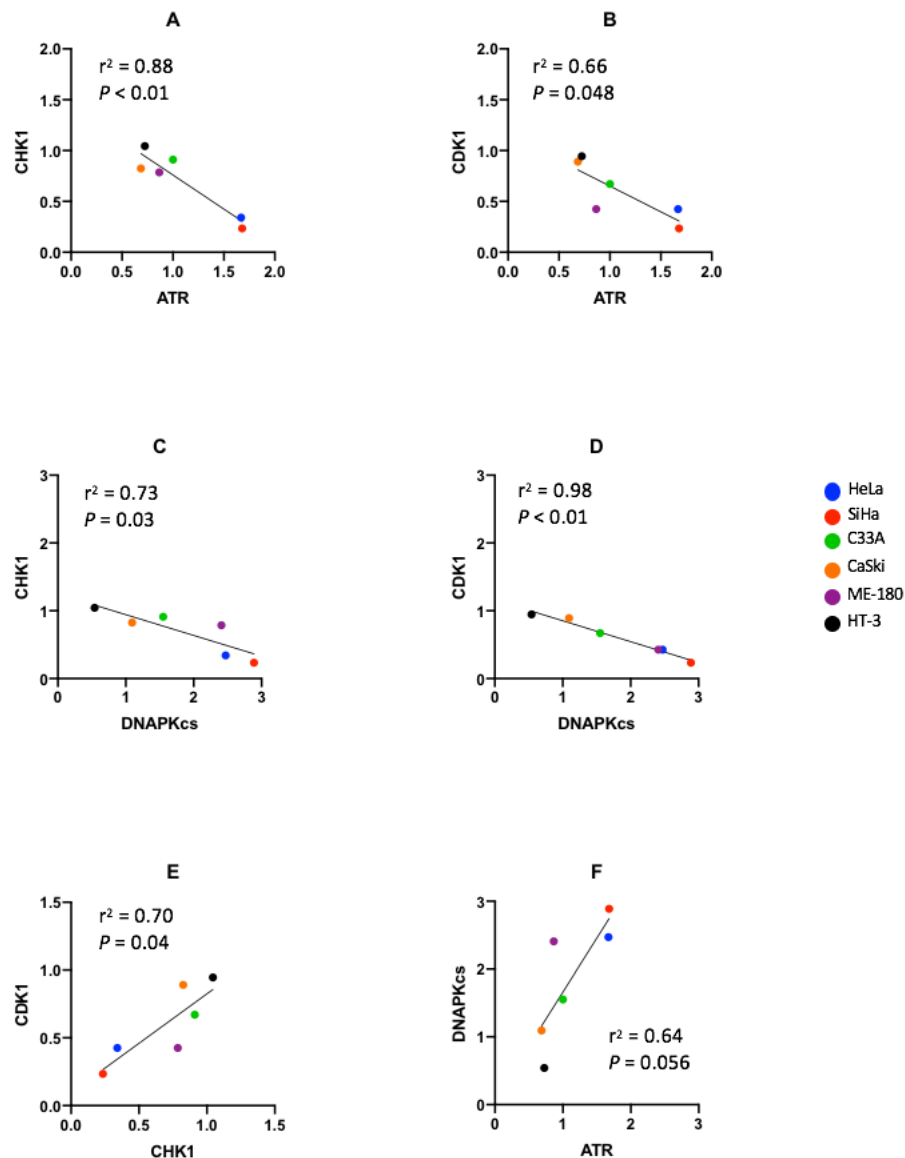


Figure 3.5 Scatter plots showing correlations between baseline protein expressions of pairs of proteins in human cervical cancer cell lines.

Correlations between all combinations of pairs of proteins was undertaken. Scatter plots for those pairs that showed significant Pearson correlations, along with the relevant p -values are shown: ATR and CHK1 (A); ATR and CDK1 (B); DNA-PKcs and CHK1 (C); and DNA-PKcs and CDK1 (D); and CHK1 and CDK1 (E). ATR and DNA-PKcs (E), though this did not reach statistical significance. Data are mean expression values, as displayed in Figure 3.4.

3.4.4 Correlations between cell growth and protein expressions

Correlation analyses were performed to determine if there was any relationship between the expression of cell cycle checkpoint or DDR proteins measured and the growth rate of the six cervical cancer cell lines. The individual scatter plots for protein expressions vs doubling time are shown in Figure 3.6. No Significant correlation was observed between the doubling times of the cell line panel and the baseline protein expression of any of the proteins measured.

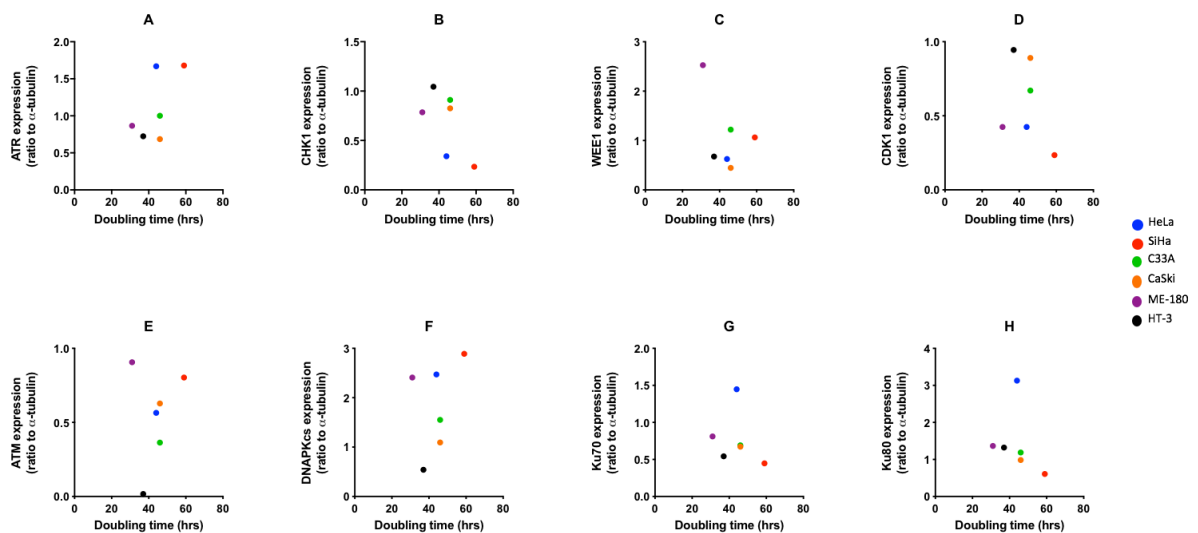


Figure 3.6 Scatter plots of cell cycle checkpoint and DDR protein expression vs cell line doubling times.

Data are mean values calculated and displayed in table 3.2 and figure 3.5.

3.5 Discussion

Knowledge of the basic growth characteristics of the cell lines under investigation allows for consistent experimental conditions to be created with respect to exposure to genotoxic agents, enzyme inhibitors and post exposure incubation for colony formation and cytotoxicity assays. The doubling times calculated for the individual cell lines during exponential growth fell within a narrow range, with a less than two-fold difference in the doubling time between the ME-180 cell line (shortest doubling time) and the SiHa cell line (longest doubling time). It should be noted that whilst the calculated doubling times of HeLa,

SiHa, C33A and ME-180 cell lines were consistent with that reported in the accepted literature (Artimo P, 2012), the calculated doubling times for CaSki and HT-3 cells were found to be significantly shorter under experimental conditions in our laboratory than that reported previously (Kalu et al., 2017). In order to ensure the most consistent conditions for the experiments described in subsequent chapters, the doubling time determined under experimental conditions in our laboratory was used to calculate appropriate post drug-exposure incubation times.

Though doubling time does not have any bearing on colony formation the demonstration of the ability of the cell lines to form colonies under non-perturbed conditions provides a second measure of their intrinsic viability. All six of the cell lines used in experiments described in this thesis demonstrated the ability to form colonies under experimental conditions described in Chapter 2. It is difficult to estimate accepted literature values for cloning efficiencies for the cell lines used, as this value will be affected by such individual experimental parameters as the cell seeding density and volume of growth media used. The experiments described in this chapter therefore provide vital information to guide the appropriate conditions (seeding densities) to be used in cytotoxicity assays described in subsequent chapters, which were conducted under similar experimental conditions.

Many researchers use the presence of mRNA as a marker for the expression of DDR pathway proteins and the lack of inclusion of mRNA data from the cell lines under investigation here, could be viewed as a potential weakness in this thesis. This approach, however, is not without disadvantage. Production and maintenance of cellular proteins requires complex integration of transcription, post-transcriptional modification and degradation processes (Vogel and Marcotte, 2012). Protein concentrations in the cell represent a dynamic balance between these processes. Several large studies comparing the transcriptome and proteome, including in human cancer systems have shown poor correlation between the two (Chen et al., 2002, Tian et al., 2004), whilst others have shown greater alignment (Orntoft et al., 2002). Overall it is estimated that between 15% and 70% of the variation of protein levels in human cells might be explained by post-transcriptional processes, rather than variation in mRNA expression (de Sousa Abreu et al., 2009).

The overall aim of this thesis is to compare a panel of checkpoint protein inhibitors in their effects on cell survival through functional inhibition of their target proteins. The primary aim of the investigations described in this chapter was to demonstrate the presence of these proteins and that of selected DDR proteins which have previously been shown to be determinants of sensitivity to ATR, CHK1 Or WEE1 inhibition (Middleton et al., 2015, Kwok et al., 2016). Protein levels, determined by Western blot were felt to be a more appropriate measure for this aim and to correlate with kinase activity (Chapter 4)

Despite the expectation that faster growing cells might have higher levels of replication stress, and therefore have higher levels of signalling to S and G2/M checkpoints via the ATR-CHK1 pathway, there was no significant correlation between growth rate (doubling time) and baseline expression of any of the key checkpoint proteins: ATR; CHK1; WEE1; and CDK1. While it is accepted that the principal activator of the ATR-CHK1 pathway is replication stress, characterised by lesions arising from stalled replication forks and the resulting dsDNA-ssDNA junction (Zeman and Cimprich, 2014), evidence suggests that this higher level of activation arises out of the complex interplay of ATR, CHK1 and their co-factors (Zeman and Cimprich, 2014, Shiotani and Zou, 2009) with the damaged DNA molecule rather than by increasing the expression of these proteins in their non-activated form. It cannot, however be ruled out that a rapidly dividing cell might adapt to increased replication stress by increasing expression of these DNA damage sensing, signalling and effector proteins.

When considering relationships between the baseline expression of cell cycle checkpoint proteins and DDR proteins, it is important to bear in mind the small sample size of cell lines under consideration in these experiments. Nevertheless, there appear to be highly significant inverse correlations between ATR and both CHK1 and CDK1. Additionally, and in-keeping with this finding is the significant positive correlation between CHK1 and CDK1. There is a paucity of published evidence to confirm any relationships between the expression of these proteins in either human cell lines or clinical tumour specimens. Whilst it might be expected that all components in a given pathway would be upregulated together, or expressed in similar quantities, this inverse relationship between ATR and CHK1/CDK1 might suggest some functional redundancy in the pathway that warrants further exploration in a larger panel of cell lines or tumour material

Concerning the positive correlation observed between CDK1 and CHK1: it could be hypothesised that a cell with high levels of CDK1 might require high levels of CHK1, acting through CDC25C and WEE1 in order to prevent inappropriate entry to mitosis at the G2/M checkpoint. These correlations, while interesting are however observed in a small panel of cell lines. The cell may have adapted to high levels of replication stress by over-expression of proteins that are not measured in these experiments. Verification of these findings would require a substantial expansion of the sample size, including in clinical tumour samples before any definitive conclusion of their significance could be drawn.

Relationships between DNA-PKcs and the G2/M cell cycle checkpoint signalling kinases were also observed. Though there is, again little in published evidence to support a relationship between DNA-PKcs expression and that of CDK1 in either pre-clinical or clinical tumour samples, correlations between CHK1 and DNA-PKcs mRNA expression levels have been observed in publicly available data sets derived from tumour samples from a variety of tissues including lung, hepatocellular, ovarian and colon carcinomas. Less convincing correlations have been observed in ovarian cancers and there was no observed correlation in breast cancer samples (Massey et al., 2016). Though no negative correlations between these two proteins were observed, cervical tissue was not included in the analysis. In this study a positive correlation was noted to be present between the expression of DNA-PKcs and ATR. This relationship has previously been shown to exist in glioma samples using mRNA expression data, following the observation that high DNA-PKcs expression conferred sensitivity to ATR inhibition (Middleton et al., 2015). Furthermore, both high ATR and high DNA-PKcs expression have been shown to correlate with survival in ovarian cancer patients, though no correlation was performed between DNA-PKcs and ATR expression in individual tumour samples in this study (Abdel-Fatah et al., 2014).

The presence of high-risk HPV (HPV 16/18) has been previously shown to have an impact on the sensitivity of head and neck squamous cell cancers (HNSCC) to PARP inhibitors through reduced recruitment or expression of NHEJ and HRR pathway proteins including DNA-PK (Weaver et al., 2015). High-risk HPV positivity has also been shown to be related to the upregulation of other proteins involved in BER and SSB repair pathways (Nickson et al.,

2017). Though the HPV negative cell lines, C33A and HT-3 showed the lowest overall expression of ATM, no other relationships were noted between high-risk HPV status and expression of any of the other DDR or cell cycle checkpoint proteins measured.

3.6 Conclusions

- The cervical cancer cell lines HeLa, SiHa, C33A, CaSki, ME-180 and HT-3 have doubling times that show a less than two-fold difference. The differences in doubling time do not correlate with expression of any of the cell cycle checkpoint or DDR proteins measured, or the HPV status of the cell line.
- The cervical cancer cell lines form colonies with cloning efficiencies that are high enough to allow for cytotoxicity clonogenic assays to be conducted using standard techniques.
- Significant correlations were observed between ATR, CHK1 and CDK1, which are all components of a common pathway signalling DNA damage to the G2/M cell cycle checkpoint.
- CHK1 expression was seen to correlate with DNA-PKcs expression in an inverse relationship, contrary to that observed in mRNA expression from other cancer tissues.
- ATR expression was seen to correlate with DNA-PKcs expression. Though this relationship was non-significant, it is consistent with previously observed correlations in brain cancer tissue.
- DDR protein expression in unperturbed cells was not influenced by HPV status

4 Target enzyme activity and single agent cytotoxicity

4.1 Introduction

A panel of six human cervical cancer cell lines, with known HPV status and pathogenic mutations of TP53 and RB1 tumour suppressor genes were characterised for doubling times, DDR protein expressions and cloning efficiencies in the previous chapter so that subsequent data could be interpreted in light of this knowledge.

The loss of G1 checkpoint control through inactivation of TP53 and/or RB1 is likely to result in increased replication stress and a reliance on the Intra-S and G2/M cell cycle checkpoints (Chapter 1.3). It might be anticipated that inhibition of ATR, CHK1 or WEE1 and hence S and G2/M checkpoints would result in increased in cell death in the face of (endogenous) DNA damage. Evidence supporting p53 mutation or loss as a sensitiser to ATR or CHK1 inhibition is derived from experiments conducted on isogenic cell lines and the results are less consistent in unmatched, wild-type and dysfunctional cells (Rundle et al., 2017). Recent evidence also suggests that p53 deficiency may only confer sensitivity to ATR-CHK1 inhibition in the presence of a genotoxic insult, such as that delivered by co-treatment with IR or gemcitabine (Middleton et al., 2018).

Defects in the DDR pathways HRR, BER and NHEJ have previously been shown to confer sensitivity to inhibition of ATR, CHK1 and WEE1 (Chapter 1.6.2). Of particular interest are observations that aberrations in the expression of components of NHEJ confer sensitivity to ATR-CHK1 pathway inhibition: overexpression of DNA-PKcs (a marker for replication stress and catalytic sub-unit of DNA-PK) is associated with sensitisation of cells to ATR and CHK1 monotherapy (Middleton et al., 2015, Massey et al., 2016). Conversely, loss or knockdown of the DNA-PK components, Ku70 and Ku80 are also associated with sensitisation of cells to ATR and CHK1 inhibition (Middleton et al., 2015, Massey et al., 2016, Sultana et al., 2013).

ATM deficiency has also been suggested as a potential sensitising characteristic for ATR, CHK1 or WEE1 inhibition, due to the complimentary functions of the ATR-CHK1 and ATM-CHK2 mediated pathways in the DDR. ATM deficiency has been shown to sensitise leukaemic

cells to ATR inhibition (Kwok et al., 2016) though convincing evidence of a similar effect on CHK1 and WEE1 inhibitors is lacking.

Investigations described in this chapter will measure the potency of the inhibitors: VE-821; PF-477736; and MK-1775 against their respective kinase targets in intact cells and investigate whether this target inhibition or the characteristics described in chapter 3, including baseline expression of DDR proteins has an impact on the cell's sensitivity to the single agent cytotoxicity of the inhibitors.

4.2 Aims and objectives

The aims of the investigations described in this chapter are:

1. To demonstrate the target enzyme inhibition of ATR, CHK1 and WEE1 by VE-821, PF-477736 and MK-1775, respectively in each cervical cancer cell line.
2. To determine the single agent cytotoxicity of VE-821, PF-477736 and MK-1775 in each cervical cancer cell line.

This will enable the following hypotheses to be tested:

1. The inhibitors will have similar potencies against their target across all cell lines.
2. The cytotoxicity of the inhibitor will be dependent on the baseline expression level of the target enzyme and its inhibition.
3. The cytotoxicity of the inhibitors will be dependent on the expression levels of other DDR proteins (ATM, DNA-PKcs, Ku70 and Ku80).

An additional aim will be to determine suitable concentrations of VE-821, PF-477736 and MK-1775 to use in cytotoxicity assays in combination with cisplatin and IR.

4.3 Materials and methods

4.3.1 Investigations of enzyme activation and inhibition by western blot

Activation of the ATR-CHK1-WEE1 pathway by cisplatin

Exponentially growing HeLa cells were exposed to cisplatin at a concentration of 3 μ M for time intervals of between 1 hour and 24 hours. Cell lysates were prepared as described in chapter 2.6 and analysed by western blot. Western blot membranes were incubated with antibodies raised against the principal phosphorylation target of ATR, CHK1 and WEE1 (Table 2.2 and section 1.4). Following HRP-conjugated secondary antibody binding and exposure to ECL substrate, the intensity of chemiluminescence at bands corresponding to pCHK1^{S345}, pCHK1^{S296} and pCDK1^{Y15} (O'Connell et al., 1997, Peasland et al., 2011, Okita et al., 2012) at each time-point was compared (Figure 4.1). Activation by cisplatin was compared to a positive control using 4-Nitroquinoline 1-oxide (4NQO), a known potent UV mimetic and activator of ATR (Chen et al., 2015).

Target enzyme inhibition as a function of inhibitor concentration

The extent to which each of the three inhibitors under investigation is able to prevent phosphorylation of the principal phosphorylation target of their respective substrate enzyme was investigated at multiple inhibitor concentrations. Exponentially growing HeLa, SiHa, C33A and CaSki cells were concurrently exposed to 3 μ M cisplatin alone or with increasing concentrations of VE-821, PF-477736 or MK-1775 for 24-hour incubations. ME-180 and HT-3 cells were exposed to 3 μ M cisplatin alone or with a single fixed concentration of inhibitor drug, determined in initial experiments with the other four cell lines. Cell lysates were prepared immediately following 24 hours exposure to the drug combinations and analysed by Western blot as described in Chapter 2.6. ATR activity was determined by measuring pCHK1^{S345}, CHK1 activity by measuring pCHK1^{S296} and WEE1 activity by measuring pCDK1^{Y15}. Percent (%) inhibition was calculated by comparison of the activity with cisplatin alone, as follows:

Control (DMSO) = *X*

3 μM Cisplatin = *Y*

3 μM Cisplatin + inhibitor = *Z*

$$\text{Fold activation by 3 } \mu\text{M cisplatin} = Y/X$$

$$\% \text{ inhibition at specific inhibitor concentration} = 100 - \left\{ \frac{(Z - X)}{(Y - X)} \times 100 \right\}$$

4.3.2 Single agent cytotoxicity of inhibitors of ATR, CHK1 and WEE1

Exponentially growing cells were seeded at known densities in 6 well plates and exposed to increasing concentrations of inhibitor in growth medium for 24 hours using an equivalent concentration of DMSO as a vehicle control as described in section 2.5. Following incubation in fresh medium for 10 - 14 days (dependent on cell growth rate) to allow colonies to form they were fixed, stained and counted. The survival at each inhibitor concentration was calculated relative to the DMSO control. Survival curves of relative colony survival against inhibitor concentrations were used to calculate the inhibitor concentration that resulted in 50% inhibition of colony survival relative to control (LC₅₀) for each of the inhibitors: VE-821; PF-477736; and MK1-775 as well as survival at a defined concentration. Inhibitor concentrations were chosen to range between those which caused minimal cytotoxicity to those which resulted in <10% colony survival in pilot experiments using HeLa cells.

4.4 Results

4.4.1 Activation of the ATR-CHK1-WEE1 pathway by cisplatin

Activation of all three enzymes, ATR, CHK1 and WEE1 by cisplatin (3 μ M), at levels comparable with positive control, 4NQO was observed at 8 hours and 24 hours (Figure 4.2). Subsequent activation and inhibition assays were therefore conducted following 24-hour exposure to cisplatin.

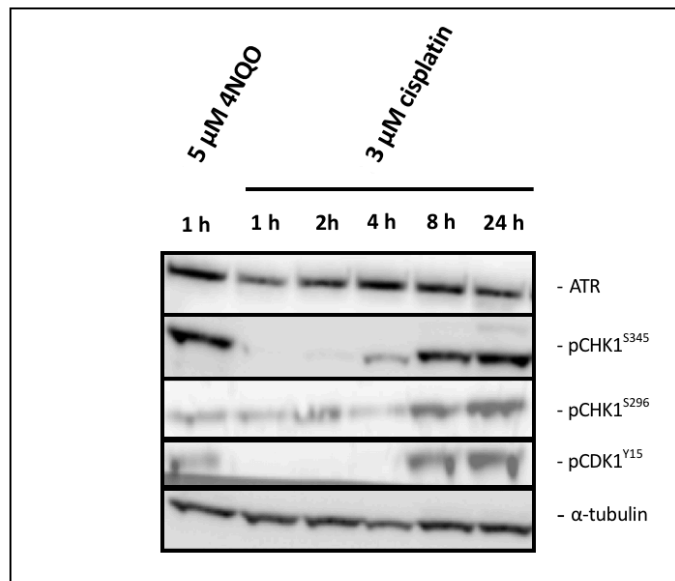


Figure 4.1 Representative Western blots showing protein bands corresponding to ATR and the principal phosphorylation targets of ATR CHK1 and WEE1 in HeLa cells.

HeLa cells were exposed to 3 μ M cisplatin for periods of time between 1 and 24 hours. Reliable activation of ATR, CHK1 and WEE1 was seen at 8 hours and 24 hours. Kinase activation by cisplatin was compared to that seen in a positive control using 4NQO

4.4.2 Target enzyme inhibition: ATR and VE-821

Concentration dependent inhibition of ATR by VE-821

HeLa, SiHa, C33A and CaSki cells were cultured in media containing 3 μ M cisplatin \pm VE-821 at increasing concentrations between 0.3 μ M and 30 μ M. After 24-hours exposure, cell lysates were prepared and analysed by Western blot as outlined, above. Concentration vs inhibition curves were used to calculate the concentration of VE-821 needed to achieve 50%

enzymatic inhibition (VE-821 IC₅₀) for each of these four cell lines. The mean IC₅₀ values for VE-821 fell over a narrow range of concentrations from 620 nM (C33A) to 840 nM (CaSki) (Figure 4.2).

Inhibition of ATR by equimolar concentrations of VE-821

Greater than 50% inhibition of ATR phosphorylation of CHK1 was observed at concentrations of VE-821 ≥ 1 μ M in all four cell lines: HeLa, SiHa, C33A and CaSki (Figure 4.2) so this concentration of VE-821 was further evaluated across the complete panel of six cell lines. To minimise inconsistencies associated with constitutive ATR activity, these assays were normalised to a control in which cells were exposed to DMSO only. This also revealed differences in the extent of ATR activation by cisplatin across the cell line panel. Activation was strongest in HeLa cells with a mean of 106-fold activation observed, and least in SiHa cells, with a mean activation of just 1.3-fold. Inhibition of cisplatin mediated ATR activation by 1 μ M VE-821 was observed to be more consistent, with greater than 50% inhibition observed in five out of the six cell lines. The greatest inhibition was seen in SiHa cells, with a mean inhibition of 93% and the lowest in ME-180 cells, with a mean inhibition of 43% (Figure 4.3).

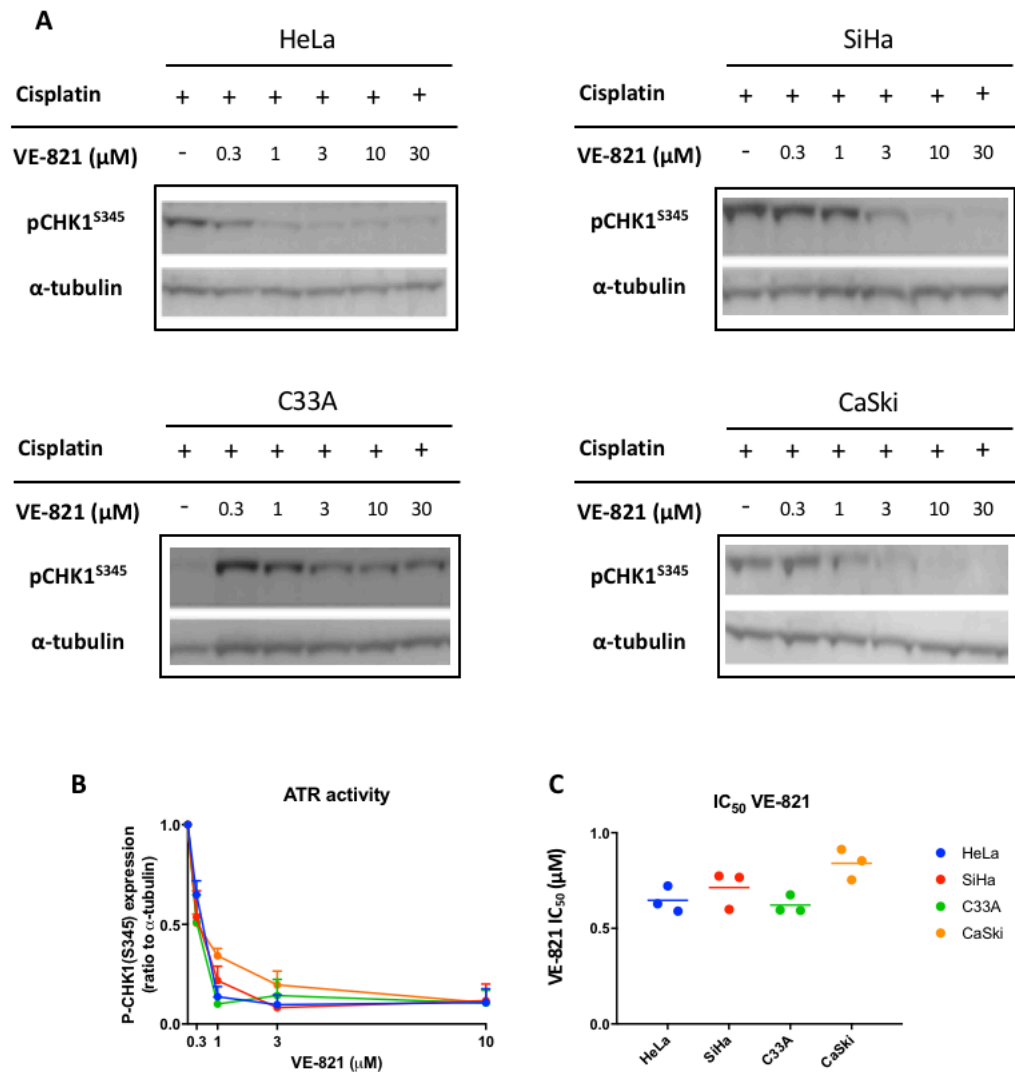


Figure 4.2 Concentration dependent inhibition of ATR by VE-821.

A: Representative Western blots for HeLa, SiHa, C33A and CaSki cells. **B:** pCHK1^{S345} levels in cells treated with cisplatin (3 μM) and increasing concentrations of VE-821 relative to levels in cells treated with cisplatin alone. Data are mean and SEM of 3 independent experiments **C:** Concentration of VE-821 required to achieve a 50% reduction in expression of pCHK1^{S345} compared to a cisplatin control (VE-821 IC₅₀) was calculated from the expression vs concentration curves (**B**). Data are the mean and individual values from three independent experiments

Cell line	HeLa			SiHa			C33A			CaSki			ME-180			HT-3		
Drug	DMSO	+C	+C +VE	DMSO	+C	+C +VE	DMSO	+C	+C +VE	DMSO	+C	+C +VE	DMSO	+C	+C +VE	DMSO	+C	+C +VE
pCHK1 ^{S345}																		
α-tubulin																		
Activation (fold)		106			1.3			3.2			17			5.6			4.8	
Inhibition (%)			80			93			79			65			43			57

Figure 4.3 Activation of ATR by cisplatin and inhibition by VE-821.

Cells were cultured with 3 μ M cisplatin (C) \pm 1 μ M VE-821 (VE). Representative Western blots are shown. Fold activation of ATR by cisplatin is given as a ratio of the pCHK1^{S345} band intensity to that of the untreated (DMSO) control. % inhibition is the percent-reduction in pCHK1^{S345} band intensity of the Cisplatin + VE-821 treated cells compared to that of cisplatin alone and normalised to the control. Figures given are a mean of at least two independent experiments. Experiments in which high levels of background ATR activity, out of keeping with other results, were excluded.

4.4.3 Target enzyme inhibition: CHK1 and PF-477736

Concentration dependent inhibition of CHK1 by PF-477736

The inhibition of CHK1 by increasing concentrations of PF-477736 (10 nM – 200 nM) was investigated in HeLa, SiHa, C33A and CaSki cells treated with 3 μ M cisplatin \pm PF-477736 prior to cell lysis and analysis of pCHK1^{S296} by Western blot. Concentration vs inhibition curves were used to calculate the concentration of VE-821 needed to achieve 50% enzymatic inhibition (PF-477736 IC₅₀) for each of these four cell lines (Figure 4.4). The mean values of PF-477736 IC₅₀ fell over a narrow (2-fold) range from 6.5 nM (CaSki) to 15 nM (SiHa).

Inhibition of CHK1 by equimolar concentrations of PF-477736

Greater than 50% inhibition of CHK1 auto-phosphorylation at Serine 296 by PF-477736 was observed at the concentrations \geq 50 nM in the cell lines for which IC₅₀ values were calculated. This concentration of inhibitor was then further evaluated in the complete panel of six cervical cancer cell lines. Normalising this panel of activation and inhibition results to an untreated control, again revealed that while there was considerable variation in the activation of CHK1 by cisplatin from just over two-fold (CaSki) to 141-fold (HeLa). Inhibition of cisplatin mediated activation of CHK1 was, however consistent across the cell line panel, with 50 nM PF-477736 causing between 79% (HT-3) and 100% (C33A) inhibition (Figure 4.5).

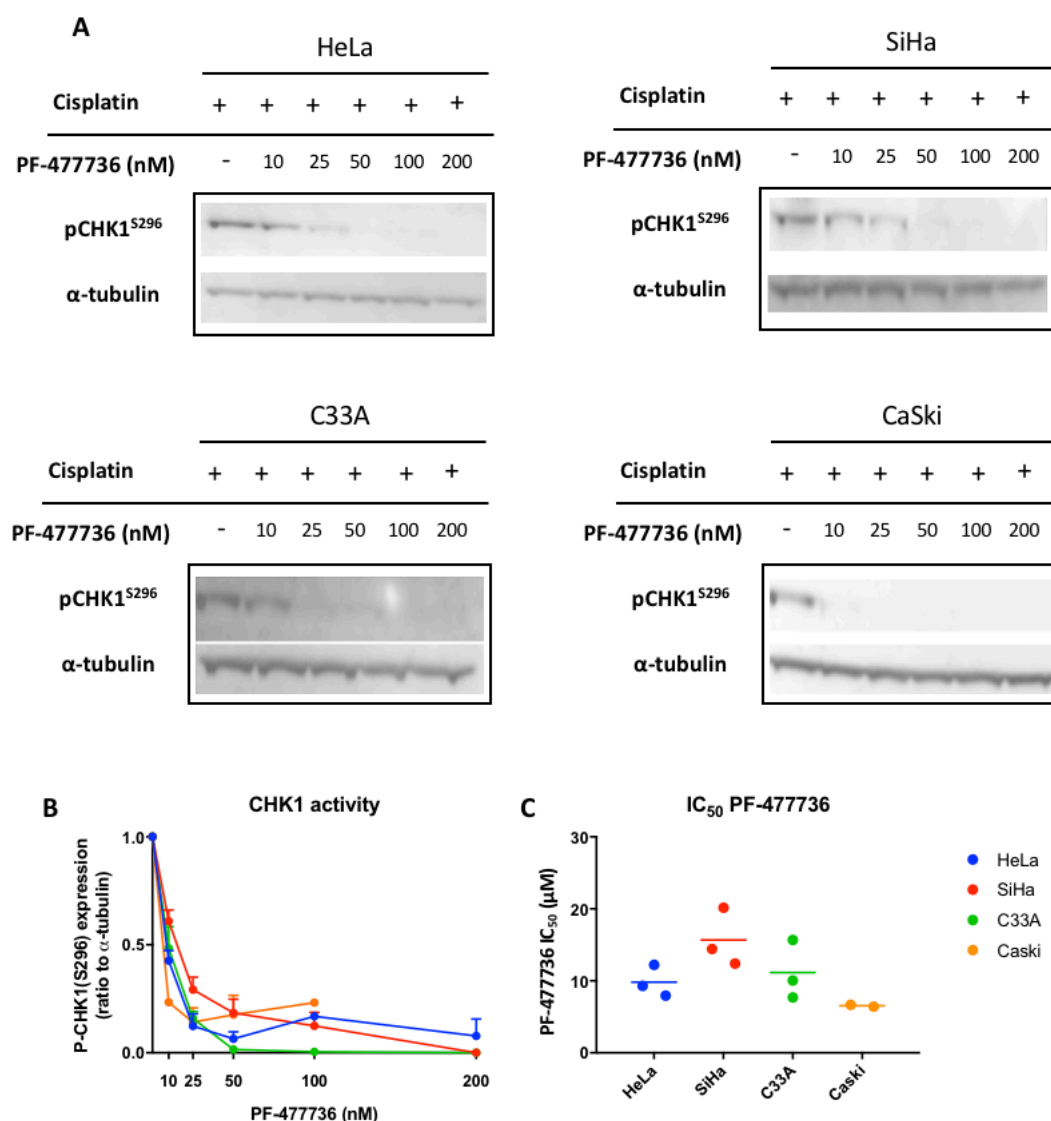


Figure 4.4 Concentration dependent inhibition of CHK1 by PF-477736.

A: Representative Western blots for HeLa, SiHa, C33A and CaSki cells. **B:** Phospho-CHK1(S296) levels in cells treated with cisplatin (3 μ M) and increasing concentrations of PF-477736 relative to levels in cells treated with cisplatin alone. Data are mean and SEM of 3 independent experiments. **C:** Concentration of PF-477736 required to achieve a 50% reduction in expression of pCHK1^{S296} compared to a cisplatin control (PF-477736 IC₅₀) was calculated from the expression vs concentration curves (**B**). Data are the mean and individual values from independent experiments.

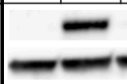
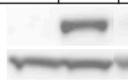
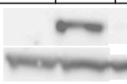
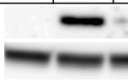
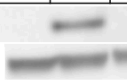
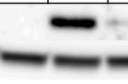






Cell line	HeLa			SiHa			C33A			CaSki			ME-180			HT-3		
Drug	DMSO	+C	+C +PF	DMSO	+C	+C +PF	DMSO	+C	+C +PF	DMSO	+C	+C +PF	DMSO	+C	+C +PF	DMSO	+C	+C +PF
pCHK1 ^{S296}																		
α -tubulin																		
Activation (fold)		141			14			43			2.2			26			6.2	
Inhibition (%)			96			85			100			82			80			79

Figure 4.5 Activation of CHK1 by cisplatin and inhibition by PF-477736.

Cells were cultured with 3 μ M cisplatin (C) \pm 50 nM PF-477736 (PF). Representative Western blots are shown. Fold activation of CHK1 by cisplatin is given as a ratio of the pCHK1^{296S} band intensity to that of the untreated (DMSO) control. % inhibition is the percent-reduction in pCHK1^{S296} band intensity of the Cisplatin + PF-477736 treated cells compared to that of cisplatin alone and normalised to the control. Figures given are a mean of at least two independent experiments. Experiments in which high levels of background CHK1 activity, out of keeping with other results, were excluded

4.4.4 Target enzyme inhibition: WEE1 and MK-1775

Concentration dependent inhibition of WEE1 by MK-1775

HeLa, SiHa, C33A and CaSki cells were cultured with 3 μ M cisplatin \pm MK-1775 at concentrations between 50 nM and 800 nM prior to probing for pCDK1^{Y15}. MK-1775 IC₅₀ was calculated for each of these four cell lines (Figure 4.6). In contrast to the results described for ATR and CHK1, the inhibition of WEE1 by MK-1775 in HeLa, SiHa, C33A and CaSki cells showed less consistency with an approximate 4-fold range in IC₅₀ values ranging from 130 nM (HeLa) to 520 nM (C33A).

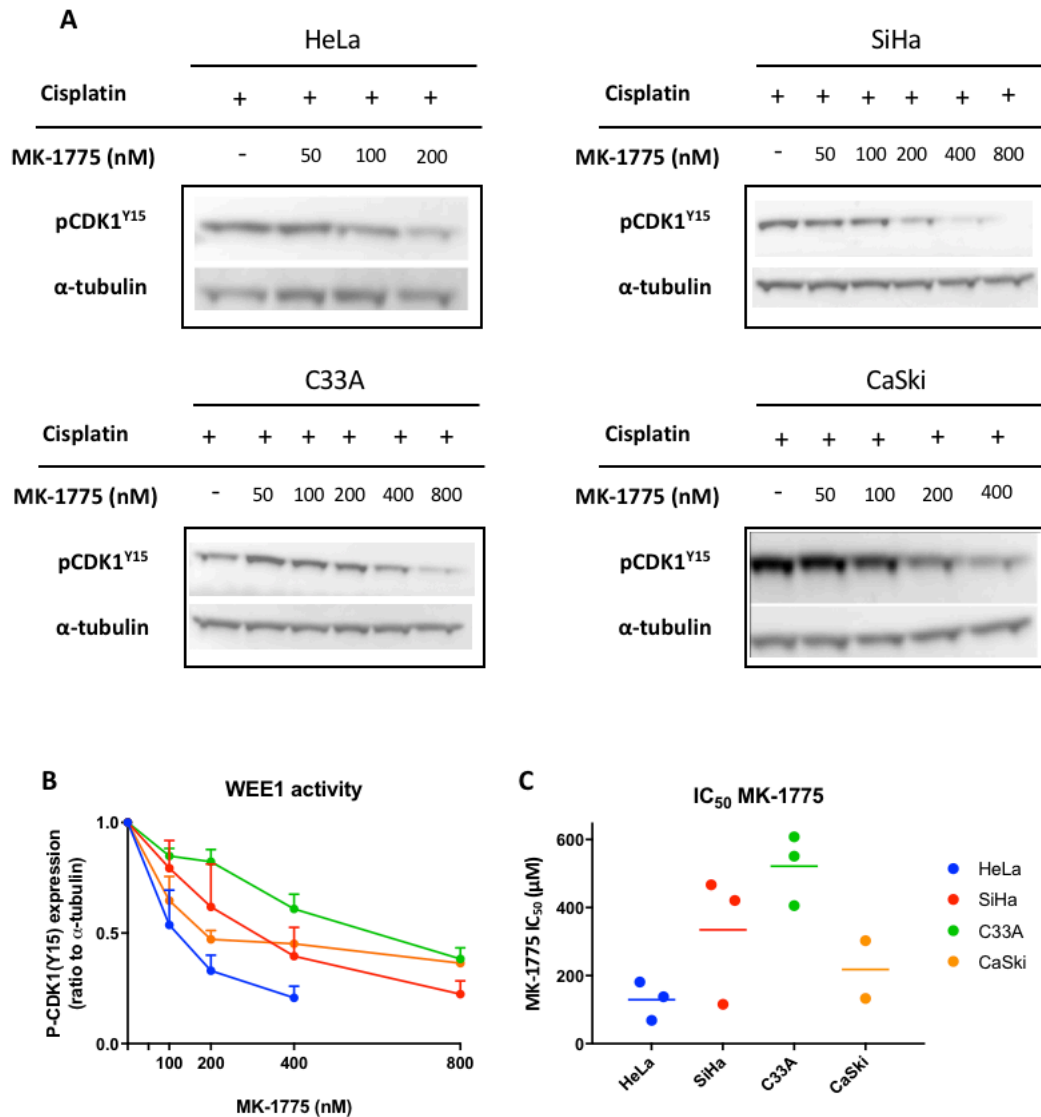


Figure 4.6 Concentration dependent inhibition of WEE1 by MK-1775.

A: Representative Western blots for HeLa, SiHa, C33A and CaSki cells. **B:** pCDK1^{Y15} levels in cells treated with cisplatin (3 μM) and increasing concentrations of MK-1775 relative to levels in cells treated with cisplatin alone. Data are mean and SEM of 3 independent experiments **C:** Concentration of MK-1775 required to achieve a 50% reduction in expression of pCDK1^{Y15} compared to a cisplatin control (MK-1775 IC₅₀) was calculated from the expression vs concentration curves. **(B).** Data are the mean and individual values from independent experiments.

Inhibition of WEE1 by equimolar concentrations of MK-1775

Greater than 50% inhibition of WEE1 by MK-1775 was not consistently observed in all four of the cell lines in the concentration range used. Given the substantial inhibition seen in HeLa and CaSki cells at 100 nM MK-1775 and the fact that higher concentrations resulted in

substantial single agent cytotoxicity (see section 4.5), a concentration of 100 nM was selected to expand into the full panel of six cervical cancer cell lines. In these experiments, a high level of constitutive pCDK1^{Y15} was noted. When the WEE1 inhibition was calculated and normalised to the background WEE1 activity, consistent inhibition of >50% was observed at 100 nM MK1775, ranging from 54% (SiHa) to >100% (ME-180): representing less than constitutive levels of phosphorylated CDK1 (Figure 4.7). Activation of WEE1 by cisplatin was more consistent than that seen of ATR and CHK1 but overall was less marked with a range of 1.2-fold (ME-180) to 2.8-fold (SiHa) (figure 4.7). This is likely to be a consequence of the high level of constitutive CDK1 phosphorylation observed.

Despite the differences described, none of the cell lines were consistently either the least or most susceptible to enzymatic inhibition by the three inhibitors under investigation. The results of these experiments confirm that the cell lines have intact ATR-CHK1-WEE1 pathways and that the individual constituent kinases are susceptible to inhibition by the small molecule inhibitors under investigation.

Cell line	HeLa			SiHa			C33A			CaSki			ME-180			HT-3		
Drug	DMSO	+C	+C +MK	DMSO	+C	+C +MK	DMSO	+C	+C +MK	DMSO	+C	+C +MK	DMSO	+C	+C +MK	DMSO	+C	+C +MK
pCDK1 ^{Y15}																		
α-tubulin																		
Activation (fold)		1.8			2.8			1.5			2.1			1.2			2.2	
Inhibition (%)			75			54			58			58			100			60

Figure 4.7 Activation of WEE1 by cisplatin and inhibition by MK-1775.

Cells were cultured with 3 μM cisplatin (C) +/- 100 nM MK-1775 (MK). Representative Western blots are shown. Fold activation of WEE1 by cisplatin is given as a ratio of the pCDK1^{Y15} band intensity to that of the untreated (DMSO) control. % inhibition is the percent reduction in pCDK1^{Y15} band intensity of the Cisplatin + MK-1775 treated cells compared to that of cisplatin alone and normalised to the control. Figures given are a mean of at least three independent experiments. Experiments in which cisplatin appeared to reduce WEE1 activity, out of keeping with other results, were excluded.

4.5 Single agent cytotoxicity

4.5.1 ATR inhibitor single agent cytotoxicity: VE-821

The single agent cytotoxicity of VE-821 at concentrations of 300 nM to 30 μ M was determined. Four out of the six, cell lines: HeLa; C33A; CaSki; and HT-3 showed very similar survival across the range of VE-821 concentrations used (Figure 4.8) and the calculated mean VE-821 LC₅₀ values fell within a narrow range for these cell lines of between 5.0 μ M (C33A) and 6.6 μ M (HeLa). The survival of both SiHa and ME-180 cells however, was substantially greater across all concentrations tested. The mean LC₅₀ for ME-180 was 14 μ M. SiHa cells failed to reach 50% survival in two out of three experiments and in a third the LC₅₀ was calculated to be 22 μ M.

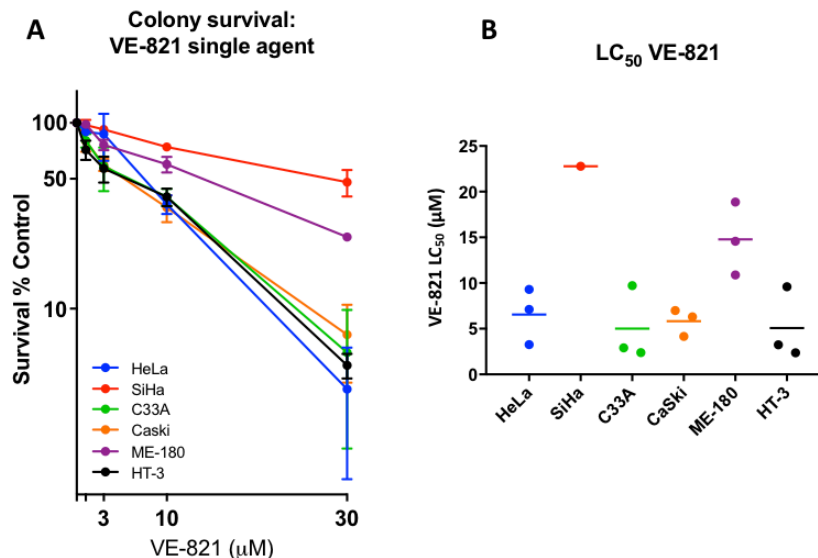


Figure 4.8 Single agent cytotoxicity of VE-821 in the cervical cancer cell line panel.

A: The Survival of six cervical cancer cell lines at increasing concentrations of VE-821. Cells were exposed to VE-821 at concentrations of 300 nM to 30 μ M in growth media for 24 hours. Following exposure, cells were incubated in fresh full growth media for at least five doubling times prior to fixation and staining. Survival is given as a percentage relative to the survival in a DMSO only control. Data are the means \pm SEM for three independent experiments. **B:** LC₅₀ values for VE-821 in six cervical cancer cell lines. The calculated mean value for the concentration of VE-821 required to achieve a 50% reduction in survival compared to a DMSO control for each of the cervical cancer cell lines, along with the individual values for three independent experiments are shown. 50% survival was reached in one out of three experiments with SiHa cells.

4.5.2 CHK1 single agent cytotoxicity: PF-477736

The single agent cytotoxicity of PF-477736 at concentrations of 100 nM to 800 nM was determined. In contrast to the results for VE-821, the cells lines showed a greater variation in survival across the range of concentrations used (Figure 4.9). Despite this, the range of PF-477736 LC₅₀ in five of the six cell lines: HeLa; SiHa; C33A; CaSki; and ME-180 fell within a < 4-fold range of between < 100 nM (CaSki) and 320 nM (ME-180). This inhibitor, however showed substantially less cytotoxicity in HT-3 cells than the other cell lines with two out of three experiments failing to reach 50% survival and a third giving an LC₅₀ value of 1300 nM. At higher concentrations of PF-477736 the survival of the cell lines appeared to diverge, with 400 nM PF-477736 giving survivals in a range from 5% (CaSki) to 36% (ME-180).

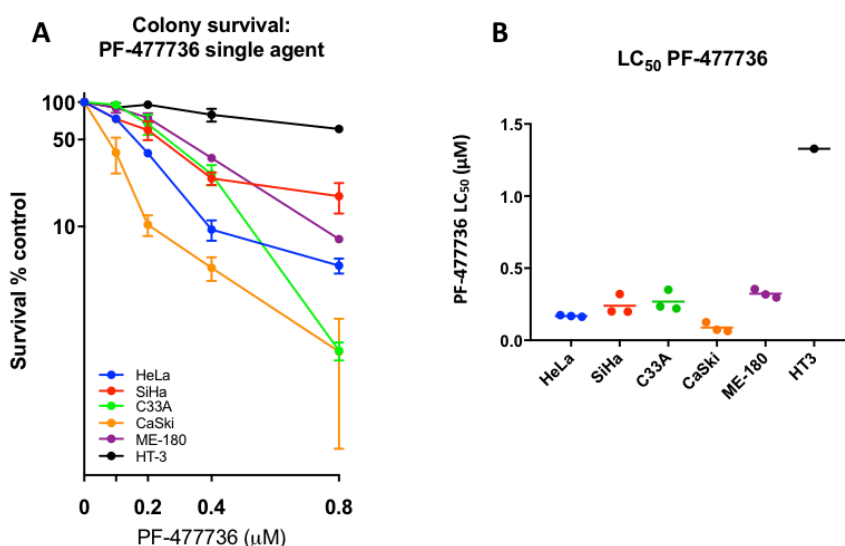


Figure 4.9 Single agent cytotoxicity of PF-477736 in the cervical cancer cell line panel.

A: The Survival of six cervical cancer cell lines at increasing concentrations of PF-477736. Cells were exposed to PF-477736 at concentrations of 100 nM to 800 nM in growth media for 24 hours. Following exposure, cells were incubated in fresh full growth media for at least five doubling times prior to fixation and staining. Survival is given as a percentage relative to the survival in a DMSO only control. Data are the means \pm SEM for three independent experiments. **B:** LC₅₀ values for PF-477736 in six cervical cancer cell lines. The calculated mean value for the concentration of PF-477736 required to achieve a 50% reduction in survival compared to a DMSO control for each of the cervical cancer cell lines, along with the individual values for three independent experiments are shown. 50% survival was reached in one out of three experiments with SiHa cells.

4.5.3 WEE1 inhibitor single agent cytotoxicity: MK-1775

The single agent cytotoxicity of MK-1775 at concentrations of 50 nM to 1.6 μ M was determined. The cell lines showed a variation in survival across the concentration range with some clustering of LC₅₀ values (Figure 4.10). Four out of the six cell lines showed MK-1775 LC₅₀ values in a narrow range of between 250 nM (C33A) and 300 nM (CaSki). ME-180 showed a slightly higher LC₅₀ of 400 nM and the value for HT-3 cells was substantially higher at 720 nM.

As with experiments using PF-477736, divergence of survival between the cell lines was seen at higher concentrations of MK-1775. At 800 nM MK-1775 the difference in survival between the least and most sensitive was greater than 20-fold, with HeLa survival being 2% and HT-3 survival being 46%.

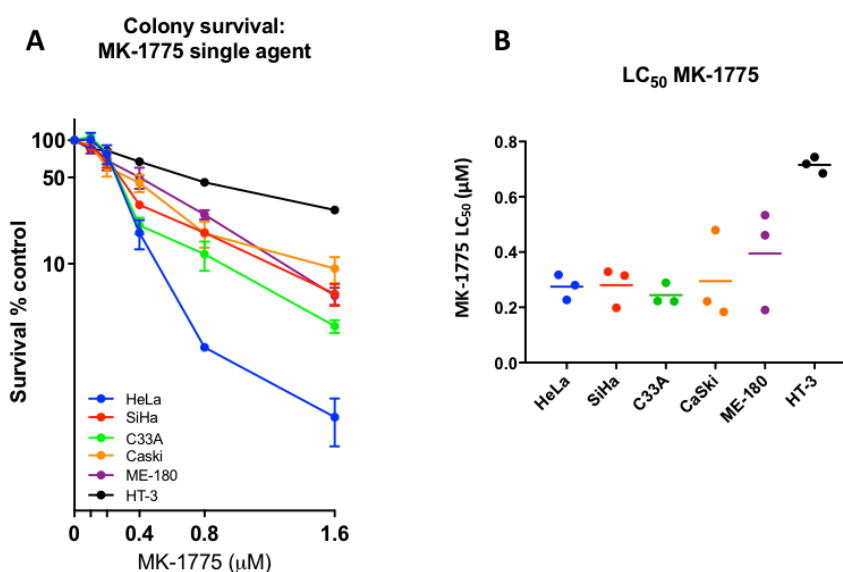


Figure 4.10 Single agent cytotoxicity of MK-1775 in the cervical cancer cell line panel.

A: The Survival of six cervical cancer cell lines at increasing concentrations of MK-1775. Cells were exposed to MK-1775 at concentrations of 100 nM to 1.6 μ M in growth media for 24 hours. Following exposure, cells were incubated in fresh full growth media for at least five doubling times prior to fixation and staining. Survival is given as a percentage relative to the survival in a DMSO only control. Data are the means \pm SEM for three independent experiments. **B:** LC₅₀ values for MK-1775 in six cervical cancer cell lines. The calculated mean value for the concentration of MK-1775 required to achieve a 50% reduction in survival compared to a DMSO control for each of the cervical cancer cell lines, along with the individual values for three independent experiments are shown.

The results of the single agent cytotoxicity assays are summarised by the inhibitor LC₅₀ values obtained as given in Table 4.1. Notable results include that SiHa cells were the most resistant to the cytotoxic effects of VE-821, despite being the cell line which showed the most overall inhibition of ATR at 1 µM. HT-3 cells were the most resistant to the cytotoxic effects of both PF-477736 and MK-1775 but showed average inhibition of CHK1 and WEE1, respectively at the concentrations tested. ME-180 cells were amongst the two most resistant cell lines for all of the inhibitors and whilst this cell line showed the greatest inhibition of WEE1 by MK-1775, it also showed the least inhibition of ATR by VE-821. The single agent cytotoxicity results are unlikely to be explained by the extent of inhibition of the target kinases alone and point to a much more complex interplay of factors that determine sensitivity to these drugs.

Cell line	VE-821 LC ₅₀ µM ± SEM	PF-477736 LC ₅₀ nM ± SEM	MK-1775 LC ₅₀ nM ± SEM
HeLa	6.6 ± 1.7	168 ± 3.0	275 ± 26
SiHa	22.7*	239 ± 20	281 ± 42
C33A	5.0 ± 2.3	268 ± 41	245 ± 22
CaSki	5.8 ± 0.8	88 ± 19	295 ± 93
ME-180	15 ± 2.3	323 ± 17	395 ± 105
HT-3	5.1 ± 2.3	1328*	716 ± 17

Table 4.1 LC₅₀ values for each VE-821, PF-477736 and MK-1775 in all six cervical cancer cell lines.

*The mean ± Standard error of the mean for three independent experiments is given (*indicates that survival fell to 50% in one-out of three experiments with this cells line and drug).*

4.6 Correlations between cell line characteristics, target inhibition and single agent cytotoxicity.

Correlation analyses were performed to investigate relationships between the cell line characteristics, described in Chapter 3, and the activity of the inhibitors determined in this chapter.

4.6.1 Correlations between enzyme inhibition and single agent cytotoxicity

It would be expected that some relationship should exist between the activity of the inhibitor against its target enzyme and the relative cytotoxicity of that inhibitor to the cancer cell. However, no correlation was observed between the cytotoxicity (LC_{50}) and target inhibition at a fixed concentration for any of the three inhibitors (Figure 4.11). When an alternative measure of cytotoxicity (colony survival at a fixed concentration of inhibitor) is used in order to avoid the clustering of LC_{50} values seen with all inhibitors, neither is there a relationship observed between cytotoxicity and target enzyme inhibition for any of the three inhibitors (Figure 4.12).

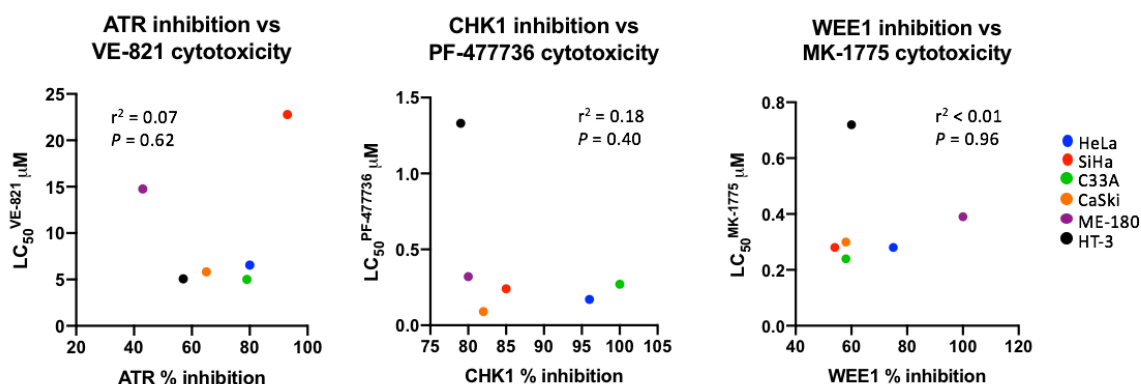


Figure 4.11 Scatter plots of target enzyme % inhibition vs cytotoxicity (LC_{50}).

Inhibition is given as the % inhibition at a fixed concentration of inhibitor drug (1 μM VE-821, 50 nM PF-477736 and 100 nM MK-1775). Cytotoxicity is given as the inhibitor specific concentration at 50% colony survival (LC_{50}).

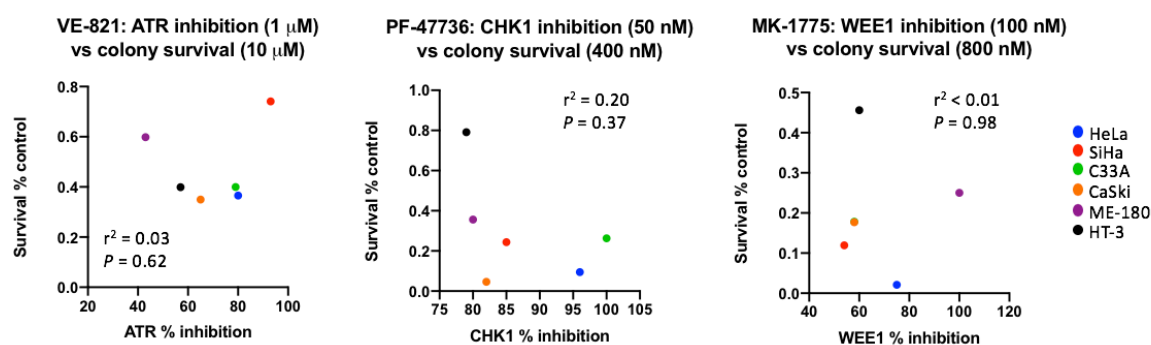


Figure 4.12 Scatter plots of target enzyme % inhibition vs cytotoxicity (% colony survival at fixed inhibitor concentrations).

Inhibition is given as the % inhibition at a fixed concentration of inhibitor drug (1 μ M VE-821, 50 nM PF-477736 and 100 nM MK-1775) as determined in experiments described in chapter 4.4). Cytotoxicity is given as % colony survival at a fixed concentration of inhibitor drug (10 μ M VE-821, 400 nM PF-477736 and 800 nM MK-1775) as determined in colony formation assays.

Given the lack of correlation between target enzyme inhibition and the LC_{50} , the % enzyme inhibition was compared to the % inhibition of colony survival at the concentrations used for the enzyme activation/ inhibition assays. This showed that at the specific concentrations used for each enzyme (1 μ M VE-821, 50 nM PF-477736 and 100 nM MK-1775) greater than 50% enzyme inhibition and less than 30% inhibition of colony survival was seen for the majority of cell line-inhibitor combinations, though ME-180 cells were particularly sensitive to VE-821 and CaSki cells were particularly sensitive to PF-477736 (Table 4.2). These concentrations of inhibitors, therefore gave a pragmatic balance between adequate enzyme inhibition without excessive single agent cytotoxicity for investigating the relative potential of the three inhibitors as sensitisers of cisplatin and ionising radiation.

Cell line	1 μ M VE-821		50 nM PF-477736		100 nM MK-1775	
	% ATR inhibition \pm SD	% inhibition of colony survival \pm SEM	% CHK1 inhibition \pm SD	% inhibition of colony survival \pm SEM*	% WEE1 inhibition \pm SD	% inhibition of colony survival \pm SEM
HeLa	79 \pm 9	10 \pm 4	96 \pm 4	30 \pm 0.3	75 \pm 20	0 \pm 13
SiHa	92 \pm 10	3 \pm 6	85 \pm 22	23 \pm 7	54 \pm 40	0 \pm 5
C33A	78 \pm 30	20 \pm 7	100 \pm 0.2	16 \pm 12	58 \pm 22	13 \pm 5
CaSki	65 \pm 4	20 \pm 10	82 \pm 25	45 \pm 9	58 \pm 59	9 \pm 5
ME-180	43 \pm 5	2 \pm 5	80 \pm 20	19 \pm 7	> 100	13 \pm 9
HT-3	57 \pm 27	29 \pm 5	79 \pm 11	7 \pm 4	60 \pm 36	15 \pm 5

Table 4.2 Concentration specific target enzyme inhibition and inhibition of colony survival for the cervical cancer cell lines using 1 μ M VE-821, 50 nM PF-477736 and 100 nM MK-1775.

*Enzyme inhibition data is derived from that given in section 4.4 and is data derived from at least 2 independent experiments. For colony survival data Mean \pm SEM is given from at least three independent experiments. *Data for colony survival at 50 nM PF-477736 is interpolated from the survival curves.*

4.6.2 Correlations with baseline protein expressions

Single agent cytotoxicity

There was no relationship between the cytotoxicity (LC₅₀) of VE-821, PF-477736 or MK-1775 and the expressions of the kinases targeted by them in this cell line panel. Neither was there any significant correlation between the expression of the key DDR proteins ATM, DNA-PKcs, Ku 70 or Ku 80 and the single agent cytotoxic effects of PF-477736 or MK-1775 (data not shown). However, ATM and DNA-PKcs did appear to show some relationship to VE-821 cytotoxicity. Neither correlation significant was significant, but HT-3 cells had particularly low ATM and DNA-PKcs expression and were the most sensitive to VE-821 (Figure 4.13).

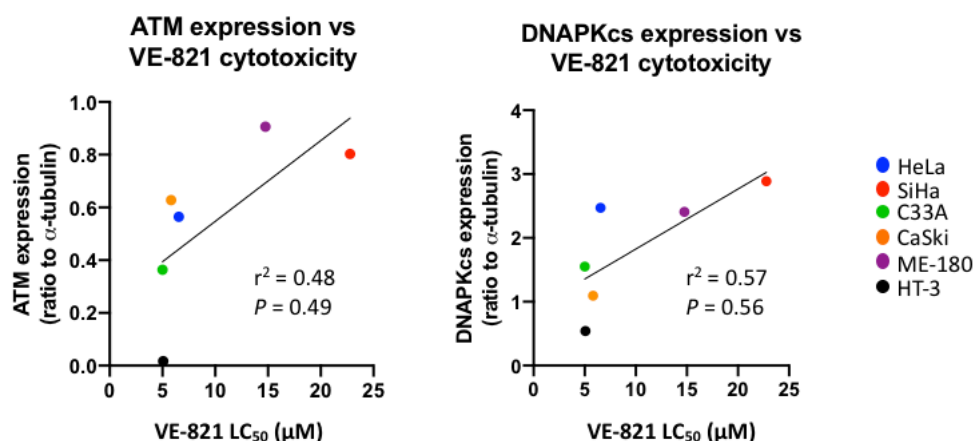


Figure 4.13 Scatter plots of ATM and DNA-PKcs expression vs single agent cytotoxicity.

The expressions of ATM and DNA-PKcs proteins are shown as a ratio to loading control (α -tubulin). Cytotoxicity is given as the inhibitor specific concentration at 50% colony survival in colony formation assays (LC_{50}).

Given the observed clustering of LC_{50} values, as described in chapter 4.5 and the apparent divergence of colony survival results at higher concentrations of PF-477736 and MK-1775, further correlations were tested using colony survival at 400 nM PF-477736 and 800 nM MK-1775 as the measure of cytotoxicity. There was however, no relationship seen between this measure of single agent cytotoxicity and baseline protein expressions using these values (data not shown).

Target enzyme inhibition

As IC_{50} values were calculable for just four of the six cervical cancer cell lines, correlations between the extent of inhibition at single inhibitor concentrations (1 μ M VE-821, 50 nM PF-477736 and 100 nM MK-1775) were tested for correlation with the baseline expression of the associated target enzyme. Potential relationships were observed between i) the baseline expression of ATR and the inhibition of ATR by VE-821, and ii) the baseline expression of WEE1 and the inhibition of WEE1 by MK-1775 (Figure 4.14). In both cases, higher baseline expression appeared to be associated with greater enzyme inhibition at the stated concentrations. Neither relationship reached significance on Pearson correlation testing, which may be due to the small number of data points. Additionally, the correlation between

WEE1 expression and inhibition by MK-1775, does appear to be driven by ME-180, which appears as an outlier in both expression and inhibition datasets.

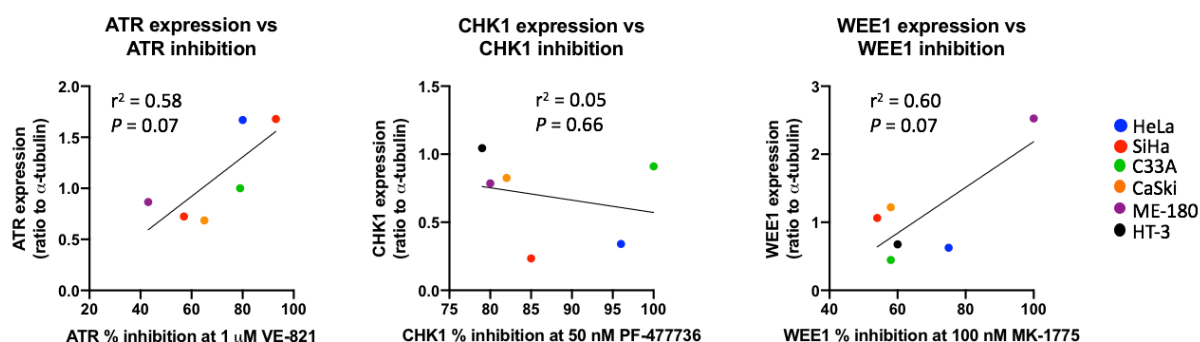


Figure 4.14 Correlations between inhibitor % target enzyme inhibition and baseline expressions of G2/M cell cycle checkpoint kinases. Scatter plots of the % inhibition of ATR, CHK1 and WEE1 at fixed concentrations vs the baseline expressions of the target enzyme for inhibition and the immediate downstream kinase or phosphorylation target. The expression of ATR, CHK1 and WEE1 are shown as a ratio to loading control (α -tubulin).

In summary, correlation analysis has revealed potential relationships between results described in this chapter and baseline characteristics of the cell lines explored in chapter 3. While there were no relationships seen between the target enzyme inhibition and single agent cytotoxicity of the ATR, CHK1 and WEE1 inhibitors, some degree of correlation was noted to exist between baseline expression of ATR and the extent of its inhibition by VE-821, and between baseline expression of WEE1 and its inhibition by MK-1775. Additionally, possible positive correlations were observed between VE-821 cytotoxicity and both ATM and DNA-PKcs baseline expression. Further correlation analysis between cell growth (doubling time) and the single agent cytotoxicity of all three inhibitors revealed no relationship (data not shown).

4.7 Discussion

Consistent, concentration dependent inhibition of ATR and CHK1 was observed when HeLa, SiHa, C33A and CaSki cells were exposed to increasing concentrations of VE-821 and PF-477736, respectively with IC_{50} values falling within narrow ranges. Inhibition of WEE1 by MK-1775 showed a greater variation in these initial assays and with a wider range of MK-1775 IC_{50} values. Expanding the inhibition assays at a fixed concentration of inhibitors to all

six cell lines and controlling for background revealed high levels of constitutive pCDK1^{Y15}. This resulted in comparatively small increases in CDK1 phosphorylation in response to WEE1 activation by cisplatin and hence a smaller dynamic range from which to measure inhibition by MK-1775. When the baseline levels of target phosphorylation were controlled for, consistent inhibition levels of > 50% were seen in all cell-inhibitor combinations except that with ME-180 cells and the ATR inhibitor VE-821.

The presence of high levels of pCDK1^{Y15} in untreated cells could suggest a high level of WEE1 activity. However, WEE1 activity promoted by high levels of replication stress would likely occur along with high levels of ATR and CHK1 activity in untreated cells, which was not seen, making an alternative explanation more likely. Phosphorylated CDK1 may exist in low levels of replication stress as phosphorylation of CDK1 at Y15 is not solely dependent on WEE1 activity. Cdc25c (whose function is also dependent on CHK1 phosphorylation) also influences the phosphorylated state of CDK1 (Sorensen and Syljuasen, 2012). CDK1 also interacts with and is phosphorylated by a number of other important kinases that are not involved in the DNA damage response. One such kinase is Myelin transcription factor 1 (MYT1), which is implicated in the G2/M checkpoint response (de Gooijer et al., 2017, Chow and Poon, 2013). MYT1 phosphorylates CDK1 at tyrosine 15 (Y15) as well as at tyrosine 14 (Y14) (Welburn et al., 2007, Chow and Poon, 2013), and the antibody used may not discriminate between these residues.

Overall, there was little consistency in the profile of cytotoxicity amongst the six cervical cancer cell lines across the three inhibitors used, however, a number of results are worthy of further discussion. ME-180 cells appeared amongst the most resistant to the cytotoxic effects of all three inhibitors. This was in keeping with the observation that these cells also expressed the highest levels of ATM: ATM having been previously described as a determinant of sensitivity to ATR inhibition (Kwok et al., 2016, Middleton et al., 2015). Consistent with this was the finding that the HPV-negative and RB1/TP53 mutated cell line HT-3 was amongst the most sensitive to the ATR inhibitor and expressed the least ATM in baseline expression assays (Chapter 3). HT3 cells were, however the least sensitive to both the CHK1 inhibitor and the WEE1 inhibitor.

This difference in the response of the HT-3 cells to the cytotoxic effects of ATR inhibition versus CHK1 or WEE1 inhibition, despite similar levels of target enzyme inhibition across the three inhibitors, points at subtle differences in the roles of the kinases in the DDR and confirms that the ATR-CHK1-WEE1 pathway does not exist or act in isolation from other responses to DNA damage. The cells response to the inhibitors was also not solely dependent on the extent of enzymatic inhibition at a given concentration. This is further confirmed by the observation that whilst SiHa cells were the most resistant to VE-821 cytotoxicity, they showed the greatest extent of inhibition of ATR at the concentration tested (Table. 4.2).

Depletion of the human Ku proteins or upregulation of DNA-PKcs has previously been shown confer sensitivity to ATR and CHK1 inhibition (Middleton et al., 2015, Massey et al., 2016). No clear relationship was observed between the levels of expression of Ku70 or Ku80 and the cytotoxicity of the inhibitors in the cell line panel. However, in contrast to this evidence the cervical cancer cells with low DNA-PKcs expression reported here were more sensitive to ATR inhibitor cytotoxicity, though this should be interpreted with caution the non-significant nature of the correlation.

4.8 Conclusions

With reference to the aims and objectives set out at the start of this chapter:

- ATR, CHK1 and WEE1 were inhibited in a concentration dependent manner by VE-821, PF-477736 and MK-1775, respectively. When the background activity or baseline phosphorylation of the downstream target kinase was controlled for, enzyme inhibitions fell within a consistent range, with similar potencies across the cell line panel.
- The cervical cancer cell lines had a variable response to the cytotoxic effects of the ATR, CHK1 and WEE1 inhibitors that was not dependent of the extent of target inhibition or the baseline level of checkpoint kinase expression.
- The cytotoxic effects of the ATR inhibitor VE-821 may be related to the baseline expression levels of both ATM and DNA-PKcs, though it is difficult to draw conclusions in this small cell line panel. VE-821 cytotoxicity did not appear to be related to expression of any of the other proteins measured

- CHK1 and WEE1 inhibition by PF-477736 and MK-1775, respectively did not show any correlation with baseline DDR proteins measured.

Experiments reported in this chapter allowed the determination of suitable fixed concentrations of VE-821, PF-477736 and MK-1775 to use in cytotoxicity assays in combination with cisplatin and IR (1 μ M VE-821, 50 nM PF-477736 and 100 nM MK-1775). These concentrations, in general, resulted in greater than 50% target enzyme inhibition while causing less than 30% inhibition of colony survival as single agents (Table 4.2).

5 Sensitisation of cervical cancer cell lines to cisplatin and ionising radiation using inhibitors of ATR, CHK1 and WEE1

5.1 Introduction

Results of experiments detailed in the previous chapter identified a spectrum of sensitivity to ATR, CHK1 and WEE1 inhibitor single agent cytotoxicity with no obvious consistency in the rank order of sensitivity or relationship with target inhibition or DDR protein expression. Western blot analysis provided confidence that substantial target enzyme inhibition was achieved at inhibitor concentrations that showed modest single agent cytotoxic effects.

The overall aim of this thesis was to determine the potential of inhibitors of the intra-S and G2/M cell cycle checkpoint kinases to improve cervical cancer treatment and to understand the underlying biological mechanisms that may underlie such improvements. The standard of care treatments for cervical cancer are cisplatin and ionising radiation (IR) used alone or in combinations as described in Chapter 1. The aim of this chapter was to compare the extent to which the inhibitors enhance the cytotoxicity of IR and cisplatin and to determine if this ability was related to any of the parameters measured in chapters 3 and 4.

Cisplatin and IR produce different DNA lesions that are repaired by different DNA repair pathways (Chapter 1). Both agents, however result in the key ATR-CHK1 activating single-strand-double-strand junctions (Hoeijmakers, 2001) and, more importantly lead to the presence of collapsed replication forks (Paulsen and Cimprich, 2007, Nam and Cortez, 2011). It would therefore be expected that both insults will invoke a strong ATR-CHK1-WEE1 pathway induction response that would be amenable to inhibition by inhibitors of these enzymes. In respect of cisplatin, this is shown in results described in Chapter 4 and the activation of this pathway by IR is established through investigations into inhibition of this pathway in radio-resistant breast cancer tissue (Zhang et al., 2016) and recently in studies involving human squamous cancers (HNSCC) (Dillon et al., 2017). The rationale for ATR, CHK1 and WEE1 inhibitor combinations as a strategy in cervical cancer treatment is therefore strong and ATR, CHK1 or WEE1 knockdown or pharmacological inhibition has been reported

to sensitise human cancer cells and xenografts to cisplatin and IR, as reviewed in Chapter 1.5.

Single agent cytotoxicity did not reflect the extent of target inhibition across the cell line panel and there are limitations in estimating this inhibition by Western blot. For these reasons a fixed concentration of each of the inhibitors, rather than concentrations that caused a defined level of target inhibition, was used to study the chemo- and radio-sensitisation. Concentrations were selected that showed good inhibition of the target enzyme as detailed in Table 4.2.

5.2 Aims and Objectives

The aims of the investigations described in this chapter were:

1. To determine the relative sensitivity of the six cervical cancer cell lines to cisplatin and ionising radiation (IR).
2. To determine the relative potential of the ATR, CHK1 and WEE 1 inhibitors: VE-821, PF-477736 and MK-1775, respectively to sensitise cervical cancer cell lines to cisplatin and ionising radiation.

This will enable the following hypotheses to be tested:

1. Sensitisation of cell lines to cisplatin by ATR, CHK1 or WEE1 inhibitors will be dependent on the intrinsic sensitivity of the cell lines to cisplatin.
2. Sensitisation of cell lines to IR by ATR, CHK1 or WEE1 inhibitors will be dependent on the intrinsic sensitivity of the cell lines to IR.
3. Sensitisation of cell lines to cisplatin or IR will depend on the single agent cytotoxicity in of the inhibitor.

5.3 Materials and methods

5.3.1 Colony formation assays with cisplatin and ionising radiation

Exponentially growing cells were seeded at known densities in 6 well plates and exposed to increasing concentrations of cisplatin or increasing doses of ionising radiation (IR) in order to

assess the cell lines' intrinsic sensitivity to cisplatin and IR. Exposure to cisplatin was for 24 hours in all cases. Following exposure to cisplatin, the growth media was changed to fresh full media and the cells were incubated for at least five doubling times as described in Chapter 2.5.1. For IR sensitivity and sensitisation assays, the IR dose was delivered in a single fraction using a D3300 X-ray system (Gulmay Medical Ltd. Chertsey, UK). For IR-only assays, the growth media was not changed prior to incubation for five doublings. For IR + inhibitor assays, the growth media was changed to fresh full media following 24-hour drug exposure as described in Chapter 2.5.4.

The results of these assays were used to determine suitable concentration and dose ranges for sensitisation experiments using fixed concentration ATR, CHK1 and WEE1 inhibitors in the cell lines. Colony formation assays assessing the sensitisation of the cell lines to cisplatin and IR were carried out as described in Chapter 2.5.3 and Chapter 2.5.4. In all sensitisation assays, fixed concentrations of inhibitor drug were used, as described in Chapter 5.1, above. These were 1 μ M VE821, 50 nM PF-477736 and 100 nM MK-1775.

5.4 Results

5.4.1 Cell line sensitivity to cisplatin and ionising radiation alone

Sensitivity to cisplatin

The six cervical cancer cell lines showed a range of sensitivity to cisplatin. There was just over a two-fold difference in Cisplatin LC₅₀ values between the least sensitive cell line (HeLa) and the most sensitive (SiHa), as shown in Table 5.1. There was no clear relationship between cisplatin cytotoxicity and cell line HPV, p53 or pRB status: the HPV negative and p53 mutated cell lines C33A and HT-3 showed average sensitivity to cisplatin across the concentration range used (Figure 5.1). Nor was there any relationship seen between cisplatin cytotoxicity and baseline expression of any of the cell cycle or DDR proteins measured, as described in Chapter 3 (data not shown).

Potential relationships were found between cisplatin cytotoxicity and cisplatin mediated activation of both ATR and CHK1 (Figure 5.2). Cisplatin induced ATR, CHK1 and WEE1 activity to differing extents across the cell lines (Chapter 4). Activation of ATR and CHK1 was greatest

in HeLa cells, which showed the least sensitivity to cisplatin. SiHa cells, which were the most sensitive to cisplatin cytotoxicity had amongst the lowest ATR activation and CHK1 activation. Though Pearson correlation analysis suggested a significant correlation in the case of ATR, the clustering of ATR activation and cisplatin LC₅₀ and the likely heavy reliance of the outlying HeLa result for both parameters indicates that whilst extremes may fit the hypothesis that cisplatin sensitivity is related to ATR/CHK1 activity, it is not possible to determine if there is a true correlation with such a small panel of cells. There was no relationship found between cisplatin activation of WEE1 and cisplatin cytotoxicity.

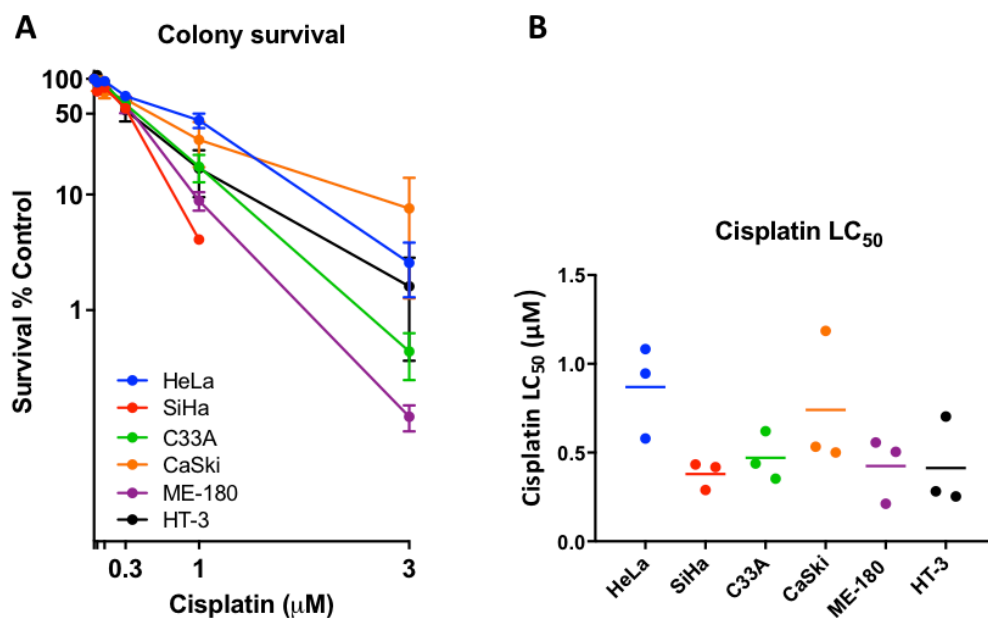


Figure 5.1 Cisplatin cytotoxicity in the cervical cell line panel.

A: The survival of six cervical cancer cell lines at increasing concentrations of cisplatin. Cells were exposed to cisplatin at concentrations of 0.03 μM to 3 μM in growth media for 24 hours. Following exposure, cells were incubated in fresh growth media for at least five doubling times prior to fixation and staining. **B:** LC₅₀ values for cisplatin in the cervical cancer cell lines. The calculated mean cisplatin concentration required to cause 50% reduction in survival compared to control, along with the individual values for three individual experiments are given. Data are from three individual experiments and normalised to control.

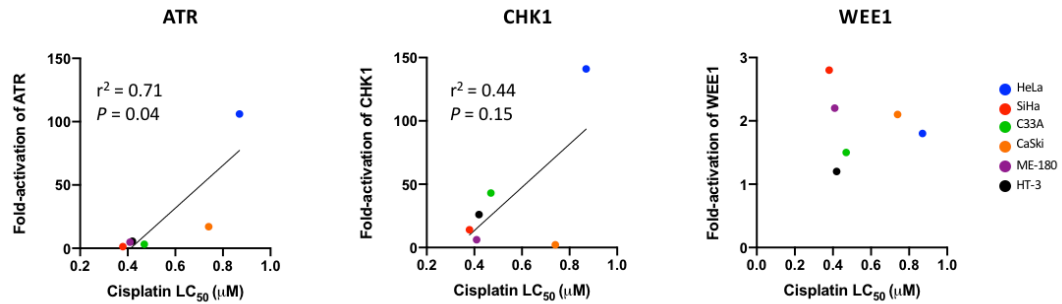


Figure 5.2 Correlations between cisplatin cytotoxicity and relative activation of target enzymes by cisplatin in cervical cancer cell lines.

Scatter plots of the concentration of cisplatin alone required to reduce colony survival to 50% compared to an untreated control vs the fold-activation over baseline of each of the enzymes: ATR, CHK1 and WEE1 in response to exposure to cisplatin, as determined in experiments described in chapter 4. All values correspond to the means of at least two independent experiments.

Sensitivity to IR

Similar to that found with cisplatin, there was some variation in the sensitivity of the cell lines to IR, but over a fairly narrow range (Figure 5.3). There was a just under two-fold difference between the dose of IR required to reduce colony survival by 50% compared to control (IR LD₅₀) between the most sensitive (C33A: 1.3 Gy) and the least sensitive (HeLa: 2.5 Gy). The four remaining cell lines all had LD₅₀ values of between 1.5 Gy and 1.8 Gy. The order of sensitivity of the cell line panel was not similar for cisplatin and IR, though ME-180 and HT-3 cells were amongst the three most sensitive cell lines and HeLa was the least sensitive in each case. The sensitivity of the cell lines to IR did not appear related to HPV, p53 or pRB status.

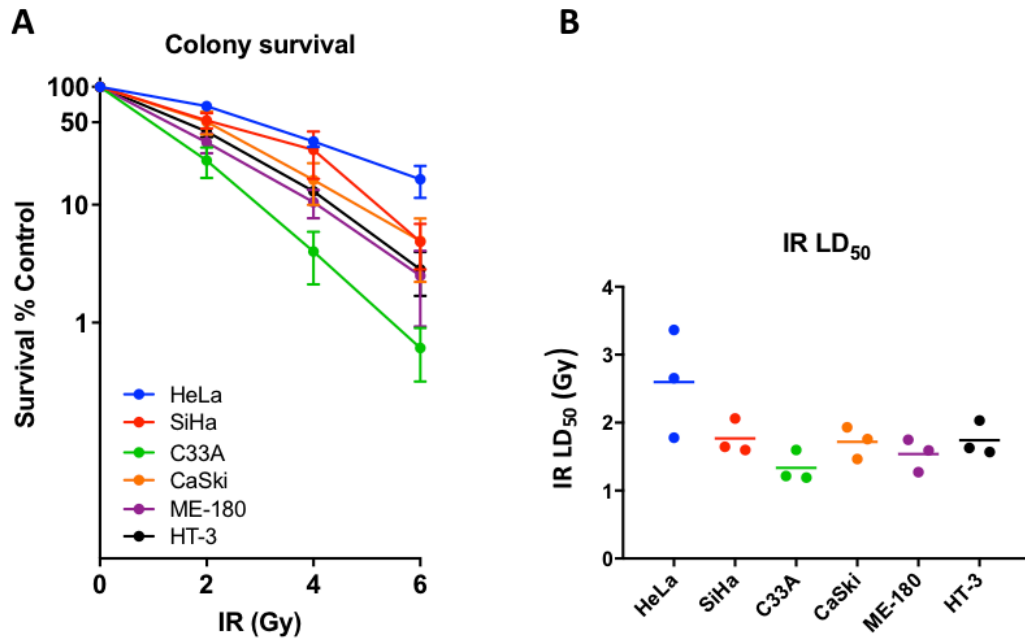


Figure 5.3 Ionising radiation cytotoxicity in the cervical cell line panel.

A: The survival of six cervical cancer cell lines at increasing doses of cisplatin. Cells in full growth media were exposed to IR at doses of 2 Gy to 6 Gy. Following exposure, cells were incubated for at least five doubling times prior to fixation and staining. Survival is given as a percentage relative to the survival of untreated cells. **B:** LD₅₀ values for IR in the cervical cancer cell lines. The calculated mean IR dose required to cause 50% reduction in survival compared to control, along with the individual values for three individual experiments are given. Data are from three individual experiments and normalised to control.

Considering the relative similarity of the IR LD₅₀ values and the impact that this could have in determining trends, an alternative measure of IR cytotoxicity: colony survival following exposure to a fixed dose of IR (4 Gy) was used to compare cytotoxicity with baseline expression of the cell cycle kinases and DRR proteins. When this alternative measure of cytotoxicity was used, potential relationships between IR cytotoxicity and both ATR and CHK1 expression were seen (Figure 5.4).

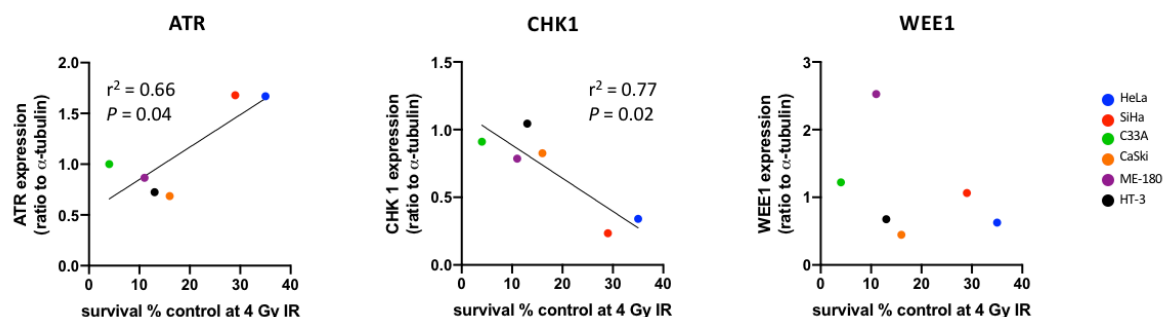


Figure 5.4 Correlations IR cytotoxicity and baseline expression of target enzymes cervical cancer cell lines.

Scatter plots of the % colony survival following exposure to 4 Gy IR vs baseline expression of the enzymes: ATR, CHK1 and WEE1, as determined in experiments described in chapter 3. All values correspond to the means of three independent experiments.

5.4.2 Sensitisation of cell lines to cisplatin by ATR, CHK1 and WEE1 inhibitors

The cytotoxicity of increasing concentrations of cisplatin \pm a fixed concentration of inhibitor drug was investigated. In addition to the survival curves, results for the sensitisation of cells to cisplatin by the inhibitors are given as potentiation factors (PF). PF₅₀ is the ratio of LC₅₀ in the absence or presence of the inhibitor. PF_{0.3-cis} is the ratio between survival at a fixed cisplatin concentration of 0.3 μ M in the absence and presence of the inhibitor drug.

VE-821

VE-821 (1 μ M) caused variable sensitisation to cisplatin cytotoxicity in the six cervical cancer cell lines. When survival curves for cisplatin \pm inhibitor (Figure 5.5) were compared using two-way ANOVA, a significant potentiation of cisplatin across the range of concentrations was confirmed in four of the cell lines: HeLa; SiHa; C33A; and ME-180. The largest magnitude of potentiation was seen in C33A cells (PF₅₀ = 5.9) and the smallest in CaSki cells (PF₅₀ = 1.8) and SiHa cells (PF₅₀ = 1.8). At higher concentrations the order of sensitisation appeared to change. The potentiation factor at 0.3 μ M cisplatin was largest in ME-180 cells (PF_{0.3-cis} = 12.7) and lowest in CaSki (PF_{0.3-cis} = 1.2) (Table 5.1).

When either measure of sensitisation to cisplatin is used, there was no relationship between sensitisation by VE-821 and expression of baseline proteins across the cell line panel. VE-821

caused the least sensitisation to cisplatin in SiHa cells and the greatest in ME-180 cells. This appears at odds with the observation that SiHa showed the greatest inhibition of ATR by the same concentration of VE-821 and ME-180 the least. When the other cell lines are included, there was no relationship between either ATR activation by cisplatin or its inhibition by VE-821 and VE-821 mediated sensitisation of the cell lines to cisplatin cytotoxicity. Neither is the extent of sensitisation to cisplatin by VE-821 predicted by single agent VE-821 cytotoxicity or cisplatin cytotoxicity.

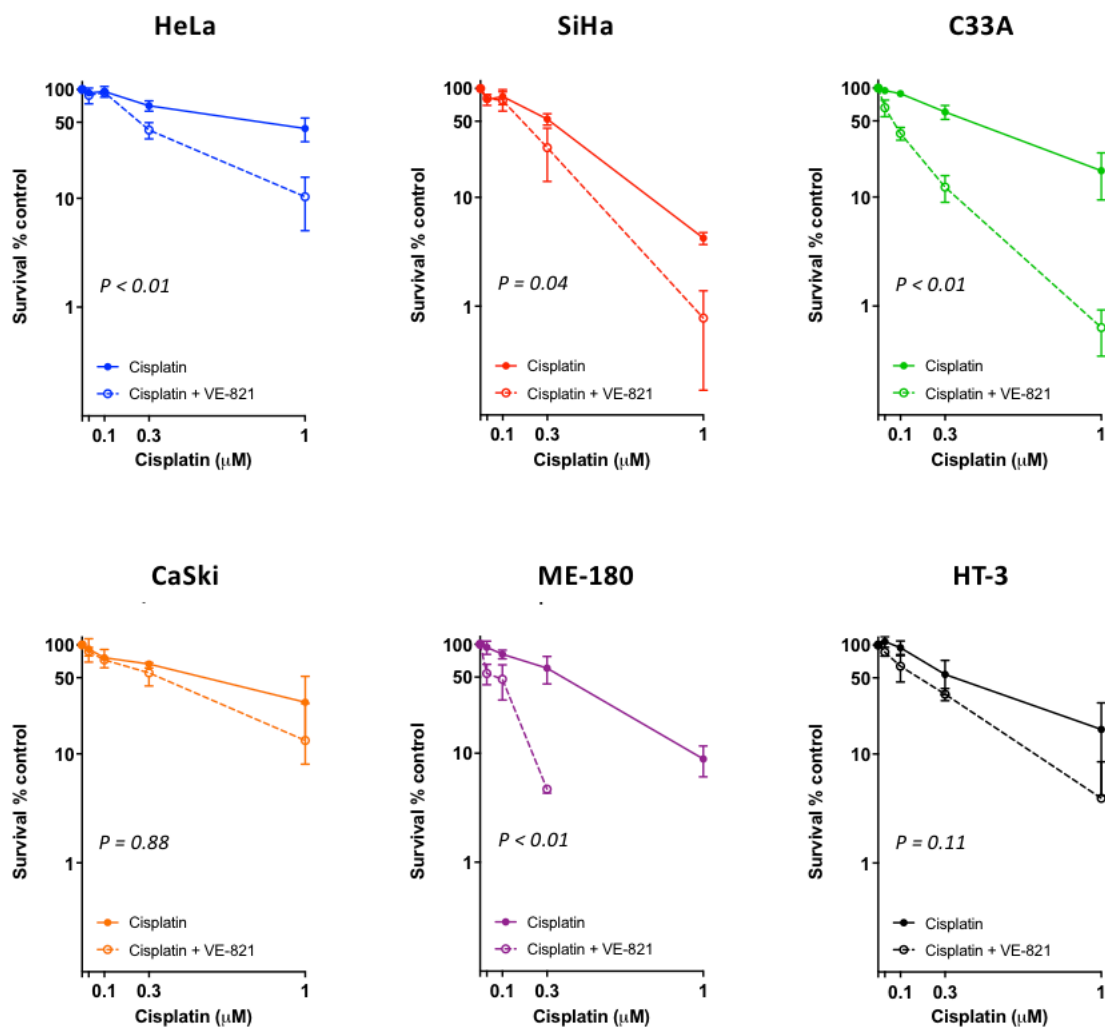


Figure 5.5 Colony survival of cervical cancer cell lines exposed to cisplatin \pm VE-821.

Cells were exposed to cisplatin at concentrations of 0.03 μM to 3 μM \pm 1 μM VE-821 in growth media for 24 hours. Following exposure, cells were incubated in fresh growth media for at least five doubling times prior to fixation and staining. Data are the means and SEM from three independent experiments. Survival is normalised to vehicle (DMSO) or VE-821 alone.

Cell Line	Concentration at 50% colony survival (LC ₅₀)			Colony survival at 0.3 μ M cisplatin		
	Cisplatin (μ M \pm SEM)	Cisplatin + VE821 (μ M \pm SEM)	VE-821 PF ₅₀ (\pm SD)	Cisplatin (% \pm SEM)	Cisplatin + VE821 (% \pm SEM)	VE-821 PF _{0.3-cis} (\pm SD)
HeLa	0.87 \pm 0.15	0.28 \pm 0.02	3.1 \pm 0.9	71 \pm 4	42 \pm 4	1.7 \pm 0.2 *
SiHa	0.38 \pm 0.05	0.21 \pm 0.04	1.8 \pm 0.2 *	56 \pm 4	27 \pm 8	2.2 \pm 0.8
C33A	0.47 \pm 0.08	0.08 \pm 0.01	5.9 \pm 1.3 *	61 \pm 5	12 \pm 2	5.0 \pm 0.9 **
CaSki	0.74 \pm 0.22	0.42 \pm 0.12	1.8 \pm 0.2	67 \pm 3	55 \pm 8	1.2 \pm 0.2
ME-180	0.42 \pm 0.11	0.10 \pm 0.02	4.9 \pm 3.2	60 \pm 10	5 \pm 0.2	12.7 \pm 2.9 *
HT-3	0.41 \pm 0.15	0.19 \pm 0.03	2.2 \pm 1.1	54 \pm 11	35 \pm 3	1.6 \pm 0.8

Table 5.1 Sensitisation of cervical cancer cell lines to cisplatin by VE-821.

*Two measures of sensitisation are given: PF₅₀ (Potentiation Factor at 50% survival) is the factor by which the mean concentration of cisplatin causing 50% colony survival vs control is reduced in the presence of 1 μ M VE-821. PF_{cis 0.3} (Potentiation Factor at 0.3 μ M cisplatin) is the factor by which % colony survival at 0.3 μ M cisplatin is reduced vs control by 1 μ M VE-821. The differences between the mean LC₅₀/LC_{0.3-cis} \pm inhibitor was compared using a paired t-test. * = $p < 0.05$, ** = $p < 0.005$*

PF-477736

Sensitisation of the cell lines to cisplatin by 50 nM PF-477736 was less than that seen for 1 μ M VE-821 (Figure 5.6), despite the observation that 50 nM PF-477736 inhibited CHK1 more than 1 μ M VE-821 inhibited ATR across the cell line panel (Chapter 4.4). ME-180 cells again showed the greatest sensitisation by PF-477736 (PF₅₀ = 2.5; PF_{0.3-cis} = 1.8). PF-477736 did not sensitise HeLa cells to cisplatin.

Analysis of the sensitisation effects of 50 nM PF477736 on cisplatin cytotoxicity in the individual cell lines were mixed. Comparison of the survival curves \pm inhibitor by two-way ANOVA suggested a significant sensitisation was seen in HT-3 cells, however this was likely to be due to the results at low cisplatin concentrations and the curves appear to converge at higher concentrations. Differences in the ME-180 survival curves approached significance but neither the difference between LC₅₀ or LC_{0.3-cis} with and without inhibitor were significant on paired t-testing (Table 5.2).

There were no significant correlations found between PF-477736 sensitisation to cisplatin and PF-477736 single agent cytotoxicity. Despite the greatest activation of CHK1 by cisplatin in HeLa cells, the strong inhibition of CHK1 by PF-477736 and the resistance of this cell line to cisplatin, PF-477736 did not enhance cisplatin cytotoxicity in HeLa cells. Across the cell line panel, sensitisation of cisplatin was not related to CHK1 activation by cisplatin or extent of inhibition of CHK1 by PF-477736 as measured in Chapter 4.4.3. In contrast to HeLa cells, ME-180 cells were most sensitive to cisplatin and were sensitised the most to cisplatin by PF-477736, though there was no relationship between cisplatin cytotoxicity and PF-477736 sensitisation across the panel.

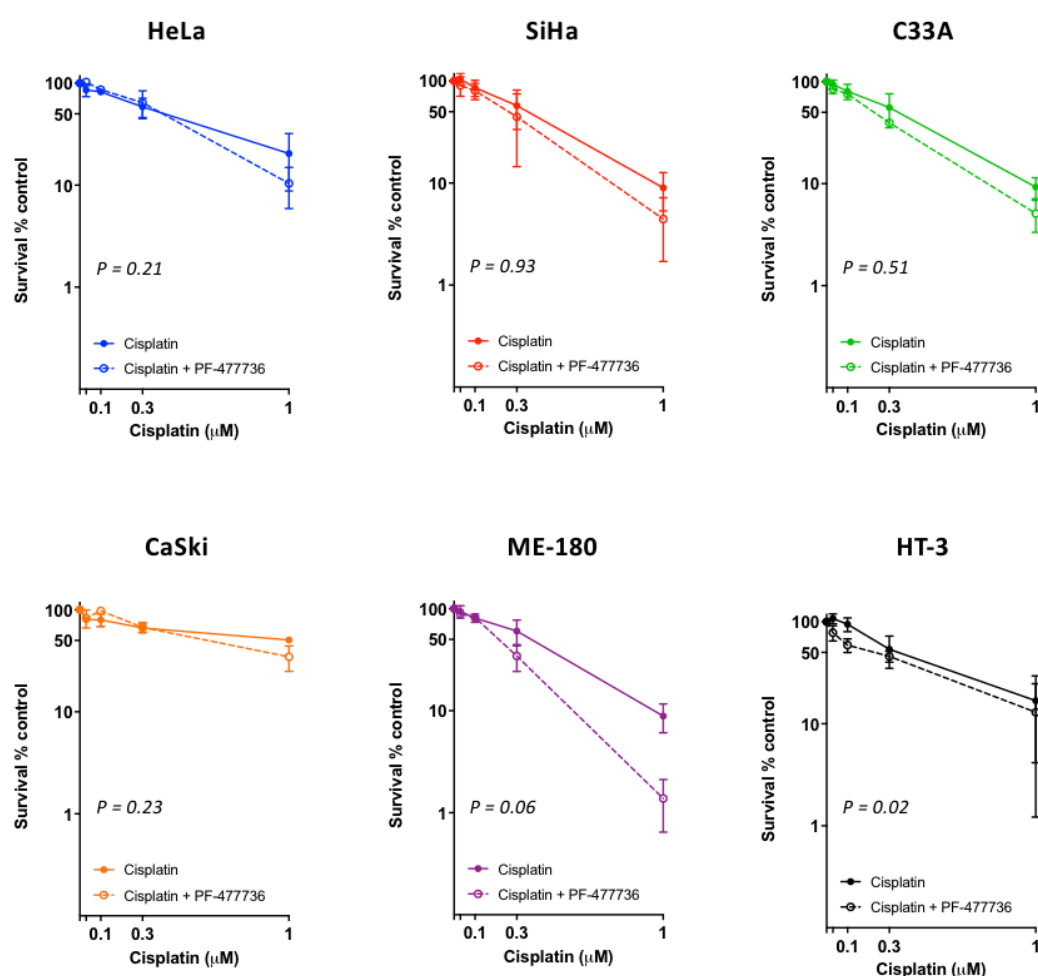


Figure 5.6 Colony survival of cervical cancer cell lines exposed to cisplatin ± PF-477736.

Cells were exposed to cisplatin at concentrations of 0.03 μM to 3 μM ± 50 nM PF-477736 in growth media for 24 hours. Following exposure, cells were incubated in fresh growth media for at least five doubling times prior to fixation and staining. Data are the means and SEM from three independent experiments. Survival is normalised to vehicle (DMSO) or PF-477736 alone.

Cell Line	Concentration at 50% colony survival (LC ₅₀)			Colony survival at 0.3 μ M cisplatin		
	Cisplatin (μ M \pm SEM)	Cisplatin + PF-477736 (μ M \pm SEM)	PF-477736 PF ₅₀ (\pm SD)	Cisplatin (% \pm SEM)	Cisplatin + PF-477736 (% \pm SEM)	PF-477736 PF _{0.3-cis} (\pm SD)
HeLa	0.48 \pm 0.11	0.48 \pm 0.11	1.0 \pm 0.1	59 \pm 7	65 \pm 11	0.9 \pm 0.1
SiHa	0.41 \pm 0.12	0.35 \pm 0.10	1.4 \pm 0.01	58 \pm 14	45 \pm 17	1.9 \pm 1.3
C33A	0.41 \pm 0.11	0.24 \pm 0.01	1.3 \pm 0.7	56 \pm 12	40 \pm 9	1.4 \pm 0.5
CaSki	1.04 \pm 0.08	0.57 \pm 0.07	1.8 \pm 0.5	66 \pm 4	67 \pm 5	1.0 \pm 0.2
ME-180	0.42 \pm 0.11	0.18 \pm 0.04	2.5 \pm 1.3	60 \pm 10	34 \pm 6	1.8 \pm 0.3
HT-3	0.41 \pm 0.15	0.23 \pm 0.06	1.9 \pm 1.1	54 \pm 11	46 \pm 3	1.2 \pm 0.5

Table 5.2 Sensitisation of cervical cancer cell lines to cisplatin by PF-477736.

Two measures of sensitisation are given: PF₅₀ (Potentiation Factor at 50% survival) is the factor by which the mean concentration of cisplatin causing 50% colony survival vs control is reduced in the presence of 50 nM PF-477736. PF_{0.3-cis} (Potentiation Factor at 0.3 μ M cisplatin) is the factor by which % colony survival at 0.3 μ M cisplatin is reduced vs control by 50 nM PF-477736. The differences between the mean LC₅₀/LC_{0.3-cis} \pm inhibitor was compared using a paired t-test.

MK-1775

There was a much smaller spectrum of potentiation of cisplatin by MK-1775 than by VE-821 or PF-477736 at the concentrations used (Figure 5.7). Comparison of the survival curves with and without inhibitor by two-way ANOVA revealed no significant differences.

Consistent with results for VE-821 and PF-477736, ME-180 showed the greatest potentiation using both PF₅₀ and PF_{0.3-cis} but paired t-testing of the differences between the means used to calculate these values again showed no significant differences (Table 5.3).

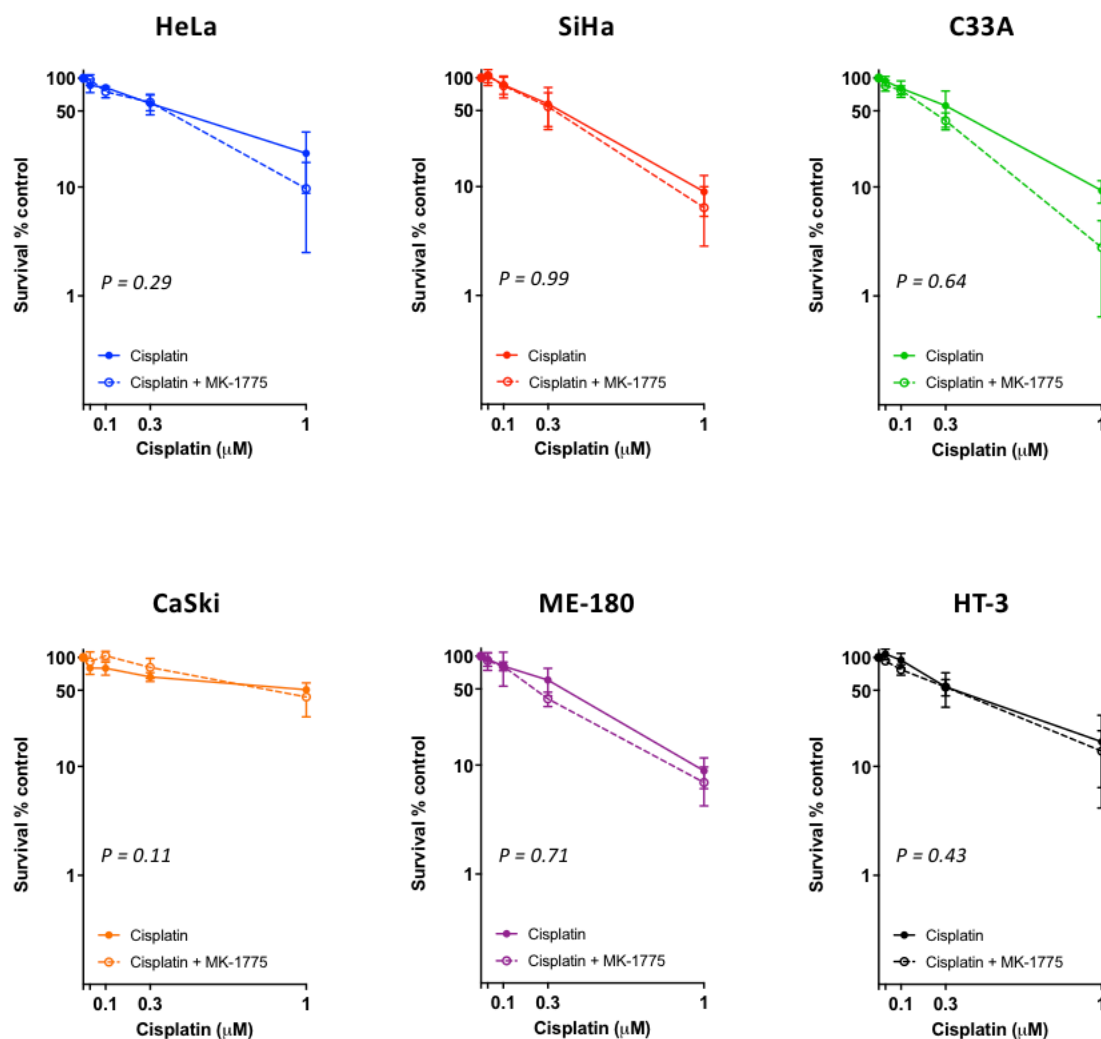


Figure 5.7 Colony survival of cervical cancer cell lines exposed to cisplatin ± MK-1775.

Cells were exposed to cisplatin at concentrations of 0.03 μM to 3 μM ± 100 nM MK-1775 in growth media for 24 hours. Following exposure, cells were incubated in fresh growth media for at least five doubling times prior to fixation and staining. Data are the means and SEM from three independent experiments. Survival is normalised to vehicle (DMSO) or MK-1775 alone.

Cell Line	Concentration at 50% colony survival (LC ₅₀)			Colony survival at 0.3 μ M cisplatin		
	Cisplatin (μ M \pm SEM)	Cisplatin + MK-1775 (μ M \pm SEM)	MK-1775 PF ₅₀ (\pm SD)	Cisplatin (% \pm SEM)	Cisplatin + MK-1775 (% \pm SEM)	MK-1775 PF _{0.3-cis} (\pm SD)
HeLa	0.56 \pm 0.03	0.46 \pm 0.08	1.4 \pm 0.6	59 \pm 7	60 \pm 6	1.0 \pm 0.3
SiHa	0.41 \pm 0.12	0.38 \pm 0.10	1.1 \pm 0.3	58 \pm 14	54 \pm 11	1.1 \pm 0.3
C33A	0.41 \pm 0.11	0.25 \pm 0.02	1.7 \pm 0.9	56 \pm 12	41 \pm 4	1.4 \pm 0.7
CaSki	1.04 \pm 0.80	0.97 \pm 0.21	1.1 \pm 0.2	66 \pm 4	81 \pm 10	0.8 \pm 0.1
ME-180	0.42 \pm 0.11	0.20 \pm 0.06	2.3 \pm 0.5	60 \pm 10	41 \pm 4	1.5 \pm 0.3
HT-3	0.41 \pm 0.15	0.41 \pm 0.07	1.0 \pm 0.3	54 \pm 11	54 \pm 5	1.0 \pm 0.2

Table 5.3 Sensitisation of cervical cancer cell lines to cisplatin by MK-1774.

Two measures of sensitisation are given: PF₅₀ (Potentiation Factor at 50% survival) is the factor by which the mean concentration of cisplatin causing 50% colony survival vs control is reduced in the presence of 100 nM MK-1775. PF_{cis 0.3} (Potentiation Factor at 0.3 μ M cisplatin) is the factor by which % colony survival at 0.3 μ M cisplatin is reduced vs control by 100 nM MK-1775. The differences between the mean LC₅₀/LC_{0.3-cis} \pm inhibitor was compared using a paired t-test.

Whilst MK-1775 was more cytotoxic as a single agent to both HT-3 and ME-180 cells than in the other cell lines, MK-1775 only sensitised ME-180 cells and there was no trend for the sensitisation by MK-1775 across the panel. Neither was sensitisation predicted by sensitivity to cisplatin alone. Despite the narrow spectrum of sensitisation to cisplatin by MK-1775 and the lack of statistical significance in the differences in survival, a significant correlation was found between the sensitisation of cells to cisplatin by MK-1775 and baseline WEE1 expression. This was observed when either measure of sensitisation was used (Figure 5.9). These results should be treated with caution due to the very small effects observed and the size of the panel, but it may be worth following up in a larger study. No relationship was seen between sensitisation and expression of any of the other proteins measured in Chapter 3 or the values for activation or inhibition of WEE1 determined in Chapter 4.

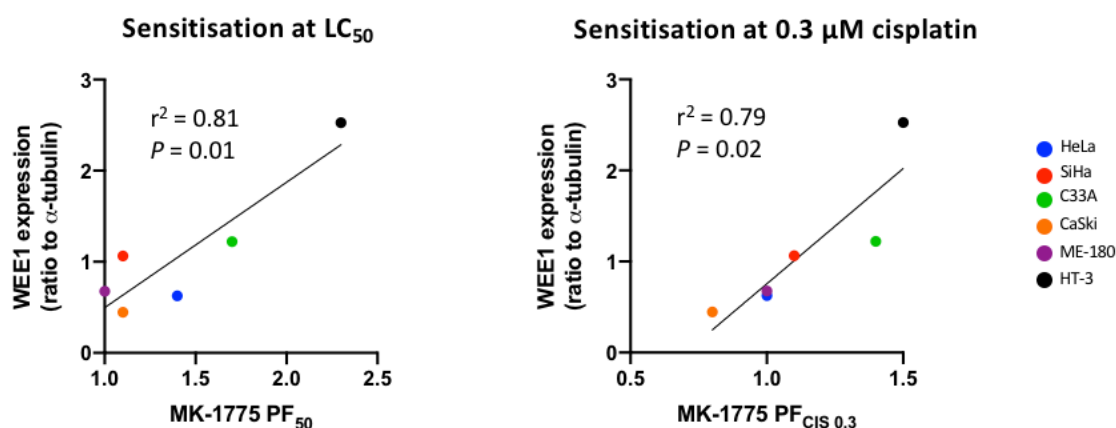


Figure 5.8 Correlations between cell line sensitisation to cisplatin by MK-1775 and baseline expression of WEE1 in cervical cancer cell lines.

Scatter plots of the calculated PF₅₀ and PF_{cis. 0.3} values for MK-1775 sensitisation to cisplatin vs WEE1 expression as determined in experiments in chapter 3. All values are the mean of three individual experiments.

5.4.3 Sensitisation of cell lines to IR by inhibitors of ATR, CHK1 and WEE1

The cytotoxicity of increasing concentrations of IR \pm a fixed concentration of inhibitor drug was investigated using the same fixed concentrations of individual inhibitors as above. In addition to the survival curves, PF₅₀ and PF_{2-IR} were calculated, as above. PF_{2-IR} is the ratio between survival at a clinically relevant fixed IR dose of 2 Gy in the absence and presence of the inhibitor drug. 2 Gy IR is a standard fractional dose for clinical radiotherapy and gives a similar range of colony survival across the cell line panel as 0.3 μ M cisplatin used for the calculation of PF_{0.3-cis}.

VE-821

VE-821 radio-sensitised HeLa cells and ME-180 cells the most (Figure 5.9, Table 5.4) and HT-3 cells were radio-sensitised the least. Comparison of the survival curves with and without inhibitor by two-way ANOVA revealed significant potentiation for HeLa and ME-180 cells. Significant potentiation of IR cytotoxicity was also seen in HT-3 cells but the magnitude of the effect was much smaller. Paired t-test of the difference in mean LD_{2-IR} revealed a significant difference in HeLa cells and CaSki cells only (Table 5.4).

HeLa cells were the most radio-resistant and had amongst the greatest sensitisation to IR by VE-821 (at the LD_{50}) whilst C33A cells were the most radio-sensitive and were amongst the least sensitised by VE-821 at the LD_{50} and at 4 Gy. VE-821 radio-sensitisation (PF_{50}) was correlated with radio-resistance across the cell line panel (Figure 5.10).

Sensitisation of cell lines to IR by VE-821 was not predicted by single agent VE-821 cytotoxicity or the extent of inhibition of ATR by VE-821 calculated in experiments in Chapter 3. VE-821 sensitisation of cell lines to IR did not correlate with cell line doubling time, HPV or p53/pRB status or baseline expression of the proteins measured in Chapter 3 (data not shown).

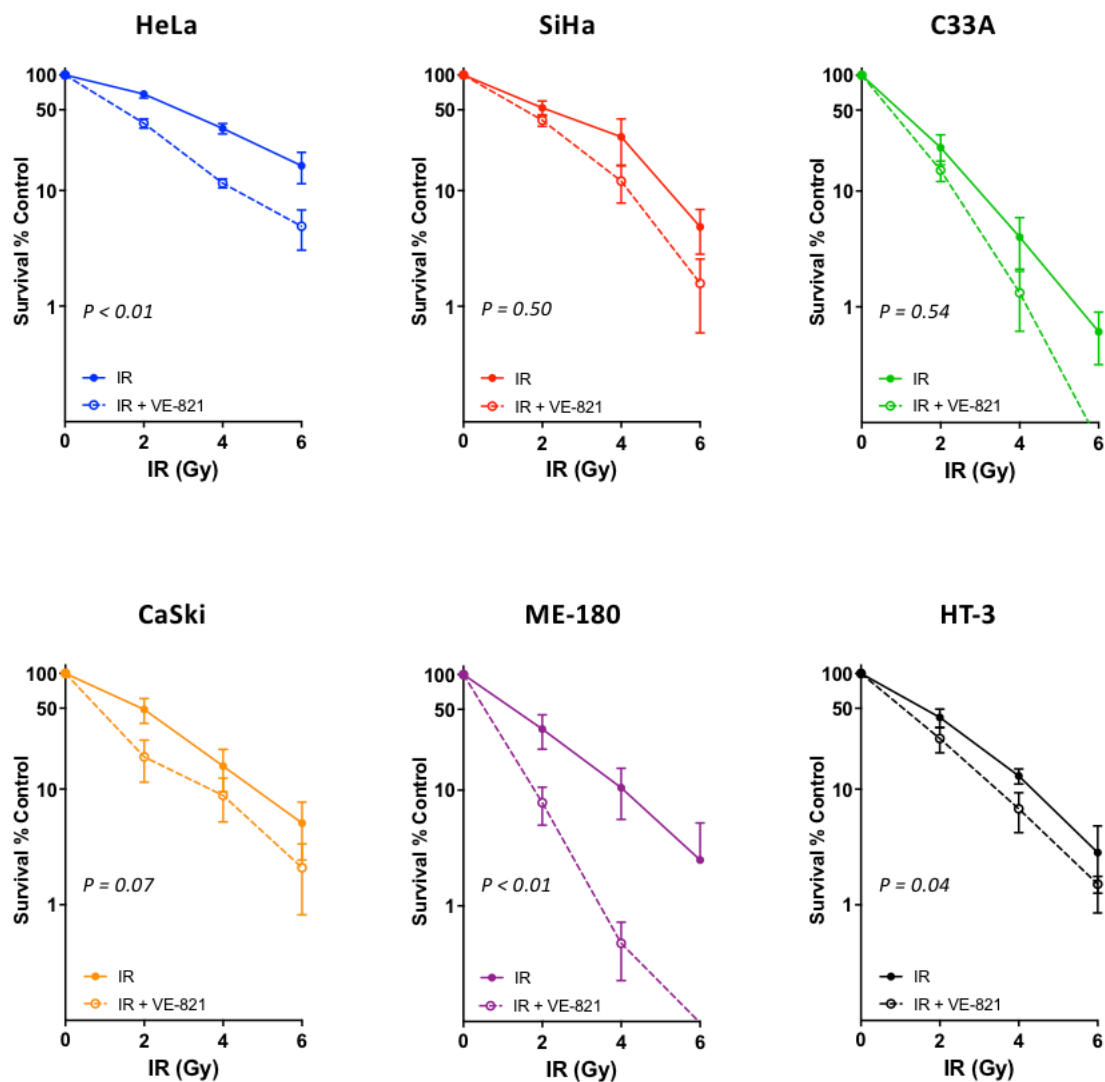


Figure 5.9 Colony survival of cervical cancer cell lines exposed to IR \pm VE-821.

Cells were exposed to 2 Gy to 6 Gy IR \pm immediate 24-hour culture with 1 μ M VE-821. After 24 hours, cells were incubated in fresh growth media for at least five doubling times prior to fixation and staining. Data are the means and SEM from three independent experiments. Survival is normalised to vehicle (DMSO) or VE-821 alone.

Cell Line	IR dose at 50% colony survival (LD ₅₀)			Colony survival at 2 Gy		
	IR (Gy ± SEM)	IR + VE-821 (Gy ± SEM)	VE-821 PF ₅₀ (± SD)	IR (% ± SEM)	IR + VE-821 (% ± SEM)	VE-821 PF _{2-IR} (± SD)
HeLa	2.6 ± 0.5	1.5 ± 0.1	1.7 ± 0.4	69 ± 5	38 ± 4	1.8 ± 0.3 *
SiHa	2.6 ± 0.8	1.7 ± 0.2	1.5 ± 0.5	52 ± 8	40 ± 5	1.3 ± 0.1
C33A	1.3 ± 0.1	1.1 ± 0.1	1.1 ± 0.2	24 ± 7	15 ± 3	1.6 ± 0.5
CaSki	2.1 ± 0.5	1.3 ± 0.1	1.6 ± 0.3	49 ± 12	19 ± 8	2.9 ± 0.7 *
ME-180	1.4 ± 0.2	1.1 ± 0.0	1.2 ± 0.2	34 ± 7	8 ± 2	5.1 ± 3.6
HT-3	1.8 ± 0.2	1.4 ± 0.7	1.3 ± 1.0	42 ± 4	27 ± 4	1.6 ± 0.3

Table 5.4 Sensitisation of cervical cancer cell lines to IR by VE-821.

Two measures of sensitisation are given: PF₅₀ (Potentiation Factor at 50% survival) is the factor by which the mean concentration of cisplatin causing 50% colony survival vs control is reduced in the presence of 1 µM VE-821. PF_{2-IR} (Potentiation Factor at 2 Gy IR) is the factor by which % colony survival at 2 Gy IR is reduced vs control by 1 µM VE-821. The differences between the mean LD₅₀/LD_{2-IR} ± inhibitor was compared using a paired t-test. * = $p < 0.05$,

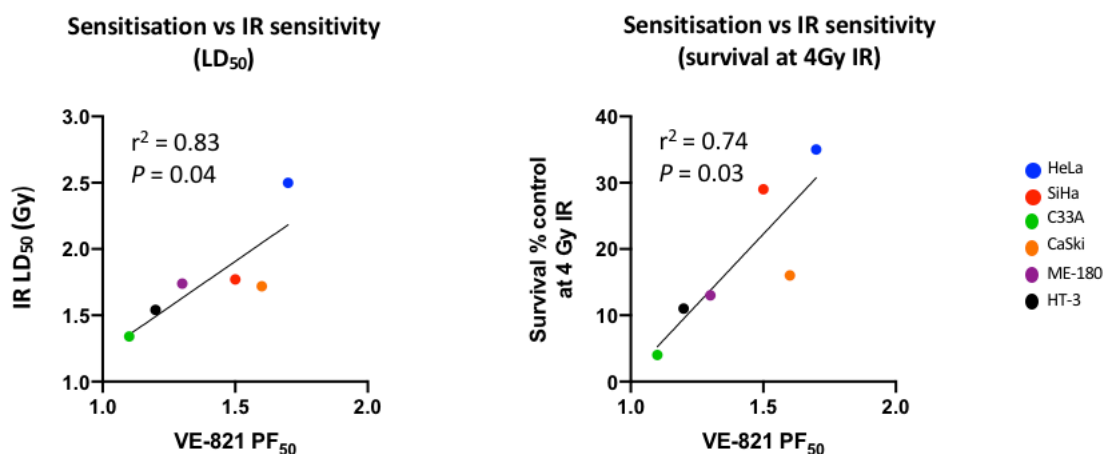


Figure 5.10 Correlations between sensitisation to IR by VE-821 and sensitivity to IR alone.

Scatter plots of calculated VE-821 PF₅₀ values vs two measures of IR sensitivity: calculated IR dose resulting in 50% colony survival (LD₅₀); and measured survival at 4 Gy IR alone. All values are means of three independent experiments.

PF-477736

Radio-sensitisation by PF-477736 was much more modest than that observed with VE-821 or cisplatin sensitisation by PF-477736 (Figure 5.11). Whilst it appeared that again, HeLa and ME-180 cells show the greatest sensitisation and HT-3 the least, there was no significant difference found between the colony survival \pm PF-477736. Unsurprisingly, given the very modest potentiation at both 50% colony survival and at 2 Gy IR (Table 5.5), no significant correlations were observed between any of the cell line characteristics, determined in experiments from Chapter 3, or the cytotoxicity of IR or PF-477736 alone (Chapter 4 and section 5.4.1, above: data not shown).

Cell Line	IR dose at 50% colony survival (LD_{50})			Colony survival at 2 Gy		
	IR (Gy \pm SEM)	IR + PF-477736 (Gy \pm SEM)	PF-477736 PF_{50} (\pm SD)	IR (% \pm SEM)	IR + PF-477736 (% \pm SEM)	PF-477736 PF_{2-IR} (\pm SD)
HeLa	2.6 \pm 0.5	2.6 \pm 0.1	1.0 \pm 0.3	69 \pm 5	52 \pm 1	1.1 \pm 0.3
SiHa	2.6 \pm 0.8	2.1 \pm 0.4	1.2 \pm 0.3	52 \pm 8	47 \pm 7	1.1 \pm 0.3
C33A	1.3 \pm 0.1	1.3 \pm 0.1	1.0 \pm 0.03	24 \pm 7	21 \pm 6	1.1 \pm 0.05
CaSki	2.1 \pm 0.5	1.8 \pm 0.3	1.2 \pm 0.3	49 \pm 12	39 \pm 10	1.4 \pm 0.6
ME-180	1.4 \pm 0.2	1.4 \pm 0.2	1.1 \pm 0.1	34 \pm 6	25 \pm 6	1.5 \pm 0.5
HT-3	1.8 \pm 0.1	1.7 \pm 0.1	1.0 \pm 0.1	42 \pm 4	41 \pm 5	1.0 \pm 0.2

Table 5.5 Sensitisation of cervical cancer cell lines to IR by PF-477736.

Two measures of sensitisation are given: PF_{50} (Potentiation Factor at 50% survival) is the factor by which the mean concentration of cisplatin causing 50% colony survival vs control is reduced in the presence of 50 nM PF-477736. $PF_{2\text{ Gy IR}}$ (Potentiation Factor at 2 Gy IR) is the factor by which % colony survival at 2 Gy IR is reduced vs control by 50 nM PF-477736. The differences between the mean $LD_{50}/LD_{2-IR} \pm$ inhibitor was compared using a paired t-test.

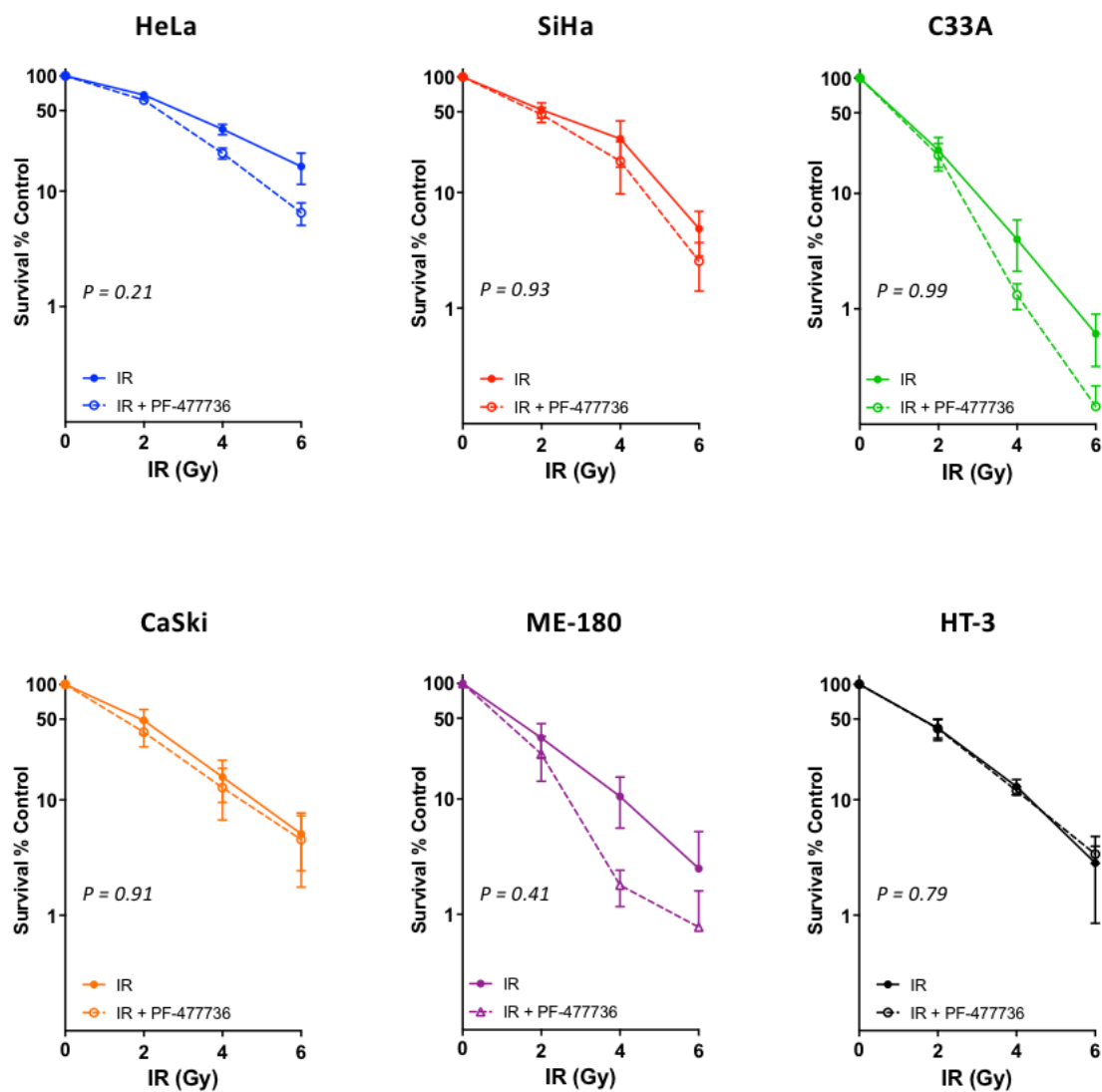


Figure 5.11 Colony survival of cervical cancer cell lines exposed to IR \pm PF-477736.

Cells were exposed to 2 Gy to 6 Gy IR \pm immediate 24-hour culture with 50 nM PF-477736. After 24 hours, cells were incubated in fresh growth media for at least five doubling times prior to fixation and staining. Data are the means and SEM from three independent experiments. Survival is normalised to vehicle (DMSO) or PF-477736 alone.

MK-1775

MK-1775 was a poor radiosensitiser. There was no relationship seen between the sensitisation of cells to IR by MK-1775 and the cells' intrinsic sensitivity to IR or MK-1775 alone or the baseline expression of WEE1. Given the modest and non-significant radiosensitisation any correlations must be taken with caution, nevertheless, a significant correlation was seen with baseline expressions of ATR, CHK1, CDK1 and DNA-PKcs (Figure 5.13). Cells with high expression of ATR and DNA-PKcs appeared to have greater sensitisation to IR by MK-1775. By contrast cells with high levels of either CHK1 or CDK1: the kinases directly upstream and downstream of WEE1, respectively at the G2/M cell cycle checkpoint, appeared to be less sensitised to IR by MK-15775. This may be a chance finding given the number of correlations investigated but is worthy of further investigation in other cell lines.

Cell Line	IR dose at 50% colony survival (LD ₅₀)			Colony survival at 2 Gy		
	IR (Gy ± SEM)	IR + MK-1775 (Gy ± SEM)	MK-1775 PF ₅₀ (± SD)	IR (% ± SEM)	IR + MK-1775 (% ± SEM)	MK-1775 PF _{2-IR} (± SD)
HeLa	2.6 ± 0.5	2.2 ± 0.4	1.3 ± 0.6	70 ± 5	53 ± 10	1.3 ± 0.4
SiHa	2.6 ± 0.8	1.8 ± 0.1	1.5 ± 0.6	52 ± 8	42 ± 3	1.2 ± 0.2
C33A	1.3 ± 0.1	1.3 ± 0.1	1.1 ± 0.1	24 ± 7	19 ± 7	1.5 ± 0.8
CaSki	2.1 ± 0.5	1.9 ± 0.2	1.1 ± 0.2	49 ± 12	44 ± 6	1.1 ± 0.2
ME-180	1.4 ± 0.2	1.3 ± 0.7	1.2 ± 0.2	34 ± 6	25 ± 3	1.3 ± 0.2
HT-3	1.7 ± 0.1	2.1 ± 0.2	0.9 ± 0.2	42 ± 4	52 ± 6	0.8 ± 0.2

Table 5.6 Sensitisation of cervical cancer cell lines to IR by MK-1775

Two measures of sensitisation are given: PF₅₀ (Potentiation Factor at 50% survival) is the factor by which the mean concentration of cisplatin causing 50% colony survival vs control is reduced in the presence of 100 nM MK-1775. PF_{2 Gy IR} (Potentiation Factor at 2 Gy IR) is the factor by which % colony survival at 2 Gy IR is reduced vs control by 100 nM MK-1775. The differences between the mean LD₅₀/LD_{2-IR} ± inhibitor was compared using a paired t-test.

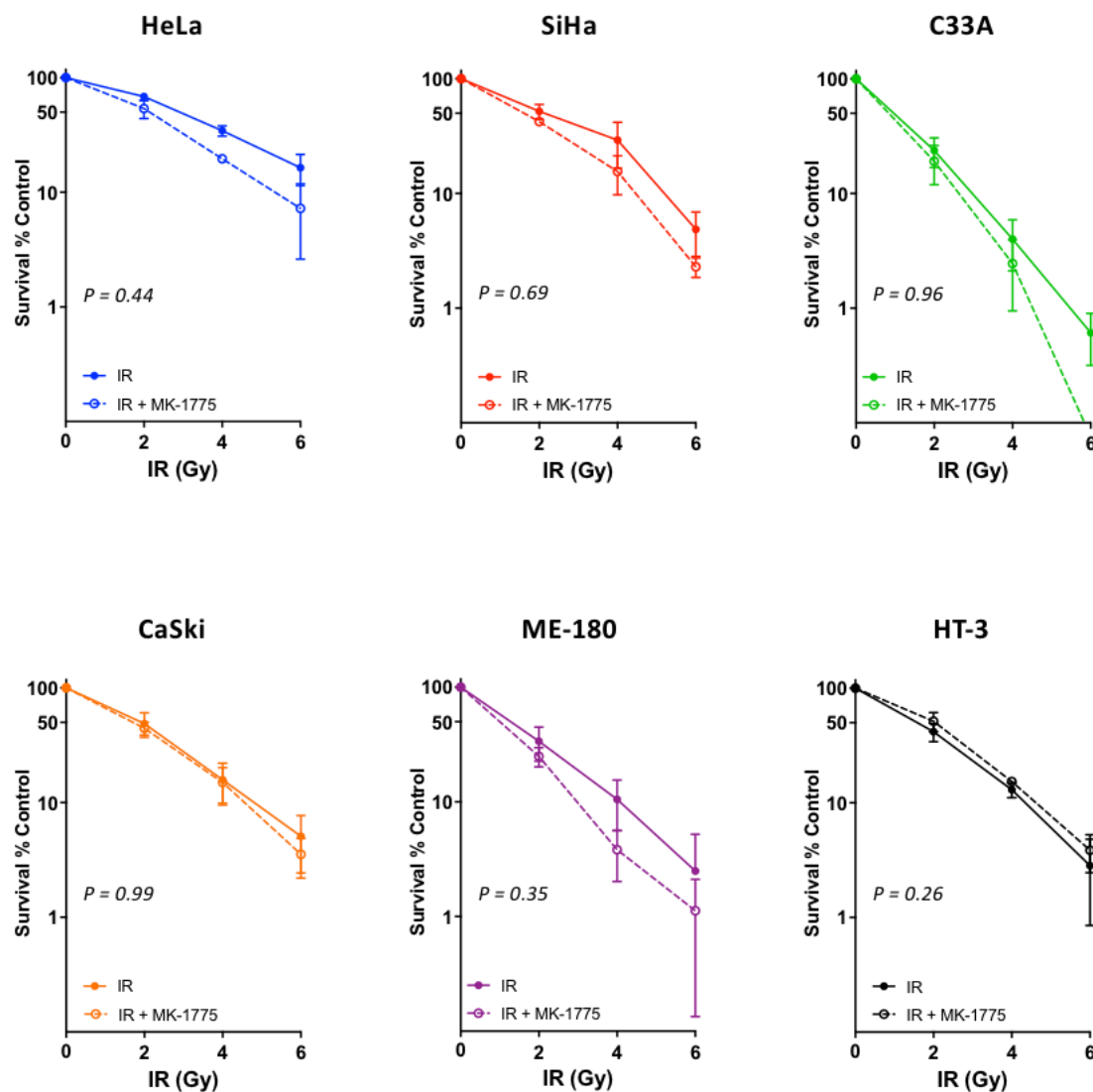


Figure 5.12 Colony survival of cervical cancer cell lines exposed to IR \pm MK-1775.

Cells were exposed to 2 Gy to 6 Gy IR \pm immediate 24-hour culture with 100 nM MK-1775. After 24 hours, cells were incubated in fresh growth media for at least five doubling times prior to fixation and staining. Data are the means and SEM from three independent experiments. Survival is normalised to vehicle (DMSO) or PF-477736 alone.

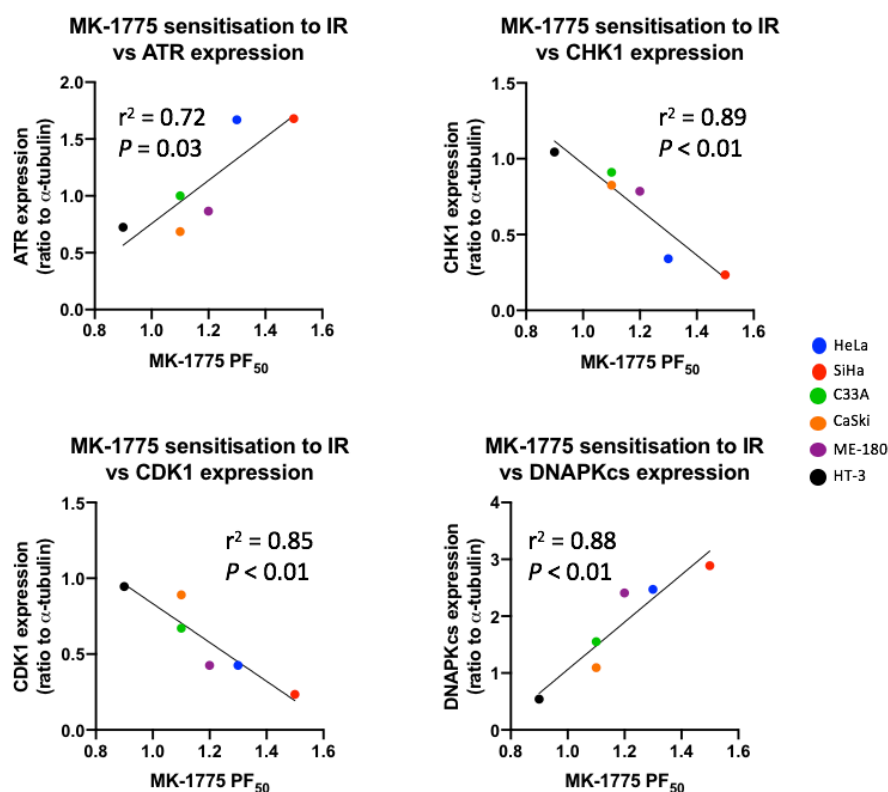


Figure 5.13 Correlations between MK-1775 sensitisation of cell lines to cisplatin cytotoxicity and baseline expression of target enzymes in cervical cancer cell lines.

Scatter plots of the calculated MK-1775 PF₅₀ values for IR sensitisation vs baseline expression of the enzymes: CHK1, CDK1 and DNA-PKcs, as determined in experiments described in chapter 3. All values correspond to the means of three independent experiments.

5.5 Discussion

The aim of this chapter was to relate the chemo- and radio-sensitivity of the cervical cancer cell lines to their baseline characteristics determined in previous chapters and to compare how effectively VE-821, PF-477736 and MK-1775 sensitise cervical cancer cell lines to cisplatin and ionising radiation. ATR, CHK1 and WEE 1 knockdown utilising siRNA/shRNA techniques have previously been used in validating these kinases as targets for inhibition with the aim of sensitising cancer cells to the effects of DNA damaging agents and are reviewed in Chapter 1.5.1. Similar experiments have not been repeated in these investigations. Whilst this raises the possibility that some of the enhanced cytotoxicity seen in combination with cisplatin or IR may be the result of off-target effects of the inhibitors, the experiments in previous chapters provide reassurance that substantial inhibition of ATR,

CHK1 and WEE1 by their inhibitors is achieved at the drug concentrations used. Though the small number of cell lines included in the cell line panel is another limitation to the wider applicability of the results, this is the first time that a direct comparison of inhibitors of ATR, CHK1 and WEE1 has been made.

Similar survival was seen for the cervical cancer cell lines over the range of cisplatin concentrations / IR exposures used to determine the cisplatin and radio-sensitivity of the cell line panel. The rank order of cytotoxicity for cisplatin and IR was not the same (Figure 5.14). Whilst no relationships were found between protein expressions and cisplatin sensitivity, potential determinants of sensitivity to IR were seen. HeLa and SiHa cells had high ATR and low CHK1 expression and were the least sensitive to IR. C33A, CaSki, ME-180 and HT-3 all expressed low ATR and high CHK1, and were more sensitive to IR. Interestingly HeLa and SiHa also showed the highest DNA-PKcs expression and SiHa showed the highest ATM expression, though no correlation was found when the other cell lines were considered.

ATM and DNA-PKcs are important in the detection of IR induced DSBs and their repair by NHEJ (Hoeijmakers, 2001) and NHEJ function has previously been reported as a determinant of sensitivity to IR (Mahaney et al., 2009). NHEJ is less important in the repair of cisplatin induced DNA damage (Hoeijmakers, 2001, Curtin, 2012). The differences in the rank order of sensitivity to cisplatin and IR and the presence of potential relationships between key NHEJ proteins and IR sensitivity, supports the hypothesis that the determinants of sensitivity to cisplatin and IR are different, owing to the different DNA repair pathways involved.

Inhibition of ATR by VE-821 caused greater cisplatin and IR sensitisation than either CHK1 inhibition by PF-477736 or WEE1 inhibition by MK-1775 at the concentrations used. This may suggest that ATR is a better target for inhibition than either CHK1 or WEE1, however the overall lower inhibition of WEE1 activity by 100 nM MK-1775 compared to ATR inhibition by 1 μ M VE-821 should be considered when making this direct comparison. The smaller magnitude of cisplatin and IR sensitisations caused by PF-477736 and MK-1775 precluded meaningful correlations with the cytotoxicity of either agent or with single agent inhibitor cytotoxicity. For VE-821 however, sensitisation of IR did appear to correlate with intrinsic IR sensitivity.

ME-180 and HeLa cells appeared to show the greatest sensitisation across all inhibitors. HT-3 cells and C33A cells were consistently amongst the least sensitised to IR (Figure 5.14), notable due to the HPV negative and TP53-/RB1- mutant status of these cell lines. Beyond those features described above it was not possible to relate any of the molecular characteristics of the cells, determined as part of this study, to intrinsic chemo- or radiosensitivity or significant sensitisation by the inhibitors. This was largely because of the size of the panel, the spectrum of sensitivity and magnitude of the sensitisation.

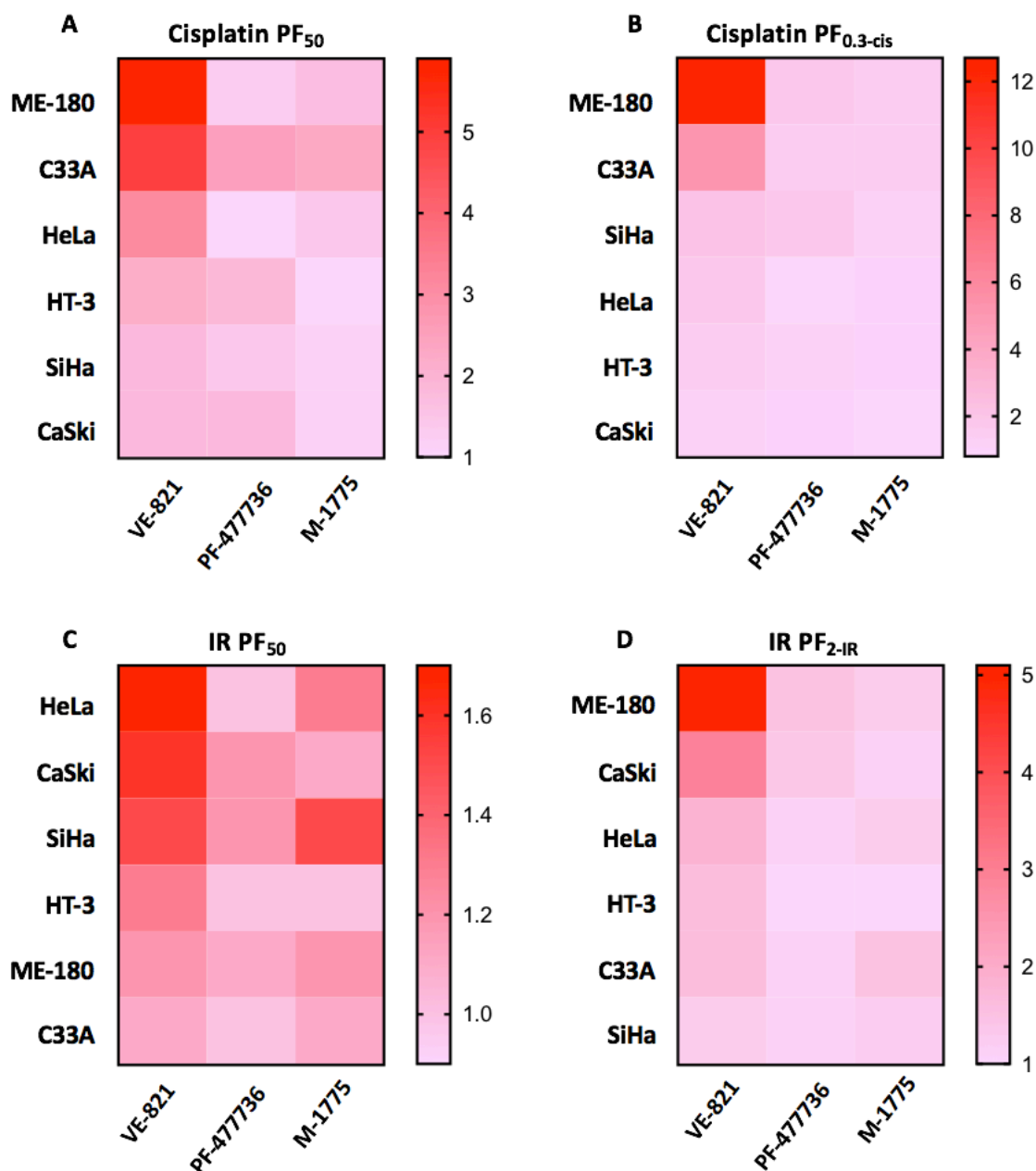


Figure 5.14 Heatmaps showing the relative sensitisation of cervical cancer cell lines to cisplatin and IR by VE-821, PF-477736 and MK-1775.

A: Cisplatin PF_{50} (potentiation factor at 50% survival) by cell line and inhibitor. **B:** Cisplatin $PF_{0.3-cis}$ (potentiation factor at 0.3 μ M cisplatin) by cell line and inhibitor. **C:** IR PF_{50} by cell line and inhibitor. **D:** IR PF_{2-IR} (potentiation factor at 2 Gy IR) by cell line and inhibitor. Data taken from Tables 5.1 to 5.6 and are derived from the mean potentiation factor from three independent experiments.

MK-1775 radio-sensitisation, though not-significant for any cell, correlated with high ATR and DNA-PKcs expression (Chapter 3). DNA-PKcs overexpression was previously described as

a determinant of sensitivity to ATR and CHK1 inhibitors (Middleton et al., 2015, Massey et al., 2016), however, this relationship has not previously been noted with respect to WEE1, either as a single agent or as a sensitising agent for IR. The very narrow and non-significant range of sensitisation by this inhibitor, however limits confidence that a true correlation exists, though it may warrant evaluation in a larger panel of cell lines.

5.6 Conclusions

With reference to the aims and objectives set out at the start of this chapter:

- The cervical cancer cell lines showed a range of sensitivity to cisplatin and IR.
- VE-821 was a more potent sensitiser to both cisplatin and IR than PF-477736 or MK-1775 at the concentrations used.
- Overall sensitisation of the cell lines to cisplatin or to IR by the inhibitors was not dependent on intrinsic sensitivity to the either agent, though a potential correlation between VE-821 sensitisation to IR and IR cytotoxicity was noted.
- Sensitisation of the cell lines to cisplatin or IR by VE-821, PF-477736 or MK-1775 was not dependent on the single agent cytotoxicity of the inhibitors.

6 Evaluation of cell cycle profile changes following cisplatin and inhibitor exposure.

6.1 Introduction

Experiments described in the previous chapters have demonstrated that in a panel of cervical cancer cell lines the spectrum of sensitivity to VE-821, PF-477736 and MK-1775 induced cytotoxicity, or their sensitisation of cisplatin or IR, could not be explained by the extent of target inhibition (Table 4.2). Furthermore, no clear determinants of sensitivity to the inhibitors have been identified. The mechanism of cisplatin sensitisation by ATR, CHK1 and WEE1 inhibitors is hypothesised to be due to abrogation of S and G2/M checkpoint function in the presence of G1/S checkpoint deficiency (Chapter 1).

ATR inhibition by VE-821 has been shown to reduce IR induced G2 arrest in a p53 independent manner in paired cell lines (Middleton et al., 2018). Another ATR inhibitor AZD6738 has also been shown to successfully abrogate a cisplatin induced G2 arrest without causing significant cell cycle perturbations as a single agent at an equivalent concentration in NSCLC cells (Vendetti et al., 2015). Whilst reports of the cell cycle effects of CHK1 combinations with platinum agents are sparse. The CHK1 inhibitor AZD7762 was shown to abrogate the intra S and G2/M checkpoints, evidenced by loss of S/G2 arrest in neuroblastoma cells treated with the anti-mitotic agent, nocodazole or the topoisomerase inhibitor, SN38 (Xu et al., 2011). SN38 mediated G2 arrest was also shown to be abolished by co-incubation with the CHK1 inhibitor SCH900776 in breast cancer cell lines (Montano et al., 2012). Likewise, the WEE1 inhibitor used in these experiments, MK-1775, has been reported to abolish G2 arrest in cisplatin treated p53-mutated ovarian cancer cells (Hirai et al., 2009).

This chapter focuses on attempts to understand the underlying mechanisms that determine the differential cisplatin sensitisation observed across the cell line and inhibitor panel: with specific reference to changes in the cell cycle in response to treatment with cisplatin with and without ATR, CHK1 or WEE1 inhibitors. Cisplatin was used as the genotoxic agent in these experiments due to the larger magnitude and range of effects seen in previous chapters with this agent compared to IR.

6.2 Aims and objectives

The aims of the investigations described in this chapter were: To determine the nature of cell cycle profile changes of the cervical cancer cell lines in response to cisplatin and inhibitors of ATR, CHK1 and WEE1 as single agents and in combination.

This will enable the following hypotheses to be tested:

1. Cisplatin will have similar effects on the cell cycle profiles of the cervical cancer cell lines, irrespective of HPV status
2. The inhibitors will have similar effects on cisplatin-induced cell cycle profile changes.
3. The effects of the inhibitors on cisplatin-induced cell cycle changes will be proportional to the degree of potentiation of cisplatin-induced cytotoxicity described in Chapter 5.
4. The effects of the inhibitors on cisplatin-induced cell cycle profile changes will correlate with baseline expression of the target enzymes.

6.3 Materials and Methods

Permeabilised and PI stained cells were prepared, as detailed in Chapter 2.7. The DNA content of cells was determined using a BD FACSCanto II flow cytometer. Data was stored and transferred to FCS Express 6® software for analysis. Doublets were excluded by gating in area versus height plots. Histograms were generated for each experimental condition for each cell line (Figure 6.1) and the percent of cells in sub-G1, G1/0, S and G2/M phases were determined by application of gates to the histograms, as shown in Figure 6.1.

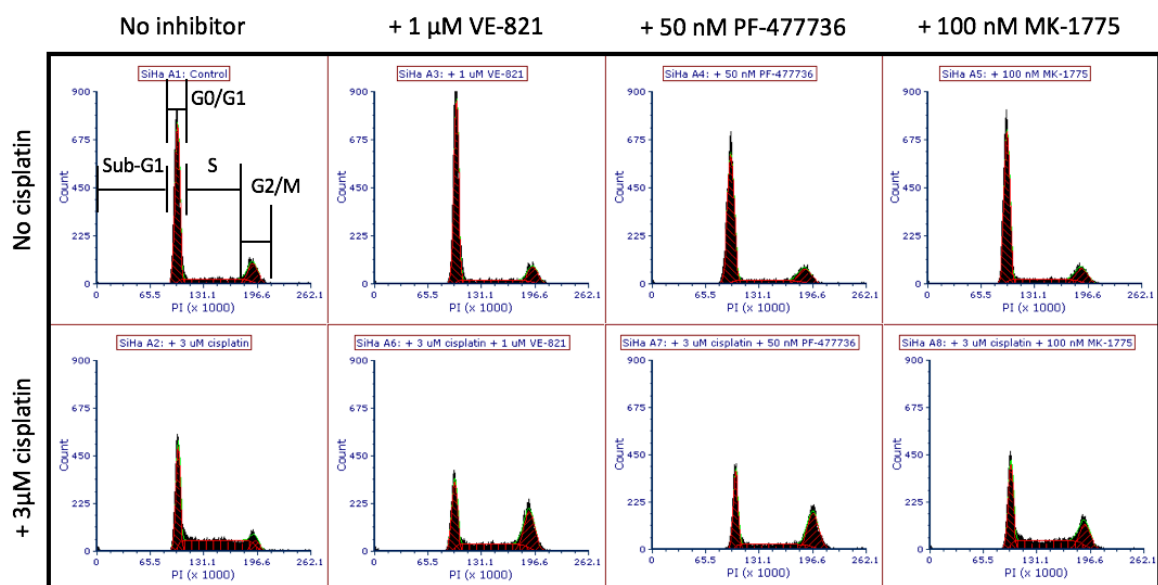


Figure 6.1 Representative example of cell cycle profile histograms showing cell cycle distributions of SiHa cells with and without treatment using cisplatin +/- VE-821, PF-477736 and MK-1775.

Cells were stained with PI and doublets were gated out using height vs area plots for more than 20000 individual events. Percent-populations of cells in sub-G1, G0/G1, S and G2/M were calculated by gating the histograms as shown. The PI content of individual cell cycle phases were determined on histograms from control cells and applied to histograms from treated cells.

6.4 Results

6.4.1 Cell cycle responses to single agents

Exposure to minimally cytotoxic concentrations of the checkpoint inhibitors alone for 24 h did not substantially affect the cell cycle profile of any of the cell lines (Table 6.1 and Figures 6.2 – 6.4). However, cisplatin at a concentration of 3 μ M for 24 hours (that causes > 90% inhibition of survival in all cell lines) resulted in marked changes in the cell cycle profiles.

The most remarkable effect of cisplatin was a substantial and significant increase in the S-phase fraction for all cell lines, which varied from 300% in HeLa to 175% in C33A. In general, this was at the expense of the G1 fraction, which was correspondingly decreased. Because the G1 population was the largest, the proportional change was less than for S-phase. The decrease in G1 ranged from 69% (HeLa) to 36% SiHa and was significant ($p < 0.05$ for all cells except CaSki ($p = 0.10$)). The shift from G1 to S could be a result of the lack of a functional G1 checkpoint. The G2/M fraction was low in control cells and cisplatin had a modest and variable effect on percentage of cells in this fraction.

6.4.2 Effect of ATR, CHK1 and WEE1 inhibitors on cisplatin-induced cell cycle profile changes.

VE-821 caused substantial reductions in cisplatin induced S-phase accumulations in HeLa (57% reduction, $p = 0.02$), SiHa (62% reduction, $p = 0.02$) and C33A (24% reduction, $p = 0.05$) cells. This was accompanied by corresponding increases in G2/M-phase populations in HeLa (250%, $p < 0.01$), SiHa (200%, $p = 0.07$) and C33A (100%, $p = 0.02$) cells. A less marked decrease in G1 cells that varied between the cell lines was observed (Figure 6.2). In contrast, co-incubation with VE-821 and cisplatin caused 50% increase in the S-phase populations in ME-180 and 30% in HT-3 cells compared to cisplatin alone, but neither increase was statistically significant due to inter-assay variability and the limited number of experiments.

Cell line	inhibitor	Cisplatin	% single cell population							
			Sub-G1		G1		S		G2/M	
			A	B	A	B	A	B	A	B
HeLa	-	-	3.7	3.8	75	69	13	17	8.5	11
	-	+	3.3	2.3	25	19	57	64	15	15
	VE-821	-	4.8	4.0	72	71	15	16	8.4	9.3
	PF-477736	-	5.4	4.1	75	68	12	18	7.1	10
	MK-1775	-	4.6	4.3	72	70	13	19	10	6.4
	VE-821	+	4.0	2.6	12	6.7	34	34	50	56
	PF-477736	+	4.9	3.8	24	17	23	27	48	52
	MK-1775	+	4.9	3.7	20	13	33	36	42	47
SiHa	-	-	0.6	0.3	68	77	17	10	14	13
	-	+	0.3	0.4	47	45	41	45	13	9.2
	VE-821	-	0.5	0.9	74	76	13	13	12	11
	PF-477736	-	0.5	0.6	75	78	12	10	12	11
	MK-1775	-	0.4	0.4	72	77	14	12	14	11
	VE-821	+	0.5	0.5	37	46	24	27	39	27
	PF-477736	+	0.6	0.6	39	53	22	20	38	26
	MK-1775	+	0.4	0.7	42	54	35	31	22	15
C33A	-	-	1.1	0.8	56	59	21	20	22	21
	-	+	0.6	0.8	25	29	56	57	18	14
	VE-821	-	1.4	0.7	57	63	20	17	21	19
	PF-477736	-	1.6	0.7	59	62	21	19	19	19
	MK-1775	-	0.6	1.2	58	61	20	22	22	16
	VE-821	+	1.6	1.3	21	15	46	50	32	34
	PF-477736	+	1.3	1.4	24	26	46	48	29	25
	MK-1775	+	0.6	0.7	16	20	53	51	30	27
CaSki	-	-	1.2	0.5	59	55	20	21	19	23
	-	+	3.7	0.2	15	36	68	53	14	11
	VE-821	-	1.4	0.4	56	55	22	21	21	24
	PF-477736	-	1.9	0.5	56	52	22	24	21	23
	MK-1775	-	1.9	0.6	55	52	19	23	24	24
	VE-821	+	6.1	0.3	30	31	53	60	11	8.8
	PF-477736	+	6.3	0.4	29	32	48	59	17	8.6
	MK-1775	+	6.3	0.4	35	37	43	53	16	10
ME-180	-	-	0.1	0.4	56	71	22	12	21	17
	-	+	0.4	1.5	30	18	60	71	8.9	9.3
	VE-821	-	0.4	0.4	62	77	22	11	16	12
	PF-477736	-	0.4	0.3	60	74	21	11	18	15
	MK-1775	-	0.9	0.5	60	76	21	10	18	13
	VE-821	+	1.1	0.4	7.2	5.4	89	87	3.1	7.0
	PF-477736	+	1.3	0.7	8.5	7.4	86	84	4.6	8.4
	MK-1775	+	1.7	0.5	17	10	77	77	3.7	13
HT-3	-	-	1.8	1.2	66	59	17	18	16	22
	-	+	1.9	2.4	26	23	48	58	24	16
	VE-821	-	1.4	1.0	66	58	15	18	17	23
	PF-477736	-	1.4	1.4	66	58	16	17	17	23
	MK-1775	-	1.8	0.9	67	54	16	18	16	27
	VE-821	+	7.3	4.1	17	18	61	65	15	12
	PF-477736	+	4.5	3.4	21	22	52	60	22	15
	MK-1775	+	4.1	2.1	21	24	51	58	24	17

Table 6.1 Percent-single cell populations per cell cycle phase for six cervical cancer cell lines exposed to cisplatin +/- inhibitors drugs.

Exponentially growing cells were treated with 1 μ M VE821, 50 nM PF-477736 or 100 nM MK-1775 +/-3 μ M cisplatin for 24 hours. Control cells were co-incubated in fresh media + DMSO at an equivalent concentration. At least 20000 events per sample were recorded. Percent-populations from single cells in each phase of the cell cycle were quantified using FCS Express (De Novo software) in two separate experiments: A and B.

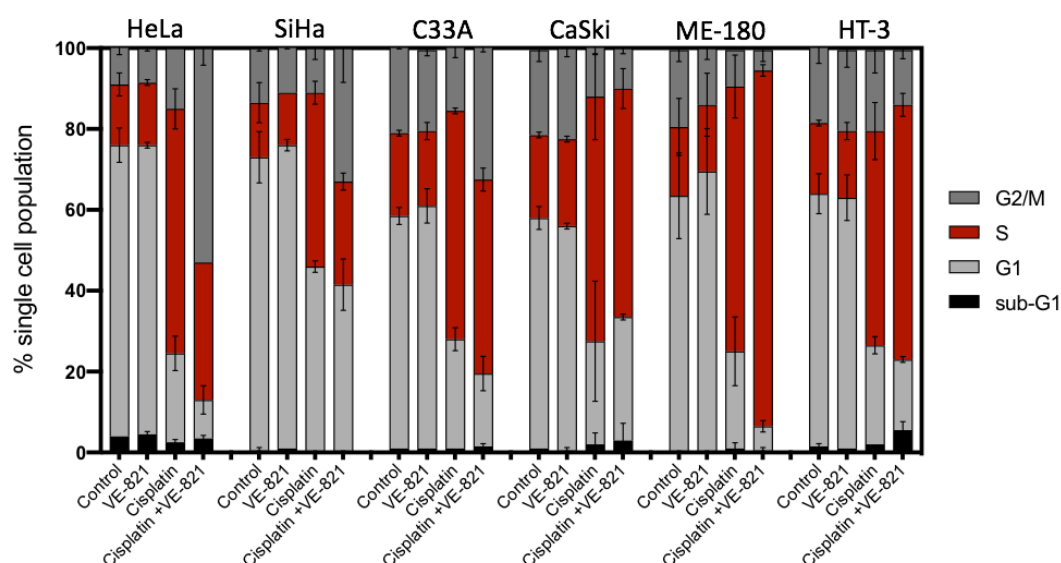


Figure 6.2 Cell cycle profiles of cervical cancer cell lines treated with VE-821 and cisplatin as single agents and in combination.

Exponentially growing cells were treated with 1 μ M VE821, 3 μ M cisplatin or both drugs in combination for 24 hours before being fixed in 70% ethanol. Cells were washed in PBS, treated with RNase and stained with PI. DNA content was analysed using a FACSCanto II flow cytometer. At least 20000 events per sample were recorded. Percent-populations from singlet cells in each phase of the cell cycle were quantified using FCS Express (De Novo software). Data are the mean and range of values from two independent experiments and are derived from values shown in Table 6.1

Similarly, co-incubation with PF-477736 (50 nM) caused reductions in cisplatin induced S-phase accumulations in HeLa (78% reduction, $p < 0.01$), SiHa (75% reduction, $p < 0.01$) and C33A (26% reduction, $p < 0.01$) cells, accompanied by a corresponding increase in the G2/M fraction of HeLa (230%, $p < 0.01$), SiHa (190%, $p = 0.08$) and C33A (68%, $p = 0.06$) cells. As with ATR inhibition, the CHK1 inhibitor increased the cisplatin-induced S-phase accumulation (by 43%) and reduced the G2/M fraction in ME-180 (23% reduction) but these were not significant. PF-477736 did not substantially affect the cell cycle changes associated with cisplatin exposure in CaSki or HT-3 cells (Figure 6.5). Co-incubations with 100 nM MK-1775 also reduced cisplatin-induced S-phase accumulation and increased the G2/M fraction in HeLa cells but to a lesser degree than with VE-821 and PF-47736. In general, the effects of MK-1775 were similar but less pronounced than with the ATR or CHK1 inhibitors.

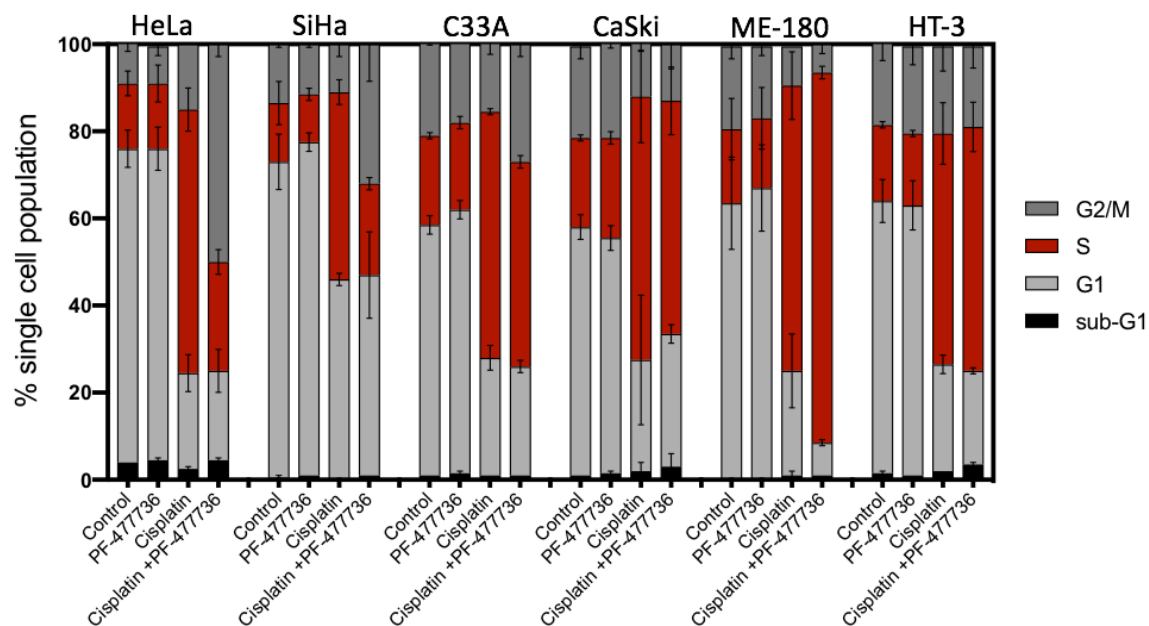


Figure 6.3 Cell cycle profiles of cervical cancer cell lines treated with PF-477736 and cisplatin as single agents and in combination.

Exponentially growing cells were treated with 50 nM PF-477736, 3 μ M cisplatin or both drugs in combination for 24 hours before being fixed in 70% ethanol. Cells were washed in PBS, treated with RNase and stained with PI. DNA content was analysed using a FACSCanto II flow cytometer. At least 20000 events per sample were recorded. Percent-populations from singlet cells in each phase of the cell cycle were quantified using FCS Express (De Novo software). Data are the mean and range of values from two independent experiments and are derived from values shown in Table 6.1

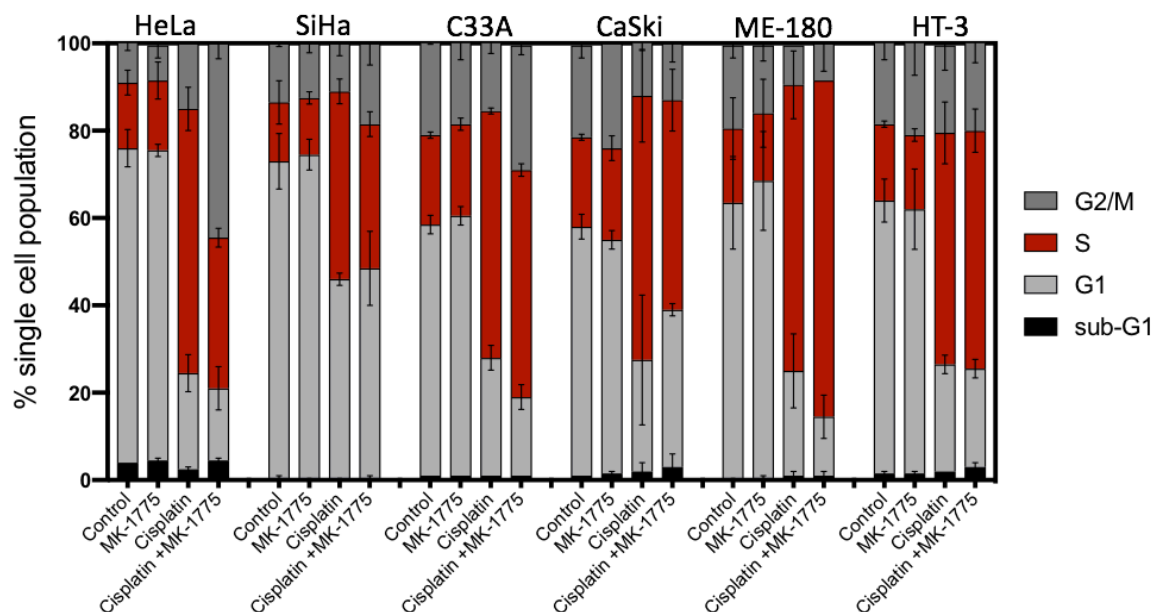


Figure 6.4 Cell cycle profiles of cervical cancer cell lines treated with MK-1775 and cisplatin as single agents and in combination.

Exponentially growing cells were treated with 100 nM MK-1775, 3 μ M cisplatin or both drugs in combination for 24 hours before being fixed in 70% ethanol. Cells were washed in PBS, treated with RNase and stained with PI. DNA content was analysed using a FACSCanto II flow cytometer. At least 20000 events per sample were recorded. Percent-populations from singlet cells in each phase of the cell cycle were quantified using FCS Express (De Novo software). Data are the mean and standard deviation of two independent experiments and are derived from values shown in Table 6.1

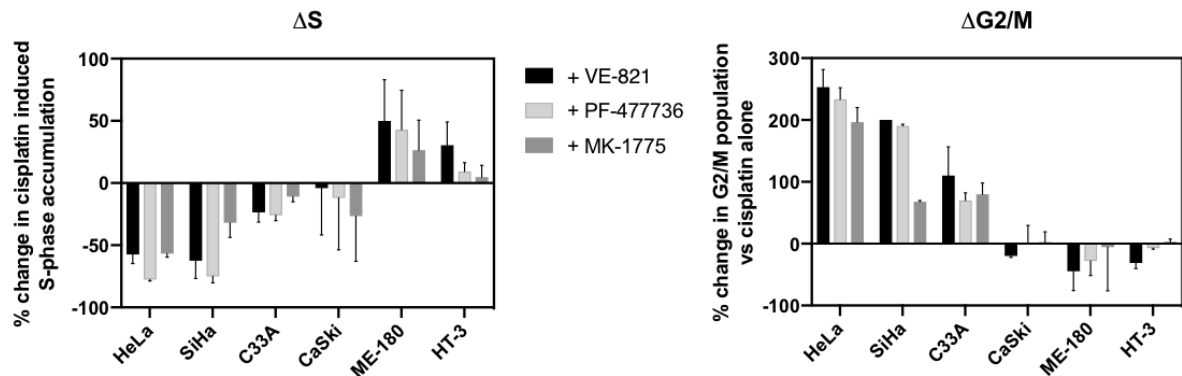


Figure 6.5 Changes in S-phase and G2/M-phase populations in cells treated with cisplatin-inhibitor combinations compared to cells treated with cisplatin alone.

A. % change in cisplatin induced S-phase accumulation of cells treated with cisplatin-inhibitor combinations. **B.** % difference in G2/M-phase populations of cells treated with cisplatin-inhibitor combinations compared to cells treated with cisplatin alone. Raw data is taken from cell cycle profiles, as displayed in figures 6.1 to 6.3 and represent mean and SD resulting from two independent experiments.

6.4.3 Correlations between cell cycle changes, cell line characteristics and cytotoxicity profiles

Changes with cisplatin exposure compared to control

Though HeLa cells are the least sensitive to cisplatin in survival assays (Chapter 5), they showed the greatest disturbance in their cell cycle profile in response to cisplatin exposure. Conversely, SiHa cells were the most sensitive to cisplatin but had one of the more modest disturbances in their cell cycle profile. When the other cell lines were considered, however no relationship was seen between sensitivity (survival) to cisplatin and the magnitude of changes G0/G1, S-phase or G2/M populations.

It would be expected that changes in the cell cycle profile in response to cisplatin would be related to the activation of ATR, CHK1 or WEE1 by cisplatin. No such correlations were found. Neither was there any relationship with the characteristics of the cell lines described in Chapter 3: baseline DDR protein expression and cell line growth rate (data not shown).

Changes with cisplatin + inhibitor co-exposure compared to cisplatin alone

The effect of 1 μ M VE-821 on cisplatin induced S-phase and G2/M cell cycle changes strongly correlated with the extent of ATR inhibition measured in the cell lines at this concentration (Chapter 4). There were, however no such relationships between cisplatin induced S-phase or G2/M changes and CHK1 or WEE1 inhibition in response to PF-477736 or MK-1775, respectively (Figure 6.6).

Unsurprisingly, given the previously noted relationship between ATR expression and the magnitude of ATR inhibition by 1 μ M VE-821, a relationship was also found to exist between baseline ATR expression and the S-Phase and G2/M changes, described above (Figure 6.7). Higher ATR expression resulted in larger reduction of the cisplatin induced S-phase accumulation in response to 1 μ M VE-821, with a corresponding increase in G2/M populations. As would be expected given the relationship between ATR and CHK1 expression (Chapter 3), an inverse relationship between these cell cycle changes and CHK1 expression was also noted, though this failed to reach statistical significance.

S-phase and G2/M-phase changes vs enzyme inhibition

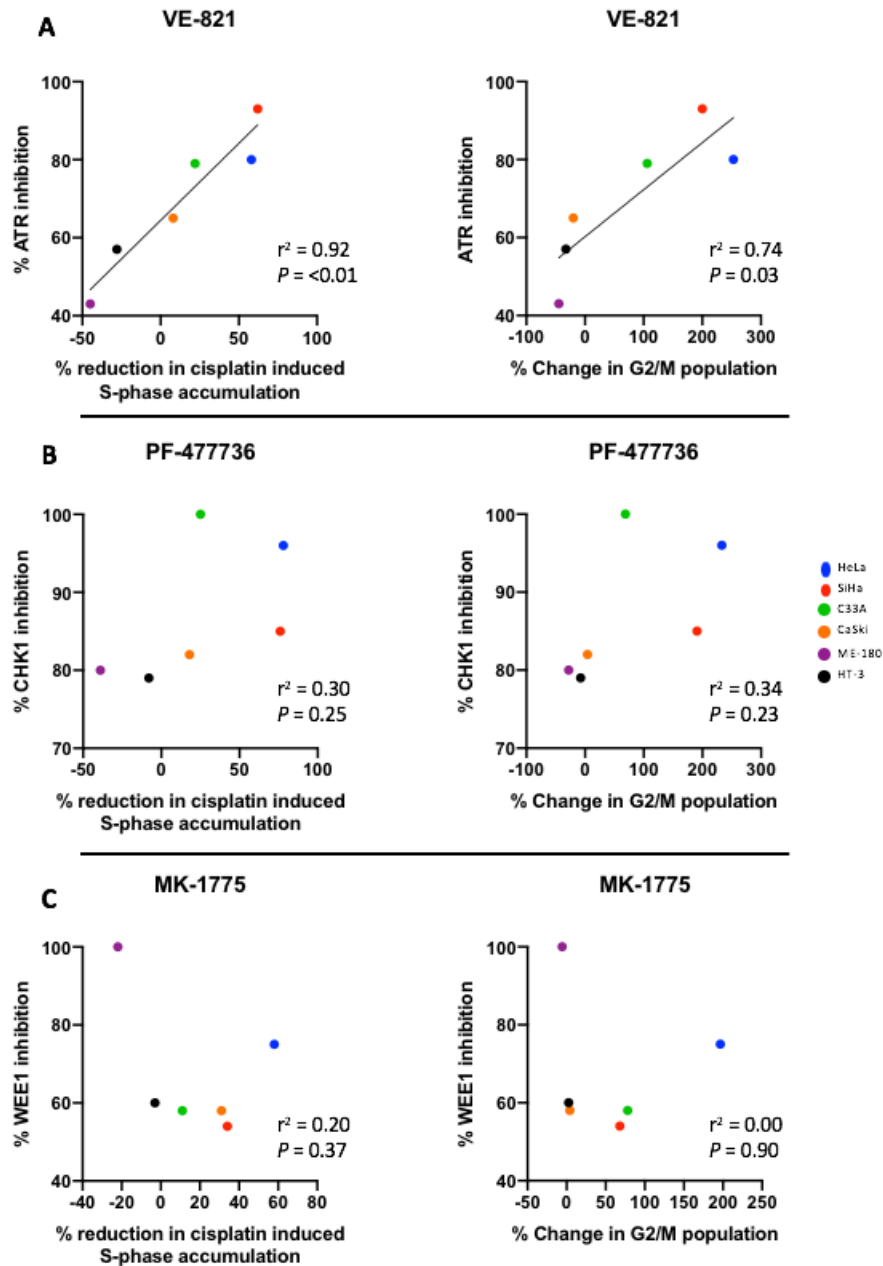


Figure 6.6 Correlations between target enzyme inhibition and effect of 1 μ M VE-821, 50 nM PF-477736 and 100 nM MK-1775 on cell cycle profile changes induced by 3 μ M cisplatin.

A: Changes in S and G2/M populations vs inhibition of ATR by 1 μ M VE-821. **B:** Changes in S and G2/M populations vs inhibition of CHK1 by 50 nM PF-477736. **C:** Changes in S and G2/M populations vs inhibition of WEE1 by 100 nM MK-1775. All exposure times were for 24 hours. Data are taken from that displayed in Figures 4.3, 4.5 and 4.7 and Figures 6.2 to 6.3 and are the mean of at least two independent experiments.

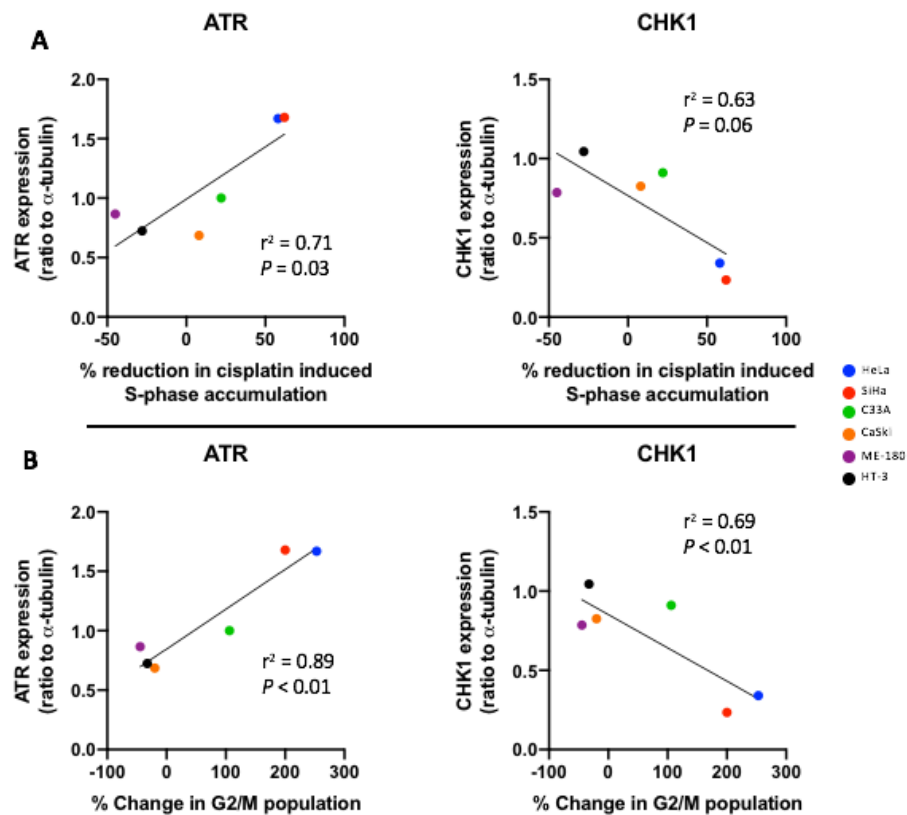


Figure 6.7 Correlations between ATR and CHK1 expression and effect of 1 μ M VE-821 on cell cycle profile changes induced by 3 μ M cisplatin.

A: Changes in cisplatin induced S-phase accumulations vs expression of ATR and CHK1. **B:** Changes in G2/M populations vs expression of ATR and CHK1. All exposure times were for 24 hours. Data are taken from that displayed in Figure 3.5 and Figures 6.2 to 6.4 and are the mean of at least two independent experiments.

Changes in cisplatin induced S-phase and G2/M changes caused by 50 μ M of the CHK1 inhibitor PF-477736 also correlated with CHK1 and ATR baseline expressions, though the relationship did not reach significance for CHK1 expression (Figure 6.8), high ATR expression and Low CHK1 expression was associated with larger reductions in cisplatin induced S-phase accumulations and also with larger increases G2/M populations. No such correlations existed for the WEE1 inhibitor, MK-1775.

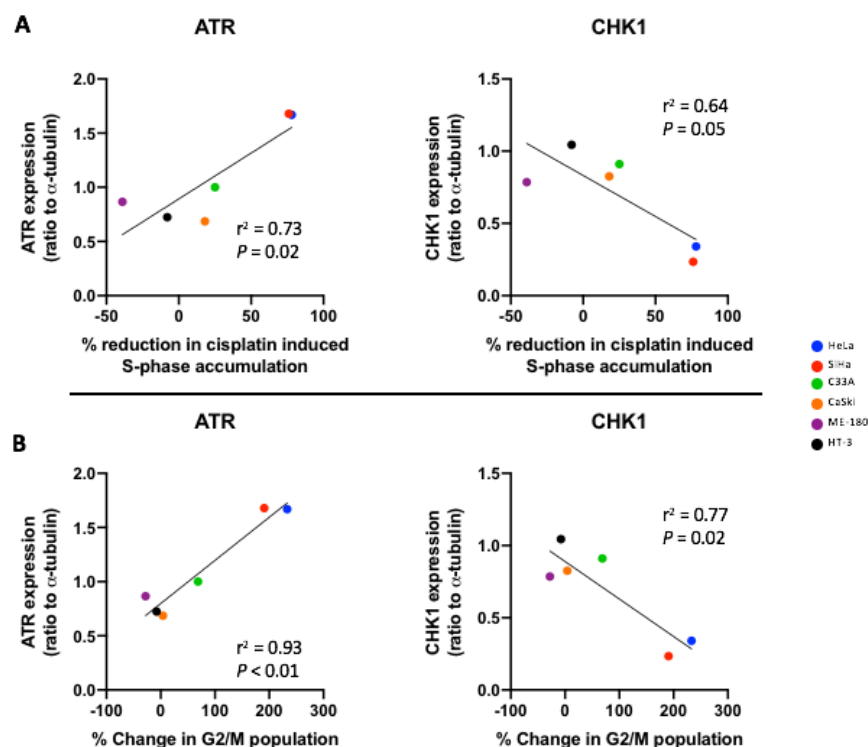


Figure 6.8 Correlations between ATR and CHK1 expression and effect of 50 nM PF-477736 on cell cycle profile changes induced by 3 μ M cisplatin.

A: Changes in S-phase populations vs expression of ATR and CHK1. **B:** Changes in G2/M populations vs expression of ATR and CHK1. All exposure times were for 24 hours. Data are taken from that displayed in Figure 3.5 and Figures 6.1 to 6.3 and are the mean of at least two independent experiments.

6.5 Discussion

Consistent with observations from previous studies (Middleton et al., 2018), at concentrations that were not profoundly cytotoxic (Table 4.2), VE-821, PF-477736 and MK-1775 had no significant impact on cell cycle distributions despite substantial target inhibition (Chapter 4). In contrast to this, treatment of the cell lines with 3 μ M cisplatin for 24 hours resulted in significant changes. Substantial increases in S-phase populations were seen, and this appeared predominantly at the expense of G1/S populations, indicative of dysfunction of the G1/S checkpoint in all cell lines. However, reductions in G2/M populations were also seen in C33A, CaSki and ME-180 cells. Only in HeLa cells did cisplatin cause an increase in G2/M cell population.

The increase in S-phase populations seen across all cell lines points towards engagement of intra-S checkpoint functions as the dominant DDR component in response to cisplatin induced DNA damage in the cervical cancer cell lines. However, physical slowing of replication forks by ICLs and engagement of repair without checkpoint signalling could also contribute. This pattern was irrespective of HR-HPV, p53 or pRB status. Increased replication stress resulting from stalled replication forks will activate ATR-CHK1-WEE1 mediated signalling to slow replication origin firing and may be responsible for arrest of the cell in S-phase, causing the measured cell cycle profile changes (Iyer and Rhind, 2017, Cimprich and Cortez, 2008, Maréchal and Zou, 2013). Consistent with this are the observations that the cells with highest ATR expression and the greatest ATR inhibition by VE-821 had the greatest reduction in cisplatin-induced S-phase arrest when treated with VE-821. However, the lack of corresponding correlations for CHK1 and WEE1, and their inhibitors make drawing conclusions on the importance of either the extent of the observed inhibition or level of baseline expressions of the enzymes difficult.

Modest but non-significant increases in cisplatin-induced S-phase accumulations, particularly by VE-821 in ME-180 and HT-3 cells (Figure 6.5), may reflect its lower target inhibition in these cells (Chapter 4) but without further studies, including in additional cell lines, the mechanisms underlying this effect cannot be elucidated. With this evidence, we can only speculate that the increase in cisplatin induced S-phase accumulations arose out of other

mechanisms related to the cells difficulty in resolving platinum induced DNA lesions and the roles the kinases and inhibitors may play in these pathways.

For HeLa, SiHa and C33A cells the decrease in S-phase accumulation was accompanied by a corresponding increase in G2/M cells and so for these cells at least, the intra-S checkpoint may be the most important for cisplatin induced DNA damage resolution. A limitation of PI staining is its inability to distinguish between G2 and M-phase cells. It could be hypothesised that in these cell lines, cells which have escaped G2 arrest and entered mitosis may be responsible for the apparent increase in G2/M phase cells, particularly as there was limited evidence for a corresponding increase in sub-G1 cell populations, indicating that most cells were still cycling at the point of fixation.

Further studies are, however needed with additional DNA damaging agents (e.g. IR), additional methods for distinguishing G2 and M-Phase cells (e.g. staining for phospho-histone-H3^{S10}) and other cell lines. This will help to elucidate whether the inhibitors always have the greatest impact on the intra-S checkpoint. Whether it was a function of the type of DNA damage caused by cisplatin that primarily engaged intra-S DDR functions and whether the changes in G2/M fractions are due to G2 arrest and escape remain to be determined.

6.6 Conclusions

With reference to the aims set out at the start of this chapter:

1. Minimally cytotoxic concentrations of all three inhibitor drugs caused little or no disturbance in the cell cycle profile of the cells across the cell line panel
2. All three inhibitors caused similar pattern changes to cisplatin induced S-phase accumulations across the cell line panel
3. The cells appeared to fall into two groups:
 - a. HeLa, SiHa and C33A cells, which showed a reduction in cisplatin-induced S-phase accumulations in response to inhibitor treatment suggesting attenuation of cisplatin induced S-phase arrest
 - b. ME-180, HT-3 (and CaSki) cells, which showed an increase in cisplatin-induced S-phase accumulations in response to inhibitor treatment and which is so far unexplained.

4. The magnitude or nature of cell cycle profile changes did not correlate with the extent of sensitisation to cisplatin across the cell line panel for any of the inhibitors.
5. Some correlations were seen between the magnitude of effect of VE-821 on cisplatin-induced S-phase accumulation and inhibition or expression of ATR and CHK1, but data with PF-477736 and MK-1775 were not convincing.

7 Exploration of checkpoint protein expression in clinical tumour samples

7.1 Introduction

Earlier experiments, described in Chapter 3, have demonstrated that cervical cancer cell lines with known HR-HPV and oncogene status display a range of cell cycle checkpoint protein expression and that there appear to be relationships between the levels of expression of some of these proteins. Despite the small number of cell lines available for investigation, positive correlations were noted between CHK1 and CDK1 and a significant inverse correlation was found between ATR and CHK1 levels. An inverse correlation was also noted between ATR and CDK1, as might be expected given this result. There appeared to be limited evidence that the expressions of cell cycle proteins were significant determinants of sensitivity to the ATR, CHK1 or WEE1 inhibitors VE-821, PF-477736 or MK-1775, respectively as single agents or sensitisers of cisplatin and IR, though WEE1 expression appeared to correlate with a narrow range of MK-1775 sensitisation of cell lines to cisplatin.

Given the absence of a clear determinant of sensitivity to the inhibitors or cisplatin and IR amongst the cell line panel a decision was taken to investigate the expression of the cell cycle proteins: ATR; CHK1; and WEE1 by immunohistochemistry (IHC) in a panel of formalin fixed and paraffin embedded (FFPE) clinical cervical cancer tumour from patients, and to supplement this with expression data from publicly available datasets. The presence of a range of level of protein expression and any similar correlations to that seen in the cell line panel would provide further validation of the cervical cancer cell lines as a useful tool in pre-clinical investigations and provide confidence in the applicability of cell line derived results to clinical cancer investigations.

7.2 Aims and Objectives

The aim of the investigations described in this chapter is to determine the range of expression of ATR, CHK1 and WEE1 in a panel of clinical cervical cancer tumour samples and to explore whether relationships between these proteins, as observed in cervical cancer cell lines, exist in clinical tumour samples. The clinical sample set will be supplemented by investigation of mRNA expression data from The Cancer Genome Atlas (TCGA) dataset.

7.3 Materials and methods

7.3.1 TMA construction and slide preparation

Women with cervical cancer who underwent treatment or investigation at the Northern Gynaecological Oncology Centre, Queen Elizabeth Hospital (QEH), Gateshead between February 2017 and January 2018 were approached under existing ethical permissions (2012 REC: 12/NE0395. R&D sponsor: NUTH NHS foundation trust No. 6579) for retrospective written consent to biobank formalin-fixed, paraffin-embedded (FFPE) diagnostic or surgical specimens (blocks) containing primary cervical cancer tissue. 29 women with cervical cancer consented. 10 blocks were available from storage at the QEH pathology lab following diagnosis or treatment that contained sufficient tumour material to allow for core extraction and inclusion in the tissue micro-array (TMA) along with one historical sample. Slides were prepared from candidate blocks by clinical scientists at the QEH laboratory and Haematoxylin and Eosin (H+E) stained prior to review by a consultant histopathologist pathologist to identify areas corresponding regions containing tumour for core extraction.

The TMA assembly contained a total of 26 x 1 mm cores: duplicate samples from 11 patients and 2 positive control blocks (human testes and a HeLa-agarose cell block). Cores were randomly assigned to TMA locations by the Galileo TMA CK3500® and associated computer software to reduce the risk of core loss or reading bias affecting results (Figure 7.1). Ideally a TMA will contain tumour known not to express the protein

under investigation to provide a further negative control. As ATR, CHK1 and WEE1 are required for viability, this was not possible.

S4	S6	S7	S10	S2	S5
S9	S1	S8	S3	Control 2	Control 1
S3	S5	Control 1	S4	S9	S11
		S10	S6	S1	Control 2
		S2	S11	S7	S8

Figure 7.1 Tissue microarray layout containing duplicate cores from 11 patient samples and 2 positive control cores.

Core locations were randomly selected by computer software. S = patient sample. Control 1= HeLa cells. Control 2 = human testes.

Individual 5 µm sections were taken by microtome and positioned on glass slides for immunohistochemical staining. HeLa block preparation and microtome sectioning of the TMA and H+E staining were undertaken by a dedicated immunohistochemistry (IHC) technician at the NICR according to local protocols.

7.3.2 Immunohistochemistry

Primary and secondary antibodies used for IHC investigation of ATR, CHK1 and WEE1 expression as well as antigen retrieval methods are given in Table 7.1. CHK1 antigen retrieval and antibody dilution optimisation was undertaken by MRES student, Mr Harry Robinson. Due to time limitations for these investigations, antigen retrieval methods for ATR and WEE1 were undertaken according to antibody manufacturer and expert advice. A range of three antibody dilutions were tested for each antibody including: the dilution advised by the manufacturer and; a single dilution more or less concentrated.

Slides were de-waxed in xylene hydrated through graded ethanol (100% to 50%) and washed in tap water. Antigen retrieval was performed using citrate buffer (pH 6) heated to at 125 °C for 30 s under pressure. Slides were rinsed in tap water before and after exposure to 3% hydrogen peroxide solution for 10 minutes. Incubations were performed with diluted primary antibody (Table 7.1) for 60 minutes each at room temperature prior to application of Menapath® IHC kit HRP-polymer +/- universal probe (A. Menari diagnostics, USA) for 30 minutes each. No-antibody negative controls slides were prepared without primary antibody staining. Slides were rinsed in Tris-buffered saline + 0.1% Tween 20 (TBST). DAB solution applied to each slide for 1 minute before neutralisation in sodium hypochlorite and a further tap water rinse. All slides were then counterstained in Gills II haematoxylin for 5 seconds and blued in Scott's Tap Water. Following dehydration through graded ethanol (50% to 100%) and Xylene, cover-slips were applied using DPX mounting medium and allowed to dry.

Antigen	Primary antibody	Dilutions (Diluent)	Secondary antibody
ATR	Anti-ATR (abcam ab222820) Rabbit polyclonal Ab	1:50, 1:100, 1:200 (TBS)	HRP polymer
CHK1	Anti-CHK1(G-4) (Santa-Cruz sc-8448) Mouse monoclonal Ab	1:500 (TBS)	Universal probe + HRP polymer
WEE1	Anti-WEE1(B-11) (Santa-Cruz sc-5285) Mouse monoclonal Ab	1:100, 1:200, 1:500 (1% BSA in TBS)	Universal probe + HRP polymer

Table 7.1 Antibodies and dilutions used for IHC staining of clinical TMA slides.

Antigen retrieval was undertaken in citrate buffer (pH 6) in a pressure cooker in all cases. Secondary antibodies were applied according to the Menapath® protocol using reagents supplied in the IHC kit.

7.3.4 Slide scanning and data analysis

Slides were scanned by Ms Xin Xu at the Newcastle University central biobank facility using Leica SCN400® slide scanner and images were accessed and viewed remotely using a web-based Leica digital image hub (slidepath.ncl.uk). A modified H-score was calculated for each core in the TMA at the antibody dilution which best allowed differentiation between stained and non-stained nuclei.

The modified H-score was calculated by multiplying the staining intensity of nuclear staining (0-3) by the proportional area of tumour positively stained (0-6), to give a minimum score of 0 and a maximum score of 18 (Table 7.2). A single score was determined for each core, as tumour staining tended to be of uniform intensity in each core. The mean score from duplicate cores was calculated. Where there was core loss or artefact impeding interpretation the score from the remaining core was used. Cores composed of less-than 20% tumour were excluded.

Pearson's correlation analysis was performed on H-scores determined experimentally using Graphpad Prism®. TCGA mRNA expression data for ATR, CHK1 and WEE1 was analysed by Pearson correlation analysis by Dr Sweta Sharma Saha. Survival analysis of TCGA patient cohorts was by Kaplan-Meier plot undertaken on open source software available at <http://www.proteinatlas.org> and significance testing for correlations between mRNA expression data and patient survival was by Log-rank test.

7.4 Results

7.4.1 Optimisation of antibody dilutions

The optimal dilution for CHK1 staining was previously determined to be 1:500 (Figure 7.2). The antibody dilutions tested for ATR staining were 1:50, 1:100 and 1:200 with an optimal dilution of 1:200 selected for quantification of ATR expression in tumour samples by modified H-score (Figure 7.3, D-F). The WEE1 antibody failed to stain satisfactorily at any of the dilutions tested (Figure 7.3, G-I) and no quantification of WEE1 expression in the tumour samples was possible.

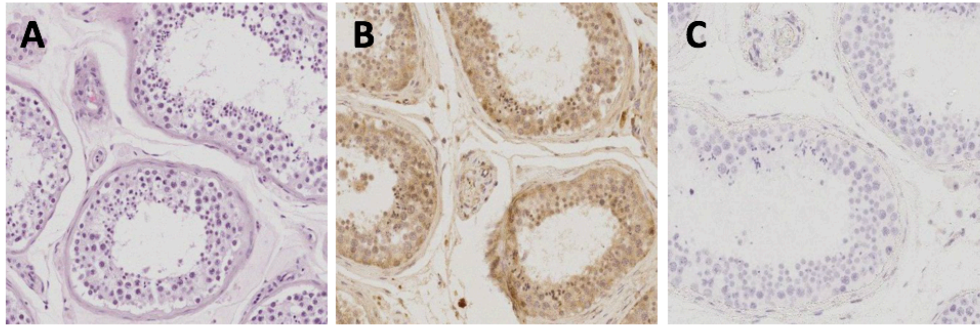


Figure 7.2 Micrographs of human testes positive control tissue demonstrating CHK1 staining.

A: H+E stained section showing cellular areas. B: Anti-CHK1 antibody staining at dilution of 1:500 with corresponding nuclear staining. C: No-primary antibody negative control with anti-mouse secondary antibody.

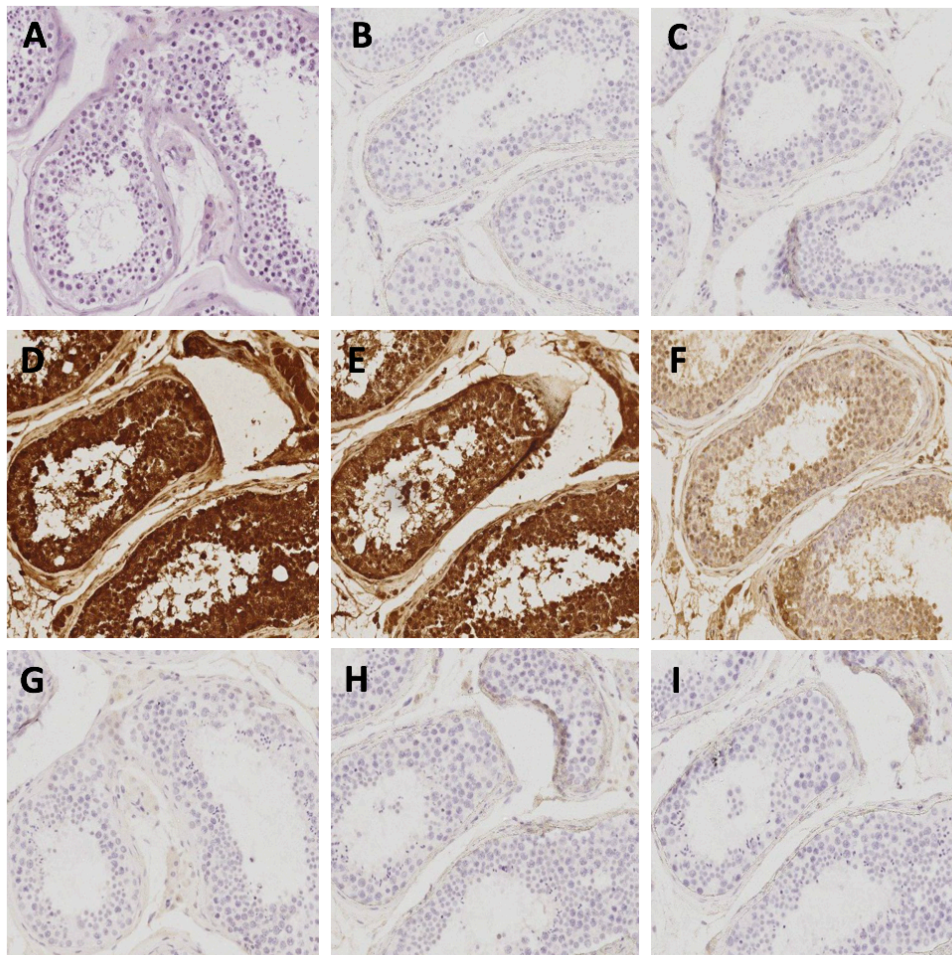


Figure 7.3 Micrographs of human testes positive control tissue demonstrating ATR staining but inadequate WEE1 staining.

A: H+E stained section showing cellular areas. B: No-primary antibody negative control with anti-rabbit secondary antibody. C: No-primary antibody negative control with anti-

mouse secondary antibody. **D-F:** Anti-ATR antibody staining at 1:50 (**D**), 1:100 (**E**) and 1:200 (**F**). **G-I:** Anti-WEE1 antibody staining at 1:100 (**G**), 1:200 (**H**) and 1:500 (**I**).

7.4.2 IHC scoring

ATR and CHK1 stained cores were scored using the method and antibody dilutions detailed in section 7.3.4. Figure 7.4 shows representative TMA cores stained for ATR and CHK1 and examples of stain intensity used to calculate the modified H-score. H-Scores for both ATR and CHK1 varied between 0 and 18 (Table 7.2). The core that scored most strongly for both proteins was later noted to be a serous cancer of the cervix, a rare tumour that is not associated with HR-HPV infection. With this core excluded, the highest H-score for ATR was 12.5 in a squamous cancer. The highest H-score for CHK1 was 10.5 in an adenocarcinoma. Due to the limited number of clinical samples and the fact that tumour-deficient exclusions were exclusively in the adenocarcinoma group, it was not possible to determine if there was a difference in the expression of ATR or CHK1 amongst the tumour sub-types.

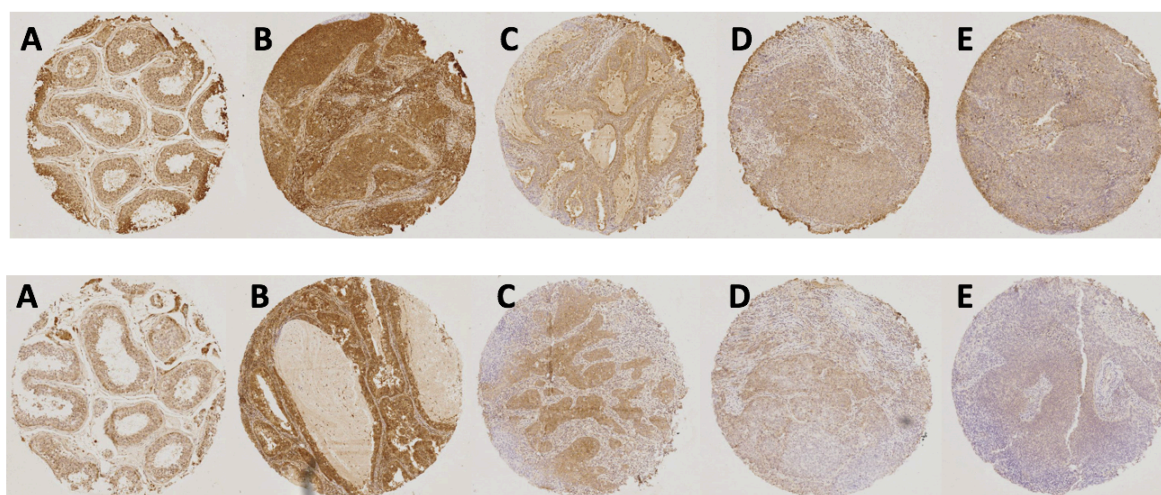


Figure 7.4 Micrographs of representative TMA cores stained for ATR (top) and CHK1 (bottom).

A: Positive control tissue (human testes). **B:** Tumour demonstrating strong stain intensity (score = 3). **C:** Tumour demonstrating moderate stain intensity (score = 2). **D:** Tumour demonstrating weak stain intensity (score = 1). **E:** Tumour demonstrating no tumour staining, including cytoplasmic staining only (score = 0). Antibody dilutions were 1:200 in 1%BSA-TBS for ATR and 1:500 in TBS for CHK1.

Sample	Clinical characteristics		Modified H-score (ATR)			Modified H-score (CHK1)		
	Pathology	Grade	Core 1	Core 2	Mean	Core 1	Core 2	Mean
S1	Squamous carcinoma	3	6	6	6	4	3	3.5
S2	Serous	3	No tumour	18	18	No tumour	18	18
S3	Adenocarcinoma	3	<20% tumour	<20% tumour	Excluded	<20% tumour	<20% tumour	Excluded
S4	Squamous carcinoma	3	<20% tumour	8	8	<20% tumour	0	0
S5	Squamous carcinoma	2	0	0	0	4	10	7
S6	Squamous carcinoma	3	15	10	12.5	0	0	0
S7	Adenocarcinoma	3	<20% tumour	<20% tumour	Excluded	<20% tumour	<20% tumour	Excluded
S8	Squamous carcinoma	3	6	6	6	3	1	2
S9	Squamous carcinoma	2	Lost core	3	3	6	12	9
S10	Adenocarcinoma	2	6	6	6	6	15	10.5
S11	Adeno-squamous	3	0	0	0	0	2	1

Table 7.2 Modified H-score results for individual cores from a cervical cancer TMA stained for ATR and CHK1.

Sample numbers correspond to the core locations detailed in Figure 7.1. Mean scores were calculated from the individual scores from duplicate cores. Where core loss or artefact impeded scoring, a single core score was used. Cores with 20% tumour were excluded. Sample S2 was later found to be a serous cancer of the cervix and was excluded from further analyses.

Given the strong negative correlation between ATR and CHK1 expression noted in Western blot analysis of baseline proteins in cervical cancer cell lines (Chapter 3), correlation analysis was conducted to determine whether a similar relationship between ATR and CHK1 existed in these clinical tumour samples. Whilst no correlation was present when the whole panel of clinical tumour samples was included, exploration of a difference observed in the squamous carcinoma sub-type revealed a significant inverse correlation between ATR and CHK1 expression (Figure 7.5) in keeping with that seen in the cervical cancer cell lines, however as the cell line data did not similarly exclude those derived from glandular cancers, and each correlation relies on a very small number of

data points. These investigations should be undertaken in a much larger set of samples before concluding that they are meaningful.

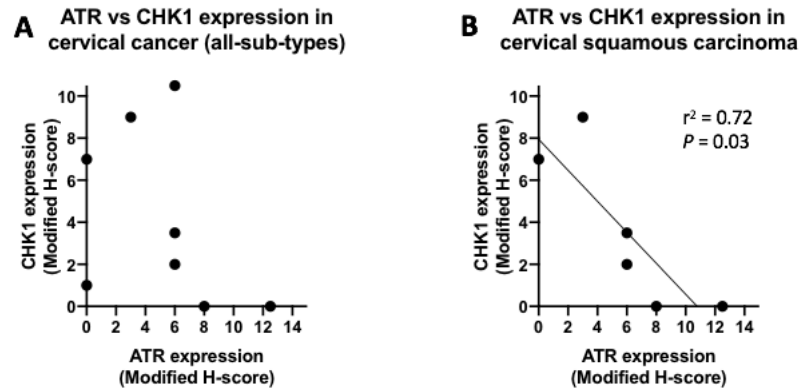


Figure 7.5 Correlations between ATR and CHK1 expression in clinical tumour samples

A: Scatter plot of ATR vs CHK1 expression for all cervical cancer sub-types. **B:** Scatter plot and linear regression of ATR vs CHK1 in cervical squamous cancers only. Data is taken from that displayed in Table 7.2.

7.4.3 ATR, CHK1 and WEE1 expression in a wider context.

In order to further explore the observed correlation between ATR and CHK1 protein expression from cell line data described in Chapter 3 (Figure 3.5) in clinical tumour samples, a correlation analysis of ATR and CHK1 mRNA expression derived from the TCGA study of cervical cancer (Cancer Genome Atlas Research et al., 2017) was performed by Dr Sweta Sharma Saha. The TCGA data included 291 clinical cervical cancer tissue samples, of which 75% were SCC. Pearson's Correlation analysis of ATR and CHK1 mRNA expression in the TCGA dataset showed no correlation between ATR and CHK1 expression (Figure 7.6). Neither protein showed correlation with WEE1 mRNA expression levels (data not shown).

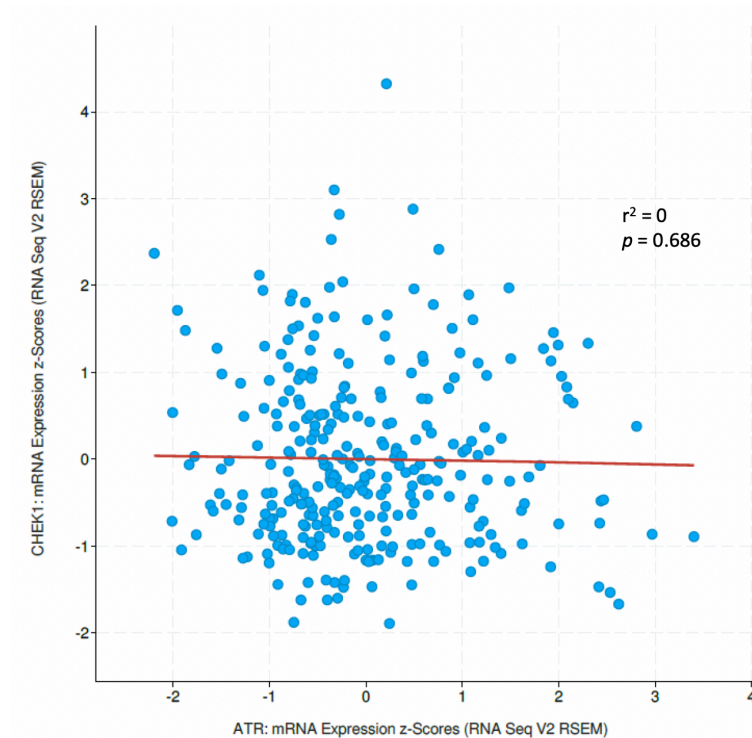


Figure 7.6 Correlation between ATR and CHK1 mRNA expression in TCGA data

Scatter plot showing ATR and CHK1 mRNA expression in 291 cervical cancers (75% SCC). The results shown here are based upon data generated by the TCGA Research Network: <https://www.cancer.gov/tcga>, analysed by Dr Sweta Sharma Saha

7.4.4 Clinical correlation

Clinical diagnostic and treatment data for the cervical cancer patients who donated tumour samples to these investigations are given in Table 7.3. The short time period between sample collection and data analysis and a median follow up interval of just 18.7 months at the time of writing, and the presence of a single a single episode of disease progression has occurred in this small patient cohort makes assessment of the prognostic significance for the expression of ATR and CHK1 in this patient cohort difficult. All patients included were treated with primary surgery and two received adjuvant radiotherapy without macroscopic disease. No correlations with response to cisplatin or IR are therefore possible.

Patient	Histology	Grade	Stage (FIGO 2009)	Primary Treatment	Adjuvant treatment	Date of 1st treatment	Date of follow up	Follow up (Months)	Status
S1	Squamous	3	1B2	Radical surgery	None	13.12.18	3.7.19	6.7	AWD
S3	Adeno.	3	1B1	Surgery	None	22.11.17	26.6.19	19.4	AWD
S4	Squamous	3	1A1	Loop excision	none	12.2.18	9.10.18	8.0	AWD
S5	Squamous	2	1B1	Radical Surgery	None	8.12.17	13.6.19	18.4	AWD
S6	Squamous	3	1B1	Radical Surgery	None	18.8.17	11.3.19	19.0	AWD
S7	Adeno.	3	1B1	Radical Surgery	None	2.10.17	4.3.19	17.3	AWD
S8	Squamous	3	2A	Radical Surgery	IR	8.11.17	1.6.19	19.0	AWD
S9	Squamous	2	1B2	Radical Surgery	None	30.11.17	3.7.19	19.3	AWD
S10	Adeno.	2	1B1	Radical Surgery	None	1.3.18	28.5.19	15.1	AWD
S11	Adeno-squamous	3	4B	Radical Surgery	IR	26.2.09	30.11.19	131.0	REC 30.11.18

Table 7.3 Clinical, diagnostic, treatment and follow-up data for cervical cancer patients who donated tumour samples to these investigations.

Loop excision = local excision with margin. Surgery = hysterectomy with pelvic lymphadenectomy. Radical surgery = radical hysterectomy or radical trachelectomy with pelvic lymphadenectomy. Patient S11 was diagnosed with primary cervical cancer on operative histology. AWD = alive without disease. REC = recurrence with date of progression/recurrence.

The TCGA study of cervical cancer (Cancer Genome Atlas Research et al., 2017) did not report survival effects of ATR, CHK1 or WEE1 gene alterations, underlining the novel nature of the data reported in this thesis. Using data from the Human Protein Atlas, available from <http://www.proteinatlas.org> (Uhlen et al., 2017), survival data for the patients included in the TCGA dataset was categorised by high (above the median) or low (below the median) expression (mRNA) of ATR, CHK1 and WEE1 (Figure 7.7 and Table 7.4). Overall, high expression of any of ATR or CHK1 was not prognostic in cervical cancer. High expression of WEE1, however showed a tendency towards increased survival. In this data, 75% of patients had SCC versus 25% with adenocarcinoma or adenosquamous cancer and 70% underwent primary surgical management.

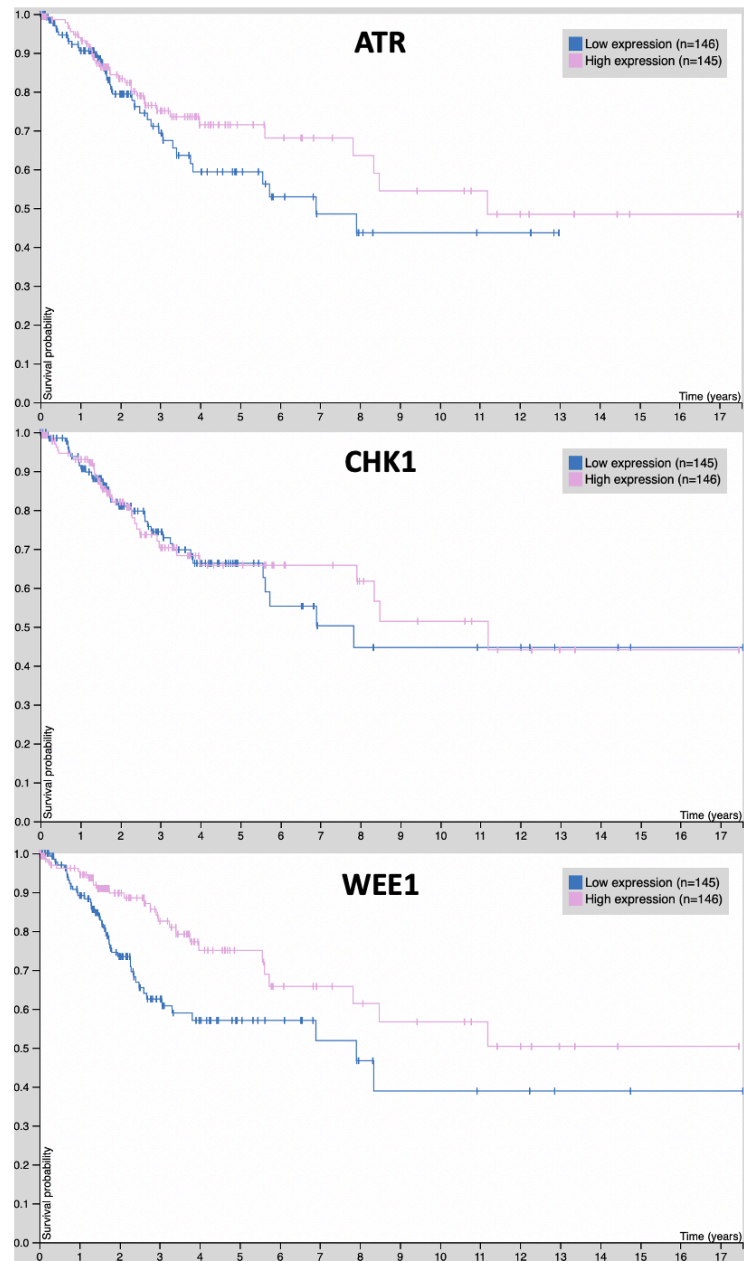


Figure 7.7 Kaplan-Meier plots showing survival of kinase high vs low expression from the TCGA study of cervical cancer dataset

Data for 291 cervical cancer patients was analysed from Human Protein Atlas data <http://www.proteinatlas.org>. Cut off for low vs high expression was the median mRNA expression for the checkpoint kinase Median follow up is 23.5 months

Kinase	Median mRNA expression (FPKM)	5 Year survival High expression (%)	5 Year survival Low expression (%)	p value
ATR	3.17	71	59	0.20
CHK1	5.45	66	66	0.82
WEE1	7.50	75	57	0.006

Table 7.4 Survival of cervical cancer patients from the TCGA study of cervical cancer dataset by checkpoint kinase expression

Data for 291 cervical cancer patients was analysed from Human Protein Atlas data <http://www.proteinatlas.org>. Cut off for low vs high expression was the median mRNA expression for the checkpoint kinase expressed as Fragments Per Kilobase of transcript per Million mapped reads (FPKM) and determined by RNA-seq. Log-rank p-value for Kaplan-Meier plot is shown. Median follow up is 23.5 months

7.5 Discussion and conclusions.

It is not possible to draw significant conclusions regarding the prognostic value of ATR or CHK1 expression in cervical cancer given the small number of tumour samples included in the investigations of protein expression by IHC. The short follow up period and the absence of non-surgical primary treatment used in this patient cohort precludes meaningful correlation with survival or comparison with primary non-surgical treatment modalities. The fact that a range of expression of both kinases was observed in the patient FFPE samples is consistent with the cell line data presented in Chapter 3 and that seen in the TCGA study of cervical cancer data set. This provides additional validation of the cervical cancer cell lines as representative clinical substitutes for the ongoing investigation of ATR-CHK1 pathway inhibition.

Published prevalence data suggests that 80% - 90% of cervical cancer worldwide is SCC (Mathew and George, 2009), but that the relative incidence of this sub-type is falling under the influence of cervical screening programmes which are better able to detect pre-cancerous squamous lesions (Castanon et al., 2016). The proportion of SCC in our limited clinical sample set was 60% and that in the TCGA data set is broadly comparable at 75% with the large majority of patients (70%) undergoing primary surgical treatment rather than platinum chemotherapy or IR based therapy. The TCGA patient cohort is

therefore a comparable group of patients to those recruited for this study and the data is applicable to the global cervical cancer population. No association between high expression of either ATR, CHK1 and survival was seen. High WEE1 expression showed a potential association with better survival, justifying ongoing investigation of WEE1 as a potential biomarker in the investigation of cervical cancer treatment.

In order to broaden the options for further investigations into the expression of DDR proteins in cervical cancer and to provide opportunity to validate any future cell line findings in clinical samples, biobanking of tissue from women with cervical cancer is ongoing. Efforts will need to be made to identify patients who have received platinum and IR, alone and in combination as their primary treatment modality so that any future identified determinants of sensitivity can be correlated with tumour response to provide prognostic data.

8 Final discussion, conclusions and future directions

The investigations in this thesis, for the first time directly compare the relative potential of ATR, CHK1 and WEE1 inhibition in cervical cancer cells using potent and selective inhibitors of these cell cycle checkpoint kinases. Furthermore, attempts were made to elucidate the determinants of sensitivity that may underpin differences in sensitivity across a cervical cancer cell line panel and to understand the mechanisms that may be responsible for differences in the sensitisation of cisplatin and IR observed between the inhibitors. The aim of these investigations was to inform future studies of the relative potential of these drugs in cervical cancer therapy so that attention may be focussed on those that are likely to provide the best solution to the urgent need for novel therapies for this disease. The exploration of the role of HPV and consequent p53/pRb inactivation as a determinant of sensitivity was somewhat confounded by the fact that the 2 HPV negative cells (C33A and HT-3) are known to harbour mutations in TP53 and RB1. The functional status of p53/pRB was not confirmed in the experiments described in this thesis. Nevertheless, the functional consequence for the cell: G1/S dysfunction is of primary importance to the rationale of the investigations and this was demonstrated in all cell lines in response to cisplatin induced DNA damage.

In order to establish that cytotoxicity or sensitisation results later attributed to the inhibitors under investigation were due to enzyme inhibition rather than absence of the enzymes, the expressions of the key enzymes in the pathway were established by Western blot. ATR, CHK1, WEE1 and CDK1 were all expressed by the cervical cancer cell lines and this expression did not appear to be related to HPV status. The level of expression of these proteins was quantified by densitometric analysis and was seen to vary across the cell line panel (Figure 3.4). The magnitude of the differences between the cell lines, the semi-quantitative nature of Western blot densitometry as well as the limited number of cell lines in the panel make drawing definite conclusions from these results difficult and these are limitations that are applicable to many of the results herein. Some of these variations and apparent relationships between them are note-worthy and novel and are discussed below.

Whilst CHK1 expression correlated with CDK1 expression, there was a negative relationship between levels of both of these kinases and ATR levels. Levels of WEE1 showed no relationships with expression of any of the kinases in this common pathway. These results along with the fact that none of the kinase expressions correlated with the cell doubling time, a marker of cell growth suggest that these cells do not have constitutively up-regulated ATR-CHK1-WEE1 pathways in response to G1/S checkpoint insufficiency induced replication stress. In fact, the inverse relationship between ATR expression and that of downstream pathway components may suggest a level of functional redundancy in the pathway that could form the basis of future investigations.

High ATR expression correlated with high DNA-PKcs expression in this cell line panel (Figure 3.5) and this relationship has previously been described. Furthermore, a functional relationship between these two enzymes has also been previously observed. High ATR and high DNA-PKcs levels have been reported to confer survival advantages in ovarian cancer patients (Abdel-Fatah et al., 2014), and High DNA-PKcs has also been shown to confer sensitivity to ATR inhibition by VE-821 (Middleton et al., 2015). A potential relationship was observed between single agent VE-821 cytotoxicity and DNA-PKcs expression across the cell line panel, though this was the inverse to previous reports and suggested that high DNA-PKcs levels conferred resistance rather than sensitivity to VE-821 cytotoxicity. The results of this should be interpreted with caution given the lack of statistical significance, and the panel size (Figure 4.13).

A further relationship between ATM expression and VE-821 single agent cytotoxicity was observed: though the correlation was not significant, the relative resistance of ME-180 cells (which expressed the most ATM) to VE-821 single agent cytotoxicity and the sensitivity of HT-3 cells (which expressed the least ATM) to VE-821 is consistent with previous reports that ATM is a determinant of sensitivity to ATR inhibition (Middleton et al., 2015, Kwok et al., 2016). Although ME-180 cells were, in fact amongst the most sensitive to all three inhibitors, clear relationships were not noted to exist between either PF-477736 or MK-1775 single agent cytotoxicity and ATM expression.

The range of sensitivities of the cell lines to the single agent effects of VE-821, PF-477736 or MK-1775 was not wholly explained by the baseline expression of any of the measured checkpoint or DDR proteins and nor were the sensitisation effects of the inhibitors on either cisplatin or IR. Interestingly, the single agent cytotoxicity of the inhibitors was also unrelated to the observed extent of target inhibition of cisplatin induced ATR, CHK1 and WEE1 activity.

The cells displayed a modest range of sensitivity to cisplatin but the difference between the most sensitive and least sensitive was only around 2-fold, making it difficult to draw conclusions regarding what determines sensitivity. HeLa cells were the most resistant to cisplatin and interestingly, the greatest cisplatin mediated ATR and CHK1 activation was seen in this cell line.

The cell cycle profile changes associated with exposure to 3 μ M cisplatin were uniform across the cell line panel with a significant increase in S-phase populations that appeared largely at the expense of G1 cells. Whilst this is consistent with a deficient G1/S checkpoint either through p53 or pRB mutation or HR-HPV infection as described in Chapter 1, a strong S-phase arrest in response to cisplatin is also consistent with the DNA lesions produced by this agent. Inter-strand cross links are difficult to resolve, requiring multiple DNA repair proteins and the process of repair could itself cause a slowing of progression through S-phase (Deans and West, 2011). Moreover, Intra-strand cross links are a key cause of replication stress and as such are likely to make the cisplatin treated cell heavily dependent on the ATR-CHK1-WEE1 pathway to engage the intra-S checkpoint. S-phase arrest associated with CHK1 phosphorylation by ATR has previously been reported as the major cell cycle response to cisplatin induced DNA damage (Cruet-Hennequart et al., 2009).

HeLa cells showed the greatest cell cycle disturbance in response to cisplatin, with the largest increase in S-phase populations (300% increase). There were no clear correlations between the size of S-phase accumulations and sensitivity to cisplatin across all cell lines, however HeLa cells were the most resistant to cisplatin. This observations is consistent with a report that increased S-phase populations in response to cisplatin may be linked to platinum resistance (Kielbik et al., 2018). This could represent a greater ability to engage cell

cycle arrest or DNA repair during S-phase, slowing the cell cycle progression in response to cisplatin and conferring a survival advantage.

In terms of chemo-sensitisation by the inhibitors, ATR inhibition by VE-821 caused the greatest sensitisation to cisplatin. Cisplatin sensitisation of over 5-fold was seen in C33A cells ($PF_{50} = 5.9 \pm 1.3$) and at higher cisplatin concentrations ME-180 cells were sensitised by over 12-fold ($PF_{0.3-cis} = 12.7 \pm 2.9$) in keeping with previous reports, which suggested up to 10-fold sensitisation of cells to cisplatin by ATR inhibitors (Reaper et al., 2011). Despite the relatively wide variation in cisplatin sensitisation by VE-821 across the cell line panel (Table 5.1) with the least sensitised cell lines (HT-3 and SiHa) being sensitised by less than 2-fold, no significant correlations with ATR expression or inhibition or baseline cisplatin sensitivity were seen. It is worth noting, however that ME-180 cells showed the least VE-821 inhibition of cisplatin induced ATR activity, contrary to what may be expected given the sizeable cisplatin sensitisation effects associated with VE-821 in this cell line.

The concentrations of the inhibitors used for chemo-and radio-sensitisation experiments: 1 μ M VE-821, 50 nM PF-477736 and 100 nM MK-1775 caused broadly similar levels of target enzyme inhibition. Despite this, CHK1 inhibition by PF-477736 caused a much smaller magnitude of sensitisation to cisplatin (Table 4.2). ME-180 cells again showed the greatest sensitisation by PF-477736 ($PF_{50} = 2.5$ and $PF_{0.3-cis} = 1.8$). In contrast with the results for VE-821, PF-477736 did not sensitise HeLa cells to cisplatin. As with VE-821, cisplatin sensitisation by PF-477736 was not related to intrinsic cisplatin sensitivity of the cell lines, despite ME-180 also being amongst the most sensitive to cisplatin alone. No clear relationships were noted with the previously determined phenotypic characteristics of the cell lines, including HPV or p53 status. MK-1775 showed the least overall sensitisation of the cell lines to cisplatin with a maximum but non-significant effect seen, in ME-180 cells ($PF_{50} = 2.3 \pm 0.5$ and $PF_{0.3-cis} = 1.5 \pm 0.5$) and no sensitisation seen in SiHa CaSki or HT-3 cells. Despite this, MK-1775 sensitisation of cisplatin did appear to correlate strongly with baseline WEE1 expression, and this may be worthy of further exploration in a wider cell line panel.

The cells showed little change in their cell cycle profiles in response to exposure to all three inhibitors alone at the concentrations used in sensitisation experiments in keeping with previous reports (Vendetti et al., 2015, Middleton et al., 2018). However, strikingly different responses to the inhibitors were seen within the cell line panel on cisplatin-induced S-phase arrest that were similar for VE-821 and PF-477736. Both inhibitors induced a substantial *reduction* in S-phase accumulation in HeLa, SiHa and C33A but a substantial further *increase* in ME-180 (and HT-3 for PF-477736). Whilst the reductions of cisplatin induced S-phase accumulations may be attributable to attenuation of ATR-Chk1 mediated S-phase arrest (Cruet-Hennequart et al., 2009), the response in ME-180 and HT-3 cells is, so far unexplained.

That such a difference in the response of the cells to ATR or Chk1 inhibition in the face of cisplatin induced DNA damage exists, along with the fact that neither the magnitude of the S-phase or other cell cycle population changes correlated with the sensitisation of the cells to cisplatin in cytotoxicity assays suggests that any observed cisplatin sensitisation by VE-821 or PF-477736 is unlikely to be directly attributable to cell cycle checkpoint abrogation. Instead it is possible that it is due to inhibition of homologous recombination DNA repair (HRR) by inhibition of the ATR-Chk1-Wee1 pathway. HRR is needed to resolve DNA damage-induced collapsed replication forks and there is emerging evidence of a coupling of ATR-mediated checkpoint activation and HRR function (Buisson et al., 2017). This should be considered in future investigations of ATR and Chk1 inhibitors in particular, and their utility as sensitisers to cisplatin or IR in cervical cancer. 100 nM MK-1775 caused a broadly similar pattern of cell cycle changes but with much smaller effects in keeping with the smaller sensitisation effects observed in chemo-sensitisation assays and the slightly lower overall target inhibition observed at this concentration compared to 1 μ M VE-821 and 50 nM PF-477736.

The rank order of sensitivity of the cells was different for IR and cisplatin, implying different determinants of sensitivity to each agent, which might be expected given their different types of DNA damage (Table 1.2). Resistance to IR correlated with high ATR and low Chk1 expression. Surprisingly, given the relationship between ATR and DNA-PKcs discussed above, no correlation existed between DNA-PKcs and IR sensitivity. NHEJ function is a

known determinant of sensitivity to IR (Mahaney et al., 2009). Although there was no correlation between IR sensitivity and expression of the key NHEJ proteins: DNA-PKcs; Ku70; or Ku80, HeLa cells (which were the most radio-resistant) expressed amongst the highest levels of all three proteins. Unexpectedly, ATM expression also showed no correlation with IR sensitivity despite its established role in the detection of IR induced DSBs (Maréchal and Zou, 2013) but SiHa with high ATM and DNA-PKcs were also radioresistant. Overall, the detection of IR induced DNA damage and the functioning of repair pathways such as NHEJ is complex (Thompson, 2012) and functional assays may need to be developed to capture the activity of the entire pathway.

Compared to the results for chemo-sensitisation assays, radio-sensitisation by VE-821 was of a smaller magnitude and over a smaller range at the LD₅₀, though still greater than that seen for PF-477736 and MK-1775. Maximum sensitisation by 1 µM VE-821 was seen in HeLa cells (PF₅₀ = 1.7 ± 0.4) compared to no sensitisation in C33A cells (PF₅₀ = 1.1 ± 0.2). Despite this smaller range of sensitisations and the lack of statistical significance, radio-sensitisation by VE-821 did correlate with intrinsic IR resistance of the cell lines. Unfortunately, it was not possible to complete cell cycle investigations using IR as the DNA damaging agent within the scope of these investigations, and therefore we are unable to relate IR cell cycle changes and the response of the cell to IR + inhibitors to the results obtained for cisplatin, described above. The cell line panel displayed not only a different rank order of sensitivity to IR and cisplatin but also chemo- and radio-sensitisation by the inhibitors, no-doubt reflecting the different nature of the DNA lesions caused by IR and cisplatin and their dependence on different DNA damage signalling and repair pathways. Future experiments should therefore aim at quantifying these differences though, for example DSB-quantification (Rogakou et al., 1998).

The data presented in these investigations comparing the effects of cell cycle checkpoint kinase inhibitors in a panel of cervical cancer specific cell lines is novel. Attempts have been made to determine whether the observed differences and similarities can be explained by relationships with previously described determinants of sensitivity, or through observation of inhibitor specific changes in the cell's engagement of cell cycle checkpoints in the presence of induced DNA damage. Previously identified determinants of sensitivity were not

confirmed, partially due to the size of the panel and the relatively narrow spectrum of data. Due to time limitations, further mechanistic studies were not undertaken. However, the data serve to highlight the difficulty in translating a determinant of sensitivity identified using genetic knockdown/ isogenic pairs of cells to the much more complex phenotype of a cancer cell. In this respect, use of these cell lines relates to the difficulty in identifying predictive biomarkers that will be useful clinically. These results do, however allow identification of future directions that have the potential to provide mechanistic evidence that might underly the observed findings using previously described assays.

8.1 *Final conclusions*

Inhibitors of ATR, CHK1 and WEE1 caused a range of single agent cytotoxicity to cervical cancer cells that was independent of HR-HPV, p53 or pRB status. The cervical cancer cell lines showed variable expressions of checkpoint and DDR proteins and clinical samples showed a range of expression of ATR and CHK1. Because the spectrum of differences in cytotoxicity and protein levels was quite narrow, no clear determinants of single agent activity to PF-477736 and MK-1775 were identified. Nevertheless, ATM deficiency appeared to correlate with VE-821 sensitivity, in keeping with prior reports.

VE-821 sensitised cervical cancer cells lines to cisplatin and IR, independent of HR-HPV, p53 or pRB status and to a greater extent than either PF-477736 and MK-1775 at concentrations that caused broadly similar levels of target enzyme inhibition, suggesting that this is the most promising candidate for future studies. This sensitisation was greatest for cisplatin and this is consistent with cisplatin induced DNA lesions causing greater replication stress and dependence on ATR signalling to cell cycle checkpoints and DNA repair than lesions typically resulting from IR.

Cell cycle analysis suggests that intra-S events predominate in the cell lines' response to cisplatin induced DNA damage. VE-821 and PF-477736 increased cisplatin induced S-phase arrest in some cells but attenuated it in others and this was not related to the extent of cisplatin sensitisation by these drugs. It seems likely, therefore that cisplatin sensitisation by ATR pathway inhibition is not solely dependent on intra-S or G2/M cell cycle checkpoint

abrogation but may be influenced by a balance between the effects of pathway inhibition on checkpoint and DNA repair pathways (Figure 8.1). The repair pathways that may influence this balance have not been determined in these investigations.

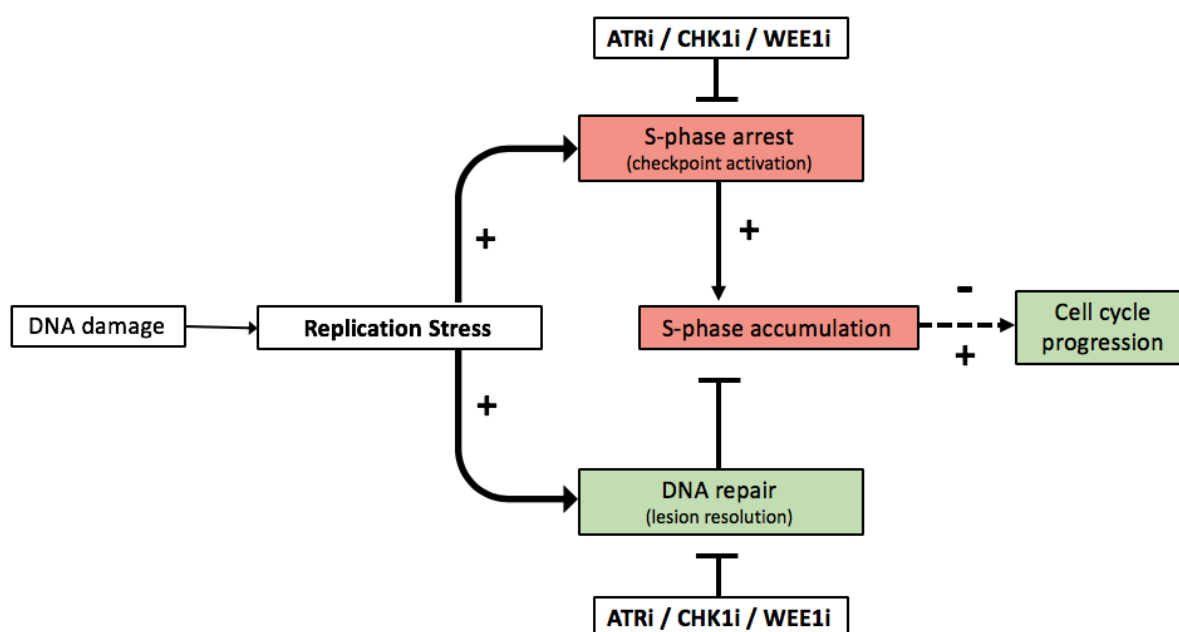


Figure 8.1 Schematic representation of proposed balance of DNA damage checkpoint and repair reactions influencing cell cycle progression in response to DNA damage.

ATR-CHK1-WEE1 inhibition is likely to lead to abrogation of S-phase arrest in cells. The relative effect of ATR-CHK1-WEE1 inhibition on DNA repair (for example on HRR or NHEJ function) is likely to influence the cells ability to overcome S-phase arrest and accumulations.

8.2 Future directions

Whilst the investigations described in this thesis did not identify clear determinants of sensitivity to ATR, CHK1 and WEE1 inhibitors, some associations between the cell lines' response to either single agent inhibitors or their sensitisation of cisplatin and IR and baseline protein expressions are worthy of expansion in wider studies. These include:

1. The relationship between ATM and DNA-PKcs expression and VE-821 single agent cytotoxicity. Despite some conflict with existing literature, the presence of potential

relationships between these enzyme expressions and cells' sensitivity to ATR inhibitors may provide a useful biomarker for future clinical use.

2. MK-1775 sensitisation of cisplatin and expression of WEE1. Though MK-1775 was, overall a poor sensitiser of cisplatin a strong correlation with WEE1 expression suggests that future studies using this agent should be targeted at cells with WEE1 overexpression for maximum effect.

Cisplatin induced S-phase arrest was not uniformly attenuated by the inhibitors across the cell line panel it is likely therefore that rather than abrogation of cell cycle checkpoints, some other function of ATR, CHK1 and to a lesser extent WEE1 are responsible for chemosensitisation. Investigation of the effects of ATR, CHK1 and WEE1 inhibition on DNA repair mechanisms implicated in the response to cisplatin and IR induced DNA damage (particularly HRR and NHEJ) may provide further insight into the reasons for the differences in the cell cycle responses seen and help identify useful determinants of sensitivity for future exploitation. Furthermore, investigations aimed at establishing the cell cycle effects of IR and IR + inhibitor combinations are needed. This is likely to provide further insight into the differences seen between IR and cisplatin with regard to both the cervical cancer cells intrinsic sensitivity to these agents and their sensitisation to them by ATR, CHK1 or WEE1 inhibitors.

There are currently over 70 ongoing early-phase clinical trials of ATR, CHK1 and WEE1 inhibitors as monotherapy or in combinations with chemotherapy agents or IR (www.clinicaltrials.gov). None specifically targets cervical cancer, though patients with advanced cervical cancer may be included in cohorts of patients with solid organ tumours. Ultimately, an understanding of the mechanisms involved in the sensitivity to these inhibitors or their sensitisation of standard of care therapies will enable better interpretation of these clinical trial results and targeting of patients who are likely to receive maximum benefits from these therapies.

References

- AARTS, M., BAJRAMI, I., HERRERA-ABREU, M. T., ELLIOTT, R., BROUGH, R., ASHWORTH, A., LORD, C. J. & TURNER, N. C. 2015. Functional Genetic Screen Identifies Increased Sensitivity to WEE1 Inhibition in Cells with Defects in Fanconi Anemia and HR Pathways. *Mol Cancer Ther*, 14, 865-76.
- ABDEL-FATAH, T. M., ARORA, A., MOSELEY, P., COVENEY, C., PERRY, C., JOHNSON, K., KENT, C., BALL, G., CHAN, S. & MADHUSUDAN, S. 2014. ATM, ATR and DNA-PKcs expressions correlate to adverse clinical outcomes in epithelial ovarian cancers. *BBA Clin*, 2, 10-7.
- ANDREASSEN, P. R., D'ANDREA, A. D. & TANIGUCHI, T. 2004. ATR couples FANCD2 monoubiquitination to the DNA-damage response. *Genes & Development*, 18, 1958-1963.
- ARTIMO P, J. M., ARNOLD K, BARATIN D, CSARDI G, DE CASTRO E, DUVAUD S, FLEGEL V, FORTIER A, GASTEIGER E, GROSDIDIER A, HERNANDEZ C, IOANNIDIS V, KUZNETSOV D, LIECHTI R, MORETTI S, MOSTAGUIR K, REDASCHI N, ROSSIER G, XENARIOS I, AND STOCKINGER H. 2012. *ExPASy Bioinformatics Resource Portal* [Online]. Swiss Institute of Bioinformatics. Available: https://web.expasy.org/cellosaurus/CVCL_0030 [Accessed 2nd February 2019].
- AZORSA, D. O., GONZALES, I. M., BASU, G. D., CHOUDHARY, A., ARORA, S., BISANZ, K. M., KIEFER, J. A., HENDERSON, M. C., TRENT, J. M., VON HOFF, D. D. & MOUSSES, S. 2009. Synthetic lethal RNAi screening identifies sensitizing targets for gemcitabine therapy in pancreatic cancer. *J Transl Med*, 7, 43.
- BALL, H. L., EHRHARDT, M. R., MORDES, D. A., GLICK, G. G., CHAZIN, W. J. & CORTEZ, D. 2007. Function of a conserved checkpoint recruitment domain in ATRIP proteins. *Molecular and Cellular Biology*, 27, 3367-3377.
- BARTUCCI, M., SVENSSON, S., ROMANIA, P., DATTILO, R., PATRIZII, M., SIGNORE, M., NAVARRA, S., LOTTI, F., BIFFONI, M., PILOZZI, E., DURANTI, E., MARTINELLI, S., RINALDO, C., ZEUNER, A., MAUGERI-SACCA, M., ERAMO, A. & DE MARIA, R. 2012. Therapeutic targeting of Chk1 in NSCLC stem cells during chemotherapy. *Cell Death Differ*, 19, 768-78.
- BECK, H., NAHSE-KUMPF, V., LARSEN, M. S. Y., O'HANLON, K. A., PATZKE, S., HOLMBERG, C., MEJLVANG, J., GROTH, A., NIELSEN, O., SYLJUASEN, R. G. & SORENSEN, C. S. 2012. Cyclin-Dependent Kinase Suppression by WEE1 Kinase Protects the Genome through Control of Replication Initiation and Nucleotide Consumption. *Molecular and Cellular Biology*, 32, 4226-4236.
- BERTOLI, C., SKOTHEIM, J. M. & DE BRUIN, R. A. 2013. Control of cell cycle transcription during G1 and S phases. *Nat Rev Mol Cell Biol*, 14, 518-28.

- BHATLA, N., AOKI, D., SHARMA, D. N. & SANKARANARAYANAN, R. 2018. Cancer of the cervix uteri. *Int J Gynaecol Obstet*, 143 Suppl 2, 22-36.
- BIZZARRI, N., GHIRARDI, V., ALESSANDRI, F., VENTURINI, P. L., VALENZANO MENADA, M., RUNDLE, S., LEONE ROBERTI MAGGIORE, U. & FERRERO, S. 2016. Bevacizumab for the treatment of cervical cancer. *Expert Opin Biol Ther*, 16, 407-19.
- BLASINA, A., HALLIN, J., CHEN, E., ARANGO, M. E., KRAYNOV, E., REGISTER, J., GRANT, S., NINKOVIC, S., CHEN, P., NICHOLS, T., O'CONNOR, P. & ANDERES, K. 2008. Breaching the DNA damage checkpoint via PF-00477736, a novel small-molecule inhibitor of checkpoint kinase 1. *Mol Cancer Ther*, 7, 2394-404.
- BOSCH, F. X., MANOS, M. M., MUNOZ, N., SHERMAN, M., JANSEN, A. M., PETO, J., SCHIFFMAN, M. H., MORENO, V., KURMAN, R. & SHAH, K. V. 1995. Prevalence of human papillomavirus in cervical cancer: a worldwide perspective. International biological study on cervical cancer (IBSCC) Study Group. *J Natl Cancer Inst*, 87, 796-802.
- BRAY, F., FERLAY, J., SOERJOMATARAM, I., SIEGEL, R. L., TORRE, L. A. & JEMAL, A. 2018. Global cancer statistics 2018: GLOBOCAN estimates of incidence and mortality worldwide for 36 cancers in 185 countries. *CA Cancer J Clin*, 68, 394-424.
- BRIDGES, K. A., HIRAI, H., BUSER, C. A., BROOKS, C., LIU, H., BUCHHOLZ, T. A., MOLKENTINE, J. M., MASON, K. A. & MEYN, R. E. 2011. MK-1775, a novel Wee1 kinase inhibitor, radiosensitizes p53-defective human tumor cells. *Clin Cancer Res*, 17, 5638-48.
- BRISTOW, R. G. & HILL, R. P. 2008. Hypoxia and metabolism. Hypoxia, DNA repair and genetic instability. *Nat Rev Cancer*, 8, 180-92.
- BROWN, E. J. & BALTIMORE, D. 2000. ATR disruption leads to chromosomal fragmentation and early embryonic lethality. *Genes & Development*, 14, 397-402.
- BRYANT, C., RAWLINSON, R. & MASSEY, A. J. 2014. Chk1 inhibition as a novel therapeutic strategy for treating triple-negative breast and ovarian cancers. *BMC Cancer*, 14, 570.
- BRYANT, H. E., SCHULTZ, N., THOMAS, H. D., PARKER, K. M., FLOWER, D., LOPEZ, E., KYLE, S., MEUTH, M., CURTIN, N. J. & HELLEDAY, T. 2005. Specific killing of BRCA2-deficient tumours with inhibitors of poly(ADP-ribose) polymerase. *Nature*, 434, 913-7.
- BUISSON, R., NIRAJ, J., RODRIGUE, A., HO, C. K., KREUZER, J., FOO, T. K., HARDY, E. J., DELLAIRE, G., HAAS, W., XIA, B., MASSON, J. Y. & ZOU, L. 2017. Coupling of Homologous Recombination and the Checkpoint by ATR. *Mol Cell*, 65, 336-346.

- BURROWS, A. E. & ELLEDGE, S. J. 2008. How ATR turns on: TopBP1 goes on ATRIP with ATR. *Genes Dev*, 22, 1416-21.
- CAIRNS, R. A. & HILL, R. P. 2004. Acute hypoxia enhances spontaneous lymph node metastasis in an orthotopic murine model of human cervical carcinoma. *Cancer Res*, 64, 2054-61.
- CANCER GENOME ATLAS RESEARCH 2017. Integrated genomic and molecular characterization of cervical cancer. *Nature*, 543, 378-384. Available: <https://www.cancer.gov/about-nci/organization/ccg/research/structural-genomics/tcga>. Accessed November 2019.
- CARRASSA, L., BROGGINI, M., ERBA, E. & DAMIA, G. 2004. Chk1, but not Chk2, is involved in the cellular response to DNA damaging agents - Differential activity in cells expressing or not p53. *Cell Cycle*, 3, 1177-1181.
- CASTANON, A., LANDY, R., PESOLA, F., WINDRIDGE, P. & SASIENI, P. 2018. Prediction of cervical cancer incidence in England, UK, up to 2040, under four scenarios: a modelling study. *Lancet Public Health*, 3, e34-e43.
- CASTANON, A., LANDY, R. & SASIENI, P. D. 2016. Is cervical screening preventing adenocarcinoma and adenosquamous carcinoma of the cervix? *Int J Cancer*, 139, 1040-5.
- CHARRIER, J. D., DURRANT, S. J., GOLEC, J. M., KAY, D. P., KNEGTEL, R. M., MACCORMICK, S., MORTIMORE, M., O'DONNELL, M. E., PINDER, J. L., REAPER, P. M., RUTHERFORD, A. P., WANG, P. S., YOUNG, S. C. & POLLARD, J. R. 2011. Discovery of potent and selective inhibitors of ataxia telangiectasia mutated and Rad3 related (ATR) protein kinase as potential anticancer agents. *J Med Chem*, 54, 2320-30.
- CHEN, C. C., KENNEDY, R. D., SIDI, S., LOOK, A. T. & D'ANDREA, A. 2009. CHK1 inhibition as a strategy for targeting fanconi anemia (FA) DNA repair pathway deficient tumors. *Molecular Cancer*, 8.
- CHEN, G., GHARIB, T. G., HUANG, C. C., TAYLOR, J. M., MISEK, D. E., KARDIA, S. L., GIORDANO, T. J., IANNETTONI, M. D., ORRINGER, M. B., HANASH, S. M. & BEER, D. G. 2002. Discordant protein and mRNA expression in lung adenocarcinomas. *Mol Cell Proteomics*, 1, 304-13.
- CHEN, J. L., HUANG, C. Y., HUANG, Y. S., CHEN, R. J., WANG, C. W., CHEN, Y. H., CHENG, J. C., CHENG, A. L. & KUO, S. H. 2014. Differential clinical characteristics, treatment response and prognosis of locally advanced adenocarcinoma/adenosquamous carcinoma and squamous cell carcinoma of cervix treated with definitive radiotherapy. *Acta Obstet Gynecol Scand*, 93, 661-8.
- CHEN, M. S., RYAN, C. E. & PIWNICA-WORMS, H. 2003. Chk1 kinase negatively regulates mitotic function of Cdc25A phosphatase through 14-3-3 binding. *Molecular and Cellular Biology*, 23, 7488-7497.

- CHEN, T., MIDDLETON, F. K., FALCON, S., REAPER, P. M., POLLARD, J. R. & CURTIN, N. J. 2015. Development of pharmacodynamic biomarkers for ATR inhibitors. *Mol Oncol*, 9, 463-72.
- CHEN, X., LOW, K. H., ALEXANDER, A., JIANG, Y., KARAKAS, C., HESS, K. R., CAREY, J. P. W., BUI, T. N., VIJAYARAGHAVAN, S., EVANS, K. W., YI, M., ELLIS, D. C., CHEUNG, K. L., ELLIS, I. O., FU, S., MERIC-BERNSTAM, F., HUNT, K. K. & KEYOMARSI, K. 2018. Cyclin E Overexpression Sensitizes Triple-Negative Breast Cancer to Wee1 Kinase Inhibition. *Clin Cancer Res*, 24, 6594-6610.
- CHOI, J. H., LINDSEY-BOLTZ, L. A., KEMP, M., MASON, A. C., WOLD, M. S. & SANCAR, A. 2010. Reconstitution of RPA-covered single-stranded DNA-activated ATR-Chk1 signaling. *Proc Natl Acad Sci U S A*, 107, 13660-5.
- CHOW, J. P. & POON, R. Y. 2013. The CDK1 inhibitory kinase MYT1 in DNA damage checkpoint recovery. *Oncogene*, 32, 4778-88.
- CIBULA, D., POTTER, R., PLANCHAMP, F., AVALL-LUNDQVIST, E., FISCHEROVA, D., HAIE MEDER, C., KOHLER, C., LANDONI, F., LAX, S., LINDEGAARD, J. C., MAHANTSHETTY, U., MATHEVET, P., MCCLUGGAGE, W. G., MCCORMACK, M., NAIK, R., NOUT, R., PIGNATA, S., PONCE, J., QUERLEU, D., RASPAGLIESI, F., RODOLAKIS, A., TAMUSSINO, K., WIMBERGER, P. & RASPOLINI, M. R. 2018. The European Society of Gynaecological Oncology/European Society for Radiotherapy and Oncology/European Society of Pathology Guidelines for the Management of Patients With Cervical Cancer. *Int J Gynecol Cancer*, 28, 641-655.
- CICCIA, A. & ELLEDGE, S. J. 2010. The DNA damage response: making it safe to play with knives. *Mol Cell*, 40, 179-204.
- CIMPRICH, K. A. & CORTEZ, D. 2008. ATR: an essential regulator of genome integrity. *Nature Reviews Molecular Cell Biology*, 9, 616-627.
- CLIBY, W. A., LEWIS, K. A., LILLY, K. K. & KAUFMANN, S. H. 2002. S phase and G2 arrests induced by topoisomerase I poisons are dependent on ATR kinase function. *J Biol Chem*, 277, 1599-606.
- CLIBY, W. A., ROBERTS, C. J., CIMPRICH, K. A., STRINGER, C. M., LAMB, J. R., SCHREIBER, S. L. & FRIEND, S. H. 1998. Overexpression of a kinase-inactive ATR protein causes sensitivity to DNA-damaging agents and defects in cell cycle checkpoints. *Embo Journal*, 17, 159-169.
- COOK, R., ZOUMPOULIDOU, G., LUCZYNSKI, M. T., RIEGER, S., MOQUET, J., SPANSWICK, V. J., HARTLEY, J. A., ROTHKAMM, K., HUANG, P. H. & MITTNACHT, S. 2015. Direct Involvement of Retinoblastoma Family Proteins in DNA Repair by Non-homologous End-Joining. *Cell Reports*, 10, 2006-2018.
- CORTEZ, D., GUNTUKU, S., QIN, J. & ELLEDGE, S. J. 2001. ATR and ATRIP: Partners in checkpoint signaling. *Science*, 294, 1713-1716.

- CRUET-HENNEQUART, S., VILLALAN, S., KACZMARCZYK, A., O'MEARA, E., SOKOL, A. M. & CARTY, M. P. 2009. Characterization of the effects of cisplatin and carboplatin on cell cycle progression and DNA damage response activation in DNA polymerase eta-deficient human cells. *Cell Cycle*, 8, 3039-50.
- CRUK. 2019. *Cancer Research UK* [Online]. Available: <https://www.cancerresearchuk.org/health-professional/cancer-statistics/statistics-by-cancer-type/cervical-cancer/mortality> [Accessed May 30th 2019].
- CURTIN, N. J. 2012. DNA repair dysregulation from cancer driver to therapeutic target. *Nature Reviews Cancer*, 12, 801-817.
- DAI, Y. & GRANT, S. 2010. New Insights into Checkpoint Kinase 1 in the DNA Damage Response Signaling Network. *Clinical Cancer Research*, 16, 376-383.
- DE GOOIJER, M. C., VAN DEN TOP, A., BOCKAJ, I., BEIJNEN, J. H., WURDINGER, T. & VAN TELLINGEN, O. 2017. The G2 checkpoint-a node-based molecular switch. *FEBS Open Bio*, 7, 439-455.
- DE SOUSA ABREU, R., PENALVA, L. O., MARCOTTE, E. M. & VOGEL, C. 2009. Global signatures of protein and mRNA expression levels. *Mol Biosyst*, 5, 1512-26.
- DE VILLIERS, E. M. 2013. Cross-roads in the classification of papillomaviruses. *Virology*, 445, 2-10.
- DE WITT HAMER, P. C., MIR, S. E., NOSKE, D., VAN NOORDEN, C. J. & WURDINGER, T. 2011. WEE1 kinase targeting combined with DNA-damaging cancer therapy catalyzes mitotic catastrophe. *Clin Cancer Res*, 17, 4200-7.
- DEANS, A. J. & WEST, S. C. 2011. DNA interstrand crosslink repair and cancer. *Nature Reviews Cancer*, 11, 467-480.
- DEMARCO, C., BUNCH, R. T., CRESWELL, D. & EASTMAN, A. 1994. The role of cell cycle progression in cisplatin-induced apoptosis in Chinese hamster ovary cells. *Cell Growth Differ*, 5, 983-93.
- DICK, F. A. & RUBIN, S. M. 2013. Molecular mechanisms underlying RB protein function. *Nature Reviews Molecular Cell Biology*, 14, 297-306.
- DILLON, M. T., BARKER, H. E., PEDERSEN, M., HAFSI, H., BHIDE, S. A., NEWBOLD, K. L., NUTTING, C. M., MCLAUGHLIN, M. & HARRINGTON, K. J. 2017. Radiosensitization by the ATR Inhibitor AZD6738 through Generation of Acentric Micronuclei. *Mol Cancer Ther*, 16, 25-34.
- DILLON, M. T. E., A.; ELLIS, S.; MOHAMMED, K.; GROVE, L. G.; MCLELLAN, L.; SMITH, S.A.; ROSS, G.; ADELEKE, S.; WOO, K.; JOSEPHIDES, E.; SPICER, J. F.; FORSTER, M. D.; HARRINGTON, K. J. 2017. A Phase I dose- escalation study of ATR inhibitor monotherapy with AZD6738 in advanced solid tumors (PATRIOT Part A) (Abstract). *Cancer Res.*, 77.
- DO, K., WILSKER, D., JI, J., ZLOTT, J., FRESHWATER, T., KINDERS, R. J., COLLINS, J., CHEN, A. P., DOROSHOW, J. H. & KUMMAR, S. 2015. Phase I

Study of Single-Agent AZD1775 (MK-1775), a Wee1 Kinase Inhibitor, in Patients With Refractory Solid Tumors. *J Clin Oncol*, 33, 3409-15.

DONAT, U., ROTHER, J., SCHAFER, S., HESS, M., HARTL, B., KOBER, C., LANGBEIN-LAUGWITZ, J., STRITZKER, J., CHEN, N. G., AGUILAR, R. J., WEIBEL, S. & SZALAY, A. A. 2014. Characterization of metastasis formation and virotherapy in the human C33A cervical cancer model. *PLoS One*, 9, e98533.

DOORBAR, J., EGAWA, N., GRIFFIN, H., KRANJEC, C. & MURAKAMI, I. 2015. Human papillomavirus molecular biology and disease association. *Rev Med Virol*, 25 Suppl 1, 2-23.

EASTMAN, A. 1990. Activation of programmed cell death by anticancer agents: cisplatin as a model system. *Cancer Cells*, 2, 275-80.

EUSTERMANN, S., WU, W. F., LANGELIER, M. F., YANG, J. C., EASTON, L. E., RICCIO, A. A., PASCAL, J. M. & NEUHAUS, D. 2015. Structural Basis of Detection and Signaling of DNA Single-Strand Breaks by Human PARP-1. *Mol Cell*, 60, 742-754.

FARMER, H., MCCABE, N., LORD, C. J., TUTT, A. N., JOHNSON, D. A., RICHARDSON, T. B., SANTAROSA, M., DILLON, K. J., HICKSON, I., KNIGHTS, C., MARTIN, N. M., JACKSON, S. P., SMITH, G. C. & ASHWORTH, A. 2005. Targeting the DNA repair defect in BRCA mutant cells as a therapeutic strategy. *Nature*, 434, 917-21.

FLATTEN, K., DAI, N. T., VROMAN, B. T., LOEGERING, D., ERLICHMAN, C., KARNITZ, L. M. & KAUFMANN, S. H. 2005. The role of checkpoint kinase 1 in sensitivity to topoisomerase I poisons. *Journal of Biological Chemistry*, 280, 14349-14355.

FOKAS, E., PREVO, R., POLLARD, J. R., REAPER, P. M., CHARLTON, P. A., CORNELISSEN, B., VALLIS, K. A., HAMMOND, E. M., OLCINA, M. M., GILLIES MCKENNA, W., MUSCHEL, R. J. & BRUNNER, T. B. 2012. Targeting ATR in vivo using the novel inhibitor VE-822 results in selective sensitization of pancreatic tumors to radiation. *Cell Death Dis*, 3, e441.

FOOTE, K. M., BLADES, K., CRONIN, A., FILLERY, S., GUICHARD, S. S., HASSALL, L., HICKSON, I., JACQ, X., JEWSEBURY, P. J., MCGUIRE, T. M., NISSINK, J. W., ODEDRA, R., PAGE, K., PERKINS, P., SULEMAN, A., TAM, K., THOMMES, P., BROADHURST, R. & WOOD, C. 2013. Discovery of 4-{4-[(3R)-3-Methylmorpholin-4-yl]-6-[1-(methylsulfonyl)cyclopropyl]pyrimidin-2-yl}-1H-indole (AZ20): a potent and selective inhibitor of ATR protein kinase with monotherapy in vivo antitumor activity. *J Med Chem*, 56, 2125-38.

FRANKEN, N. A., RODERMOND, H. M., STAP, J., HAVEMAN, J. & VAN BREE, C. 2006. Clonogenic assay of cells in vitro. *Nat Protoc*, 1, 2315-9.

- FRIEDEL, A. M., PIKE, B. L. & GASSER, S. M. 2009. ATR/Mec1: coordinating fork stability and repair. *Curr Opin Cell Biol*, 21, 237-44.
- GANZINELLI, M., CARRASSA, L., CRIPPA, F., TAVECCHIO, M., BROGGINI, M. & DAMIA, G. 2008. Checkpoint kinase 1 down-regulation by an inducible small interfering RNA expression system sensitized in vivo tumors to treatment with 5-fluorouracil. *Clinical Cancer Research*, 14, 5131-5141.
- GILAD, O., NABET, B. Y., RAGLAND, R. L., SCHOPPY, D. W., SMITH, K. D., DURHAM, A. C. & BROWN, E. J. 2010. Combining ATR Suppression with Oncogenic Ras Synergistically Increases Genomic Instability, Causing Synthetic Lethality or Tumorigenesis in a Dosage-Dependent Manner. *Cancer Research*, 70, 9693-9702.
- GUZI, T. J., PARUCH, K., DWYER, M. P., LABROLI, M., SHANAHAN, F., DAVIS, N., TARICANI, L., WISWELL, D., SEGHEZZI, W., PENAFLORE, E., BHAGWAT, B., WANG, W., GU, D., HSIEH, Y., LEE, S., LIU, M. & PARRY, D. 2011. Targeting the replication checkpoint using SCH 900776, a potent and functionally selective CHK1 inhibitor identified via high content screening. *Mol Cancer Ther*, 10, 591-602.
- HALL, A. B., NEWSOME, D., WANG, Y., BOUCHER, D. M., EUSTACE, B., GU, Y., HARE, B., JOHNSON, M. A., MILTON, S., MURPHY, C. E., TAKEMOTO, D., TOLMAN, C., WOOD, M., CHARLTON, P., CHARRIER, J. D., FUREY, B., GOLEC, J., REAPER, P. M. & POLLARD, J. R. 2014. Potentiation of tumor responses to DNA damaging therapy by the selective ATR inhibitor VX-970. *Oncotarget*, 5, 5674-85.
- HARRIS, P. S., VENKATARAMAN, S., ALIMOVA, I., BIRKS, D. K., BALAKRISHNAN, I., CRISTIANO, B., DONSON, A. M., DUBUC, A. M., TAYLOR, M. D., FOREMAN, N. K., REIGAN, P. & VIBHAKAR, R. 2014. Integrated genomic analysis identifies the mitotic checkpoint kinase WEE1 as a novel therapeutic target in medulloblastoma. *Molecular Cancer*, 13.
- HIRAI, H., IWASAWA, Y., OKADA, M., ARAI, T., NISHIBATA, T., KOBAYASHI, M., KIMURA, T., KANEKO, N., OHTANI, J., YAMANAKA, K., ITADANI, H., TAKAHASHI-SUZUKI, I., FUKASAWA, K., OKI, H., NAMBU, T., JIANG, J., SAKAI, T., ARAKAWA, H., SAKAMOTO, T., SAGARA, T., YOSHIZUMI, T., MIZUARAI, S. & KOTANI, H. 2009. Small-molecule inhibition of Wee1 kinase by MK-1775 selectively sensitizes p53-deficient tumor cells to DNA-damaging agents. *Molecular Cancer Therapeutics*, 8, 2992-3000.
- HOEIJMAKERS, J. H. J. 2001. DNA repair mechanisms. *Maturitas*, 38, 17-22.
- HOFFMAN, R. M. 1991. In vitro sensitivity assays in cancer: a review, analysis, and prognosis. *J Clin Lab Anal*, 5, 133-43.
- HONG, D., INFANTE, J., JANKU, F., JONES, S., NGUYEN, L. M., BURRIS, H., NAING, A., BAUER, T. M., PIHA-PAUL, S., JOHNSON, F. M., KURZROCK, R., GOLDEN, L., HYNES, S., LIN, J., LIN, A. B. & BENDELL, J. 2016. Phase I

- Study of LY2606368, a Checkpoint Kinase 1 Inhibitor, in Patients With Advanced Cancer. *J Clin Oncol*, 34, 1764-71.
- HUANG, P. H., COOK, R. & MITTNACHT, S. 2015. RB in DNA repair. *Oncotarget*, 6, 20746-20747.
- HUIBREGTSE, J. M., SCHEFFNER, M., BEAUDENON, S. & HOWLEY, P. M. 1995. A family of proteins structurally and functionally related to the E6-AP ubiquitin-protein ligase. *Proc Natl Acad Sci U S A*, 92, 5249.
- ITAMOCHI, H., NISHIMURA, M., OUMI, N., KATO, M., OISHI, T., SHIMADA, M., SATO, S., NANIWA, J., SATO, S., KUDOH, A., KIGAWA, J. & HARADA, T. 2014. Checkpoint kinase inhibitor AZD7762 overcomes cisplatin resistance in clear cell carcinoma of the ovary. *Int J Gynecol Cancer*, 24, 61-9.
- IYER, D. R. & RHIND, N. 2017. The Intra-S Checkpoint Responses to DNA Damage. *Genes (Basel)*, 8.
- JEON, S., ALLEN-HOFFMANN, B. L. & LAMBERT, P. F. 1995. Integration of human papillomavirus type 16 into the human genome correlates with a selective growth advantage of cells. *J Virol*, 69, 2989-97.
- JIRICNY, J. 2006. The multifaceted mismatch-repair system. *Nature Reviews Molecular Cell Biology*, 7, 335-346.
- KALU, N. N., MAZUMDAR, T., PENG, S., SHEN, L., SAMBANDAM, V., RAO, X., XI, Y., LI, L., QI, Y., GLEBER-NETTO, F. O., PATEL, A., WANG, J., FREDERICK, M. J., MYERS, J. N., PICKERING, C. R. & JOHNSON, F. M. 2017. Genomic characterization of human papillomavirus-positive and -negative human squamous cell cancer cell lines. *Oncotarget*, 8, 86369-86383.
- KASTAN, M. B. & BARTEK, J. 2004. Cell-cycle checkpoints and cancer. *Nature*, 432, 316-323.
- KATANYOO, K., SANGUANRUNGSIRIKUL, S. & MANUSIRIVITHAYA, S. 2012. Comparison of treatment outcomes between squamous cell carcinoma and adenocarcinoma in locally advanced cervical cancer. *Gynecol Oncol*, 125, 292-6.
- KAUR, G. & DUFOUR, J. M. 2012. Cell lines: Valuable tools or useless artifacts. *Spermatogenesis*, 2, 1-5.
- KIELBIK, M., KRZYZANOWSKI, D., PAWLIK, B. & KLINK, M. 2018. Cisplatin-induced ERK1/2 activity promotes G1 to S phase progression which leads to chemoresistance of ovarian cancer cells. *Oncotarget*, 9, 19847-19860.
- KING, C., DIAZ, H., BARNARD, D., BARDA, D., CLAWSON, D., BLOSSER, W., COX, K., GUO, S. & MARSHALL, M. 2014. Characterization and preclinical development of LY2603618: a selective and potent Chk1 inhibitor. *Invest New Drugs*, 32, 213-26.

- KNIGHT, Z. A. & SHOKAT, K. M. 2005. Features of selective kinase inhibitors. *Chem Biol*, 12, 621-37.
- KRAJEWSKA, M., FEHRMANN, R. S., SCHOONEN, P. M., LABIB, S., DE VRIES, E. G., FRANKE, L. & VAN VUGT, M. A. 2015. ATR inhibition preferentially targets homologous recombination-deficient tumor cells. *Oncogene*, 34, 3474-81.
- KUMAGAI, A. & DUNPHY, W. G. 2000. Claspin, a novel protein required for the activation of Chk1 during a DNA replication checkpoint response in *Xenopus* egg extracts. *Molecular Cell*, 6, 839-849.
- KWOK, M., DAVIES, N., AGATHANGGELOU, A., SMITH, E., OLDREIVE, C., PETERMANN, E., STEWART, G., BROWN, J., LAU, A., PRATT, G., PARRY, H., TAYLOR, M., MOSS, P., HILLMEN, P. & STANKOVIC, T. 2016. ATR inhibition induces synthetic lethality and overcomes chemoresistance in TP53- or ATM-defective chronic lymphocytic leukemia cells. *Blood*, 127, 582-95.
- LANDY, R., CASTANON, A., HAMILTON, W., LIM, A. W., DUDDING, N., HOLLINGWORTH, A. & SASIENI, P. D. 2016. Evaluating cytology for the detection of invasive cervical cancer. *Cytopathology*, 27, 201-9.
- LEE, J. M. 2016. A phase II study of the cell cyclecheckpoint kinases 1 and 2 inhibitor (LY2606368;Prexasertib monomesylate monohydrate) in sporadic high- grade serous ovarian cancer (HGSOC) andgermline BRCA mutation- associated ovarian cancer(gBRCAm+ OvCa). . *Ann. Oncol.* , 27, 8550.
- LEIJEN, S., VAN GEEL, R. M., SONKE, G. S., DE JONG, D., ROSENBERG, E. H., MARCHETTI, S., PLUIM, D., VAN WERKHOVEN, E., ROSE, S., LEE, M. A., FRESHWATER, T., BEIJNEN, J. H. & SCHELLENS, J. H. 2016. Phase II Study of WEE1 Inhibitor AZD1775 Plus Carboplatin in Patients With TP53-Mutated Ovarian Cancer Refractory or Resistant to First-Line Therapy Within 3 Months. *J Clin Oncol*, 34, 4354-4361.
- LI, R. & SHEN, Y. 2013. An old method facing a new challenge: re-visiting housekeeping proteins as internal reference control for neuroscience research. *Life Sci*, 92, 747-51.
- LIU, Q. H., GUNTUKU, S., CUI, X. S., MATSUOKA, S., CORTEZ, D., TAMAI, K., LUO, G. B., CARATTINI-RIVERA, S., DEMAYO, F., BRADLEY, A., DONEHOWER, L. A. & ELLEDGE, S. J. 2000. Chk1 is an essential kinase that is regulated by Atr and required for the G(2)/M DNA damage checkpoint. *Genes & Development*, 14, 1448-1459.
- LIU, S., BEKKER-JENSEN, S., MAILAND, N., LUKAS, C., BARTEK, J. & LUKAS, J. 2006. Claspin operates downstream of TopBP1 to direct ATR signaling towards Chk1 activation. *Molecular and Cellular Biology*, 26, 6056-6064.
- LIVNEH, I., COHEN-KAPLAN, V., COHEN-ROSENZWEIG, C., AVNI, N. & CIECHANOVER, A. 2016. The life cycle of the 26S proteasome: from birth, through regulation and function, and onto its death. *Cell Res*, 26, 869-85.

- LODISH H, B. A., ZIPURSKY SL, MOLECULAR CELL BIOLOGY. 4TH EDITION. NEW YORK: W. H. FREEMAN; 2000. SECTION 12.2, THE DNA REPLICATION MACHINERY. 2000. The DNA Replication Machinery. 4th Edition. *Molecular Cell Biology*. New York: W. H. Freeman.
- LONGUET, M., BEAUDENON, S. & ORTH, G. 1996. Two novel genital human papillomavirus (HPV) types, HPV68 and HPV70, related to the potentially oncogenic HPV39. *J Clin Microbiol*, 34, 738-44.
- LORD, C. J. & ASHWORTH, A. 2017. PARP inhibitors: Synthetic lethality in the clinic. *Science*, 355, 1152-1158.
- LUCEY, B. P., NELSON-REES, W. A. & HUTCHINS, G. M. 2009. Henrietta Lacks, HeLa cells, and cell culture contamination. *Arch Pathol Lab Med*, 133, 1463-7.
- MACDOUGALL, C. A., BYUN, T. S., VAN, C., YEE, M. C. & CIMPRICH, K. A. 2007. The structural determinants of checkpoint activation. *Genes & Development*, 21, 898-903.
- MAHANEY, B. L., MEEK, K. & LEES-MILLER, S. P. 2009. Repair of ionizing radiation-induced DNA double-strand breaks by non-homologous end-joining. *Biochem J*, 417, 639-50.
- MARÉCHAL, A. & ZOU, L. 2013. DNA Damage Sensing by the ATM and ATR Kinases. *Cold Spring Harbor Perspectives in Biology*, 5, a012716.
- MARTEIJN, J. A., LANS, H., VERMEULEN, W. & HOEIJMAKERS, J. H. J. 2014. Understanding nucleotide excision repair and its roles in cancer and ageing. *Nature Reviews Molecular Cell Biology*, 15, 465-481.
- MASSAGUE, J. 2004. G1 cell-cycle control and cancer. *Nature*, 432, 298-306.
- MASSEY, A. J., STEPHENS, P., RAWLINSON, R., MCGURK, L., PLUMMER, R. & CURTIN, N. J. 2016. mTORC1 and DNA-PKcs as novel molecular determinants of sensitivity to Chk1 inhibition. *Molecular Oncology*, 10, 101-112.
- MASSEY, A. J., STOKES, S., BROWNE, H., FOLOPPE, N., FIUMANA, A., SCRACE, S., FALLOWFIELD, M., BEDFORD, S., WEBB, P., BAKER, L., CHRISTIE, M., DRYSDALE, M. J. & WOOD, M. 2015. Identification of novel, in vivo active Chk1 inhibitors utilizing structure guided drug design. *Oncotarget*, 6, 35797-812.
- MATHESON, C. J., BACKOS, D. S. & REIGAN, P. 2016. Targeting WEE1 Kinase in Cancer. *Trends Pharmacol Sci*, 37, 872-881.
- MATHEW, A. & GEORGE, P. S. 2009. Trends in incidence and mortality rates of squamous cell carcinoma and adenocarcinoma of cervix--worldwide. *Asian Pac J Cancer Prev*, 10, 645-50.

- MATTHEWS, T. P., JONES, A. M. & COLLINS, I. 2013. Structure-based design, discovery and development of checkpoint kinase inhibitors as potential anticancer therapies. *Expert Opin Drug Discov*, 8, 621-40.
- MCBRIDE, A. A. & WARBURTON, A. 2017. The role of integration in oncogenic progression of HPV-associated cancers. *PLoS Pathog*, 13, e1006211.
- MIDDLETON, F. K., PATTERSON, M. J., ELSTOB, C. J., FORDHAM, S., HERRIOTT, A., WADE, M. A., MCCORMICK, A., EDMONDSON, R., MAY, F. E. B., ALLAN, J. M., POLLARD, J. R. & CURTIN, N. J. 2015. Common cancer-associated imbalances in the DNA damage response confer sensitivity to single agent ATR inhibition. *Oncotarget*, 6, 32396-32409.
- MIDDLETON, F. K., POLLARD, J. R. & CURTIN, N. J. 2018. The Impact of p53 Dysfunction in ATR Inhibitor Cytotoxicity and Chemo- and Radiosensitisation. *Cancers (Basel)*, 10.
- MILLER, B. E., MILLER, F. R. & HEPPNER, G. H. 1984. Assessing tumor drug sensitivity by a new in vitro assay which preserves tumor heterogeneity and subpopulation interactions. *J Cell Physiol Suppl*, 3, 105-16.
- MITCHELL, J. B., CHOUDHURI, R., FABRE, K., SOWERS, A. L., CITRIN, D., ZABLUDOFF, S. D. & COOK, J. A. 2010. In vitro and in vivo radiation sensitization of human tumor cells by a novel checkpoint kinase inhibitor, AZD7762. *Clin Cancer Res*, 16, 2076-84.
- MIZUARAI, S., YAMANAKA, K., ITADANI, H., ARAI, T., NISHIBATA, T., HIRAI, H. & KOTANI, H. 2009. Discovery of gene expression-based pharmacodynamic biomarker for a p53 context-specific anti-tumor drug Wee1 inhibitor. *Mol Cancer*, 8, 34.
- MOHNI, K. N., KAVANAUGH, G. M. & CORTEZ, D. 2014. ATR pathway inhibition is synthetically lethal in cancer cells with ERCC1 deficiency. *Cancer Res*, 74, 2835-45.
- MOLINARI, M. 2000. Cell cycle checkpoints and their inactivation in human cancer. *Cell Proliferation*, 33, 261-274.
- MONTANO, R., CHUNG, I., GARNER, K. M., PARRY, D. & EASTMAN, A. 2012. Preclinical development of the novel Chk1 inhibitor SCH900776 in combination with DNA-damaging agents and antimetabolites. *Mol Cancer Ther*, 11, 427-38.
- MORGADO-PALACIN, I., DAY, A., MURGA, M., LAFARGA, V., ANTON, M. E., TUBBS, A., CHEN, H. T., ERGAN, A., ANDERSON, R., BHANDoola, A., PIKE, K. G., BARLAAM, B., CADOGAN, E., WANG, X., PIERCE, A. J., HUBBARD, C., ARMSTRONG, S. A., NUSSENZWEIG, A. & FERNANDEZ-CAPETILLO, O. 2016. Targeting the kinase activities of ATR and ATM exhibits antitumoral activity in mouse models of MLL-rearranged AML. *Sci Signal*, 9, ra91.

- MORGAN, M. A., PARSELS, L. A., ZHAO, L., PARSELS, J. D., DAVIS, M. A., HASSAN, M. C., ARUMUGARAJAH, S., HYLANDER-GANS, L., MOROSINI, D., SIMEONE, D. M., CANMAN, C. E., NORMOLLE, D. P., ZABLUDOFF, S. D., MAYBAUM, J. & LAWRENCE, T. S. 2010. Mechanism of radiosensitization by the Chk1/2 inhibitor AZD7762 involves abrogation of the G2 checkpoint and inhibition of homologous recombinational DNA repair. *Cancer Res*, 70, 4972-81.
- MUELLER, S. & HAAS-KOGAN, D. A. 2015. WEE1 Kinase As a Target for Cancer Therapy. *Journal of Clinical Oncology*, 33, 3485-+.
- MUELLER, S., HASHIZUME, R., YANG, X. D., KOLKOWITZ, I., OLOW, A. K., PHILLIPS, J., SMIRNOV, I., TOM, M. W., PRADOS, M. D., JAMES, C. D., BERGER, M. S., GUPTA, N. & HAAS-KOGAN, D. A. 2014. Targeting Wee1 for the treatment of pediatric high-grade gliomas. *Neuro-Oncology*, 16, 352-360.
- MUNGER, K., SCHEFFNER, M., HUIBREGTSE, J. M. & HOWLEY, P. M. 1992. Interactions of HPV E6 and E7 oncoproteins with tumour suppressor gene products. *Cancer Surv*, 12, 197-217.
- MUNGER, K., WERNESS, B. A., DYSON, N., PHELPS, W. C., HARLOW, E. & HOWLEY, P. M. 1989. Complex formation of human papillomavirus E7 proteins with the retinoblastoma tumor suppressor gene product. *EMBO J*, 8, 4099-105.
- MUNOZ, N., BOSCH, F. X., DE SANJOSE, S., HERRERO, R., CASTELLSAGUE, X., SHAH, K. V., SNIJDERS, P. J., MEIJER, C. J. & INTERNATIONAL AGENCY FOR RESEARCH ON CANCER MULTICENTER CERVICAL CANCER STUDY, G. 2003. Epidemiologic classification of human papillomavirus types associated with cervical cancer. *N Engl J Med*, 348, 518-27.
- MURGA, M., CAMPANER, S., LOPEZ-CONTRERAS, A. J., TOLEDO, L. I., SORIA, R., MONTANA, M. F., D'ARTISTA, L., SCHLEKER, T., GUERRA, C., GARCIA, E., BARBACID, M., HIDALGO, M., AMATI, B. & FERNANDEZ-CAPETILLO, O. 2011. Exploiting oncogene-induced replicative stress for the selective killing of Myc-driven tumors. *Nature Structural & Molecular Biology*, 18, 1331-U38.
- NAM, E. A. & CORTEZ, D. 2011. ATR signalling: more than meeting at the fork. *Biochem J*, 436, 527-36.
- NGHIEM, P., PARK, P. K., KIM, Y. S., VAZIRI, C. & SCHREIBER, S. L. 2001. ATR inhibition selectively sensitizes G(1) checkpoint-deficient cells to lethal premature chromatin condensation. *Proceedings of the National Academy of Sciences of the United States of America*, 98, 9092-9097.
- NICKSON, C. M., MOORI, P., CARTER, R. J., RUBBI, C. P. & PARSONS, J. L. 2017. Misregulation of DNA damage repair pathways in HPV-positive head and neck squamous cell carcinoma contributes to cellular radiosensitivity. *Oncotarget*, 8, 29963-29975.

- NIN, D. S., YEOW, C. W., TAY, S. K. & DENG, L. W. 2014. Targeted silencing of MLL5beta inhibits tumor growth and promotes gamma-irradiation sensitization in HPV16/18-associated cervical cancers. *Mol Cancer Ther*, 13, 2572-82.
- NISHIDA, H., TATEWAKI, N., NAKAJIMA, Y., MAGARA, T., KO, K. M., HAMAMORI, Y. & KONISHI, T. 2009. Inhibition of ATR protein kinase activity by schisandrin B in DNA damage response. *Nucleic Acids Res*, 37, 5678-89.
- O'CARRIGAN B, J. D. M. L. M., PAPADATOS-PASTOS D, BROWN J, TUNARIU N, PEREZ R, GANEGODA M, RIISNAES R, FIGUEIREDO I, CARREIRA S, HARE B, YANG F, MCDERMOTT K, PENNEY M, POLLARD J, LOPEZ JS, BANERJI U, DE BONO JS, FIELDS SZ, YAP TA. 2016. Phase I trial of a first-in-class ATR inhibitor VX-970 as monotherapy (mono) or in combination (combo) with carboplatin (CP) incorporating pharmacodynamics (PD) studies (Astract). *Journal of Clinical Oncology*, 34, s2054.
- O'CONNELL, M. J., RALEIGH, J. M., VERKADE, H. M. & NURSE, P. 1997. Chk1 is a wee1 kinase in the G2 DNA damage checkpoint inhibiting cdc2 by Y15 phosphorylation. *EMBO J*, 16, 545-54.
- O'DRISCOLL, M., RUIZ-PEREZ, V. L., WOODS, C. G., JEGGO, P. A. & GOODSHIP, J. A. 2003. A splicing mutation affecting expression of ataxia-telangiectasia and Rad3-related protein (ATR) results in Seckel syndrome. *Nat Genet*, 33, 497-501.
- OKITA, N., MINATO, S., OHMI, E., TANUMA, S. & HIGAMI, Y. 2012. DNA damage-induced CHK1 autophosphorylation at Ser296 is regulated by an intramolecular mechanism. *FEBS Lett*, 586, 3974-9.
- ORNTOFT, T. F., THYKJAER, T., WALDMAN, F. M., WOLF, H. & CELIS, J. E. 2002. Genome-wide study of gene copy numbers, transcripts, and protein levels in pairs of non-invasive and invasive human transitional cell carcinomas. *Mol Cell Proteomics*, 1, 37-45.
- OZA, A. 2015. An international, biomarker- directed, randomized, phase II trial of AZD1775 plus paclitaxel and carboplatin (P/C) for the treatment of women with platinum- sensitive, TP53-mutant ovarian cancer. *Journal of Clinical Oncology* 33, 5506.
- OZA, V., ASHWELL, S., ALMEIDA, L., BRASSIL, P., BREED, J., DENG, C., GERO, T., GRONDINE, M., HORN, C., IOANNIDIS, S., LIU, D., LYNE, P., NEWCOMBE, N., PASS, M., READ, J., READY, S., ROWSELL, S., SU, M., TOADER, D., VASBINDER, M., YU, D., YU, Y., XUE, Y., ZABLUDOFF, S. & JANETKA, J. 2012. Discovery of checkpoint kinase inhibitor (S)-5-(3-fluorophenyl)-N-(piperidin-3-yl)-3-ureidothiophene-2-carboxamide (AZD7762) by structure-based design and optimization of thiophenecarboxamide ureas. *J Med Chem*, 55, 5130-42.
- PAN, Y., REN, K. H., HE, H. W. & SHAO, R. G. 2009. Knockdown of Chk1 sensitizes human colon carcinoma HCT116 cells in a p53-dependent manner to lidamycin

- through abrogation of a G(2)/M checkpoint and induction of apoptosis. *Cancer Biology & Therapy*, 8, 1559-1566.
- PANEK, R. L., LU, G. H., KLUTCHKO, S. R., BATLEY, B. L., DAHRING, T. K., HAMBY, J. M., HALLAK, H., DOHERTY, A. M. & KEISER, J. A. 1997. In vitro pharmacological characterization of PD 166285, a new nanomolar potent and broadly active protein tyrosine kinase inhibitor. *J Pharmacol Exp Ther*, 283, 1433-44.
- PAPPANO, W. N., ZHANG, Q., TUCKER, L. A., TSE, C. & WANG, J. 2014. Genetic inhibition of the atypical kinase Wee1 selectively drives apoptosis of p53 inactive tumor cells. *BMC Cancer*, 14, 430.
- PARSELS, L. A., MORGAN, M. A., TANSKA, D. M., PARSELS, J. D., PALMER, B. D., BOOTH, R. J., DENNY, W. A., CANMAN, C. E., KRAKER, A. J., LAWRENCE, T. S. & MAYBAUM, J. 2009. Gemcitabine sensitization by checkpoint kinase 1 inhibition correlates with inhibition of a Rad51 DNA damage response in pancreatic cancer cells. *Mol Cancer Ther*, 8, 45-54.
- PARSELS, L. A., PARSELS, J. D., TANSKA, D. M., MAYBAUM, J., LAWRENCE, T. S. & MORGAN, M. A. 2018. The contribution of DNA replication stress marked by high-intensity, pan-nuclear gammaH2AX staining to chemosensitization by CHK1 and WEE1 inhibitors. *Cell Cycle*, 17, 1076-1086.
- PAULSEN, R. D. & CIMPRICH, K. A. 2007. The ATR pathway: fine-tuning the fork. *DNA Repair (Amst)*, 6, 953-66.
- PEASLAND, A., WANG, L. Z., ROWLING, E., KYLE, S., CHEN, T., HOPKINS, A., CLIBY, W. A., SARKARIA, J., BEALE, G., EDMONDSON, R. J. & CURTIN, N. J. 2011. Identification and evaluation of a potent novel ATR inhibitor, NU6027, in breast and ovarian cancer cell lines. *Br J Cancer*, 105, 372-81.
- PILIE, P. G., TANG, C., MILLS, G. B. & YAP, T. A. 2019. State-of-the-art strategies for targeting the DNA damage response in cancer. *Nat Rev Clin Oncol*, 16, 81-104.
- PIRES, I. M., OLCINA, M. M., ANBALAGAN, S., POLLARD, J. R., REAPER, P. M., CHARLTON, P. A., MCKENNA, W. G. & HAMMOND, E. M. 2012. Targeting radiation-resistant hypoxic tumour cells through ATR inhibition. *British Journal of Cancer*, 107, 291-299.
- POMMIER, Y., O'CONNOR, M. J. & DE BONO, J. 2016. Laying a trap to kill cancer cells: PARP inhibitors and their mechanisms of action. *Sci Transl Med*, 8, 362ps17.
- RACEY, C. S., ALBERT, A., DONKEN, R., SMITH, L., SPINELLI, J. J., PEDERSEN, H., DE BRUIN, P., MASARO, C., MITCHELL-FOSTER, S., SADARANGANI, M., DAWAR, M., KRAJDEN, M., NAUS, M., VAN NIEKERK, D. & OGILVIE, G. 2020. Cervical Intraepithelial Neoplasia Rates in British Columbia Women: A

Population-Level Data Linkage Evaluation of the School-Based HPV Immunization Program. *J Infect Dis*, 221, 81-90.

- RAMANAKUMAR, A. V., NAUD, P., ROTELI-MARTINS, C. M., DE CARVALHO, N. S., DE BORBA, P. C., TEIXEIRA, J. C., BLATTER, M., MOSCICKI, A. B., HARPER, D. M., ROMANOWSKI, B., TYRING, S. K., RAMJATTAN, B., SCHUIND, A., DUBIN, G., FRANCO, E. L. & GROUP, H. P. V. S. 2016. Incidence and duration of type-specific human papillomavirus infection in high-risk HPV-naïve women: results from the control arm of a phase II HPV-16/18 vaccine trial. *BMJ Open*, 6, e011371.
- RASTOGI, N., DUGGAL, S., SINGH, S. K., PORWAL, K., SRIVASTAVA, V. K., MAURYA, R., BHATT, M. L. & MISHRA, D. P. 2015. Proteasome inhibition mediates p53 reactivation and anti-cancer activity of 6-gingerol in cervical cancer cells. *Oncotarget*, 6, 43310-25.
- REAPER, P. M., GRIFFITHS, M. R., LONG, J. M., CHARRIER, J. D., MACCORMICK, S., CHARLTON, P. A., GOLEC, J. M. & POLLARD, J. R. 2011. Selective killing of ATM- or p53-deficient cancer cells through inhibition of ATR. *Nat Chem Biol*, 7, 428-30.
- REBOLJ, M., RIMMER, J., DENTON, K., TIDY, J., MATHEWS, C., ELLIS, K., SMITH, J., EVANS, C., GILES, T., FREW, V., TYLER, X., SARGENT, A., PARKER, J., HOLBROOK, M., HUNT, K., TIDBURY, P., LEVINE, T., SMITH, D., PATNICK, J., STUBBS, R., MOSS, S. & KITCHENER, H. 2019. Primary cervical screening with high risk human papillomavirus testing: observational study. *BMJ*, 364, l240.
- ROBERTS, J. J. & KOTSAKI-KOVATSI, V. P. 1986. Potentiation of sulphur mustard or cisplatin-induced toxicity by caffeine in Chinese hamster cells correlates with formation of DNA double-strand breaks during replication on a damaged template. *Mutat Res*, 165, 207-20.
- ROGAKOU, E. P., PILCH, D. R., ORR, A. H., IVANOVA, V. S. & BONNER, W. M. 1998. DNA double-stranded breaks induce histone H2AX phosphorylation on serine 139. *J Biol Chem*, 273, 5858-68.
- ROSEN, V. M., GUERRA, I., MCCORMACK, M., NOGUEIRA-RODRIGUES, A., SASSE, A., MUNK, V. C. & SHANG, A. 2017. Systematic Review and Network Meta-Analysis of Bevacizumab Plus First-Line Topotecan-Paclitaxel or Cisplatin-Paclitaxel Versus Non-Bevacizumab-Containing Therapies in Persistent, Recurrent, or Metastatic Cervical Cancer. *Int J Gynecol Cancer*, 27, 1237-1246.
- ROSKOSKI, R., JR. 2015. A historical overview of protein kinases and their targeted small molecule inhibitors. *Pharmacol Res*, 100, 1-23.
- RUNDLE, S., BRADBURY, A., DREW, Y. & CURTIN, N. J. 2017. Targeting the ATR-CHK1 Axis in Cancer Therapy. *Cancers (Basel)*, 9.

- SAILER, C., OFFENSPERGER, F., JULIER, A., KAMMER, K. M., WALKER-GRAY, R., GOLD, M. G., SCHEFFNER, M. & STENGEL, F. 2018. Structural dynamics of the E6AP/UBE3A-E6-p53 enzyme-substrate complex. *Nat Commun*, 9, 4441.
- SALMON, S. E., HAMBURGER, A. W., SOEHNLEN, B., DURIE, B. G., ALBERTS, D. S. & MOON, T. E. 1978. Quantitation of differential sensitivity of human-tumor stem cells to anticancer drugs. *N Engl J Med*, 298, 1321-7.
- SANCAR, A., LINDSEY-BOLTZ, L. A., UNSAL-KACMAZ, K. & LINN, S. 2004. Molecular mechanisms of mammalian DNA repair and the DNA damage checkpoints. *Annual Review of Biochemistry*, 73, 39-85.
- SARKARIA, J. N., BUSBY, E. C., TIBBETTS, R. S., ROOS, P., TAYA, Y., KARNITZ, L. M. & ABRAHAM, R. T. 1999. Inhibition of ATM and ATR kinase activities by the radiosensitizing agent, caffeine. *Cancer Res*, 59, 4375-82.
- SCATCHARD, K., FORREST, J. L., FLUBACHER, M., CORNES, P. & WILLIAMS, C. 2012. Chemotherapy for metastatic and recurrent cervical cancer. *Cochrane Database Syst Rev*, 10, CD006469.
- SENDEROWICZ, A. M. 2000. Small molecule modulators of cyclin-dependent kinases for cancer therapy. *Oncogene*, 19, 6600-6.
- SHAPIRO, G., WESOLOWSKI, R., MIDDLETON, M., DEVOE, C., CONSTANTINIDOU, A., PAPADATOS-PASTOS, D., FRICANO, M., ZHANG, Y., KARAN, S., POLLARD, J., XCANCER RES. 2016. 2016. Phase 1 trial of first-in-class ATR inhibitor VX-970 in combination with cisplatin (Cis) in patients (pts) with advanced solid tumors (NCT02157792) (Abstract). 2016. *Cancer Res*.
- SHIGECHI, T., TOMIDA, J., SATO, K., KOBAYASHI, M., EYKELENBOOM, J. K., PESSINA, F., ZHANG, Y. B., UCHIDA, E., ISHIAI, M., LOWNDES, N. F., YAMAMOTO, K., KURUMIZAKA, H., MAEHARA, Y. & TAKATA, M. 2012. ATR-ATRIP Kinase Complex Triggers Activation of the Fanconi Anemia DNA Repair Pathway. *Cancer Research*, 72, 1149-1156.
- SHIOTANI, B. & ZOU, L. 2009. ATR signaling at a glance. *Journal of Cell Science*, 122, 301-304.
- SHRIVASTAV, M., DE HARO, L. P. & NICKOLOFF, J. A. 2008. Regulation of DNA double-strand break repair pathway choice. *Cell Research*, 18, 134-147.
- SIDDIK, Z. H. 2003. Cisplatin: mode of cytotoxic action and molecular basis of resistance. *Oncogene*, 22, 7265-79.
- SIMMS, K. T., STEINBERG, J., CARUANA, M., SMITH, M. A., LEW, J. B., SOERJOMATARAM, I., CASTLE, P. E., BRAY, F. & CANFELL, K. 2019. Impact of scaled up human papillomavirus vaccination and cervical screening and the potential for global elimination of cervical cancer in 181 countries, 2020-99: a modelling study. *Lancet Oncol*, 20, 394-407.

- SKEHAN, P., STORENG, R., SCUDIERO, D., MONKS, A., MCMAHON, J., VISTICA, D., WARREN, J. T., BOKESCH, H., KENNEY, S. & BOYD, M. R. 1990. New colorimetric cytotoxicity assay for anticancer-drug screening. *J Natl Cancer Inst*, 82, 1107-12.
- SKLOOT, R. 2010. *The Immortal Life of Henrietta Lacks*, New York, Crown/Random House.
- SMITH, P. K., KROHN, R. I., HERMANSON, G. T., MALLIA, A. K., GARTNER, F. H., PROVENZANO, M. D., FUJIMOTO, E. K., GOEKE, N. M., OLSON, B. J. & KLENK, D. C. 1985. Measurement of protein using bicinchoninic acid. *Anal Biochem*, 150, 76-85.
- SMITS, V. A. & GILLESPIE, D. A. 2015. DNA damage control: regulation and functions of checkpoint kinase 1. *FEBS J*, 282, 3681-92.
- SONGOCK, W. K., KIM, S. M. & BODILY, J. M. 2017. The human papillomavirus E7 oncoprotein as a regulator of transcription. *Virus Res*, 231, 56-75.
- SORENSEN, C. S., HANSEN, L. T., DZIEGIELEWSKI, J., SYLJUASEN, R. G., LUNDIN, C., BARTEK, J. & HELLEDAY, T. 2005. The cell-cycle checkpoint kinase Chk1 is required for mammalian homologous recombination repair. *Nature Cell Biology*, 7, 195-U121.
- SORENSEN, C. S. & SYLJUASEN, R. G. 2012. Safeguarding genome integrity: the checkpoint kinases ATR, CHK1 and WEE1 restrain CDK activity during normal DNA replication. *Nucleic Acids Research*, 40, 477-486.
- SULTANA, R., ABDEL-FATAH, T., PERRY, C., MOSELEY, P., ALBARAKTI, N., MOHAN, V., SEEDHOUSE, C., CHAN, S. & MADHUSUDAN, S. 2013. Ataxia telangiectasia mutated and Rad3 related (ATR) protein kinase inhibition is synthetically lethal in XRCC1 deficient ovarian cancer cells. *PLoS One*, 8, e57098.
- TAINIO, K., ATHANASIOU, A., TIKKINEN, K. A. O., AALTONEN, R., CARDENAS, J., HERNANDES, GLAZER-LIVSON, S., JAKOBSSON, M., JORONEN, K., KIVIHARJU, M., LOUVANTO, K., OKSJOKI, S., TAHTINEN, R., VIRTANEN, S., NIEMINEN, P., KYRGIU, M. & KALLIALA, I. 2018. Clinical course of untreated cervical intraepithelial neoplasia grade 2 under active surveillance: systematic review and meta-analysis. *BMJ*, 360, k499.
- TAKAI, H., TOMINAGA, K., MOTOYAMA, N., MINAMISHIMA, Y. A., NAGAHAMA, H., TSUKIYAMA, T., IKEDA, K., NAKAYAMA, K. & NAKANISHI, N. 2000. Aberrant cell cycle checkpoint function and early embryonic death in Chk1(-/-) mice. *Genes & Development*, 14, 1439-1447.
- TENG, P. N., BATEMAN, N. W., DARCY, K. M., HAMILTON, C. A., MAXWELL, G. L., BAKKENIST, C. J. & CONRADT, T. P. 2015. Pharmacologic inhibition of ATR and ATM offers clinically important distinctions to enhancing platinum or

- radiation response in ovarian, endometrial, and cervical cancer cells. *Gynecol Oncol*, 136, 554-61.
- THOMAS, M., PIM, D. & BANKS, L. 1999. The role of the E6-p53 interaction in the molecular pathogenesis of HPV. *Oncogene*, 18, 7690-7700.
- THOMPSON, L. H. 2012. Recognition, signaling, and repair of DNA double-strand breaks produced by ionizing radiation in mammalian cells: the molecular choreography. *Mutat Res*, 751, 158-246.
- TIAN, Q., STEPANIANTS, S. B., MAO, M., WENG, L., FEETHAM, M. C., DOYLE, M. J., YI, E. C., DAI, H., THORSSON, V., ENG, J., GOODLETT, D., BERGER, J. P., GUNTER, B., LINSELEY, P. S., STOUGHTON, R. B., AEBERSOLD, R., COLLINS, S. J., HANLON, W. A. & HOOD, L. E. 2004. Integrated genomic and proteomic analyses of gene expression in Mammalian cells. *Mol Cell Proteomics*, 3, 960-9.
- TIBBETTS, R. S., CORTEZ, D., BRUMBAUGH, K. M., SCULLY, R., LIVINGSTON, D., ELLEDGE, S. J. & ABRAHAM, R. T. 2000. Functional interactions between BRCA1 and the checkpoint kinase ATR during genotoxic stress. *Genes & Development*, 14, 2989-3002.
- TOLEDO, L. I., MURGA, M., ZUR, R., SORIA, R., RODRIGUEZ, A., MARTINEZ, S., OYARZABAL, J., PASTOR, J., BISCHOFF, J. R. & FERNANDEZ-CAPETILLO, O. 2011. A cell-based screen identifies ATR inhibitors with synthetic lethal properties for cancer-associated mutations. *Nat Struct Mol Biol*, 18, 721-7.
- TOMMASINO, M., ACCARDI, R., CALDEIRA, S., DONG, W., MALANCHI, I., SMET, A. & ZEHBE, I. 2003. The role of TP53 in Cervical carcinogenesis. *Hum Mutat*, 21, 307-12.
- UHLEN, M., ZHANG, C., LEE, S., SJOSTEDT, E., FAGERBERG, L., BIDKHORI, G., BENFEITAS, R., ARIF, M., LIU, Z., EDFORS, F., SANLI, K., VON FEILITZEN, K., OKSVOLD, P., LUNDBERG, E., HOBER, S., NILSSON, P., MATTSSON, J., SCHWENK, J. M., BRUNNSTROM, H., GLIMELIUS, B., SJOBLUM, T., EDQVIST, P. H., DJUREINOVIC, D., MICKE, P., LINDSKOG, C., MARDINOGLU, A. & PONTEN, F. 2017. A pathology atlas of the human cancer transcriptome. *Science*, 357.
- VENDETTI, F. P., LAU, A., SCHAMUS, S., CONRADS, T. P., O'CONNOR, M. J. & BAKKENIST, C. J. 2015. The orally active and bioavailable ATR kinase inhibitor AZD6738 potentiates the anti-tumor effects of cisplatin to resolve ATM-deficient non-small cell lung cancer in vivo. *Oncotarget*, 6, 44289-305.
- VINK, M. A., BOGAARDS, J. A., VAN KEMENADE, F. J., DE MELKER, H. E., MEIJER, C. J. & BERKHOF, J. 2013. Clinical progression of high-grade cervical intraepithelial neoplasia: estimating the time to preclinical cervical cancer from doubly censored national registry data. *Am J Epidemiol*, 178, 1161-9.

- VOGEL, C. & MARCOTTE, E. M. 2012. Insights into the regulation of protein abundance from proteomic and transcriptomic analyses. *Nat Rev Genet*, 13, 227-32.
- WAGNER, J. M. & KARNITZ, L. M. 2009. Cisplatin-Induced DNA Damage Activates Replication Checkpoint Signaling Components that Differentially Affect Tumor Cell Survival. *Molecular Pharmacology*, 76, 208-214.
- WALBOOMERS, J. M., JACOBS, M. V., MANOS, M. M., BOSCH, F. X., KUMMER, J. A., SHAH, K. V., SNIJDERS, P. J., PETO, J., MEIJER, C. J. & MUNOZ, N. 1999. Human papillomavirus is a necessary cause of invasive cervical cancer worldwide. *J Pathol*, 189, 12-9.
- WALBOOMERS, J. M. & MEIJER, C. J. 1997. Do HPV-negative cervical carcinomas exist? *J Pathol*, 181, 253-4.
- WALLACE, S. S. 2014. Base excision repair: a critical player in many games. *DNA Repair (Amst)*, 19, 14-26.
- WALTON, M. I., EVE, P. D., HAYES, A., HENLEY, A. T., VALENTI, M. R., DE HAVEN BRANDON, A. K., BOX, G., BOXALL, K. J., TALL, M., SWALES, K., MATTHEWS, T. P., MCHARDY, T., LAINCHBURY, M., OSBORNE, J., HUNTER, J. E., PERKINS, N. D., AHERNE, G. W., READER, J. C., RAYNAUD, F. I., ECCLES, S. A., COLLINS, I. & GARRETT, M. D. 2016. The clinical development candidate CCT245737 is an orally active CHK1 inhibitor with preclinical activity in RAS mutant NSCLC and Emicro-MYC driven B-cell lymphoma. *Oncotarget*, 7, 2329-42.
- WALTON, M. I., EVE, P. D., HAYES, A., VALENTI, M. R., DE HAVEN BRANDON, A. K., BOX, G., HALLSWORTH, A., SMITH, E. L., BOXALL, K. J., LAINCHBURY, M., MATTHEWS, T. P., JAMIN, Y., ROBINSON, S. P., AHERNE, G. W., READER, J. C., CHESLER, L., RAYNAUD, F. I., ECCLES, S. A., COLLINS, I. & GARRETT, M. D. 2012. CCT244747 is a novel potent and selective CHK1 inhibitor with oral efficacy alone and in combination with genotoxic anticancer drugs. *Clin Cancer Res*, 18, 5650-61.
- WALWORTH, N. C. & BERNARDS, R. 1996. rad-dependent response of the chk1-encoded protein kinase at the DNA damage checkpoint. *Science*, 271, 353-356.
- WALWORTH, N. C., WAN, S., LIU, H. Y., CAPASSO, H., RAO, H., CHEN, L. & NEFSKY, B. S. 2000. DNA damage checkpoint signaling through the protein kinase Chk1. *Faseb Journal*, 14, A1582-A1582.
- WANG, X., ZOU, L., LU, T., BAO, S., HUROV, K. E., HITTELMAN, W. N., ELLEDGE, S. J. & LI, L. 2006. Rad17 phosphorylation is required for claspin recruitment and Chk1 activation in response to replication stress. *Molecular Cell*, 23, 331-341.

- WANG, Y., DECKER, S. J. & SEBOLT-LEOPOLD, J. 2004. Knockdown of Chk1, Wee1 and Myt1 by RNA interference abrogates G2 checkpoint and induces apoptosis. *Cancer Biol Ther*, 3, 305-13.
- WEAVER, A. N., COOPER, T. S., RODRIGUEZ, M., TRUMMELL, H. Q., BONNER, J. A., ROSENTHAL, E. L. & YANG, E. S. 2015. DNA double strand break repair defect and sensitivity to poly ADP-ribose polymerase (PARP) inhibition in human papillomavirus 16-positive head and neck squamous cell carcinoma. *Oncotarget*, 6, 26995-7007.
- WELBURN, J. P., TUCKER, J. A., JOHNSON, T., LINDERT, L., MORGAN, M., WILLIS, A., NOBLE, M. E. & ENDICOTT, J. A. 2007. How tyrosine 15 phosphorylation inhibits the activity of cyclin-dependent kinase 2-cyclin A. *J Biol Chem*, 282, 3173-81.
- WILLIAMSON, C. T., MILLER, R., PEMBERTON, H. N., JONES, S. E., CAMPBELL, J., KONDE, A., BADHAM, N., RAFIQ, R., BROUGH, R., GULATI, A., RYAN, C. J., FRANCIS, J., VERMULEN, P. B., REYNOLDS, A. R., REAPER, P. M., POLLARD, J. R., ASHWORTH, A. & LORD, C. J. 2016. ATR inhibitors as a synthetic lethal therapy for tumours deficient in ARID1A. *Nat Commun*, 7, 13837.
- WU, X., SHELL, S. M., LIU, Y. & ZOU, Y. 2007. ATR-dependent checkpoint modulates XPA nuclear import in response to UV irradiation. *Oncogene*, 26, 757-764.
- XU, H., CHEUNG, I. Y., WEI, X. X., TRAN, H., GAO, X. & CHEUNG, N. K. 2011. Checkpoint kinase inhibitor synergizes with DNA-damaging agents in G1 checkpoint-defective neuroblastoma. *Int J Cancer*, 129, 1953-62.
- YANG, H., YOON, S. J., JIN, J., CHOI, S. H., SEOL, H. J., LEE, J. I., NAM, D. H. & YOO, H. Y. 2011. Inhibition of checkpoint kinase 1 sensitizes lung cancer brain metastases to radiotherapy. *Biochem Biophys Res Commun*, 406, 53-8.
- YAP, T. A. 2016. Phase I modular study of AZD6738, a novel oral, potent and selective ataxia telangiectasia Rad3-related (ATR) inhibitor in combination (combo) with carboplatin, olaparib or durvalumab in patients (pts) with advanced cancers (Abstract). *Eur. J. Cancer* 69
- YAZLOVITSKAYA, E. M. & PERSONS, D. L. 2003. Inhibition of cisplatin-induced ATR activity and enhanced sensitivity to cisplatin. *Anticancer Res*, 23, 2275-9.
- ZEHBE, I. & WILANDER, E. 1997. Human papillomavirus infection and invasive cervical neoplasia: a study of prevalence and morphology. *J Pathol*, 181, 270-5.
- ZEMAN, M. K. & CIMPRICH, K. A. 2014. Causes and consequences of replication stress. *Nat Cell Biol*, 16, 2-9.

- ZENVIRT, S., KRAVCHENKO-BALASHA, N. & LEVITZKI, A. 2010. Status of p53 in human cancer cells does not predict efficacy of CHK1 kinase inhibitors combined with chemotherapeutic agents. *Oncogene*, 29, 6149-59.
- ZHANG, Y., LAI, J., DU, Z., GAO, J., YANG, S., GORITYALA, S., XIONG, X., DENG, O., MA, Z., YAN, C., SUSANA, G., XU, Y. & ZHANG, J. 2016. Targeting radioresistant breast cancer cells by single agent CHK1 inhibitor via enhancing replication stress. *Oncotarget*, 7, 34688-702.
- ZHENG, H., SHAO, F., MARTIN, S., XU, X. & DENG, C. X. 2017. WEE1 inhibition targets cell cycle checkpoints for triple negative breast cancers to overcome cisplatin resistance. *Sci Rep*, 7, 43517.

Appendix

Poster presentations at scientific conferences

1. Targeting replication stress in cervical cancer by inhibiting checkpoint signalling. **Rundle, S** and Curtin, N J. 6th EU-US Conference on the repair of endogenous DNA damage. Udine, Italy. September 24th -28th 2017.
2. Exploiting endogenous replication stress in cervical cancer by inhibition of checkpoint signalling. **Rundle, S**. Drew, Y. Kucukmetin, A K and Curtin, N J. National Cancer Research Institute Conference. Liverpool, UK. 5th – 8th September 2017.